

Sliding Mode Control and Estimation for
Systems With Mismatched Uncertainties
Described by Polytopic Models

Thesis submitted for the degree of
Doctor of Philosophy
at the University of Leicester

by

José Manuel ANDRADE DA SILVA

Engineer's Degree in Electrical Engineering

Master's Degree (With Hons.) in Control Systems

Department of Engineering

University of Leicester

March 2010

UMI Number: U641602

All rights reserved

INFORMATION TO ALL USERS

The quality of this reproduction is dependent upon the quality of the copy submitted.

In the unlikely event that the author did not send a complete manuscript and there are missing pages, these will be noted. Also, if material had to be removed, a note will indicate the deletion.



UMI U641602

Published by ProQuest LLC 2015. Copyright in the Dissertation held by the Author.
Microform Edition © ProQuest LLC.

All rights reserved. This work is protected against
unauthorized copying under Title 17, United States Code.



ProQuest LLC
789 East Eisenhower Parkway
P.O. Box 1346
Ann Arbor, MI 48106-1346



To my beloved wife Zoraya and my wonderful sons Emmanuel Jesús and Angel Manuel with thanks for your understanding, encouragement, support and being patient even knowing this effort would make our invaluable time of sharing missed and lost forever.

To my dear mother María Teresa Souto De Andrade who made the impossible to be possible in order to provide me with the best education.

To my dear godmother María Conceição De Andrade Souto (in memoriam) who made me fall in love with mathematics when I was just a child.

Thanks to God Father, Son and Holy Spirit, for the gift of life, wisdom,
perseverance and discernment. Thanks for giving me the strength
to bring out the best of me in everything I undertake,
for making my ideas roll down like an ever-flowing stream,
for enlightening my mind with the fire of wisdom and for sowing in me,
as seeds in fertile ground, every one of the talents you have given me.
Thanks My Lord, Thanks!

Acknowledgements

There is a number of people without whom my doctoral studies and this PhD thesis might not have been possible, and to whom I am greatly indebted and heartily thankful.

First and foremost, I owe my deepest and sincere gratitude to my supervisor, Prof. Christopher EDWARDS, for providing me with sound advice, careful and detailed guidance, and encouragement at any time since the very beginning of my PhD. I am so thankful for his professional and personal support of the most invaluable kind. He has inspired me for his hard work as a researcher and scientist. Indeed, it has been a honour and I was so fortunate to have been able to study and work under his supervision. Thank you very much indeed for believing in my abilities!

I am grateful to Prof. Sarah K. SPURGEON for admitting me at the Control and Instrumentation Research Group of the Engineering Department at the University of Leicester. Many thanks for her advice and contribution during part of my PhD.

I wish to acknowledge my gratitude to the Department of Engineering at the University of Leicester for the diligence and support I have consistently obtained throughout my doctoral studies. Specially to Prof. Ian POSTLETHWAITE, head of the Control and Instrumentation Research Group, who was the first person I contacted in order to find out the possibility to register as a PhD student and from whom I got the following reply "your interests are well covered by our group". Also, I am thankful to Dr. Fernando S. SCHLINDWEIN for his advice as the postgraduate tutor of the Engineering Department. Many thanks to all members of the Engineering Department's General Office for their support, specially to Mrs. Michelle PRYCE, Ms. Julie CLAYTON, Mr. Andy CHORLEY, Mrs. Jenny RUANE and Ms. Debbie RICHARDSON.

I want to express my gratitude and heartily acknowledgement to the Roberto Rocca Education Program (RREP) for its generous support and encouragement during my PhD. The RREP made its support available in many ways and its team looked after my family, me and my PhD since I was awarded

a RREP fellowship. Special thanks to Mr. Daniel KRISHOCK director of the RREP. My family and I have unforgettable memories from his visits.

Many thanks to Mr. Alfredo J. COHEN KOHN, Mrs. Thalma COHEN DE GRUSZKA and Mrs. Aylin GRUSZKA DE COHEN who supported me during part of the first year of my PhD. Also, I am grateful to Ms. Regina das Neves DE JESUS PESTANA for her support, encouragement and reminder “Don’t give up. Never give up!”. Thanks for providing me the comfort of her house and everything I needed for working on my research project when staying in Ponta do Sol on Madeira Island, Portugal.

I am thankful to Ms. Jennifer M. WARREN for teaching me English language but more specially for her sincere friendship.

I want to thank the camaraderie of my fellows of the Control & Instrumentation Research Group: Halim ALWI, Sajjad FEKRI, Naeem KHAN, Rosli OMAR and Sohail IQBAL. Also to Taher BIALA, Carlos PEDREIRA and Juan MARTINEZ of the Bioengineering Group. My special thanks to Federico CARDONA-ROCHA of the Bioengineering Group for his truly friendship and time spent in many conversations about a vast number of topics. Thanks to Ricardo BAUTISTA-QUINTERO of the Embedded Systems Research Group for his friendship and for providing me with plenty of information based on the experience he had obtained for being in Leicester before than me. Thanks to Srinath GOVINDASWAMY of the Instrumentation, Control and Embedded Systems Research Group at the University of Kent for being keen to discuss several topics on control engineering, and also for his friendship.

I wish to express my love and gratitude to my beloved wife Zoraya and my tender sons Emmanuel Jesús and Angel Manuel for their never-ending love, support and understanding. My deepest thanks to my parents, specially to my mother María Teresa SOUTO DE ANDRADE who always has believed in my abilities. Thanks to my brothers Carlos Alberto and Victor José.

I offer my best wishes and blessings to all of those referred to above who supported and motivated me in any respect during my PhD. God bless all of you today, tomorrow and forever!

José Manuel ANDRADE-DA SILVA
Leicester - U.K., March-1st, 2k + 10

Abstract

Sliding Mode Control and Estimation for Systems With Mismatched Uncertainties Described by Polytopic Models

José Manuel ANDRADE DA SILVA

The problem of designing *variable structure systems with sliding modes* for uncertain continuous-time plants involving *mismatched parametric uncertainties* and matched uncertainties, nonlinearities and/or disturbances is addressed in this thesis. *Sliding mode control and estimation schemes* are proposed for this class of plants. Full and partial state information cases are considered. The latter scenario corresponds to sliding mode controllers using only measurable output signals, and comprises static and dynamic output feedback approaches. The proposed synthesis frameworks are based on *linear matrix inequality methods* and involve *polytopic models*. The multi-model paradigm is also explored to study the use of a finite set of *Lyapunov* matrices instead of a single *Lyapunov* matrix. Thus, a wider number of systems and control engineering problems can be dealt with. Control strategies using only measurable output signals are proposed for designing a single sliding mode controller for the simultaneous stabilisation of a finite collection of plant models. Design methodologies for sliding mode static and dynamic output feedback controllers based on linear matrix inequalities are described. The problem of state reconstruction using a discontinuous observer with sliding modes for systems with matched and mismatched parametric uncertainties is also studied in this dissertation. The mismatched uncertain component is considered as a disturbance whose effect on the output estimation error has to be minimised. The observer gain is synthesised by solving a convex optimisation problem involving linear matrix inequalities, with a polytopic description of the reduced-order error system, in terms of \mathcal{H}_∞ performance. A detailed stability analysis is carried out for the sliding mode observer and the class of uncertain systems considered. Throughout this thesis, several design examples illustrate the proposed sliding mode control and estimation schemes, and computer simulations are used to demonstrate their efficacy.

“I have yet to see any problem, however complicated,
which, when you looked at it in the right way,
did not become still more complicated.”

Poul Anderson (1926–2001)
New Scientist (September 25, 1969)

Contents

Nomenclature	xv
1 Introduction	1
1.1 A Brief Historical Overview of Sliding Modes	1
1.2 Motivation and Literature Review	4
1.2.1 Full State Information Approaches	4
1.2.2 Output Feedback Methods	6
1.2.3 Observer Schemes	7
1.3 Objectives	9
1.4 Methodology	9
1.5 Structure of the Thesis and Contributions	10
2 Variable Structure Systems With Sliding Modes	14
2.1 Introduction	14
2.2 Ideal Sliding Mode Existence and Uniqueness of Solution	18
2.3 Sliding Surface Design Problem	20
2.3.1 The Regular Form Approach	21
2.3.2 The Output Feedback Canonical Form Approach	24
2.4 Properties of Sliding Mode Control	26
2.5 Variable Structure Control Laws	31
2.5.1 The Reachability Problem	31
2.5.2 Existence of a Pseudo-Sliding Mode	32
2.5.3 Structure of the Control Law	34
2.5.4 Continuous Approximation of the Control Law	35
2.6 A Sliding Mode Observer	36
2.7 Summary	38

CONTENTS

3	Linear Matrix Inequalities and Polytopic Models	40
3.1	Introduction	40
3.2	Linear Matrix Inequalities	40
3.2.1	Convexity	41
3.2.2	Canonical and Other Forms of Representing LMIs	46
3.2.3	Standard LMI Problems	47
3.2.4	LMI Properties and Features	49
3.2.5	Fundamental Mathematical Operations on LMIs	49
3.2.6	LMI Regions	52
3.3	Parametric Uncertainty Description: Polytopic Models	56
3.4	Summary	61
4	State Feedback SMC for Systems With Mismatched Uncertainties	63
4.1	Introduction	63
4.2	System Description and Problem Formulation	64
4.3	State Feedback SMC Design Framework	65
4.3.1	Sliding Surface Design	65
4.3.2	Control Law Synthesis	69
4.3.3	Design Example	76
4.4	Summary	82
5	Sliding Mode Output Feedback Control: A Polytopic Approach	84
5.1	Introduction	84
5.2	System Description and Statement of Problems	85
5.3	Sliding Mode Static Output Feedback Control	88
5.3.1	Sliding Surface Design	88
5.3.2	Control Law Synthesis	91
5.3.3	Design and Computer Simulation Examples: SMSOFC	98
5.4	Sliding Mode Dynamic Output Feedback Control	104
5.4.1	Compensator-based Sliding Surface Design	104
5.4.2	Compensator-based Control Law Synthesis	107

CONTENTS

5.4.3	Design and Computer Simulation Examples: SMDOFC	110
5.5	Summary	114
6	Sliding Mode Output Feedback Control: Simultaneous Stabilisation	115
6.1	Introduction	115
6.2	System Description and Statement of Problems	116
6.3	SMSOFSS: Synthesis Framework	119
6.3.1	Switching Surface Design	119
6.3.2	Control Law Design	121
6.4	Design and Computer Simulation Example	127
6.5	SMDOFSS: Synthesis Framework	131
6.5.1	Compensator-based Sliding Hyperplane Design	131
6.5.2	Control Law Design	133
6.6	Design and Computer Simulation Examples	137
6.7	Summary	146
7	Sliding Mode Observer	147
7.1	Introduction	147
7.2	System Description and Statement of Problem	148
7.3	Stability Analysis	155
7.4	Design Framework	166
7.5	Design and Simulation Example	172
7.6	Summary	181
8	Conclusions	182
8.1	Concluding Remarks	182
8.2	Brief Suggestion for Future Research	186
A	High-level Implementation of LMIs	188

List of Figures

2.1	Block diagram of a double integrator system under VSC	14
2.2	Regions of the phase plane defined by the switching function $\sigma(t) = y(t)\dot{y}(t)$	15
2.3	Phase portrait of a double integrator system under VSC	15
2.4	Phase portrait of a double integrator system under SMC	17
2.5	Construction of Filippov's solution $\mathbf{F}_{av}(t, \mathbf{x}_\sigma)$	20
2.6	A practical sliding motion (adapted from (Edwards & Spurgeon, 1998a))	33
2.7	Approximation of the signum function by a sigmoid-like function (figure adapted from (Edwards & Spurgeon, 1998b) pages 16 and 62)	36
3.1	Convex set \mathcal{C}_1 and non-convex set \mathcal{C}_2	41
3.2	2-D and 3-D Polyhedra	43
3.3	Geometric interpretation of convex hull of a set of points in 2-D and 3-D	44
3.4	Geometric interpretation of convex and concave functions.	45
3.5	Elementary LMI Region: Half-plane $\mathcal{H}(h)$	53
3.6	Elementary LMI Region: Cone $\mathcal{C}((0,0)_c, \alpha)$	54
3.7	Elementary LMI Region: Disk $\mathcal{D}(c_n, r_d)$	55
3.8	Elementary LMI Region: Vertical strip $\mathcal{V}_s(h_1, h_2)$	56
3.9	Mapping of a Parameter Box in a Polytope of System Matrices.	60
4.1	LMI Region $\mathcal{D}(h, c_n, r_d, \alpha)$	69
4.2	Schematic Diagram of a DC Motor (Figure adapted from (Franklin <i>et al.</i> , 2002) page 55)	76
4.3	Electric and Mechanic Diagram of a DC Motor (Figure adapted from (Franklin <i>et al.</i> , 2002) page 54)	77
4.4	Angular position $\vartheta(t)$ [rad].	80
4.5	Angular speed $d\vartheta(t)/dt$ [rad/sec].	80
4.6	Armature current i_a [A].	81

LIST OF FIGURES

4.7	Armature voltage $v_a(t)$ [V].	81
4.8	Switching functions.	82
5.1	LMI Region $\mathcal{D}(h, c_n, r_d)$	97
5.2	Closed-loop poles obtained when using only the linear part of the control law	100
5.3	Closed-loop response	100
5.4	Control signal $u(t)$ and switching function $\sigma(t)$	101
5.5	Time evolution of the output signals $y_1(t)$, $y_2(t)$ and $y_3(t)$	103
5.6	Control signals $u_1(t) = \delta_r(t)$ and $u_2(t) = \delta_a(t)$	103
5.7	Time evolution of switching functions $\sigma_1(t)$ and $\sigma_2(t)$	104
5.8	Root locus for the system triple $(\tilde{\mathbf{A}}_{111}, \tilde{\mathbf{A}}_{121}, \mathbf{C}_{11})$ for $\theta = \underline{\theta} = -0.2$. . .	111
5.9	Root locus for the system triple $(\tilde{\mathbf{A}}_{112}, \tilde{\mathbf{A}}_{122}, \mathbf{C}_{12})$ for $\theta = \bar{\theta} = +0.2$. . .	112
5.10	Response of the uncertain plant using the SMDOF controller	112
5.11	Control signal $u(t)$	113
5.12	Time evolution of the switching function $\sigma(t)$	113
6.1	LMI Region $\mathcal{D}(h, c_n, r_d)$	126
6.2	Time evolution of the output signals using the designed sliding mode output feedback controller.	129
6.3	Control signals $\zeta(t)$ and $\tau(t)$	130
6.4	Switching functions vs time.	130
6.5	Time evolution of the output signals y_1 and y_2 , and the unmeasurable state x_1 for both operation modes of the plant	139
6.6	Control signal $u(t)$ for both operation modes of the plant	139
6.7	Switching function $\sigma(t)$ for both operation modes of the plant	140
6.8	Schematic Diagram of an n plates Gas absorber [adapted from (Luus, 2000)]	141
6.9	Eigenvalues of the sliding mode reduced-order system at each operating condition of the gas absorber plant.	143
6.10	Eigenvalues of $(\hat{\mathbf{A}}_{a_i} - \hat{\mathbf{B}}_a \mathbf{G}_a \hat{\mathbf{C}}_a)$ for the set of operating conditions of the gas absorber plant.	144

LIST OF FIGURES

6.11 Time evolution of the output signals (continuous lines), and the unmeasured state variables (dotted lines) for the set of operating conditions of the gas absorber plant	144
6.12 Control signals $u_1(t)$ and $u_2(t)$ for the set of operating conditions of the gas absorber plant	145
6.13 Switching functions $\sigma_1(t)$ and $\sigma_2(t)$ for the set of operating conditions of the gas absorber plant	145
7.1 Convex Region $\mathcal{D}(h, c_n, r_d, \alpha) = \mathcal{D}(0.1, 0, 6, \pi/4)$ for robust pole placement of a full state feedback controller	175
7.2 Time evolution of the uncertain parameters $\theta_1(t)$, $\theta_2(t)$ and $\theta_3(t)$	176
7.3 Time evolution of the true and estimated state $x_1(t)$	176
7.4 Time evolution of the true and estimated state $x_2(t)$	177
7.5 Time evolution of the true and estimated state $x_3(t)$	177
7.6 Time evolution of the true and estimated state $x_4(t)$	178
7.7 Estimation error $e_1(t) = \hat{x}_1(t) - x_1(t)$	178
7.8 Estimation error $e_2(t) = \hat{x}_2(t) - x_2(t)$	179
7.9 Estimation error $e_3(t) = \hat{x}_3(t) - x_3(t)$	179
7.10 Estimation error $e_4(t) = \hat{x}_4(t) - x_4(t)$	180
7.11 Time evolution of switching functions $\mathbf{e}_y(t) \in \mathfrak{R}^2$	180

Nomenclature

Symbols

\bar{s}	The complex conjugate of s
\mathbb{C}	The field of complex numbers
\mathbb{C}_-	The open left-half complex plane
\mathbf{S}	The System Matrix
\mathbb{Z}_+	The set of strictly positive integer numbers
$\mathbf{\Gamma}$	The switchig gain matrix
\mathbf{A}	The state matrix
\mathbf{B}	The input distribution matrix
\mathbf{C}	The output distribution matrix
\mathbf{M}^\dagger	The left <i>Moore-Penrose</i> pseudo-inverse of the matrix \mathbf{M}
$\mathcal{N}(\mathbf{M})$	Null sub-space of the matrix \mathbf{M}
$\mathcal{R}(\mathbf{M})$	Range sub-space of the matrix \mathbf{M}
\mathcal{P}	Projector
$\text{Im}[s]$	The imaginary part of the complex number z
$\text{Re}[s]$	The real part of the complex number z
$\mathcal{C}((0,0)_{\mathbb{C}}, \alpha)$	Conic region centered at the origin of the complex plane \mathbb{C} and at an angle α with respect to the real axis of the complex left half-plane
$\mathcal{D}(c_n, r_d)$	Disk region centered at $(-c_n, 0)$ in the complex plane \mathbb{C} with radius r_d
$\mathcal{H}(h)$	Half-plane delimited by a vertical line at $(-h, 0)$ in the complex plane.
$\mathcal{H}^{n \times n}$	The set of $n \times n$ <i>Hermitian</i> matrices
$\mathcal{R}(s)$	The <i>Rosenbrock's</i> system matrix
\mathcal{X}	State space

Nomenclature

max	maximise
min	minimise
\mathfrak{R}	The field of real numbers
$\mathfrak{R}^{n \times m}$	The set of $n \times m$ dimensional real matrices
\mathfrak{R}_+	The set of strictly positive real numbers
$I(\epsilon_1, \epsilon_2)$	The index set $I(\epsilon_1, \epsilon_2) = \{\epsilon_1, \epsilon_1 + 1, \dots, \epsilon_2\}$ where $\epsilon_1, \epsilon_2 \in \mathbb{Z}_+$ and $\epsilon_1 < \epsilon_2$
s	The complex variable

Acronyms and Abbreviations

BMI	Bilinear Matrix Inequality
DC	Direct Current
DOF	Dynamic Output Feedback
dps	decimal places
emf	electromotive force
EVP	Eigenvalue Problem
FTC	Fault Tolerant Control
GEVP	Generalised Eigenvalue Problem
HOSMO	High Order Sliding Mode Observer
KVL	<i>Kirchhoff's</i> Voltage Law
LMI	Linear Matrix Inequality
LOMP	Linear Objective Minimisation Problem
LTI	Linear Time Invariant
MIMO	Multiple-Input Multiple-Output
n.d.	negative definite
p.d.	positive definite
PDP	Positive Definite Programming
QMI	Quadratic Matrix Inequality

Nomenclature

R.H.S.	Right Hand Side
s.p.d.	symmetric positive definite
s.t.	subject to
SDP	Semidefinite Programming
SISO	Single-Input Single-Output
SMC	Sliding Mode Control/Controller
SMDOF	Sliding Mode Dynamic Output Feedback
SMDOFC	Sliding Mode Dynamic Output Feedback Control/Controller
SMDOFSS	Sliding Mode Dynamic Output Feedback Simultaneous Stabilisation
SMO	Sliding Mode Observer
SMOF	Sliding Mode Output Feedback
SMSOF	Sliding Mode Static Output Feedback
SMSOFC	Sliding Mode Static Output Feedback Control/Controller
SMSOFSS	Sliding Mode Static Output Feedback Simultaneous Stabilisation
SOF	Static Output Feedback
VSC	Variable Structure Control
VSS	Variable Structure System

*"All truths are easy to understand
once they were discovered;
the point is to discover them."*

Galileo Galilei (1564 - 1642)

1

Introduction

1.1 A Brief Historical Overview of Sliding Modes

Mathematical control systems theory is a sub-field of applied mathematics whose objects of analysis and design are signals and systems. This theory, built on a wide range of disciplines such as algebra, matrix theory (linear algebra), differential or difference equations, optimisation, differential geometry, functional analysis and so on, represents the abstract language of control systems engineering. Control theory deals with modelling and analysis of dynamical systems, and the subsequent synthesis of controllers and/or estimators satisfying a predefined set of performance requirements. The latter might be required to reconstruct some variables of the system or when the overhead costs associated with sensors may be prohibitive. Further tasks tackled in control engineering are implementation, testing and tuning of controllers and estimators.

Variable Structure Control (VSC) is a nonlinear control scheme consisting of a switched control law and a decision function which induces a discontinuous change in the structure of a system. A particular class of variable structure controllers, which use switched control action across a sliding surface, is Sliding Mode Control (SMC). A sliding motion, governed by the dynamics associated with a sliding surface completely defined by the designer, is the major mode of operation in Variable Structure Systems (VSS) (Utkin, 1992). These control schemes appeared and were initially developed in the former Soviet Union. *V. Kulebakin* and *G. Nikolski* can be considered as the pioneers of SMC due to their work in the early 1930s (Utkin *et al.*, 1999). The work by *Kulebakin* was concerned with the application of a vibration controller¹ for voltage control of an aircraft DC generator (Kulebakin, 1932), whilst *Nikolski* investigated

¹*Sliding mode control* corresponds to *vibration control* in contemporary terminology (Utkin *et al.*, 1999).

1.1 A Brief Historical Overview of Sliding Modes

the stability under sliding mode relays of a ship on a given course (Nikolski, 1934). Nevertheless, VSC was formally studied and presented from a mathematical viewpoint between the late 1950s and 1967 by *S. V. Emel'yanov* of the Institute of Control Science in Moscow in the following publications (Emel'yanov, 1957) (Emel'yanov, 1959a) (Emel'yanov, 1959b)¹ (Emel'yanov, 1967), and *E. A. Barbashin's* work on stability theory (Barbashin, 1967) at the Institute of Mathematics and Mechanics in Sverdlovsk. These seminal publications defined a milestone establishing a new research area in control systems theory. However, as in the case of the stability theory of *Lyapunov*, VSC theory was not known in western countries because all published work had been written in Russian. VSC theory was expanded beyond the borders of the Soviet Union and introduced in the West through several publications in English (Utkin, 1971) (Utkin, 1972) (Utkin, 1974) (Fuller, 1974) (Utkin, 1977) and (Itkis, 1976) making the fundamentals of this control scheme accessible to other researchers and engineers who became interested in this new control theory.

Before the high potential of SMC was exploited, these control schemes had to confront the scepticism of engineers in many practical applications due to the high-frequency nature of the discontinuous control signal. Although this feature might be appropriate in some applications, *e.g.* electric drives such as converters, in many others it is counterproductive and not applicable to actuators because of the risk of deterioration or even their complete break-down. Moreover, the high-frequency switching control signal exhibited by sliding mode controllers (SMCs) can excite unmodelled fast dynamics of the plant causing a finite frequency and finite amplitude oscillating trajectory of the system along the sliding surface (Utkin *et al.*, 1999). This system motion is termed chattering. Note that in an ideal sliding mode, *i.e.* control signal switching at infinite frequency, the system trajectory is constrained to lie on the sliding surface, and hence there is no chattering phenomenon at all (Edwards & Spurgeon, 1998b). Obviously, such infinite frequency switching cannot be achieved physically. The chattering phenomenon overshadowed the SMC theory until the advantageous characteristics of order reduction (Utkin, 1992) (Edwards & Spurgeon, 1998b) and the invariance property (Draženović, 1969) attracted the attention of researchers and engineers. A system in a sliding mode is governed by reduced-order dynamics specified by the designer when synthesising the sliding surface associated with the sliding mode controller. Furthermore, a sliding mode controller, when appropriately designed, provides complete insensitivity with respect to a class of uncertainty known as matched uncertainty: that is, any uncertainty and/or disturbance signal enter through the input channel of the system. In addition, the chattering problem was studied and several approaches to mitigate the effects were proposed. For instance, the boundary layer approach (Slotine & Sastry, 1983) (Slotine, 1984), observer-based approaches (Bondarev *et al.*, 1985),

¹Even though the term *variable structure system* did not appear explicitly in any of these three papers, the concept of change of structure by using a switching logic was illustrated (Utkin, 2002).

1.1 A Brief Historical Overview of Sliding Modes

cascade control using regular form or the block control principle approach (Drakunov *et al.*, 1990a) (Drakunov *et al.*, 1990b) and the disturbance rejection approach (this approach is a special case of integral sliding mode presented in (Utkin & Shi, 1996)). Details of these chattering reduction solutions can be found in (Utkin *et al.*, 1999). In addition to the methods previously cited, it is possible to reduce (eliminate) the high frequency oscillations exhibited by the switched control law by means of approximating the discontinuous term. Saturation, power law interpolation and differentiable approximations have all been employed to replace the switching term (signum or unit vector). Note that the saturation approximation corresponds to the boundary layer method. The power law interpolation smooths the relay function within a neighbourhood of the origin. On the other hand, the differentiable approximation method does not imply a boundary layer. Details regarding the approximations can be found in (Edwards & Spurgeon, 1998b).

The concepts involving VSC were demonstrated, at the very beginning, for second-order systems. However, several developments including different classes of systems and mathematical descriptions have taken place over the years. Furthermore, various forms of switching functions and control laws have been under constant study within the VSS research community. In (Hung *et al.*, 1993) three main periods have been defined. The early stage of VSC from the late 1950s to 1970 represents the study of VSC in which single input systems described using high-order linear differential equations or the controllable canonical state-space form, and quadratic switching functions were considered. Later, multi-input linear systems represented in a general state-space form not restricted to the controllable canonical form, and linear switching functions in vector form were employed during the period 1970-1980. From the 1980s onwards, more complex systems were considered, *e.g.* discrete-time systems, non-linear systems, large-scale (or interconnected) systems, stochastic systems and delayed systems. Furthermore, other control problems have been considered, *e.g.* tracking control, model following, adaptive control, optimal control, static and dynamic output-feedback control using only measurable state variables and so forth. The estimation problem of state variables and faults applying sliding mode concepts has been also under continuous study. Surveys, tutorials, chapters in books on nonlinear control, and text books have been published describing the theoretical fundamentals of sliding mode theory, for example (Utkin, 1977) (DeCarlo *et al.*, 1988) (Slotine & Li, 1991) (Utkin, 1992) (Hung *et al.*, 1993) (Zinober, 1994) (Edwards & Spurgeon, 1998b) (Utkin *et al.*, 1999) (Emel'yanov & Korovin, 2000). SMC theory has been applied for solving a large number of control engineering problems in different fields, *e.g.* chemical processes, electrical systems, mechanical systems, electromechanical systems, aircrafts, biological/biochemical systems, and so on (Dote & Hoft, 1980) (Hashimoto *et al.*, 1987) (Young, 1993) (Hung *et al.*, 1993) (Utkin, 1993) (Fossas *et al.*, 2001) (Msirdi & Nadjar-Gauthier, 2002) (Biel-Sole & Fossas-Colet, 2004) (Sabanovic & Jezernik, 2004)

1.2 Motivation and Literature Review

(Utkin & Chang, 2004) (Goh *et al.*, 2004) (Bartolini *et al.*, 2004) (Herrmann *et al.*, 2008) (Alwi *et al.*, 2008) (Tan & Edwards, 2008) (Pan *et al.*, 2008) (Tan *et al.*, 2008) among other references.

1.2 Motivation and Literature Review

Uncertainties in mathematical models may arise from unknown dynamics, either unknown or approximated numerical values of the parameters in the model, varying parameters, and approximations in the modelling process. Closed-loop stability and an appropriate robust performance in the presence of parametric or non-structured uncertainties, external disturbances, measurement noise and unmodelled dynamics are requirements to be considered when synthesising a control system. A sliding mode controller, when appropriately designed, will guarantee closed-loop stability and complete rejection of a class of uncertainty known as *matched uncertainty*. Although some systems can be categorised as uncertain plants with matched uncertainty, there are many practical plants affected by mismatched uncertainties. The reduced-order sliding mode dynamics will be affected by any *mismatched uncertainty* in the system. Most of the research carried out on SMC and sliding mode estimation using Sliding Mode Observers (SMOs) consider matched uncertainty, nonlinearities and/or disturbances. Comparatively few papers have studied the control (state feedback, static and dynamic output feedback) and estimation (state reconstruction) problems for systems with mismatched uncertainties.

Sliding mode control synthesis comprises two design problems. Firstly, the sliding mode existence problem consists of synthesising a sliding surface in such a way that the reduced-order dynamics exhibit the desired behaviour established by the designer. Secondly, the reachability problem involves the design of a discontinuous control law to drive the trajectory of the system onto the sliding surface and then to lie in the subspace defined by the sliding surface.

1.2.1 Full State Information Approaches

There are several sliding surface design frameworks assuming that all state variables are available. Initially, sliding mode controllers were developed for the class of systems with only matched uncertainties, disturbances and/or nonlinearities. Thus, synthesis methodologies for sliding surfaces involving the so-called regular form and based on quadratic minimization, eigenvalue and eigenstructure assignment were presented in (Utkin & Young, 1978) (El-Ghezawi *et al.*, 1983) (Dorling & Zinober, 1986). Subsequently, design approaches using Linear Matrix Inequalities (LMIs) (Boyd *et al.*, 1994) have been proposed in (Choi, 1997) and (Edwards, 2004). It is important to

1.2 Motivation and Literature Review

highlight that the design approaches cited above, concerned with pole placement, are pointwise eigenvalue assignment methods.

The problem of sliding surface design for plants with full-state information and mismatched uncertainties has been studied and several approaches have been proposed. The robust eigenstructure assignment method described in (Edwards & Spurgeon, 1998b) seeks to minimise the effect of the variations of the mismatched parameters. A sliding mode control scheme which minimises the effects of the mismatched uncertainty on the performance associated with the sliding surface has been presented in (Spurgeon & Davies, 1993). In (Kim *et al.*, 2000) an approach based on a *Riccati* inequality has been proposed. A design methodology using pointwise pole placement is presented in (Chen & Chang, 2000). Such a methodology considers the overall closed-loop system instead of the sliding mode reduced-order system. The design of adaptive sliding surfaces to tackle mismatched uncertainty has also been considered in (Chang & Cheng, 2007).

Some sliding surface design approaches using LMIs have already been proposed. For instance, quadratic stabilisation and pole assignment in a convex region of the left-half complex plane was considered in (Arzelier *et al.*, 1997) for a class of systems with norm-bounded mismatched uncertainty. Arzelier *et al.* suggested, in the concluding remarks of (Arzelier *et al.*, 1997), the use of a polytopic representation as an extension of their work. However, such an extension considering a polytopic description of the system has not appeared in the literature. In (Takahashi & Peres, 1999) an \mathcal{H}_2 guaranteed cost design for systems with structured mismatched uncertainties (represented in polytopic form) and mismatched disturbance signals was proposed. However, LMI regions were not considered. In (Choi, 2003) the sliding mode existence problem was considered for mismatched uncertainties represented in a norm-bounded form, and an invariance property was proposed. These publications, based on LMI methods for systems with mismatched uncertainties, have tackled only the sliding mode existence problem and have not studied the reachability problem, and furthermore no design methodology for the control law was proposed either. A sliding mode controller synthesis for systems with norm-bounded mismatched uncertainties was proposed in (Sellami *et al.*, 2007). The class of system considered in (Sellami *et al.*, 2007) has only norm-bounded uncertainties affecting the state matrix, and takes into account uncertainty in both the sliding mode existence and reachability problems. The sliding surface synthesis is LMI-based involving pole placement in LMI regions, whilst the full-state feedback control law (consisting of linear and smoothed discontinuous parts) is designed algebraically following the ‘unit vector’ approach described in (Ryan & Corless, 1984). The particular form of the norm-bounded uncertainty is considered when designing the scalar gain in the smoothed discontinuous component of the control law.

1.2 Motivation and Literature Review

As referred to previously, many of the early SMC approaches assumed that the state vector is accessible, and hence all state variables are available to the control law. Although this assumption has allowed real applications to be tackled, *e.g.* (Utkin, 1993) and (Tan *et al.*, 2008), this assumption is quite restrictive, as in many applications only a subset of the state variables are physically measurable. This has given rise to developments in two main directions. On the one hand, *observer-based sliding mode control*, *e.g.* (Xie, 2007) and (Pan *et al.*, 2008), in which a state estimator or observer is applied to reconstruct the state variables by means of measuring the input and output signals of the plant. Then, a state feedback sliding mode controller can be designed. State estimators, however, unless properly designed, can undermine the robustness properties of state feedback control. On the other hand, *Sliding Mode Output Feedback Control* (SMOFC) uses only plant output signals (Edwards & Spurgeon, 1995). This kind of control can be classified into *static* (Žak & Hui, 1993) (El-Khazali & DeCarlo, 1995) (Edwards & Spurgeon, 1995) (Edwards *et al.*, 2001) or *dynamic* (Kwan, 2001) (Teixeira *et al.*, 2006) (Chen & Saif, 2008). Details on the limitations of some existing SMOFC designs are discussed in (Edwards & Spurgeon, 2000).

1.2.2 Output Feedback Methods

In general, static output feedback (SOF) is still an open problem, although several approaches have been developed (Syrmos *et al.*, 1997). Simplicity is the most attractive feature of SOF whilst non-convexity is an important drawback when an LMI framework is applied. Another relevant aspect of the SOF problem is that the dynamic output feedback (DOF) control problem via compensator-based control can be recast as a SOF problem (Syrmos *et al.*, 1997). DOF control implies that further dynamics are added to the control system in order to achieve some application dependent performance requirements defined by the designer.

A small number of papers have considered Sliding Mode Output Feedback (SMOF) controller design based on LMIs for systems with mismatched uncertainties. For instance, an LMI-based SOF variable structure controller was developed in (Choi, 2002). The proposed control law is a high gain control law which for some practical engineering systems is not desirable as it may saturate the system actuators. This drawback can be overcome through a dynamic variable structure output feedback control law. In (Choi, 2008a) an LMI-based sliding surface design approach considering \mathcal{H}_2 performance was presented. More recently, a compensator-based SMOF controller considering several performance criteria (Choi, 2008b), and uncertain fuzzy systems (Choi, 2009) were proposed. Another Sliding Mode Static Output Feedback (SMSOF) approach using LMIs was developed in (Xiang *et al.*, 2006) which neither requires coordinate transformations nor solves a SOF problem. Again, the proposed control law belongs to the

1.2 Motivation and Literature Review

class of high gain control laws. The LMIs involved in the design algorithm are relatively complex and as the algorithm is iterative, its convergence depends on the chosen initial conditions. Recently, in (Park *et al.*, 2007) a dynamic output feedback variable structure controller was presented.

In some particular cases when the *Kimura-Davison* conditions (Kimura, 1975) (Kimura, 1977) (Davison, 1970) are not satisfied (Edwards & Spurgeon, 1998a), SMSOF control may not be applied. In such situations, an appropriately dimensioned dynamic compensator is required in order to introduce extra dynamics to increase the degrees of design freedom. This approach belongs to the class of dynamic output feedback controllers.

The control theory problem of so-called simultaneous stabilisation consists of designing a single controller, if such a controller exists, to stabilise a finite set of plant models. The problem of simultaneous stabilisation can be formulated in several different contexts (Lee & Soh, 2004) (Wu & Lee, 2005) (Lavaei & Aghdam, 2007). For instance, in the case of stabilising a nonlinear system, the envelope of operation may be split into a finite number of operating conditions. Then, a linear model for each operating point is generated in order to formulate the simultaneous stabilisation problem. Another significant application lies in the control engineering field of fault tolerant control (FTC) systems. In this context a finite set of plant models is defined associated with the fault-free and faulty behaviour of the plant. The fault-free condition corresponds to an operating condition whilst the faulty behaviour is defined through a finite sub-set of faults. These faults stem from plant, actuator and/or sensor malfunctions which deteriorate the performance of the system or worse, cause a break-down in the system. Also the simultaneous stabilisation problem can be considered to correspond to a finite collection of plant models of an uncertain plant. In this case, the uncertain parameters vary continuously or piece-wise continuously within a hyper-rectangle defined by the upper and lower bounds of each uncertain parameter.

The problem of simultaneous stabilisation was initially introduced in (Birdwell *et al.*, 1979) for a particular class of LTI systems in the context of FTC. Nevertheless, a literature review suggests that it was not until a few years later that the term appeared in (Saeks & Murray, 1982) and (Vidyasagar & Viswanadham, 1982). The problem of simultaneous stability still remains open despite research efforts to solve this problem analytically. However, it is argued in (Cao & Sun, 1998) that numerical algorithms can be applied when the analytical solution may not exist.

1.2.3 Observer Schemes

An observer or estimator is a dynamical system proposed initially to reconstruct unmeasurable state variables using only input and output signals (Luenberger, 1964).

1.2 Motivation and Literature Review

However, over the years, its potential for monitoring systems has been widely exploited, more precisely, in model-based fault detection schemes (Isermann, 2006). The state estimation problem has been addressed from different paradigms, *e.g.* *Luenberger* observers (Luenberger, 1964), *Kalman* filters (Kalman, 1960), high-gain observers (Gauthier *et al.*, 1992), adaptive observers (Marino & Tomei, 1995) and sliding mode observers (Edwards & Spurgeon, 1998b). A sliding mode observer (SMO) is a subclass of nonlinear observer consisting of a nonlinear (possibly discontinuous) injection signal which guarantees convergence of the state error vector in finite time and robustness with respect to a particular class of uncertainties.

A discontinuous observer which induces a sliding motion on the output estimation error space was presented in (Utkin, 1981) (Utkin, 1992). An SMO involving linear and nonlinear output error feedback was proposed in (Slotine *et al.*, 1986). In this paper, the relationship between performance and the discontinuous component of the proposed SMO is studied. In (Walcott & Žak, 1987), an SMO consisting of a *Luenberger*-like component and a discontinuous injection signal was presented. The synthesis framework considers bounded uncertainties/non-linearities and involves a constrained *Lya-punov* problem requiring symbolic algebraic manipulation. A discontinuous observer with a sliding mode was proposed in (Edwards & Spurgeon, 1994) where a systematic design methodology considering a canonical form and norm-bounded uncertainties is described. In (Sira-Ramirez & Spurgeon, 1994) the matching condition in the context of SMOs for linear systems was studied. The equivalent control concept and the block form for designing SMOs was considered in (Drakunov & Utkin, 1995). SMOs (based on the *Walcott & Žak* and *Edwards & Spurgeon* observers described above), which do not require the upper bound of the matched uncertainty/disturbance to be known, were proposed in (Chen & Saif, 2006). The observer nonlinear injection signals are functions of a time-varying gain computed using a first-order dynamic law. A synthesis approach based on LMIs is described in (Tan & Edwards, 2001) for generating the gain matrices of an SMO of the same form as in (Edwards & Spurgeon, 1994). An LMI-based design methodology was proposed in (Choi & Ro, 2005) which does not necessitate change of coordinates to obtain the canonical form required in (Tan & Edwards, 2001). *Only systems with matched uncertainties have been considered in the references cited above.*

In all the work described previously the effects of the matched uncertainties are rejected by the discontinuous injection signal. This is consistent with the invariance property of sliding modes with respect to this class of uncertainty. Nevertheless, the invariance property is not guaranteed with respect to any mismatched uncertainty in the error system. Comparatively few papers have been devoted to the problem of designing SMOs for systems with mismatched uncertainties. A notable exception is the work (Koshkouei & Zinober, 2004) in which the problem is tackled via algebraic *Riccati* equations. High order sliding mode observers (HOSMOs) built on the sliding mode differentiator (Levant, 1998) have been employed to address the problem of state

estimation for systems with unknown inputs. Results reported in (Fridman *et al.*, 2006), (Bejarano *et al.*, 2007), (Floquet & Bardot, 2007) and (Chen & Saif, 2008) represent significant contributions in this direction. (Fridman *et al.*, 2008) presented an overview of the recent contributions on HOSMOs and proposed estimation schemes (observation, identification and fault detection) for linear systems with unknown inputs which do not require a matching condition.

1.3 Objectives

The aims of this thesis are twofold. One aim is to study the sliding mode existence and reachability problems for uncertain linear continuous-time systems with mismatched parametric uncertainties. This class of uncertainty is of great relevance in practical engineering applications. Matched uncertainties, nonlinearities and/or disturbances have to be also considered. The second aim is to propose synthesis frameworks for designing sliding mode controllers (full state and only output information) and sliding mode observers for plants with mismatched parametric uncertainties and matched uncertainties, nonlinearities and/or disturbances. As discussed in Section 1.2, comparatively few papers have studied the state feedback, static and dynamic output feedback control problems, as well as the state reconstruction problem using sliding modes for systems with mismatched uncertainties.

The stability of the reduced-order sliding mode dynamics will be formally analysed considering each class of sliding mode controller and sliding mode observer proposed in this thesis.

This dissertation contributes to the study and analysis of newly proposed systematic design methodologies for variable structure control systems with sliding modes for plants with mismatched parametric uncertainties. Thus, control engineers will have analysis and design tools enabling them to solve practical problems involving the class of systems considered in this thesis. This research not only offers a breakthrough in the theory of variable structure systems with sliding modes, but also in providing design algorithms that can be used by engineers without the need to go into the mathematical details which support the proposed synthesis methodologies.

1.4 Methodology

Abstract mathematical models for describing physical real world phenomena were first used by astronomers and mathematicians, *e.g.* Eudoxus, Ptolemy and Archimedes, in ancient Greece (Haddad & Chellaboina, 2008). In this thesis, a mathematical model constructed through a convex combination of N vertices defined in a matrix space,

1.5 Structure of the Thesis and Contributions

referred to in this thesis as a *polytopic model*, is considered to describe mismatched parametric uncertainties. The associated stability analysis is carried out using *Lya-punov* theory. LMIs (Boyd *et al.*, 1994) represent a powerful mathematical tool for formulating and solving problems in control and systems engineering which consist of a set of matrix variables that may have specific structures defined by the designer. In (Gahinet *et al.*, 1995) it is asserted that LMIs have the following attractive features: several problems can be recast as LMIs, such problems can be solved numerically in an efficient way by means of convex optimisation algorithms, moreover, some mathematical programming problems with multiple constraints or objective functions which cannot be solved analytically can be tractable using LMI techniques. In this dissertation, LMI methods are the main mathematical tool applied for solving the analysis and synthesis problems posed within this research work in the context of sliding mode theory.

Design studies and computer simulations are performed in order to illustrate the proposed design methodologies. Numerical examples and mathematical models of plants with physical meaning are used throughout this dissertation to demonstrate the efficacy of each proposed approach.

1.5 Structure of the Thesis and Contributions

The structure of this thesis and its contributions are presented in the sequel:

Chapter 2 describes the theoretical fundamentals of variable structure systems with sliding modes. Existence and uniqueness of an ideal sliding mode is discussed from two different perspectives: the *Filippov* method and the ‘equivalent control’ approach. The existence problem is studied in detail and two canonical forms employed in this dissertation are presented. Then, the main properties of sliding modes are demonstrated. Next, the reachability problem is dealt with. The structure of the control laws considered in this thesis is given in general form in this chapter. In order to reduce high frequency switching in the control law, due to the discontinuous term, a differentiable approximation of the unit vector structure is presented. The state reconstruction problem using SMOs for systems with matched uncertainties is studied and the form of the SMO considered in this thesis is presented. Finally, some concluding remarks are drawn.

Chapter 3 comprises two parts: The first part presents the LMI methods as the main mathematical tool applied in this thesis, whilst the second part describes the representation of uncertain systems considering polytopic models. LMI methods are formally discussed: this includes a study of the convexity property and different forms of representation of LMIs. A formulation of the standard LMI problems is given.

1.5 Structure of the Thesis and Contributions

The main properties and characteristics of LMIs are studied in this chapter. Finally, parametric uncertainty representations employing polytopic models are described in detail.

The sliding mode control design problem for uncertain plants with both matched and mismatched uncertainty considering full state information is discussed in Chapter 4. A synthesis methodology is proposed for the design of sliding mode controllers for both types of uncertainties. The proposed approach employs robust pole clustering in convex regions of the left-half complex plane using LMI methods and polytopic models for solving both the sliding mode existence and reachability problems. This design methodology is an extension of the approach in (Arzelier *et al.*, 1997). The sliding mode existence problem is formulated as a state feedback problem for the reduced-order system using a polytopic description, considering the mismatched uncertainty affecting the state matrix. The control law is made up of linear and nonlinear components, and their design is not independent, since one of the matrix variables obtained when designing the linear component is part of the nonlinear term. The linear component is synthesised via LMIs and a polytopic description of the system takes into account the mismatched parametric uncertainties. The matched uncertainties, disturbances and/or nonlinearities are rejected completely by means of the nonlinear component. Another feature of the design framework presented in this chapter is its simplicity when compared to the other approaches cited in the earlier literature review. The approach proposed in this chapter has been reported in (Andrade-Da Silva & Edwards, 2010a).

A design approach based on LMIs is presented in Chapter 5 for synthesising SOF and compensator-based sliding mode controllers. This work is an extension of (Edwards & Spurgeon, 2003) where only matched uncertainties were considered. The existence and reaching problems are formulated from a polytopic perspective. The switching surface design problem is recast in terms of LMIs as a static output feedback problem with mismatched uncertainties. Even though several available numerical algorithms can be applied in this chapter, the non-iterative algorithm proposed in (Benton & Smith, 1999) is considered because of its simplicity. The control law consists of linear and nonlinear parts. The problem of synthesising the linear part is solved via LMI methods considering a convex region of the complex left half-plane defined by the designer. The design of the nonlinear component counteracts matched uncertainties, disturbances and/or nonlinearities. The control law proposed in this chapter is different to the high gain control laws presented in the other cited references for SMOF control. In addition, the approach proposed here is less complex. Results regarding the static output feedback approach developed in this chapter have been presented in (Andrade-Da Silva *et al.*, 2008a) and (Andrade-Da Silva *et al.*, 2008b). The sliding mode compensator-based scheme proposed in this chapter appears in (Andrade-Da Silva *et al.*, 2009a). Furthermore, a compressed version of this chapter can be found in (Andrade-Da Silva *et al.*, 2009b).

1.5 Structure of the Thesis and Contributions

Different classes of plants and controllers have been considered in terms of simultaneous stabilisation (Howitt & Luus, 1991). In Chapter 6 variable structure controllers with a sliding mode, using only measured output information, are explored. The plant model belongs to the class of continuous-time systems described in the state-space by a finite set of different state matrices, but common input and output matrices. Static and dynamic sliding mode output feedback control strategies are proposed. The dynamic output feedback is compensator-based. The design methodologies proposed in this chapter consists of two stages. Firstly, the sliding mode existence problem is formulated as a static output feedback problem considering a family of LTI plant models. Then, the algorithm presented in (Cao & Sun, 1998) is re-cast in the context of such an existence problem. Secondly, the reachability problem is formulated using LMIs (Boyd *et al.*, 1994). The synthesis framework proposed in this chapter is an extension of the work on sliding mode static output feedback control presented in (Edwards *et al.*, 2001) which allows only one plant model to be considered. Furthermore, the design methodology differs from the approach in Chapter 4 as the conservatism in the solution of the sliding mode existence problem is reduced by considering a *Lyapunov* matrix for each model, instead of using a common *Lyapunov* matrix for all models. A key feature of the proposed approaches is that it allows the application of sliding mode static or dynamic output feedback control to the problem of stabilisation of a nonlinear plant linearised at several equilibria, uncertain plants with both matched and mismatched uncertainties, fault tolerant control, and plants with several operational modes. This is a useful contribution since most of the existing approaches, *e.g.* (Žak & Hui, 1993) (Heck *et al.*, 1995) (Edwards & Spurgeon, 1995) (Edwards *et al.*, 2001), for designing sliding mode output feedback control systems, are not able to be applied in such contexts. The sliding mode simultaneous stabilisation approaches proposed in this chapter have been presented in (Andrade-Da Silva & Edwards, 2009a) and (Andrade-Da Silva & Edwards, 2009b).

In Chapter 7 a sliding mode observer (SMO) analysis and design framework is proposed for systems with mismatched uncertainties in the state matrix. The stability of the state estimation error system considering mismatched uncertainties is addressed using the concept of uniform ultimate bounded stability (also known as practical stability). The design methodology is based on LMI methods and employs a polytopic description of the mismatched uncertainty for designing the gain matrices of the SMO. The observer gains are obtained by solving an LMI optimisation problem for which powerful computational tools are available, *e.g.* (Gahinet *et al.*, 1995). An important contribution of this work is that mismatched uncertainties are considered when synthesising the gain matrices of the SMO rather than using only the nominal state and output matrices. This feature is of practical interest since real world plants are affected by parametric uncertainties. A compressed version of this chapter appears in (Andrade-Da Silva & Edwards, 2010b).

1.5 Structure of the Thesis and Contributions

Finally, Chapter 8 provides the concluding remarks of this thesis and highlights future research work including potential problems to be studied and possible extensions of the contributions proposed in this dissertation.

"A mathematical theory is not to be considered complete until you have made it so clear that you can explain it to the first man whom you meet in the street"

David Hilbert (1862 - 1943)

2

Variable Structure Systems With Sliding Modes

2.1 Introduction

A Variable Structure System (VSS) is a class of nonlinear system whose structure changes discontinuously based on a decision function called switching function. A Variable Structure Control (VSC) is a nonlinear control scheme consisting of a switched control law and a switching function. The main concepts of VSC are introduced in the sequel by means of a classical example concerning a double integrator system. To this end, consider the system in block diagram form shown in Figure 2.1.

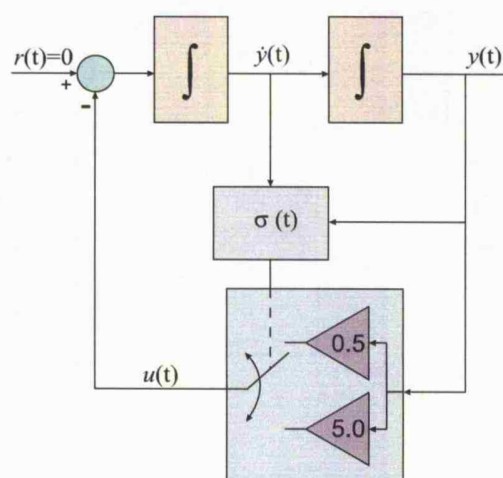


Figure 2.1: Block diagram of a double integrator system under VSC

The control law is of the form

$$u(t) = \begin{cases} -0.5y(t) & \text{if } y(t)\dot{y}(t) < 0 \\ -5y(t) & \text{otherwise} \end{cases} \quad (2.1)$$

Notice that the decision rule which defines how the structure of the system changes is given by $\sigma(t) = y(t)\dot{y}(t)$. This switching function delimits two main regions in the phase plane $(y(t), \dot{y}(t))$ depending on the sign of $\sigma(t)$ as shown in Figure 2.2. The dynamical behaviour of the VSC system is depicted in the phase portrait in Figure 2.3. It is easy to see the effect on the system's trajectory produced by changing the structure of the system.

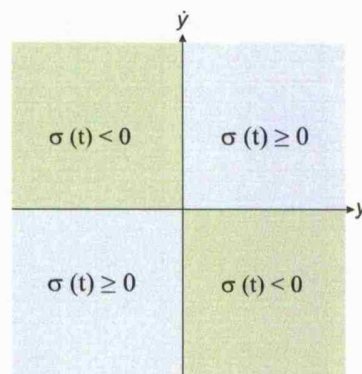


Figure 2.2: Regions of the phase plane defined by the switching function $\sigma(t) = y(t)\dot{y}(t)$

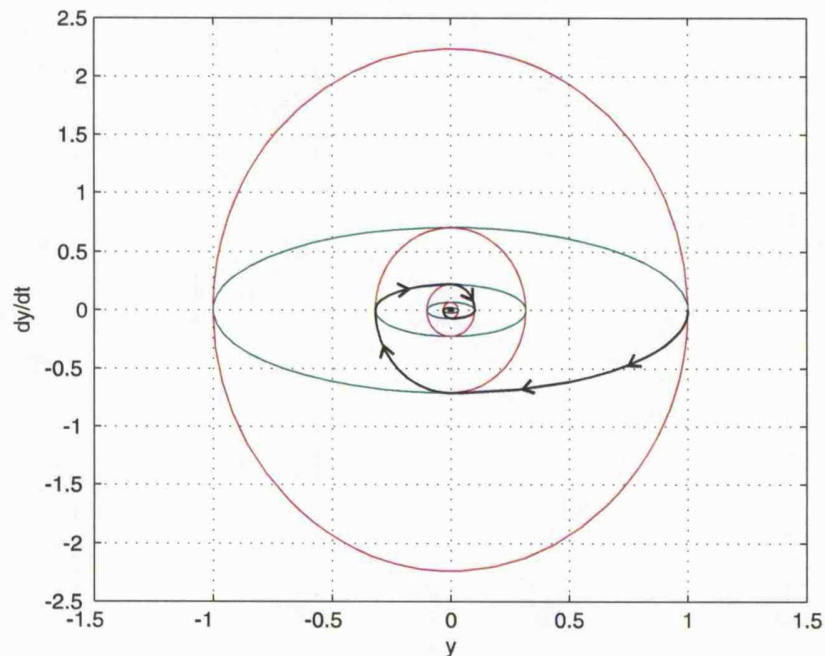


Figure 2.3: Phase portrait of a double integrator system under VSC

2.1 Introduction

Remark 2.1 *Figure 2.3 shows a phase portrait of an asymptotically stable VSC involving two simple harmonic motions (center points plotted in red and green colours).*

SMC is a class of VSC which employs a switched control action across a sliding surface defined through a switching function. SMC theory has aroused interest among researchers due to its robust nature, its ability to decouple high-dimensional systems into a set of lower-dimensional sub-systems, and for its applicability to SISO and MIMO linear and nonlinear systems.

The state trajectory of a system under SMC usually consists of two dynamical modes: the reaching mode and the sliding mode. These modes are also called the sliding phase or the sliding motion, and the reaching phase respectively (Hung *et al.*, 1993) (Edwards & Spurgeon, 1998b).

Consider the uncertain linear time invariant (LTI) system described by

$$\dot{\mathbf{x}}(t) = \mathbf{A}\mathbf{x}(t) + \mathbf{B}\mathbf{u}(t) + \mathbf{D}\mathbf{f}(t, \mathbf{x}, \mathbf{u}) \quad (2.2)$$

where $\mathbf{x} \in \mathfrak{R}^n$ is the state vector, $\mathbf{u} \in \mathfrak{R}^m$ is the input vector, $\mathbf{A} \in \mathfrak{R}^{n \times n}$ is the state matrix, $\mathbf{B} \in \mathfrak{R}^{n \times m}$ is the input distribution matrix, $\mathbf{D} \in \mathfrak{R}^{n \times l}$ is the uncertainty distribution matrix which is known, and the function $\mathbf{f} : \mathfrak{R}_+ \times \mathfrak{R}^n \times \mathfrak{R}^m \rightarrow \mathfrak{R}^l$ represents the lumped sum of nonlinearities and/or uncertainties. This function is unknown but norm bounded.

The *sliding surface* \mathcal{S}_{SF} is defined as follows

$$\mathcal{S}_{SF} = \{ \mathbf{x} \in \mathfrak{R}^n : \boldsymbol{\sigma}(t) = \boldsymbol{\Gamma}\mathbf{x}(t) = \mathbf{0} \} \quad (2.3)$$

where $\boldsymbol{\sigma} \in \mathfrak{R}^m$ is the *switching function* and $\boldsymbol{\Gamma} \in \mathfrak{R}^{m \times n}$ is the *switching gain matrix* to be designed.

Notice that although the sliding surface defined above corresponds to a hyperplane because of the linear switching function, some applications require nonlinear or time-varying switching functions to be constructed (DeCarlo *et al.*, 1988).

Definition 2.1 *Let \mathcal{S}_{SF} be a sliding surface. The system trajectory $\mathbf{x}(t) \in \mathfrak{R}^n$ between an initial point $\mathbf{x}(t_0) = \mathbf{x}_0 \notin \mathcal{S}_{SF}$ and any point $\mathbf{x}(t_\sigma) = \mathbf{x}_\sigma \in \mathcal{S}_{SF}$ such that $t \leq t_\sigma < \infty$ where t_σ is the reaching time, is said to be in the reaching mode.*

The condition which guarantees the system state trajectory is driven towards the sliding surface is the so-called reaching condition.

Definition 2.2 *Let \mathcal{S}_{SF} be a sliding surface. If the system trajectory $\mathbf{x}(t) \in \mathcal{S}_{SF}$ for all $t \geq t_\sigma$, then the system is said to be in an ideal sliding mode.*

Recall the double integrator system, and define the following sliding surface

$$\mathcal{S}_{SF} = \{\mathbf{x} \in \mathbb{R}^n : \sigma(t) = y(t) + \dot{y}(t) = 0\} \quad (2.4)$$

together with the discontinuous control law

$$u(t) = -10\text{sgn}(\sigma(t)) \quad (2.5)$$

where sgn denotes the sign function. The phase portrait of the VSC system with a sliding mode is shown in Figure 2.4. This plot illustrates the reaching and sliding motions of the system when applied to the double integrator system.

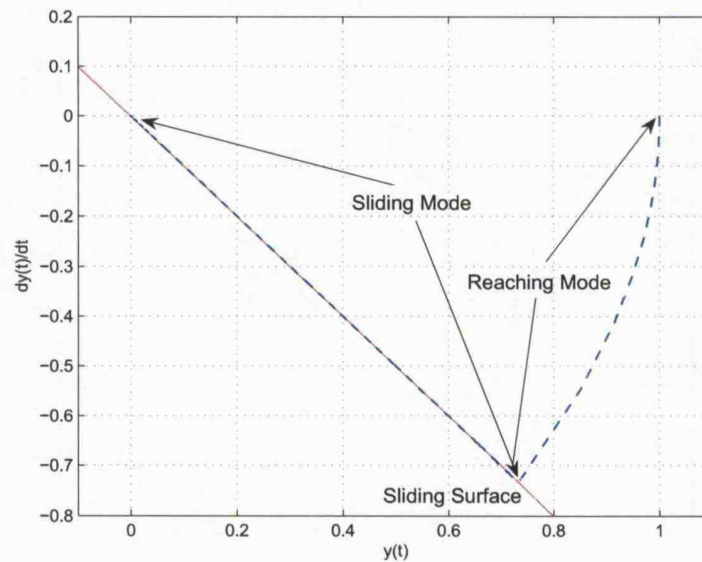


Figure 2.4: Phase portrait of a double integrator system under SMC

Generally speaking there are two main overarching control problems: the stabilisation or regulation problem, and the tracking problem. In an ideal sliding motion, the stabilisation problem consists of driving the states of the system towards an equilibrium point, typically the origin of the state space, whilst constrained to the sliding surface \mathcal{S}_{SF} . For the tracking problem, when in an ideal sliding mode, the system's output signals track a time-varying trajectory called the reference signal, while the system trajectory is restricted to the sliding hyperplane \mathcal{S}_{SF} . The model-reference paradigm belongs to the class of tracking control approaches, whereby the dynamics of the plant follow the dynamics of an ideal reference-model. In (Edwards & Spurgeon, 1998b) a reference-model approach via sliding modes is presented.

The remainder of this chapter is structured as follows: Section 2.2 presents the concept of an ideal sliding mode, and its existence and uniqueness of solution from

2.2 Ideal Sliding Mode Existence and Uniqueness of Solution

two paradigms. *Filippov's* method is built on the theory of differential equations with discontinuous right-hand sides. The other paradigm proposed in (Utkin, 1977) is the equivalent control approach. In Section 2.3, the sliding surface design problem is studied and two useful state space canonical forms are exhaustively described. That is, the regular form (employed in the full state feedback case) and the output feedback canonical form. VSC with sliding modes has several attractive features. The main characteristics are introduced in Section 2.4 including the feature that the reduced-order sliding mode dynamics have an invariance property (the robustness property of SMC). Another noteworthy concept concerned with SMC is the notion of invariant zeros which are related to the eigenvalues of the reduced-order motion governing the sliding dynamics. The reachability problem is stated formally and the existence of a pseudo-sliding mode is studied. The structure of the control law considered throughout this thesis is presented and approaches to create continuous approximations of the control law are also dealt with. An observer based upon sliding mode theory is introduced in Section 2.6. Finally, some concluding remarks are drawn in Section 2.7.

2.2 Ideal Sliding Mode Existence and Uniqueness of Solution

The classical theory of differential equations cannot be applied to VSS since the equation

$$\dot{\mathbf{x}}(t) = \mathbf{F}_{CL}(t, \mathbf{x}) \quad (2.6)$$

which describes the closed-loop dynamical behaviour of the system (2.2), is discontinuous with respect to the state vector $\mathbf{x}(t)$. In this case, the function $\mathbf{F}_{CL} : \mathfrak{R} \times \mathfrak{R}^n \rightarrow \mathfrak{R}^n$ does not satisfy the so-called *Lipschitz* condition

$$\|\mathbf{F}_{CL}(t, \mathbf{x}_1) - \mathbf{F}_{CL}(t, \mathbf{x}_2)\| \leq L\|\mathbf{x}_1 - \mathbf{x}_2\| \quad (2.7)$$

where L is the *Lipschitz* constant (Michel & Herget, 1981b). The function $\mathbf{F}_{CL}(t, \mathbf{x})$ in (2.6) is said to be non-analytic (Marsden, 1974) (Utkin, 1992). This means that $\mathbf{F}_{CL}(t, \mathbf{x})$ is not defined at the discontinuity points, and hence the uniqueness of the solution of is not guaranteed at that point.

The right-hand side of (2.6) can be classified as follows (Hung *et al.*, 1993):

1. Relay type discontinuity: $\mathbf{F}_{CL}(t, \mathbf{x})$ is a finite non-analytical function.
2. Relay type discontinuity with hysteresis: $\mathbf{F}_{CL}(t, \mathbf{x})$ is a double-valued non-analytical function.

2.2 Ideal Sliding Mode Existence and Uniqueness of Solution

The theory proposed in (Filippov, 1964) allows a solution for (2.6) to be calculated as the ‘average’ of the solutions obtained when the discontinuity point is approached from different directions.

The sliding surface \mathcal{S}_F divides the state space \mathcal{X} into two domains: \mathcal{S}^+ and \mathcal{S}^- . The closed-loop dynamics defined in (2.6) exhibit two structures:

$$\mathbf{F}_{CL}(t, \mathbf{x}) = \begin{cases} \mathbf{F}^+(t, \mathbf{x}) & \text{if } \mathbf{x} \in \mathcal{S}^+ \\ \mathbf{F}^-(t, \mathbf{x}) & \text{if } \mathbf{x} \in \mathcal{S}^- \end{cases} \quad (2.8)$$

Let $\mathbf{x}_\sigma \in \mathcal{S}_F$ be a point of discontinuity. Furthermore, let $\mathbf{F}^+(t, \mathbf{x}_\sigma)$ and $\mathbf{F}^-(t, \mathbf{x}_\sigma)$ be defined as follows

$$\mathbf{F}^+(t, \mathbf{x}_\sigma) = \lim_{\substack{\mathbf{x} \in \mathcal{S}^+ \\ \mathbf{x} \rightarrow \mathbf{x}_\sigma}} \mathbf{F}(t, \mathbf{x}) \quad (2.9)$$

and

$$\mathbf{F}^-(t, \mathbf{x}_\sigma) = \lim_{\substack{\mathbf{x} \in \mathcal{S}^- \\ \mathbf{x} \rightarrow \mathbf{x}_\sigma}} \mathbf{F}(t, \mathbf{x}) \quad (2.10)$$

The Filippov’s solution is obtained from

$$\dot{\mathbf{x}}(t) = \mu \mathbf{F}^+(t, \mathbf{x}_\sigma) + (1 - \mu) \mathbf{F}^-(t, \mathbf{x}_\sigma) \quad (2.11)$$

where the scalar $0 \leq \mu \leq 1$ is such that the vector

$$\mathbf{F}_{av}(t, \mathbf{x}_\sigma) \triangleq \mu \mathbf{F}^+(t, \mathbf{x}_\sigma) + (1 - \mu) \mathbf{F}^-(t, \mathbf{x}_\sigma) \quad (2.12)$$

is tangential to the sliding surface \mathcal{S}_F . Figure 2.5 depicts the construction of the Filippov’s solution.

The equivalent control approach, proposed in (Utkin, 1977), is another method for describing the dynamics of a VSS with a sliding mode. The equivalent control law, if it exists, guarantees an ideal sliding mode on \mathcal{S}_F . In order to define the notion of equivalent control, consider the uncertain system given in (2.2). Furthermore, assume that the uncertain term $\mathbf{f}(t, \mathbf{x}, \mathbf{u})$ in (2.2) is completely neglected, and the system trajectory is in a sliding mode, *i.e.* $\sigma(t) = \Gamma \mathbf{x}(t) = \mathbf{0}$. Differentiating $\sigma(t)$ with respect to time yields

$$\dot{\sigma} = \Gamma(\mathbf{A}\mathbf{x}(t) + \mathbf{B}\mathbf{u}(t)) = \mathbf{0} \quad \text{for } t \geq t_\sigma \quad (2.13)$$

then, it follows from (2.13) that the equivalent control law is straightforwardly calculated as

$$\mathbf{u}_{EQ}(t) = -(\Gamma \mathbf{B})^{-1} \Gamma \mathbf{A} \mathbf{x}(t) \quad (2.14)$$

which corresponds to the unique solution to the algebraic equation (2.13) by setting $\dot{\sigma}(t) = 0$. The uniqueness of this solution requires the matrix $(\Gamma\mathbf{B})$ to be nonsingular, or from a geometrical viewpoint that the null sub-space of Γ and the range sub-space of \mathbf{B} (denoted by $\mathcal{N}(\Gamma)$ and $\mathcal{R}(\mathbf{B})$ (Michel & Herget, 1981b)), are complementary, *i.e.* $\mathcal{N}(\Gamma) \cap \mathcal{R}(\mathbf{B}) = \{0\}$, (El-Ghezawi *et al.*, 1983) (Dorling & Zinober, 1986).

The dynamics of the ideal sliding mode are given by

$$\dot{\mathbf{x}}(t) = \mathbf{A}_{EQ}\mathbf{x}(t) = (\mathbf{I}_n - \mathbf{B}(\Gamma\mathbf{B})^{-1}\Gamma)\mathbf{A}\mathbf{x}(t) \quad (2.15)$$

by substituting for (2.14) in (2.2) supposing $\mathbf{f}(t, \mathbf{x}, \mathbf{u}) = \mathbf{0}$. This assumption is completely valid when the uncertainty under consideration is matched as will be demonstrated later in the sub-section on sliding mode properties. Notice that the closed-loop dynamics depend on the switching matrix Γ , which is synthesised by the designer beforehand based upon design specifications. Furthermore, the dynamics do not appear to be directly influenced by the control action.

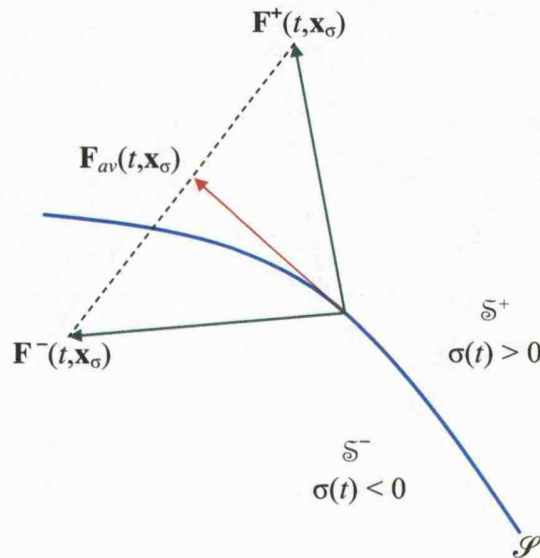


Figure 2.5: Construction of Filippov's solution $\mathbf{F}_{av}(t, \mathbf{x}_\sigma)$

2.3 Sliding Surface Design Problem

The problem of synthesising a sliding surface can be posed either as a state feedback or an output feedback problem depending on the availability of measurable state variables. Two canonical forms are appealing for this purpose. Namely, the regular form presented by Utkin in one of his seminal works on sliding mode control (Utkin,

2.3 Sliding Surface Design Problem

1977), and the output feedback canonical form proposed in (Edwards & Spurgeon, 1995). The following two sections describe both canonical forms.

2.3.1 The Regular Form Approach

Consider the dynamical system described in state-space form $\forall t \geq 0$ given in (2.2), assuming that the uncertain term $\mathbf{f}(t, \mathbf{x}, \mathbf{u})$ is equal to zero, *i.e.*,

$$\dot{\mathbf{x}}(t) = \mathbf{A}\mathbf{x}(t) + \mathbf{B}\mathbf{u}(t) \quad (2.16)$$

and the sliding surface is defined in (2.3).

The following assumptions are made:

- A-2.1** All state variables are measurable.
- A-2.2** The input matrix is full rank, *i.e.* $\text{rank}(\mathbf{B}) = m$.
- A-2.3** The nominal pair (\mathbf{A}, \mathbf{B}) is controllable.
- A-2.4** The matrix $(\mathbf{\Gamma}\mathbf{B})$ is nonsingular.

From postulate **A-2.2**, there exists an orthogonal matrix $\mathbf{T}_R \in \mathfrak{R}^{n \times n}$ such that

$$\mathbf{T}_R \mathbf{B} = \begin{bmatrix} \mathbf{0} \\ \tilde{\mathbf{B}}_2 \end{bmatrix} \quad (2.17)$$

where $\tilde{\mathbf{B}}_2 \in \mathfrak{R}^{m \times m}$ is nonsingular.

Remark 2.2 Although the Gaussian elimination method can be applied to find the transformation matrix \mathbf{T}_R , QR decomposition is more appealing from a computational viewpoint as an orthogonal matrix \mathbf{T}_R is obtained. This allows the inverse of \mathbf{T}_R to be straightforwardly computed by transposition.

Using the similarity transformation $\mathbf{x}(t) \mapsto \mathbf{T}_R \mathbf{x}(t) = \tilde{\mathbf{x}}(t)$, the system pair (\mathbf{A}, \mathbf{B}) in (2.16) can be written in the so-called regular form (Utkin, 1977):

$$\tilde{\mathbf{A}} = \begin{bmatrix} \tilde{\mathbf{A}}_{11} & \tilde{\mathbf{A}}_{12} \\ \tilde{\mathbf{A}}_{21} & \tilde{\mathbf{A}}_{22} \end{bmatrix} \quad \tilde{\mathbf{B}} = \begin{bmatrix} \mathbf{0} \\ \tilde{\mathbf{B}}_2 \end{bmatrix} \quad (2.18)$$

where $\tilde{\mathbf{A}}_{11} \in \mathfrak{R}^{(n-m) \times (n-m)}$, $\tilde{\mathbf{A}}_{12} \in \mathfrak{R}^{(n-m) \times m}$, $\tilde{\mathbf{A}}_{21} \in \mathfrak{R}^{m \times (n-m)}$, $\tilde{\mathbf{A}}_{22} \in \mathfrak{R}^{m \times m}$ and $\tilde{\mathbf{B}}_2 \in \mathfrak{R}^{m \times m}$ are known constant matrices. Moreover, the input matrix sub-block $\tilde{\mathbf{B}}_2$ is such that $\det(\tilde{\mathbf{B}}_2) \neq 0$.

2.3 Sliding Surface Design Problem

Thus, the system (2.16) in the regular form is given by

$$\dot{\tilde{\mathbf{x}}}_1(t) = \tilde{\mathbf{A}}_{11}\tilde{\mathbf{x}}_1(t) + \tilde{\mathbf{A}}_{12}\tilde{\mathbf{x}}_2(t) \quad (2.19)$$

$$\dot{\tilde{\mathbf{x}}}_2(t) = \tilde{\mathbf{A}}_{21}\tilde{\mathbf{x}}_1(t) + \tilde{\mathbf{A}}_{22}\tilde{\mathbf{x}}_2(t) + \tilde{\mathbf{B}}_2\mathbf{u}(t) \quad (2.20)$$

where equation (2.19) corresponds to the dynamics associated with the null space $\mathcal{N}(\mathbf{\Gamma})$ whilst (2.20) describes the dynamics of the range space $\mathcal{R}(\mathbf{B})$.

Conformably with the partition in (2.19)-(2.20), let

$$\mathbf{\Gamma}\mathbf{T}_R^T = \begin{bmatrix} \mathbf{\Gamma}_1 & \mathbf{\Gamma}_2 \end{bmatrix} \quad (2.21)$$

where $\mathbf{\Gamma}_1 \in \mathfrak{R}^{m \times (n-m)}$ and $\mathbf{\Gamma}_2 \in \mathfrak{R}^{m \times m}$.

From assumption **A-2.4**, it follows that $\det(\mathbf{\Gamma}\mathbf{B}) \neq 0$, then

$$\det(\mathbf{\Gamma}\mathbf{B}) = \det(\mathbf{\Gamma}\mathbf{T}_R^T\mathbf{T}_R\mathbf{B}) = \det(\mathbf{\Gamma}_2\tilde{\mathbf{B}}_2) = \det(\mathbf{\Gamma}_2)\det(\tilde{\mathbf{B}}_2) \iff \det(\mathbf{\Gamma}_2) \neq 0 \quad (2.22)$$

since $\det(\tilde{\mathbf{B}}) \neq 0$.

The switching function $\sigma(t)$ is identically equal to zero when in the sliding mode (Utkin, 1977):

$$\sigma(t) = \mathbf{\Gamma}_1\tilde{\mathbf{x}}_1(t) + \mathbf{\Gamma}_2\tilde{\mathbf{x}}_2(t) = \mathbf{0} \quad (2.23)$$

and hence

$$\tilde{\mathbf{x}}_2 = -(\mathbf{\Gamma}_2)^{-1}\mathbf{\Gamma}_1\tilde{\mathbf{x}}_1 \quad \forall t \geq t_\sigma \quad (2.24)$$

Define the gain matrix $\mathbf{K}_{SF} \in \mathfrak{R}^{m \times (n-m)}$ as

$$\mathbf{K}_{SF} \triangleq \mathbf{\Gamma}_2^{-1}\mathbf{\Gamma}_1 \quad (2.25)$$

Consequently, the dynamics associated with the null space $\mathcal{N}(\mathbf{\Gamma})$, which describe the sliding mode dynamics, are given by

$$\dot{\tilde{\mathbf{x}}}_1(t) = (\tilde{\mathbf{A}}_{11} - \tilde{\mathbf{A}}_{12}\mathbf{K}_{SF})\tilde{\mathbf{x}}_1(t) \quad (2.26)$$

Remark 2.3 *The matrix $\mathbf{\Gamma}_2$ has no direct effect on the sliding mode dynamics since it represents a scaling term of the switching matrix $\mathbf{\Gamma}$.*

From (2.21) and (2.25) the switching gain matrix $\mathbf{\Gamma}$ can be straightforwardly parameterised as follows (Edwards & Spurgeon, 1998b):

$$\mathbf{\Gamma} = \mathbf{\Gamma}_2 \begin{bmatrix} \mathbf{K}_{SF} & \mathbf{I}_m \end{bmatrix} \mathbf{T}_R \quad (2.27)$$

2.3 Sliding Surface Design Problem

The sliding surface design problem consists of synthesising a gain matrix \mathbf{K}_{sF} such that the reduced-order system (2.26) is stable, and then the switching gain matrix Γ given in (2.27) can be calculated.

Remark 2.4 *The design of the switching gain matrix Γ defined in (2.27) is equivalent to a state feedback problem for the reduced-order system pair $(\tilde{\mathbf{A}}_{11}, \tilde{\mathbf{A}}_{12})$ in which the designer tackles the synthesis requirements associated with the desired dynamics of the sliding mode reduced-order system (2.26).*

The controllability property of the pair $(\tilde{\mathbf{A}}_{11}, \tilde{\mathbf{A}}_{12})$ is required to be able to find a gain matrix \mathbf{K}_{sF} which stabilises the sliding mode dynamics given in (2.26). As asserted in (Edwards & Spurgeon, 1998b), the controllability of the system (2.16) is related to the controllability of the pair $(\tilde{\mathbf{A}}_{11}, \tilde{\mathbf{A}}_{12})$. This equivalence is presented and demonstrated formally in the sequel.

Theorem 2.1 (Edwards & Spurgeon, 1998b): *The matrix pair $(\tilde{\mathbf{A}}_{11}, \tilde{\mathbf{A}}_{12})$ is controllable if and only if the pair (\mathbf{A}, \mathbf{B}) is controllable.*

△

Proof (Edwards & Spurgeon, 1998b): From the controllability of the pair (\mathbf{A}, \mathbf{B}) , it follows the rank condition holds

$$\text{rank} \begin{bmatrix} (s \mathbf{I}_n - \mathbf{A}) & \mathbf{B} \end{bmatrix} = n \quad \forall s \in \mathbb{C} \quad (2.28)$$

Expression (2.28) can be written, using the state and input matrices in the regular form given in (2.18), as

$$\text{rank} \begin{bmatrix} (s \mathbf{I}_{(n-m)} - \tilde{\mathbf{A}}_{11}) & -\tilde{\mathbf{A}}_{12} & 0 \\ -\tilde{\mathbf{A}}_{21} & (s \mathbf{I}_m - \tilde{\mathbf{A}}_{22}) & \tilde{\mathbf{B}}_2 \end{bmatrix} = n \quad \forall s \in \mathbb{C} \quad (2.29)$$

Since by construction $\det(\tilde{\mathbf{B}}_2) \neq 0$ and $\tilde{\mathbf{B}}_2 \in \mathfrak{R}^{m \times m}$, then $\text{rank}(\tilde{\mathbf{B}}_2) = m$. This implies

$$\text{rank} \begin{bmatrix} (s \mathbf{I}_n - \mathbf{A}) & \mathbf{B} \end{bmatrix} = \text{rank} \begin{bmatrix} (s \mathbf{I}_{(n-m)} - \tilde{\mathbf{A}}_{11}) & \tilde{\mathbf{A}}_{12} \end{bmatrix} + m \quad (2.30)$$

for all $s \in \mathbb{C}$. Therefore,

$$\text{rank} \begin{bmatrix} (s \mathbf{I}_n - \mathbf{A}) & \mathbf{B} \end{bmatrix} = n \iff \text{rank} \begin{bmatrix} (s \mathbf{I}_{(n-m)} - \tilde{\mathbf{A}}_{11}) & \tilde{\mathbf{A}}_{12} \end{bmatrix} = n - m \quad (2.31)$$

for all $s \in \mathbb{C}$.

As argued in (Edwards & Spurgeon, 1998b), the controllability equivalence between the (\mathbf{A}, \mathbf{B}) and $(\tilde{\mathbf{A}}_{11}, \tilde{\mathbf{A}}_{12})$ follows from the Popov-Belevitch-Hautus rank test.

Q.E.D.

2.3 Sliding Surface Design Problem

2.3.2 The Output Feedback Canonical Form Approach

The output feedback canonical form (Edwards & Spurgeon, 1995) is an approach for designing sliding surfaces when only a subset of the state variables of the system are measurable. This canonical form is based on a similarity transformation in which the last p state variables correspond to the output signals of the system. Then, the sliding surface design problem is formulated as a static output feedback problem.

Consider a dynamical system described in state-space form $\forall t \geq 0$ by

$$\left. \begin{aligned} \dot{\mathbf{x}}(t) &= \mathbf{A}\mathbf{x}(t) + \mathbf{B}\mathbf{u}(t) \\ \mathbf{y}(t) &= \mathbf{C}\mathbf{x}(t) \end{aligned} \right\} \quad (2.32)$$

where $\mathbf{x} \in \mathbb{R}^n$, $\mathbf{u} \in \mathbb{R}^m$ and $\mathbf{y} \in \mathbb{R}^p$.

In the output feedback case, the sliding surface is denoted by \mathcal{S}_{OF} and defined as follows

$$\mathcal{S}_{OF} = \{ \mathbf{x} \in \mathbb{R}^n : \sigma(t) = \Gamma\mathbf{C}\mathbf{x}(t) = \Gamma\mathbf{y}(t) = \mathbf{0} \} \quad (2.33)$$

where $\sigma \in \mathbb{R}^m$ and $\Gamma \in \mathbb{R}^{m \times p}$.

The following are assumed:

A-2.5 The order of the system and the number of output and input signals satisfy $n > p > m$.

A-2.6 The input and output matrices are both full rank, *i.e.* $\text{rank}(\mathbf{B}) = m$ and $\text{rank}(\mathbf{C}) = p$.

A-2.7 In the nominal triple $(\mathbf{A}, \mathbf{B}, \mathbf{C})$, $\text{rank}(\mathbf{CB}) = m$.

Since $\text{rank}(\mathbf{CB}) = m$, there exists a similarity transformation $\mathbf{x} \mapsto \mathbf{T}_C\mathbf{x} = \tilde{\mathbf{x}}$ where $\mathbf{T}_C \in \mathbb{R}^{n \times n}$ has the form

$$\mathbf{T}_C = \begin{bmatrix} \mathbf{N}_C^T \\ \mathbf{C} \end{bmatrix} \quad (2.34)$$

in which $\mathbf{N}_C \in \mathbb{R}^{n \times (n-p)}$ and the columns span the sub-space $\mathcal{N}(\mathbf{C})$.

In the new coordinate system, the output and input distribution matrices \mathbf{C} and \mathbf{B} are transformed into

$$\tilde{\mathbf{C}} = \mathbf{C}\mathbf{T}_C^{-1} = \begin{bmatrix} \mathbf{0} & \mathbf{I}_p \end{bmatrix} \quad (2.35)$$

2.3 Sliding Surface Design Problem

and

$$\tilde{\mathbf{B}} = \mathbf{T}_C \mathbf{B} = \begin{bmatrix} \tilde{\mathbf{B}}_{C_1} \\ \tilde{\mathbf{B}}_{C_2} \end{bmatrix} \quad (2.36)$$

where $\tilde{\mathbf{B}}_{C_1} \in \mathfrak{R}^{(n-p) \times m}$ and $\tilde{\mathbf{B}}_{C_2} \in \mathfrak{R}^{p \times m}$.

From (2.35) and (2.36), it follows that $\tilde{\mathbf{C}}\tilde{\mathbf{B}} = \tilde{\mathbf{B}}_{C_2}$ and $\text{rank}(\tilde{\mathbf{B}}_{C_2}) = m$ because of assumption **A.2-6**. Then, the left pseudo-inverse $\tilde{\mathbf{B}}_{C_2}^{\dagger_L}$ can be defined as

$$\tilde{\mathbf{B}}_{C_2}^{\dagger_L} \triangleq (\tilde{\mathbf{B}}_{C_2}^T \tilde{\mathbf{B}}_{C_2})^{-1} \tilde{\mathbf{B}}_{C_2}^T \quad (2.37)$$

Also, there exists an orthogonal matrix $\mathbf{T} \in \mathfrak{R}^{p \times p}$ such that

$$\mathbf{T}^T \tilde{\mathbf{B}}_{C_2} = \begin{bmatrix} \mathbf{0} \\ \tilde{\mathbf{B}}_2 \end{bmatrix} \quad (2.38)$$

where $\tilde{\mathbf{B}}_2 \in \mathfrak{R}^{m \times m}$ has the property $\det(\tilde{\mathbf{B}}_2) \neq 0$.

The similarity transformation $\tilde{\mathbf{x}} \mapsto \mathbf{T}_B \tilde{\mathbf{x}} = \bar{\mathbf{x}}$ where

$$\mathbf{T}_B = \begin{bmatrix} \mathbf{I}_{(n-p)} & -\tilde{\mathbf{B}}_{C_1} \tilde{\mathbf{B}}_{C_2}^{\dagger_L} \\ \mathbf{0} & \mathbf{T}^T \end{bmatrix} \quad (2.39)$$

brings the triple $(\tilde{\mathbf{A}}, \tilde{\mathbf{B}}, \tilde{\mathbf{C}})$ into the output feedback canonical form (Edwards & Spurgeon, 1995):

$$\bar{\mathbf{A}} = \begin{bmatrix} \bar{\mathbf{A}}_{11} & \bar{\mathbf{A}}_{12} \\ \bar{\mathbf{A}}_{21} & \bar{\mathbf{A}}_{22} \end{bmatrix} \quad \bar{\mathbf{B}} = \begin{bmatrix} \mathbf{0} \\ \bar{\mathbf{B}}_2 \end{bmatrix} \quad \bar{\mathbf{C}} = \begin{bmatrix} \mathbf{0} & \mathbf{T} \end{bmatrix} \quad (2.40)$$

where $\bar{\mathbf{A}}_{11} \in \mathfrak{R}^{(n-m) \times (n-m)}$, $\bar{\mathbf{A}}_{12} \in \mathfrak{R}^{(n-m) \times m}$, $\bar{\mathbf{A}}_{21} \in \mathfrak{R}^{m \times (n-m)}$ and $\bar{\mathbf{A}}_{22} \in \mathfrak{R}^{m \times m}$. The state vector $\bar{\mathbf{x}}$ is partitioned conformably with (2.40) as follows

$$\bar{\mathbf{x}}(t) = \begin{bmatrix} \bar{\mathbf{x}}_1(t) \\ \bar{\mathbf{x}}_2(t) \end{bmatrix} \quad (2.41)$$

Let

$$\mathbf{\Gamma} \mathbf{T} = \begin{bmatrix} \mathbf{\Gamma}_1 & \mathbf{\Gamma}_2 \end{bmatrix} \quad (2.42)$$

where $\mathbf{\Gamma}_1 \in \mathfrak{R}^{m \times (p-m)}$, $\mathbf{\Gamma}_2 \in \mathfrak{R}^{m \times m}$ and $\det(\mathbf{\Gamma}_2) \neq 0$.

2.4 Properties of Sliding Mode Control

Define $\mathbf{C}_1 \in \mathfrak{R}^{(p-m) \times (n-m)}$ as

$$\mathbf{C}_1 \triangleq \begin{bmatrix} \mathbf{0}_{(p-m) \times (n-p)} & \mathbf{I}_{(p-m)} \end{bmatrix} \quad (2.43)$$

and the gain $\mathbf{K}_{OF} \in \mathfrak{R}^{m \times (p-m)}$ as

$$\mathbf{K}_{OF} \triangleq \mathbf{\Gamma}_2^{-1} \mathbf{\Gamma}_1 \quad (2.44)$$

During the sliding mode the switching function $\sigma(t)$ is identically equal to zero and hence $\dot{\bar{\mathbf{x}}}_2(t) = -\mathbf{K}_{OF} \mathbf{C}_1 \bar{\mathbf{x}}_1(t)$. Moreover, the null space dynamics satisfy

$$\dot{\bar{\mathbf{x}}}_1(t) = \bar{\mathbf{A}}_{11} \bar{\mathbf{x}}_1(t) + \bar{\mathbf{A}}_{12} \bar{\mathbf{x}}_2(t) \quad (2.45)$$

it follows that

$$\dot{\bar{\mathbf{x}}}_1(t) = (\bar{\mathbf{A}}_{11} - \bar{\mathbf{A}}_{12} \mathbf{K}_{OF} \mathbf{C}_1) \bar{\mathbf{x}}_1(t) \quad (2.46)$$

The reduced-order dynamics (2.46) correspond to an output feedback problem.

From (2.42) and (2.44), as shown in (Edwards & Spurgeon, 1995), the switching gain matrix $\mathbf{\Gamma}$ can be parameterised as follows

$$\mathbf{\Gamma} = \mathbf{\Gamma}_2 \begin{bmatrix} \mathbf{K}_{OF} & \mathbf{I}_m \end{bmatrix} \mathbf{T}^T \quad (2.47)$$

where $\mathbf{\Gamma}_2 \in \mathfrak{R}^{m \times m}$.

Remark 2.5 *The matrix $\mathbf{\Gamma}_2$ represents a scaling of $\mathbf{\Gamma}$. In this thesis, it is assumed that $\mathbf{\Gamma}_2 = \bar{\mathbf{B}}_2^{-1}$ to obtain $\mathbf{\Gamma} \bar{\mathbf{C}} \bar{\mathbf{B}} = \mathbf{I}_m$.*

The sliding mode output feedback existence problem consists of finding a gain matrix \mathbf{K}_{OF} in such a way that (2.46) is stable and hence the switching gain matrix $\mathbf{\Gamma}$ defined in (2.47) can be straightforwardly synthesised.

2.4 Properties of Sliding Mode Control

Fundamental linear algebra notions (Michel & Herget, 1981a) (Cullen, 1990) and the theory of projectors (El-Ghezawi *et al.*, 1983) are used to describe the properties of variable structure systems with a sliding mode.

The following lemma will be useful when demonstrating that the dynamics of the sliding motion are governed by a reduced-order system.

2.4 Properties of Sliding Mode Control

Lemma 2.1 (Bernstein, 2005): *Let $\mathbf{M}_1 \in \mathfrak{R}^{n \times m}$ and $\mathbf{M}_2 \in \mathfrak{R}^{m \times l}$. Then,*

$$\text{rank}(\mathbf{M}_1 \mathbf{M}_2) = \text{rank}(\mathbf{M}_1) \quad (2.48)$$

if and only if

$$\mathcal{R}(\mathbf{M}_1 \mathbf{M}_2) = \mathcal{R}(\mathbf{M}_1) \quad (2.49)$$

△

Proof See (Bernstein, 2005).

Proposition 2.1 (El-Ghezawi *et al.*, 1983) (Edwards & Spurgeon, 1998b): *The dynamics of the ideal sliding mode described by*

$$\dot{\mathbf{x}}(t) = \underbrace{(\mathbf{I}_n - \mathbf{B}(\mathbf{\Gamma}\mathbf{B})^{-1}\mathbf{\Gamma})}_{\mathbf{A}_{EQ}} \mathbf{A} \mathbf{x}(t) \quad (2.50)$$

correspond to a reduced-order system whose dimension is $n - m$, and the eigenvectors associated with any non-zero eigenvalues of the state matrix \mathbf{A}_{EQ} are contained in the null space of the switching gain matrix $\mathbf{\Gamma}$.

△

Proof By defining

$$\mathcal{P}_1 \triangleq \mathbf{B}(\mathbf{\Gamma}\mathbf{B})^{-1}\mathbf{\Gamma} \quad (2.51)$$

it is straightforward to verify that $\mathcal{P}_1^2 = \mathcal{P}_1$, *i.e.* \mathcal{P}_1 is idempotent, and hence \mathcal{P}_1 is a projector.

Since by assumption $\text{rank}(\mathbf{B}) = m$ and $\text{rank}(\mathbf{\Gamma}\mathbf{B}) = m$, it follows $\text{rank}((\mathbf{\Gamma}\mathbf{B})^{-1}\mathbf{\Gamma}) = m$. Thus, by applying Lemma 2.1, it follows that

$$\text{rank}(\mathcal{P}_1) = \text{rank}(\mathbf{B}) \quad (2.52)$$

and equivalently

$$\mathcal{R}(\mathcal{P}_1) = \mathcal{R}(\mathbf{B}) \quad (2.53)$$

Therefore, the projector \mathcal{P}_1 defined above, projects the space \mathfrak{R}^n on the range sub-space $\mathcal{R}(\mathbf{B})$ along the null sub-space $\mathcal{N}(\mathbf{\Gamma})$.

As before, since $\text{rank}(\mathbf{B}) = m$ and $\text{rank}(\mathbf{\Gamma}\mathbf{B}) = m$, $\text{rank}(\mathbf{B}(\mathbf{\Gamma}\mathbf{B})^{-1}) = m$. Using similar arguments as above, it follows that

$$\mathcal{N}(\mathcal{P}_1) = \mathcal{N}(\mathbf{\Gamma}) \quad (2.54)$$

2.4 Properties of Sliding Mode Control

Defining

$$\mathcal{P}_2 \triangleq (\mathbf{I}_n - \mathcal{P}_1) \quad (2.55)$$

yields the following projector

$$\mathcal{P}_2 \triangleq \mathbf{I}_n - \mathbf{B}(\mathbf{B}\mathbf{B}^{-1}\mathbf{B} + \mathbf{B}\mathbf{B}^{-1}\mathbf{B})^{-1}\mathbf{B} \quad (2.56)$$

which projects the space \mathfrak{R}^n on the null sub-space $\mathcal{N}(\mathbf{B})$ along $\mathcal{R}(\mathbf{B})$.

Since

$$\mathcal{R}(\mathbf{I}_n - \mathbf{B}(\mathbf{B}\mathbf{B}^{-1}\mathbf{B} + \mathbf{B}\mathbf{B}^{-1}\mathbf{B})^{-1}\mathbf{B}) = \mathcal{N}(\mathbf{B}(\mathbf{B}\mathbf{B}^{-1}\mathbf{B} + \mathbf{B}\mathbf{B}^{-1}\mathbf{B})^{-1}\mathbf{B}) = \mathcal{N}(\mathbf{B}) \quad (2.57)$$

and

$$\text{rank}(\mathbf{I}_n - \mathbf{B}(\mathbf{B}\mathbf{B}^{-1}\mathbf{B} + \mathbf{B}\mathbf{B}^{-1}\mathbf{B})^{-1}\mathbf{B}) = n - \text{rank}(\mathbf{B}(\mathbf{B}\mathbf{B}^{-1}\mathbf{B} + \mathbf{B}\mathbf{B}^{-1}\mathbf{B})^{-1}\mathbf{B}) = n - m \quad (2.58)$$

then the dimension of $\mathcal{N}(\mathbf{B})$ is $n - m$.

Therefore, the system (2.15), in which the projector $\mathcal{P}_2 = \mathbf{I}_n - \mathbf{B}(\mathbf{B}\mathbf{B}^{-1}\mathbf{B} + \mathbf{B}\mathbf{B}^{-1}\mathbf{B})^{-1}\mathbf{B}$ maps the columns of the state matrix \mathbf{A} on the null sub-space $\mathcal{N}(\mathbf{B})$, is of order $n - m$. That is, the dynamics of the sliding motion are described by a reduced-order system.

Let λ_j be a non-zero eigenvalue of $\mathbf{A}_{EQ} \in \mathfrak{R}^{n \times n}$, and let \mathbf{v}_j be the associated eigenvector. From (2.56), the following properties of the projector \mathcal{P}_2 can be verified

$$\mathbf{B}\mathcal{P}_2 = \mathbf{0} \quad (2.59)$$

and

$$\mathbf{B}\mathbf{A}_{EQ} = \mathbf{B}\mathcal{P}_2\mathbf{A} = \mathbf{0} \quad (2.60)$$

Moreover, considering the definition of the j^{th} eigenvector \mathbf{v}_j in terms of its associated eigenvalue λ_j , along with (2.60), yields

$$\mathbf{B}\mathcal{P}_2\mathbf{A}\mathbf{v}_j = \lambda_j\mathbf{B}\mathbf{v}_j = \mathbf{0} \quad (2.61)$$

This implies

$$\mathbf{B}\mathbf{v}_j = \mathbf{0} \quad (2.62)$$

and

$$\mathbf{v}_j \in \mathcal{N}(\mathbf{B}) \quad (2.63)$$

where \mathbf{v}_j denotes the set of eigenvectors of the nonzero eigenvalues. This means that the matrix \mathbf{A}_{EQ} only can have up to $n - m$ nonzero eigenvalues.

Q.E.D.

2.4 Properties of Sliding Mode Control

The sliding mode invariance property has been the key property which attracted attention to variable structure systems with a sliding mode. This characteristic is presented as a proposition and subsequently demonstrated applying projector theory.

Consider the uncertain dynamical system given in (2.2) and the sliding hyperplane

$$\mathcal{S}_{SF} = \{\mathbf{x} \in \mathbb{R}^n : \boldsymbol{\sigma}(t) = \Gamma\mathbf{x}(t) = \mathbf{0}\} \quad (2.64)$$

Proposition 2.2 (Draženović, 1969) (El-Ghezawi *et al.*, 1983): *The ideal sliding motion of the uncertain system given in (2.2) is invariant or, equivalently, insensitive to the uncertainty $\mathbf{f}(t, \mathbf{x}, \mathbf{u})$ if $\mathcal{R}(\mathbf{D}) \subset \mathcal{R}(\mathbf{B})$.*

△

Proof The time derivative of $\boldsymbol{\sigma}(t) = \Gamma\mathbf{x}(t)$ is given by

$$\dot{\boldsymbol{\sigma}}(t) = \Gamma(\mathbf{A}\mathbf{x}(t) + \mathbf{B}\mathbf{u}(t) + \mathbf{D}\mathbf{f}(t, \mathbf{x}, \mathbf{u})) \quad (2.65)$$

Assume the system (2.2) is in a sliding mode, which can be written mathematically as

$$\boldsymbol{\sigma}(t) = \mathbf{0} \quad \text{and} \quad \dot{\boldsymbol{\sigma}}(t) = \mathbf{0} \quad (2.66)$$

Then, the equivalent control law, resulting from (2.65) when considering (2.66) and the premise that $\det(\Gamma\mathbf{B}) \neq 0$, can be written as follows

$$\mathbf{u}_{EQ} = -(\Gamma\mathbf{B})^{-1}\Gamma(\mathbf{A}\mathbf{x}(t) + \mathbf{D}\mathbf{f}(t, \mathbf{x}, \mathbf{u})) \quad (2.67)$$

From the definition of \mathcal{P}_2 in (2.56) and using (2.67) as the control signal in (2.2) yields

$$\dot{\mathbf{x}}(t) = \mathcal{P}_2\mathbf{A}\mathbf{x}(t) + \mathcal{P}_2\mathbf{D}\mathbf{f}(t, \mathbf{x}, \mathbf{u}) \quad (2.68)$$

Assuming $\mathcal{R}(\mathbf{D}) \subset \mathcal{R}(\mathbf{B})$, *i.e.* the uncertainty is matched, then

$$\mathbf{D} = \mathbf{B}\mathbf{M}_D \quad (2.69)$$

where $\mathbf{M}_D \in \mathbb{R}^{m \times l}$ is a matrix constructed by means of elementary column operations.

Since \mathcal{P}_2 is a projector (as demonstrated in the proof of the Proposition 2.1), the following property follows straightforwardly

$$\mathcal{P}_2\mathbf{B} = \mathbf{0} \quad (2.70)$$

Consequently

$$\mathcal{P}_2\mathbf{D} = \mathcal{P}_2\mathbf{B}\mathbf{M}_D = \mathbf{0} \quad (2.71)$$

2.4 Properties of Sliding Mode Control

Therefore, the uncertain system given in (2.2) is invariant, or equivalently insensitive to the uncertain function $\mathbf{f}(t, \mathbf{x}, \mathbf{u})$.

Q.E.D.

In the following proposition and proof, the concept of invariant zeros in the context of VSS with sliding modes is tackled. It is assumed that the state matrix \mathbf{A} and the input distribution matrix \mathbf{B} are in the regular form described in Section 2.3.1. For the sake of simplicity and succinctness of notation, the switching gain matrix $\mathbf{\Gamma}$ in the coordinates of the regular form, defined in (2.21), is written as $\tilde{\mathbf{\Gamma}}$, that is

$$\mathbf{\Gamma} \mathbf{T}_R^T = \begin{bmatrix} \mathbf{\Gamma}_1 & \mathbf{\Gamma}_2 \end{bmatrix} =: \tilde{\mathbf{\Gamma}} \quad (2.72)$$

where $\mathbf{\Gamma}_1 \in \mathfrak{R}^{m \times (n-m)}$ and $\mathbf{\Gamma}_2 \in \mathfrak{R}^{m \times m}$.

Proposition 2.3 (*Edwards & Spurgeon, 1998b*): *The eigenvalues of the sliding motion are the invariant zeros of the system triple $(\tilde{\mathbf{A}}, \tilde{\mathbf{B}}, \tilde{\mathbf{\Gamma}})$.*

△

Proof (*Edwards & Spurgeon, 1998b*): The invariant zeros of $(\tilde{\mathbf{A}}, \tilde{\mathbf{B}}, \tilde{\mathbf{\Gamma}})$ are given by

$$\{s \in \mathbb{C} : \mathcal{R}(s) \text{ loses normal rank}\} \quad (2.73)$$

where $\mathcal{R}(s)$ is the *Rosenbrock's* matrix

$$\mathcal{R}(s) = \begin{bmatrix} (s\mathbf{I}_n - \tilde{\mathbf{A}}) & \tilde{\mathbf{B}} \\ -\tilde{\mathbf{\Gamma}} & \mathbf{0} \end{bmatrix} \quad (2.74)$$

Notice that the system triple $(\tilde{\mathbf{A}}, \tilde{\mathbf{B}}, \tilde{\mathbf{\Gamma}})$ corresponds to a square systems, *i.e.* the number of input and output signals are equal. This means that (2.74) loses rank if and only if $\det(\mathcal{R}(s)) = 0$. Re-writing the matrix (2.74) using the regular form given in (2.18) and the switching matrix $\tilde{\mathbf{\Gamma}}$ partitioned as in (2.72) yields

$$\mathcal{R}(s) = \begin{bmatrix} s\mathbf{I}_{(n-m)} - \tilde{\mathbf{A}}_{11} & -\tilde{\mathbf{A}}_{12} & \mathbf{0} \\ -\tilde{\mathbf{A}}_{21} & s\mathbf{I}_m - \tilde{\mathbf{A}}_{22} & \tilde{\mathbf{B}}_2 \\ -\mathbf{\Gamma}_1 & -\mathbf{\Gamma}_2 & \mathbf{0} \end{bmatrix} \quad (2.75)$$

Since $\det(\tilde{\mathbf{B}}_2) \neq 0$, it follows that

$$\det(\mathcal{R}(s)) = 0 \iff \det \begin{bmatrix} s\mathbf{I}_{(n-m)} - \tilde{\mathbf{A}}_{11} & -\tilde{\mathbf{A}}_{12} \\ -\mathbf{\Gamma}_1 & -\mathbf{\Gamma}_2 \end{bmatrix} = 0 \quad (2.76)$$

2.5 Variable Structure Control Laws

The matrix in the right-hand side of the statement (2.76) accepts the following factorization because, as shown in (2.22), $\det(\Gamma_2) \neq 0$:

$$\begin{bmatrix} s\mathbf{I}_{(n-m)} - \tilde{\mathbf{A}}_{11} & -\tilde{\mathbf{A}}_{12} \\ -\Gamma_1 & -\Gamma_2 \end{bmatrix} = \begin{bmatrix} \mathbf{I}_{(n-m)} & \tilde{\mathbf{A}}_{12}\Gamma_2^{-1} \\ \mathbf{0} & \mathbf{I}_m \end{bmatrix} \begin{bmatrix} s\mathbf{I}_{(n-m)} - \tilde{\mathbf{A}}_{11\sigma} & \mathbf{0} \\ \mathbf{0} & -\Gamma_2 \end{bmatrix} \begin{bmatrix} \mathbf{I}_{(n-m)} & \mathbf{0} \\ \mathbf{K}_{SF} & \mathbf{I}_m \end{bmatrix} \quad (2.77)$$

where \mathbf{K}_{SF} is defined in (2.25) and $\tilde{\mathbf{A}}_{11\sigma} \triangleq \tilde{\mathbf{A}}_{11} - \tilde{\mathbf{A}}_{12}\mathbf{K}_{SF}$. Note that the inner and outer matrices in (2.77) have determinant equal to unity and only one matrix among these matrices depends on s , hence

$$\det \begin{bmatrix} s\mathbf{I}_{(n-m)} - \tilde{\mathbf{A}}_{11} & -\tilde{\mathbf{A}}_{12} \\ -\Gamma_1 & -\Gamma_2 \end{bmatrix} = \det \begin{bmatrix} s\mathbf{I}_{(n-m)} - \tilde{\mathbf{A}}_{11\sigma} & \mathbf{0} \\ \mathbf{0} & -\Gamma_2 \end{bmatrix} \quad (2.78)$$

$$= \det(s\mathbf{I}_{(n-m)} - \tilde{\mathbf{A}}_{11\sigma}) \det(-\Gamma_2) \quad (2.79)$$

From (2.22), it follows that

$$\det(\mathcal{R}(s)) = 0 \iff \det(s\mathbf{I}_{(n-m)} - \tilde{\mathbf{A}}_{11\sigma}) = 0 \quad (2.80)$$

which means that the eigenvalues of $\tilde{\mathbf{A}}_{11\sigma}$ are the invariant zeros of the system triple $(\tilde{\mathbf{A}}, \tilde{\mathbf{B}}, \tilde{\mathbf{\Gamma}})$.

Q.E.D.

2.5 Variable Structure Control Laws

2.5.1 The Reachability Problem

The reachability problem is related to the sufficient conditions which guarantee the sliding surface

$$\mathcal{S} = \{ \mathbf{x} \in \mathbb{R}^n : \sigma(t) = \mathbf{0}, \sigma \in \mathbb{R}^m \} \quad (2.81)$$

is reached from any arbitrary initial point $\mathbf{x}_0 = \mathbf{x}(t_0) \notin \mathcal{S}$ in the state space \mathcal{X} . Therefore, a control law has to be designed such that the system trajectories are driven to the sliding surface and remain on the surface thereafter.

The reachability conditions can be classified in terms of the domain of attraction and the reaching time t_σ . Thus, there are local and global reachability conditions. The reaching conditions most frequently found in the literature are: the direct switching function condition (Emel'yanov, 1967) (Utkin, 1977) (Utkin & Yang, 1986), the *Lya-punov* function condition (Itkis, 1976), the η - reachability condition (Slotine & Li, 1991), and the reaching law condition (Hung *et al.*, 1993).

2.5 Variable Structure Control Laws

Let $\Omega_{\mathcal{S}} \subset \mathfrak{R}^n$ be a domain containing the origin of the state space $\mathcal{X} \subseteq \mathfrak{R}^n$. A local reachability condition presented in (Utkin, 1977) (Hung *et al.*, 1993) is given by

$$\lim_{\sigma_j \rightarrow 0^+} \dot{\sigma}_j < 0 \quad \text{and} \quad \lim_{\sigma_j \rightarrow 0^-} \dot{\sigma}_j > 0 \quad \text{for } j \in I(1, m) \quad (2.82)$$

where $\dot{\sigma}_j$ denotes the time derivative of the j -th component of the vector $\sigma \in \mathfrak{R}^m$, and $I(1, m)$ is the index set given by $I(1, m) = \{1, 2, \dots, m\}$.

For this condition, as stated in (Edwards & Spurgeon, 1998b), the sliding surface is the set

$$\mathcal{S} = \mathcal{S} \cap \Omega_{\mathcal{S}} = \{\mathbf{x} \in \Omega_{\mathcal{S}} : \sigma(t) = \mathbf{0}\} \quad (2.83)$$

The global counterparts of the condition (2.82), *i.e.* when $\Omega_{\mathcal{S}} = \mathfrak{R}^n$, were presented in (Emel'yanov, 1967) and (Itkis, 1976). These conditions are defined as

$$\dot{\sigma}_j \sigma_j < 0 \quad \text{for } j \in I(1, m) \quad (2.84)$$

and the *Lyapunov* function based reachability condition

$$\dot{V}(t) < 0 \quad \text{when } \sigma(t) \neq \mathbf{0} \quad (2.85)$$

where

$$V(t) = \sigma^T(t)\sigma(t) > 0 \quad (2.86)$$

The main drawback of the reachability conditions defined above is that there is no guarantee the sliding surface will be reached in finite time. In order to overcome this disadvantage the following conditions have been proposed. In (Hung *et al.*, 1993), condition (2.85) is rewritten as

$$\dot{V}(t) < -\epsilon_{\sigma} \quad \text{when } \sigma(t) \neq \mathbf{0} \quad (2.87)$$

where ϵ_{σ} is a positive scalar. The η -reachability condition (Slotine & Li, 1991) is given by

$$\frac{1}{2} \frac{d}{dt} \sigma_j^2 \leq -\eta_j |\sigma_j| \quad \text{with } \eta_j > 0 \quad \text{for } j \in I(1, m) \quad (2.88)$$

2.5.2 Existence of a Pseudo-Sliding Mode

In the non-ideal sliding mode (also referred as pseudo-sliding) the states are forced to lie arbitrarily close to the sliding surface \mathcal{S} , instead of on the surface (Edwards & Spurgeon, 1998b).

Definition 2.3 Let ϵ and δ be positive scalars such that for any ϵ there exists a δ determining a sliding mode domain $\mathcal{D}_\mathcal{S} \subset \mathcal{S}$. Thus, any motion starting in a δ -neighbourhood of $\mathcal{D}_\mathcal{S}$ may leave an ϵ -neighbourhood of $\mathcal{D}_\mathcal{S}$ only through such an ϵ -neighbourhood of the boundary of $\mathcal{D}_\mathcal{S}$.

Figure 2.6 illustrates graphically the definition of the sliding domain $\mathcal{D}_\mathcal{S} \subset \mathcal{S}$ presented above.

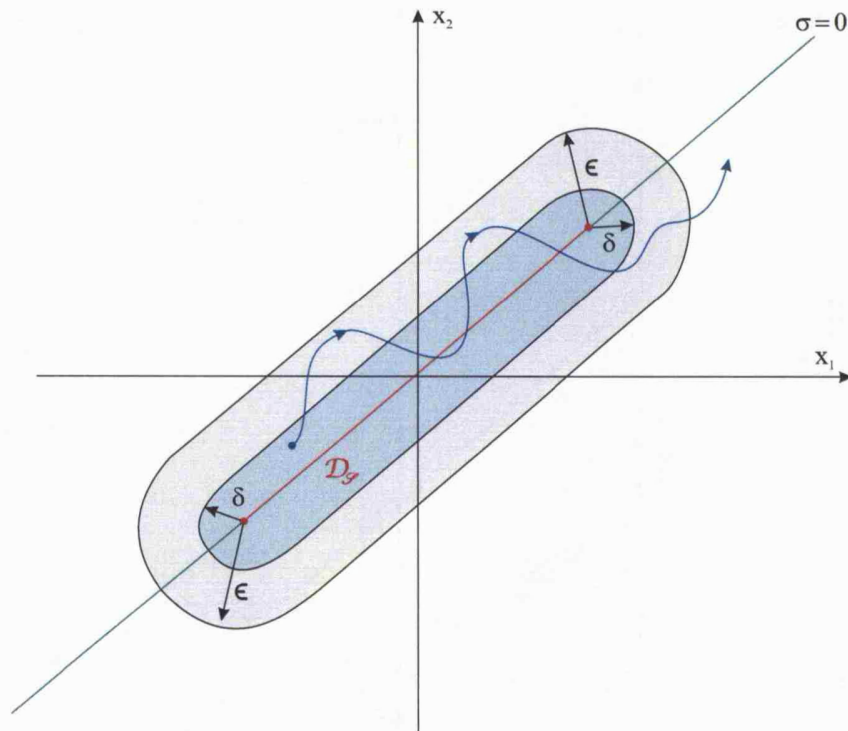


Figure 2.6: A practical sliding motion (adapted from (Edwards & Spurgeon, 1998a))

Lyapunov theory is applied to establish sufficient conditions for the existence of a non-ideal sliding mode. The following theorem establish such conditions (Utkin, 1992). This result is directly related with the continuous approximation of the discontinuous control law presented later in this chapter.

Theorem 2.2 (Utkin, 1992): Let Ω be some region contained in \mathbb{R}^n such that $\mathcal{D}_\mathcal{S} \subset \Omega$. If there exists a continuously differentiable scalar function $V : \mathbb{R}_+ \times \Omega \times \mathbb{R}^m \rightarrow \mathbb{R}$ satisfying the following conditions:

1. $V(t, \mathbf{x}, \boldsymbol{\sigma}) > 0$ if $\boldsymbol{\sigma} \neq \mathbf{0} \quad \forall \mathbf{x} \in \Omega$. Moreover, on the spheres $\|\boldsymbol{\sigma}\| = r_\sigma \quad \forall \mathbf{x} \in \Omega$

$$(a) \quad \inf_{\|\boldsymbol{\sigma}\|=r_\sigma} V(t, \mathbf{x}, \boldsymbol{\sigma}) = h_{r_\sigma} \text{ and } h_{r_\sigma} > 0 \text{ for } r_\sigma \neq 0$$

2.5 Variable Structure Control Laws

$$(b) \sup_{\|\sigma\|=r_\sigma} V(t, \mathbf{x}, \sigma) = H_{r_\sigma} > 0 \quad \text{and} \quad \lim_{r_\sigma \rightarrow 0} H_{r_\sigma} = 0$$

where h_{r_σ} and H_{r_σ} depend on r_σ .

2. The total time derivative of $V(t, \mathbf{x}, \sigma)$ has a negative supremum $\forall \mathbf{x} \in \Omega$ exempting those points on the sliding surface where the control signal may be not defined, and consequently $\dot{V}(t, \mathbf{x}, \sigma)$ does not exist.

Then, $\mathcal{D}_\mathcal{S}$ is said to be a sliding mode domain.

△

Proof A detailed proof and remarks of the theorem above can be found in (Utkin, 1992) pages 47-49. Also in (Utkin, 1978) pages 83-86.

2.5.3 Structure of the Control Law

Several forms of variable structure control laws can be found in the literature, *e.g.* switching scheme based control laws, relay control laws, unit vector control laws, and so on (Hung *et al.*, 1993) (Edwards & Spurgeon, 1998b). Many of the variable structure control laws consist of two components: a linear term with either a state or output feedback gain, and a discontinuous component. The control laws considered in this thesis have the form

$$\mathbf{u}(t) = \mathbf{u}_L(t) + \mathbf{u}_{NL}(t) \quad (2.89)$$

The linear component $\mathbf{u}_L(t)$ is of the form

$$\mathbf{u}_L(t) = -\mathbf{G}\mathbf{z}(t) \quad (2.90)$$

where $\mathbf{z}(t)$ is either the state vector $\mathbf{x}(t)$ or the output vector $\mathbf{y}(t)$ in the case of state or output feedback SMC respectively. The nonlinear term is given by

$$\mathbf{u}_{NL}(t) = \begin{cases} -\rho(\cdot)\Lambda^{-1} \frac{\Xi\sigma(t)}{\|\Xi\sigma(t)\|} & \text{if } \Xi\sigma(t) \neq \mathbf{0} \\ \mathbf{0} & \text{otherwise} \end{cases} \quad (2.91)$$

where $\rho(t, \mathbf{z}(t), \mathbf{u}(t))$ is a positive scalar function to be designed based on the norm bounded matched uncertainty, Λ and Ξ are appropriately dimensioned matrices to be designed which depend on the problem addressed, and $\sigma(t)$ is the switching function.

2.5.4 Continuous Approximation of the Control Law

The discontinuous term (2.91) produces finite high-frequency switching which induces an oscillatory behaviour in the trajectory of the system along the sliding surface. This phenomenon is the so-called chattering. In the case of an ideal sliding mode, the switching action would be infinitely fast (DeCarlo *et al.*, 1988). High frequency switching in the control law is undesirable because it may excite the unmodelled dynamics of the system, and also it can affect the useful life time of the plant's actuators and other components. It is argued in (Utkin, 1993) that chattering implies inaccurate control, high heat losses in electrical power systems and high wear of moving mechanical elements. A decrease in chattering or even more its total avoidance, is at the cost of degradation in terms of the invariance property. Therefore, a trade-off between insensitivity and chattering reduction has to be considered when designing a VSC system with a sliding mode. Many efforts have been made to reduce or even avoid chattering. For example: the boundary layer approach (Slotine & Sastry, 1983) (Slotine, 1984) whereby a continuous approximation of the discontinuity is used, the regular form solution (the block control principle) (Drakunov *et al.*, 1990a) (Drakunov *et al.*, 1990b) using a cascade control system with a sliding mode controller in the inner loop, the observer based approach (Bondarev *et al.*, 1985) for generating a sliding mode in an observer loop, and the disturbance rejection approach (Utkin & Shi, 1996)-(Utkin *et al.*, 1999) consisting of an integral sliding mode in an auxiliary control loop. Nevertheless, the most commonly applied approach, especially for relay and unit vector control laws, is to smooth the discontinuous term of the control law. The continuous approximation presented in (Burton & Zinober, 1986) and (Spurgeon & Davies, 1993) is considered in this thesis and is given by

$$\mathbf{u}_{NL}(t) = -\rho(\cdot)\Lambda^{-1} \frac{\Xi\sigma(t)}{\|\Xi\sigma(t)\| + \varepsilon} \quad (2.92)$$

where $\varepsilon \in \mathfrak{R}_+$ is a small constant defined by the designer. The continuous approximation introduced above replaces the discontinuous function signum

$$\text{sgn}(\Xi\sigma(t)) = \frac{\Xi\sigma(t)}{\|\Xi\sigma(t)\|} \quad (2.93)$$

by the sigmoid-like function

$$\nu_\varepsilon = \frac{\Xi\sigma(t)}{\|\Xi\sigma(t)\| + \varepsilon} \quad (2.94)$$

Figure 2.7 shows the signum function and the differentiable approximation given by a sigmoid-like function.

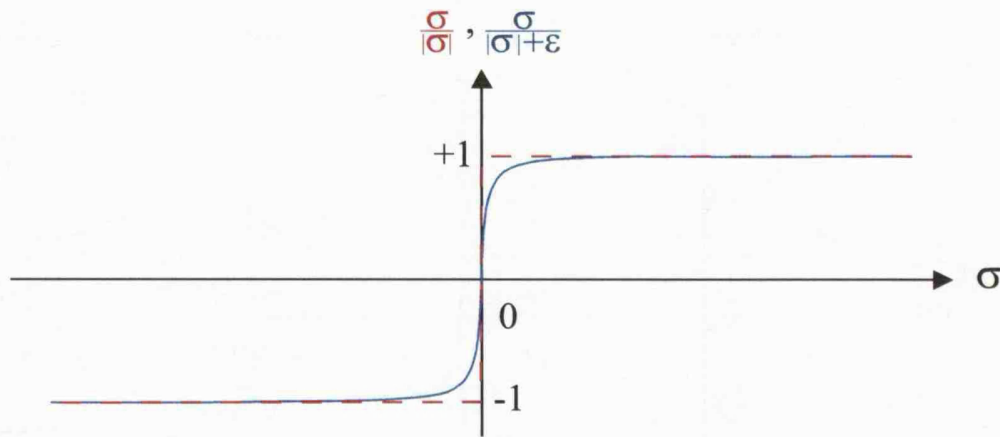


Figure 2.7: Approximation of the signum function by a sigmoid-like function (figure adapted from (Edwards & Spurgeon, 1998b) pages 16 and 62)

The choice of ϵ is a trade-off between performance (namely the invariance property) and the requirement to produce a smooth control signal.

2.6 A Sliding Mode Observer

The problem of state estimation using measurable output and input signals has been studied in the context of the sliding mode theory. The main structural difference between sliding mode and Luenberger observers lies in using discontinuous output error injection vectors. This provides the very distinctive property of insensitivity with regard to a matched type of external disturbance and/or system uncertainty. Thus, sliding mode observers (SMOs) are more robust than the Luenberger counterpart. The discontinuous injection signal, when appropriately synthesised, forces the observer's trajectories to reach in finite time and remain within a particular domain in the error space which defines a sliding surface in terms of the state estimation error. The finite time convergence of the estimation error exhibited by sliding mode observers differs radically from the asymptotic behaviour of the estimation error in other observer schemes. Furthermore, the structural constraint of observability, required in other observer synthesis methodologies, is no longer imposed in some sliding mode observer designs as demonstrated in (Edwards & Spurgeon, 1998b).

Although several forms of sliding mode observer have been proposed (Utkin, 1981) (Walcott & Žak, 1987) (Utkin, 1992), the structure of the observer proposed in (Edwards & Spurgeon, 1994) is adopted in this thesis. The main aspects and arguments for the *Edwards & Spurgeon* observer are introduced succinctly in the sequel. For more details the reader is referred to (Edwards & Spurgeon, 1994) and (Edwards & Spurgeon, 1998b).

2.6 A Sliding Mode Observer

Consider an LTI uncertain dynamical system governed by

$$\left. \begin{aligned} \dot{\mathbf{x}}(t) &= \mathbf{A}\mathbf{x}(t) + \mathbf{B}\mathbf{u}(t) + \mathbf{D}\mathbf{f}(t, \mathbf{x}, \mathbf{u}) \\ \mathbf{y}(t) &= \mathbf{C}\mathbf{x}(t) \end{aligned} \right\} \quad (2.95)$$

where $\mathbf{x} \in \mathbb{R}^n$, $\mathbf{u} \in \mathbb{R}^m$ and $\mathbf{y} \in \mathbb{R}^p$. Matrices \mathbf{A} , \mathbf{B} , \mathbf{C} and \mathbf{D} are known constant real matrices of compatible dimensions.

The following assumptions are imposed on the system in (2.95):

A-2.8 The order of the system and the number of output and input signals are such that $n > p > m$.

A-2.9 The matrices \mathbf{B} and \mathbf{C} are full rank.

A-2.10 In the nominal triple $(\mathbf{A}, \mathbf{D}, \mathbf{C})$, $\text{rank}(\mathbf{CD}) = m$.

A-2.11 The matching condition $\mathcal{R}(\mathbf{D}) \subset \mathcal{R}(\mathbf{B})$ is satisfied.

A-2.12 The uncertain vector function $\mathbf{f} : \mathbb{R}_+ \times \mathbb{R}^n \times \mathbb{R}^m \rightarrow \mathbb{R}^n$ is norm bounded.

Consider a sliding mode observer of the form (Edwards & Spurgeon, 1994):

$$\dot{\hat{\mathbf{x}}}(t) = \mathbf{A}\hat{\mathbf{x}}(t) + \mathbf{B}\mathbf{u}(t) - \mathbf{G}_L \mathbf{e}_y(t) + \mathbf{G}_{NL} \nu \quad (2.96)$$

$$\hat{\mathbf{y}}(t) = \mathbf{C}\hat{\mathbf{x}}(t) \quad (2.97)$$

where $\mathbf{G}_L \in \mathbb{R}^{n \times p}$ and $\mathbf{G}_{NL} \in \mathbb{R}^{n \times p}$ are design gain matrices. The matrix \mathbf{G}_L is a *Luenberger* type gain matrix. The vector $\nu \in \mathbb{R}^p$ is the discontinuous output error injection vector and will be specified in the sequel.

By defining the state estimation error as

$$\mathbf{e}(t) \triangleq \hat{\mathbf{x}}(t) - \mathbf{x}(t) \quad (2.98)$$

it follows that the estimation error system dynamics are governed by

$$\dot{\mathbf{e}}(t) = (\mathbf{A} - \mathbf{G}_L \mathbf{C})\mathbf{e}(t) + \mathbf{G}_{NL} \nu - \mathbf{D}\mathbf{f}(t, \mathbf{x}, \mathbf{u}) \quad (2.99)$$

Utilising the assumptions **A-2.8–A-2.12** there exists a similarity transformation $\mathbf{x} \mapsto \mathbf{T}_o \mathbf{x} = \bar{\mathbf{x}}$ with the state vector partition

$$\bar{\mathbf{x}} = \begin{bmatrix} \bar{\mathbf{x}}_1^T \\ \bar{\mathbf{x}}_2^T \end{bmatrix}^T \quad (2.100)$$

2.7 Summary

where $\bar{\mathbf{x}}_1 \in \mathfrak{R}^{(n-p)}$ and $\bar{\mathbf{x}}_2 \in \mathfrak{R}^p$ in which the state equation given in (2.95) can be written as follows

$$\dot{\bar{\mathbf{x}}}_1(t) = \mathcal{A}_{11}\bar{\mathbf{x}}_1(t) + \mathcal{A}_{12}\bar{\mathbf{x}}_2(t) + \mathcal{B}_1\mathbf{u}(t) \quad (2.101)$$

$$\dot{\bar{\mathbf{x}}}_2(t) = \mathcal{A}_{21}\bar{\mathbf{x}}_1(t) + \mathcal{A}_{22}\bar{\mathbf{x}}_2(t) + \mathcal{B}_2\mathbf{u}(t) + \mathcal{D}_2\mathbf{f}(t, \bar{\mathbf{x}}, \mathbf{u}) \quad (2.102)$$

The observer state equation given in (2.96), in the new coordinates, takes the form

$$\dot{\hat{\mathbf{x}}}_1(t) = \mathcal{A}_{11}\hat{\mathbf{x}}_1(t) + \mathcal{A}_{12}\hat{\mathbf{x}}_2(t) + \mathcal{B}_1\mathbf{u}(t) - \mathcal{G}_{L1}\mathbf{e}_y(t) \quad (2.103)$$

$$\dot{\hat{\mathbf{x}}}_2(t) = \mathcal{A}_{21}\hat{\mathbf{x}}_1(t) + \mathcal{A}_{22}\hat{\mathbf{x}}_2(t) + \mathcal{B}_2\mathbf{u}(t) - \mathcal{G}_{L2}\mathbf{e}_y(t) + \mathcal{G}_{NL2}\nu \quad (2.104)$$

where $\mathbf{e}_y = \hat{\mathbf{y}} - \mathbf{y}$ is the output estimation error vector. The discontinuous output error injection vector is given by

$$\nu = \begin{cases} -\rho(t, \mathbf{y}, \mathbf{u}) \|\mathcal{D}_2\| \frac{\mathbf{P}_2 \mathbf{e}_y(t)}{\|\mathbf{P}_2 \mathbf{e}_y(t)\|} & \text{if } \mathbf{e}_y(t) \neq \mathbf{0} \\ \mathbf{0} & \text{otherwise} \end{cases} \quad (2.105)$$

where $\mathbf{P}_2 \in \mathfrak{R}^{p \times p}$ is a s.p.d. matrix, and the scalar function $\rho : \mathfrak{R}_+ \times \mathfrak{R}^p \times \mathfrak{R}^m \rightarrow \mathfrak{R}_+$ is designed in such a way that the estimation error system dynamics are completely insensitive to the matched uncertainty $\mathbf{f}(\cdot)$.

Remark 2.6 *The form of the uncertain system given in (2.101)-(2.102) is similar to the output feedback canonical form introduced in Section 2.3.2. Later in Chapter 7, the discontinuous observer canonical form proposed in (Edwards & Spurgeon, 1994) is extended to the class of systems with uncertainties in the state matrix.*

Remark 2.7 *Most of the existing design methodologies for the Edwards & Spurgeon sliding mode observer, e.g. (Edwards & Spurgeon, 1994), (Edwards & Spurgeon, 1998b), (Tan & Edwards, 2001) and (Choi & Ro, 2005) among others, deal only with uncertain systems involving matched uncertainties. In this thesis, a new synthesis framework is presented for designing sliding mode observers of the form proposed in (Edwards & Spurgeon, 1994) but considering matched and mismatched uncertainties.*

2.7 Summary

In this chapter concepts regarding VSC with sliding modes and state estimation using a sliding mode observer have been discussed. The problem of synthesising sliding surfaces considering nominal system matrices was formulated for the cases of full state and output feedback control. Two canonical forms used in each of the aforementioned cases were described in detail. The properties of VSS with a sliding mode have also

2.7 Summary

been reviewed. The reachability problem has been studied and the form of the control law considered in the remainder of this thesis was presented. Moreover, an approach for reducing or even suppressing the high frequency switching of the control signal has been described. The structure of a discontinuous observer, known as the *Edwards & Spurgeon* sliding mode observer, was presented. It is worth pointing out that only nominal LTI systems and LTI systems with matched uncertainties were considered in this chapter.

The objective has been to introduce the theoretical foundations concerning VSS with sliding modes underlying the analysis and design contributions of this thesis. The next chapter introduces a useful mathematical tool applied in systems theory for analysis and design purposes: that is, Linear Matrix Inequality methods. This technique along with concepts of *Lyapunov* theory are the main tools employed in this thesis for analysis and design.

"You know my methods. Apply them!"

Sherlock Holmes – The Hound of the Baskervilles

Sir Arthur Conan Doyle (1859 - 1930)

3

Linear Matrix Inequalities and Polytopic Models

3.1 Introduction

Since the sliding mode design approaches proposed in this thesis are based upon Linear Matrix Inequality (LMI) methods, some of the most relevant theoretical elements concerned with this technique are reviewed in this chapter. Another subject addressed in this chapter is the description of uncertain systems through a mathematical model involving a convex combination of vertices of the system matrices when considering the upper and lower bound of each uncertain parameter in the plant. This is the so-called polytopic representation of uncertain systems within a convex bounded polyhedral domain.

This chapter is divided into two sections: LMIs are introduced in Section 3.2 where basic definitions, LMI representations and key features of LMIs are presented. In addition, standard LMI problems are formulated and the main mathematical tools frequently applied when dealing with LMIs are also described. Section 3.3 is devoted to a discussion of the sources of uncertainty inherent in real-world systems and polytopic representations of uncertain plants. This is the mathematical description used in this thesis for modelling uncertain systems with parametric uncertainties.

3.2 Linear Matrix Inequalities

This section offers a brief revision of the main concepts of LMIs used throughout this thesis. To this end, firstly, fundamental definitions regarding convex and affine sets and functions are stated. Then, the key concepts of LMIs are derived using these

definitions. Most of the material presented in this section is based upon the theory described in (Boyd *et al.*, 1994) (Gahinet *et al.*, 1995) (Scherer & Weiland, 1999) (Boyd & Vandenberghe, 2008).

3.2.1 Convexity

Definition 3.1 (Convex Set): Let \mathcal{V} be a linear vector space. A set $\mathcal{C} \subset \mathcal{V}$ is said to be a convex set if

$$\mu v_1 + (1 - \mu)v_2 \in \mathcal{C} \quad (3.1)$$

for any points $v_1, v_2 \in \mathcal{C}$ and any $\mu \in \mathbb{R}$ such that $0 \leq \mu \leq 1$. That is, the line segment joining any two points of \mathcal{C} also lies in the set \mathcal{C} . Otherwise, such a set is called non-convex.

Convexity and non-convexity is illustrated geometrically in Figure 3.1. Clearly, set \mathcal{C}_1 is convex since it is always possible to select two points v_1 and v_2 in \mathcal{C}_1 such that a segment of line also belongs to the set \mathcal{C}_1 . On the other hand, there are points v_1 and v_2 in \mathcal{C}_2 whose straight line segments have some points not in \mathcal{C}_2 .



Figure 3.1: Convex set \mathcal{C}_1 and non-convex set \mathcal{C}_2

Definition 3.2 (Affine Set): Let \mathcal{A} be a subset of a linear vector space \mathcal{V} . \mathcal{A} is an affine set if

$$v_3 = \mu v_1 + (1 - \mu)v_2 \in \mathcal{A} \quad (3.2)$$

$\forall v_1, v_2 \in \mathcal{A}$ and $\mu \in \mathbb{R}$.

An affine set is also a convex set. This follows from the definition of convex set given in 3.1.

Convex sets possess several important properties which are used to construct other definitions presented in this section. For purposes of completeness, some of such properties are listed (Scherer & Weiland, 1999):

3.2 Linear Matrix Inequalities

Let \mathcal{C}_1 and \mathcal{C}_2 be any convex sets and let \mathcal{V}_N be a normed vector space. Let α_1 and α_2 be any scalars, then:

1. The set

$$\alpha_1 \mathcal{C}_1 := \left\{ v : v = \alpha_1 c_1 \text{ with } c_1 \in \mathcal{C}_1 \right\} \quad (3.3)$$

is convex. Furthermore, the distributive property

$$(\alpha_1 + \alpha_2) \mathcal{C}_1 = \alpha_1 \mathcal{C}_1 + \alpha_2 \mathcal{C}_1 \quad (3.4)$$

holds for any $\alpha_1 \geq 0$ and $\alpha_2 \geq 0$.

2. The sum

$$\mathcal{C}_1 + \mathcal{C}_2 := \left\{ v : v = c_1 + c_2 \text{ with } c_1 \in \mathcal{C}_1 \text{ and } c_2 \in \mathcal{C}_2 \right\} \quad (3.5)$$

is convex.

3. Any linear transformation $\mathcal{T} : \mathcal{V}_N \rightarrow \mathcal{V}_N$ preserves the property of convexity, *i.e.* both the image set

$$\mathcal{T} \mathcal{C}_1 := \left\{ \bar{v}_1 : \bar{v}_1 = \mathcal{T} v_1 \text{ with } v_1 \in \mathcal{C}_1 \right\} \quad (3.6)$$

and the inverse image set

$$\mathcal{T}^{-1} \mathcal{C}_1 := \left\{ \bar{v}_1 : \mathcal{T} \bar{v}_1 \in \mathcal{C}_1 \right\} \quad (3.7)$$

are convex sets.

4. The intersection set of two convex sets is convex. Formally,

$$\mathcal{C}_1 \cap \mathcal{C}_2 := \left\{ v_1 : v_1 \in \mathcal{C}_1 \text{ and } v_1 \in \mathcal{C}_2 \right\} \quad (3.8)$$

5. The closure and the interior point of a convex set \mathcal{C}_1 are convex.

Let \mathcal{V} be a vector space and \mathbf{v} a vector in \mathcal{V} , $\mathbf{a} \in \mathbb{R}^n$, $\mathbf{c} \in \mathbb{R}^n$ are column vectors such that $\mathbf{a}, \mathbf{c} \neq \mathbf{0}$, and scalars $b, d \in \mathbb{R}$. The following are examples of convex sets (Boyd & Vandenberghe, 2008):

1. Hyperplanes defined by $\mathcal{C} = \left\{ \mathbf{v} : \mathbf{a}^T \mathbf{v} = b \right\}$.
2. Closed and open half-spaces given by $\mathcal{C} = \left\{ \mathbf{v} : \mathbf{a}^T \mathbf{v} \leq b \right\}$ and $\mathcal{C} = \left\{ \mathbf{v} : \mathbf{a}^T \mathbf{v} < b \right\}$ respectively. Note that half-spaces are convex sets but not affine sets.

3. Polyhedra (which stem from the intersection of hyperplanes and half-spaces) defined by

$$\mathcal{C} = \left\{ \mathbf{v} : \mathbf{a}_i^T \mathbf{v} \leq b_i \text{ for } i \in I(1, m), \mathbf{c}_j^T \mathbf{v} = d_j \text{ for } j \in I(1, p) \right\} \quad (3.9)$$

or in compact form

$$\mathcal{C} = \left\{ \mathbf{v} : \mathbf{A}\mathbf{v} \preceq \mathbf{b}, \mathbf{C}\mathbf{v} = \mathbf{d} \right\} \quad (3.10)$$

where

$$\mathbf{A} = \begin{bmatrix} \mathbf{a}_1 & \mathbf{a}_2 & \cdots & \mathbf{a}_m \end{bmatrix} \quad \mathbf{C} = \begin{bmatrix} \mathbf{c}_1 & \mathbf{c}_2 & \cdots & \mathbf{c}_p \end{bmatrix} \quad (3.11)$$

Here, the binary relation symbol \preceq stands for componentwise inequality (also called vector inequality) in \mathbb{R}^n , e.g. $\mathbf{u} \preceq \mathbf{v}$ means $u_i \leq v_i$ for $i \in I(1, n)$. A bounded/compact¹ polyhedron is called a polytope.

Figure 3.3 shows polyhedra in \mathbb{R}^2 and \mathbb{R}^3 respectively.

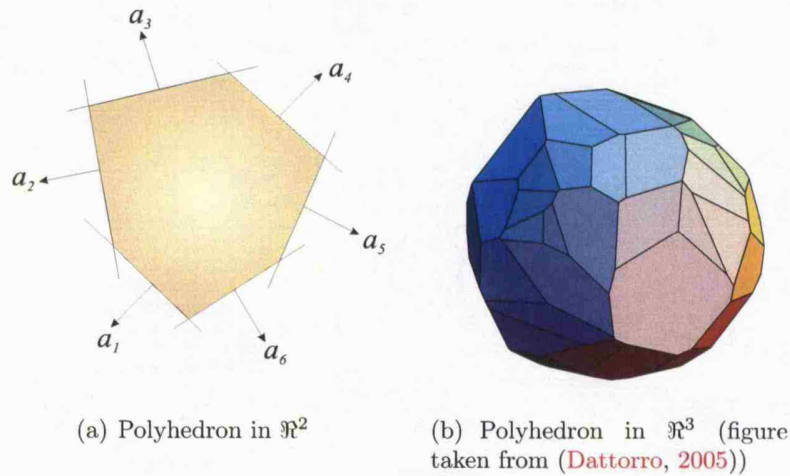


Figure 3.2: 2-D and 3-D Polyhedra

Definition 3.3 [Convex combination]: Let \mathcal{V} be a vector space and $\mathcal{C} \subset \mathcal{V}$. A point given by

$$\mathbf{v} = \sum_{j=1}^n \mu_j \mathbf{v}_j \quad (3.12)$$

is said to be a convex combination of the points $\mathbf{v}_j \in \mathcal{C}$ for $j \in I(1, n)$, if scalars μ_j satisfy

$$\mu_j \geq 0 \text{ for } j \in I(1, n) \text{ and } \sum_{j=1}^n \mu_j = 1 \quad (3.13)$$

¹A closed and bounded set is a compact set in an Euclidean space.

Note that the set containing all convex combinations of the points v_j for $j \in I(1, n)$ is a convex set.

Definition 3.4 [Convex hull]: The convex hull of a set \mathcal{C} , denoted by $\text{conv}(\mathcal{C})$ is the set of all convex combinations of points in \mathcal{C} , i.e.

$$\text{conv}(\mathcal{C}) = \left\{ \sum_{j=1}^n \mu_j v_j : v_j \in \mathcal{C}, \mu_j \geq 0 \text{ for } j \in I(1, n) \text{ and } \sum_{j=1}^n \mu_j = 1 \right\} \quad (3.14)$$

The convex hull of a finite collection of points is a polytope (note that a polytope is a closed convex polyhedron) and since convexity is closely related to the set operation of intersection, then the convex hull is also a convex set (Scherer & Weiland, 1999). The convex hull $\text{conv}(\mathcal{C})$ is the smallest convex set containing \mathcal{C} (Boyd & Vandenberghe, 2008). Figure 3.3 shows graphically two examples of convex hulls. Note that further points, besides the points at the vertices, are contained within each convex hull.

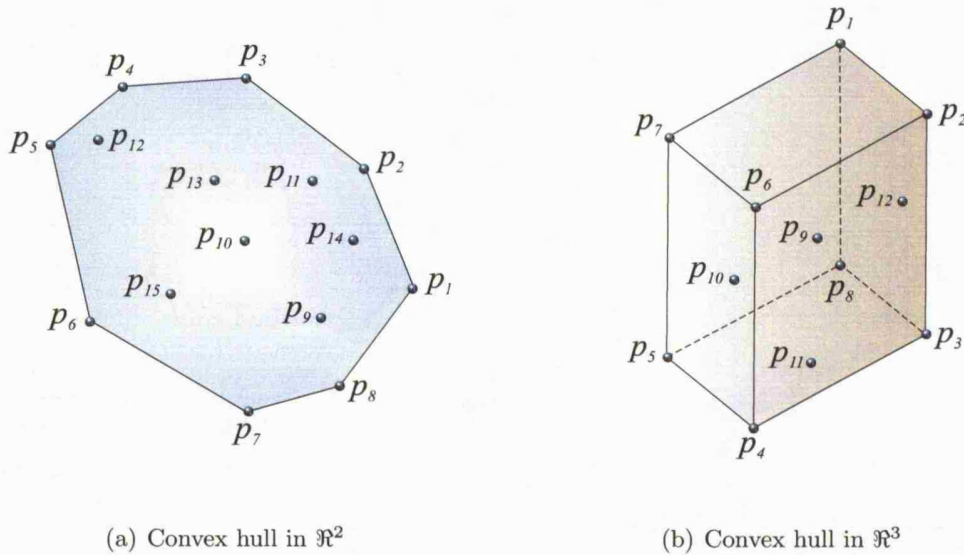


Figure 3.3: Geometric interpretation of convex hull of a set of points in 2-D and 3-D

Any convex optimisation problem consists of a convex objective function (also called a convex cost function) and constraint functions. Since convex optimisation problems are formulated throughout this thesis, a formal definition of a convex function is given below.

Definition 3.5 Let \mathcal{C} be a nonempty convex set. A function $f : \mathcal{C} \rightarrow \mathbb{R}$ is said to be a convex function if

$$f(\mu v_1 + (1 - \mu)v_2) \leq \mu f(v_1) + (1 - \mu)f(v_2) \quad (3.15)$$

for any points $v_1, v_2 \in \mathcal{C}$ and any $\mu \in \mathbb{R}$ such that $0 \leq \mu \leq 1$. The function f is called strictly convex, if inequality (3.15) is a strict inequality whenever $v_1 \neq v_2$ and $0 < \mu < 1$. The function f is said to be either concave or strictly concave, if $-f$ is convex or strictly convex.

Note that an important feature of convexity is that any local minimum over a convex set \mathcal{C} corresponds to a global minimum.

Figure 3.4 shows examples of convex and concave functions to illustrate definition 3.5.

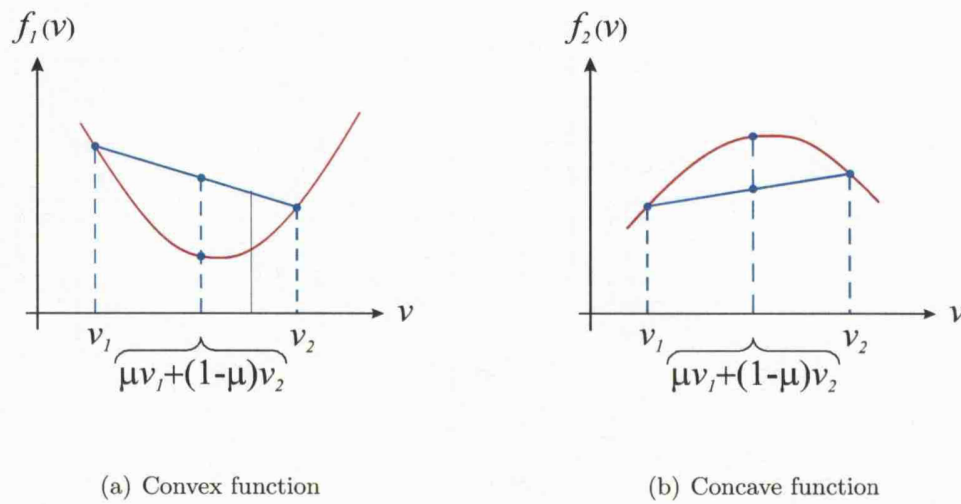


Figure 3.4: Geometric interpretation of convex and concave functions.

Remark 3.1 Although the definition of a convex function has been given considering a real valued function, it also applies to matrix (Hermitian¹ and symmetric²) valued functions. In such cases the inequality symbols $<$, \leq , $>$ and \geq (defining binary relations between real elements) are replaced by \prec , \preceq , \succ and \succeq respectively.

Definition 3.6 Let \mathcal{C}_1 and \mathcal{C}_2 be convex sets. A function $f : \mathcal{C}_1 \rightarrow \mathcal{C}_2$ is said to be affine if

$$f(\mu v_1 + (1 - \mu)v_2) = \mu f(v_1) + (1 - \mu)f(v_2) \quad (3.16)$$

for any points $v_1, v_2 \in \mathcal{C}_1$ and any $\mu \in \mathbb{R}$

If the convex sets \mathcal{C}_1 and \mathcal{C}_2 are finite dimensional, then any function $f : \mathcal{C}_1 \rightarrow \mathcal{C}_2$ consisting of a linear function $F : \mathcal{C}_1 \rightarrow \mathcal{C}_2$ and a constant $f_0 \in \mathcal{C}_2$, i.e. $f(v) = F(v) + f_0$ where $v \in \mathcal{C}_1$, is an affine function.

¹A matrix $M = M^* \in \mathcal{H}^{n \times n}$ where $*$ denotes transpose complex conjugate of M , and $\mathcal{H}^{n \times n}$ stands for the set of matrices whose entries are complex numbers.

²Any matrix $M = M^T \in \mathbb{R}^{n \times n}$.

3.2 Linear Matrix Inequalities

Remark 3.2 A function $f : \mathfrak{R}^n \rightarrow \mathfrak{R}^m$ is said to be affine if

$$f(\mathbf{x}) = \Xi \mathbf{x} + \beta \quad (3.17)$$

where $\Xi \in \mathfrak{R}^{m \times n}$ is a constant matrix and $\beta \in \mathfrak{R}^m$ is a constant vector. Thus, an affine function consists of a linear function, i.e. $\Xi \mathbf{x}$ and a constant denoted in this case by β .

Remark 3.3 All affine (and also linear) functions are both convex and concave functions. Conversely, any convex and concave function is affine (Boyd & Vandenberghe, 2008).

All concepts formally defined above are used to describe the elements of a powerful mathematical tool coined by *J. C. Willems* in (Willems, 1971) as Linear Matrix Inequalities. This technique has been in constant deployment from theoretical and practical viewpoints. The rest of this section is completely devoted to present fundamental definitions and concepts of LMIs used throughout this thesis.

3.2.2 Canonical and Other Forms of Representing LMIs

An affine matrix valued function of the form

$$\mathbf{F}(\mathbf{x}) = \mathbf{F}_0 + \sum_{i=1}^m \mathbf{x}_i \mathbf{F}_i \succ 0 \quad (3.18)$$

is said to be a *Linear Matrix Inequality* where $\mathbf{x} \in \mathfrak{R}^m$ is the vector of decision variables whilst $\mathbf{F}_0, \dots, \mathbf{F}_m$ are *Hermitian* (or symmetric real) matrices.

Any LMI of the form given in (3.18) is said to be in the canonical form. Notice that LMIs can be described in different forms. The most common representation forms used in control systems are the following (Gahinet *et al.*, 1995):

1. *Matrix description of a set of LMIs:* A system of LMIs given by

$$\left. \begin{array}{l} \mathbf{F}_1(\mathbf{x}) \succ 0 \\ \mathbf{F}_2(\mathbf{x}) \succ 0 \\ \vdots \\ \mathbf{F}_q(\mathbf{x}) \succ 0 \end{array} \right\} \quad (3.19)$$

can be recast as a single LMI as follows

3.2 Linear Matrix Inequalities

$$\begin{pmatrix} \mathbf{F}_1(\mathbf{x}) & 0 & \cdots & 0 \\ 0 & \mathbf{F}_2(\mathbf{x}) & & \vdots \\ \vdots & & \ddots & 0 \\ 0 & \cdots & 0 & \mathbf{F}_q(\mathbf{x}) \end{pmatrix} \succ 0 \quad (3.20)$$

2. *General Representation:* In a large number of cases (for example, in control engineering problems), LMI constraints are affine functions of matrix variables \mathbf{X}_j for $j \in I(1, m)$. That is,

$$\mathbf{L}(\mathbf{X}_1, \mathbf{X}_2, \dots, \mathbf{X}_m) \prec \mathbf{R}(\mathbf{X}_1, \mathbf{X}_2, \dots, \mathbf{X}_m) \quad (3.21)$$

The matrix variables \mathbf{X}_j for $j \in I(1, m)$ usually have some sort of structure which depends on the problem dealt with. For instance, the *Lyapunov* inequality $\mathbf{A}^T \mathbf{P} + \mathbf{P} \mathbf{A} \prec 0$ requires the *Lyapunov* matrix $\mathbf{P} \succ 0$, which is the matrix variable in this case, to be symmetric.

Particular cases of (3.21) are

$$\left. \begin{array}{l} \mathbf{L}_1(\mathbf{X}_1, \mathbf{X}_2, \dots, \mathbf{X}_m) \prec 0 \\ \mathbf{L}_2(\mathbf{X}_1, \mathbf{X}_2, \dots, \mathbf{X}_m) \prec 0 \\ \vdots \\ \mathbf{L}_q(\mathbf{X}_1, \mathbf{X}_2, \dots, \mathbf{X}_m) \prec 0 \end{array} \right\} \quad (3.22)$$

or

$$\left. \begin{array}{l} \mathbf{L}_1(\mathbf{X}_1, \mathbf{X}_2, \dots, \mathbf{X}_m) \prec 0 \\ \mathbf{L}_2(\mathbf{X}_1, \mathbf{X}_2, \dots, \mathbf{X}_m) \prec 0 \\ \vdots \\ \mathbf{L}_k(\mathbf{X}_1, \mathbf{X}_2, \dots, \mathbf{X}_m) \prec 0 \\ \mathbf{L}_{k+1}(\mathbf{X}_1, \mathbf{X}_2, \dots, \mathbf{X}_m) \prec \mathbf{R}_1(\mathbf{X}_1, \mathbf{X}_2, \dots, \mathbf{X}_m) \\ \mathbf{L}_{k+2}(\mathbf{X}_1, \mathbf{X}_2, \dots, \mathbf{X}_m) \prec \mathbf{R}_2(\mathbf{X}_1, \mathbf{X}_2, \dots, \mathbf{X}_m) \\ \vdots \\ \mathbf{L}_q(\mathbf{X}_1, \mathbf{X}_2, \dots, \mathbf{X}_m) \prec \mathbf{R}_{q-k}(\mathbf{X}_1, \mathbf{X}_2, \dots, \mathbf{X}_m) \end{array} \right\} \quad (3.23)$$

3.2.3 Standard LMI Problems

LMI problems can be classified into three main groups (Boyd *et al.*, 1994):

3.2 Linear Matrix Inequalities

1. *The Feasibility Problem* : This problem consists of determining whether a feasible solution \mathbf{x}^{feas} , satisfying LMI constraints, exists or not, and finding such a solution if one exists. It must be pointed out that this kind of problem is not concerned with the optimality of the solution and such a feasible solution may not be unique.
2. *The Linear Objective Minimisation Problem (LOMP) - The Eigenvalue Problem (EVP)* : This optimisation problem corresponds to minimising a linear objective function (also called a linear functional on the decision variable \mathbf{x}) subject to an LMI constraint affine with respect to \mathbf{x} . It can be formulated as

$$\left. \begin{array}{l} \min_{\mathbf{x}} \quad \mathbf{c}^T \mathbf{x} \\ \text{s.t.} \\ \mathbf{F}(\mathbf{x}) \succ 0 \end{array} \right\} \quad (3.24)$$

This formulation is said to be *Positive Definite Programming* (PDP) whilst if the constraint is of the form $\mathbf{F}(\mathbf{x}) \succeq 0$ then it is said to be *Semidefinite Programming* (SDP). Within the linear objective minimisation problem lies *the Eigenvalue Problem (EVP)* which is formulated as

$$\left. \begin{array}{l} \min_{\lambda, \mathbf{x}} \quad \lambda \\ \text{s.t.} \\ \lambda \mathbf{I} - \mathbf{F}_1(\mathbf{x}) \succ 0 \\ \mathbf{F}_2(\mathbf{x}) \succ 0 \end{array} \right\} \quad (3.25)$$

where \mathbf{F}_1 and \mathbf{F}_2 are symmetric matrices depending affinely on \mathbf{x} .

3. *The Generalised Eigenvalue Problem (GEVP)* : This problem corresponds to one of minimising the maximum generalised eigenvalue of two affine dependent matrices of \mathbf{x} . This LMI problem can be stated as

$$\left. \begin{array}{l} \min_{\lambda, \mathbf{x}} \quad \lambda \\ \text{s.t.} \\ \lambda \mathbf{F}_1(\mathbf{x}) - \mathbf{F}_2(\mathbf{x}) \succ 0 \\ \mathbf{F}_1(\mathbf{x}) \succ 0 \\ \mathbf{F}_3(\mathbf{x}) \succ 0 \end{array} \right\} \quad (3.26)$$

where \mathbf{F}_1 , \mathbf{F}_2 and \mathbf{F}_3 are symmetric matrices depending affinely on \mathbf{x} . Two aspects must be highlighted with respect to this LMI problem. The first one is regarding the quasi-convex characteristic of the GEVP instead of the convex feature of the LOMP or EVP. The second one is that in some cases a GEVP can be restated as a LOMP by means of a change of variables.

3.2 Linear Matrix Inequalities

Remark 3.4 *Convex programming is a particular type of mathematical optimisation which includes least squares, linear programming, quadratically constrained quadratic programming, quadratic programming, semidefinite programming, second-order cone programming and geometric programming (Vandenberghe & Boyd, 1996) (Boyd & Vandenberghe, 2008). This classification arises from the characteristics of both the cost function and the constraints. For instance, a semidefinite program is concerned with a linear objective function and an affine combination of symmetric positive definite (s.p.d.) matrices (Vandenberghe & Boyd, 1996).*

3.2.4 LMI Properties and Features

An LMI of the form (3.18) or (3.21) defines a convex constraint on the decision variables. This is a key feature which implies that efficient numerical algorithms, *e.g.* the *Ellipsoid Algorithm* and the *Interior-Point Methods* (details on these algorithms can be found in (Bland *et al.*, 1981), (Boyd *et al.*, 1994) and (Scherer & Weiland, 1999)), can be applied. Such algorithms can determine whether or not an LMI constraint is feasible and if it is, then find a feasible point. Also, this sort of methods allows convex optimisation problems with LMIs constraints to be solved. Furthermore, convergence to a global minimum in polynomial-time is guaranteed by means of these numerical algorithms (Boyd *et al.*, 1994). In this thesis, the LMI control toolbox of MATLAB (Gahinet *et al.*, 1995) and the toolbox SeDuMi (Sturm, 1999) are used for implementing and solving LMI problems. In the Appendix A of this dissertation, examples of code using commands from both toolboxes are shown in order to illustrate the implementation of LMIs under the MATLAB environment.

Uncertain systems can be dealt with via LMI methods using different uncertainty descriptions. For instance, uncertain state-space representations such as polytopic models or affine parameter-dependent models; also, linear-fractional models of uncertainty (Gahinet *et al.*, 1995).

Another characteristic is concerned with the possibility of formulating optimisation problems involving different criteria, *e.g.* \mathcal{H}_2 and \mathcal{H}_∞ , as a mixed problem via LMIs. This makes the LMI formulation more attractive and advantageous than classical optimisation methods since other performance or design requirements can be easily incorporated rather than using a combination of criteria as a single one (Scherer & Weiland, 1999).

3.2.5 Fundamental Mathematical Operations on LMIs

The most common LMI mathematical tools applied in this dissertation are outlined in the sequel. The material presented here draws heavily on (Boyd *et al.*, 1994) and (Scherer & Weiland, 1999).

3.2 Linear Matrix Inequalities

1. **Change of Variables** : This operation allows some *Nonlinear Matrix Inequalities* (NMIs) to be written as LMIs. It can be carried out through defining new variables depending on the original decision variables. Nevertheless, there is a fundamental condition new variables must fulfill: namely that the original ones have to be recovered uniquely from the new decision variables.
2. **Congruence Transformation** :

Definition 3.7 $\mathbf{P} \in \mathfrak{R}^{n \times n}$ and $\mathbf{M} \in \mathfrak{R}^{n \times n}$ are said to be congruent matrices if there exists a nonsingular transformation matrix $\mathbf{T} \in \mathfrak{R}^{n \times n}$ such that

$$\mathbf{M} = \mathbf{T}^T \mathbf{P} \mathbf{T} \quad (3.27)$$

Theorem 3.1 If $\mathbf{P} \in \mathfrak{R}^{n \times n}$ and $\mathbf{M} \in \mathfrak{R}^{n \times n}$ are congruent matrices then $\mathbf{M} \succ 0$ if and only if $\mathbf{P} \succ 0$.

△

Proof This proof follows the same argument postulated in (Scherer & Weiland, 1999).

If $\mathbf{P} \succ 0$ then $\mathbf{x}^T \mathbf{P} \mathbf{x} > 0 \quad \forall \mathbf{x} \in \mathfrak{R}^n$ and $\mathbf{x} \neq 0$. Furthermore, since \mathbf{P} and \mathbf{M} are congruent matrices then according to definition 3.7 there exists a nonsingular matrix $\mathbf{T} \in \mathfrak{R}^{n \times n}$ such that (3.27) holds and $\mathbf{y} = \mathbf{T}^{-1} \mathbf{x} \quad \forall \mathbf{x} \neq 0$. So, $\mathbf{P} \succ 0 \iff \mathbf{x}^T \mathbf{P} \mathbf{x} > 0$ but $\mathbf{y} = \mathbf{T}^{-1} \mathbf{x} \quad \forall \mathbf{x} \neq 0$. Then $\mathbf{x}^T \mathbf{P} \mathbf{x} = \mathbf{y}^T \mathbf{T}^T \mathbf{P} \mathbf{T} \mathbf{y} = \mathbf{y}^T \mathbf{M} \mathbf{y} > 0 \iff \mathbf{M} \succ 0$.

Q.E.D.

Remark 3.5 Theorem 3.1 means that definiteness of any positive definite (p.d.) matrix is invariant under post and pre multiplication by a full rank real matrix.

3. **Schur Complement** : Nonlinear convex inequalities, e.g. quadratic matrix inequalities, can be transformed into LMIs by means of the *Schur* complement Lemma (Boyd *et al.*, 1994).

Lemma 3.1 [*Schur Complement Lemma*] : Let $\mathbf{Q}(\mathbf{x}) = \mathbf{Q}^T(\mathbf{x})$, $\mathbf{R}(\mathbf{x}) = \mathbf{R}^T(\mathbf{x})$ and $\mathbf{S}(\mathbf{x})$ be given affine matrices on \mathbf{x} . Let

$$\mathbf{F}(\mathbf{x}) = \begin{bmatrix} \mathbf{Q}(\mathbf{x}) & \mathbf{S}(\mathbf{x}) \\ \mathbf{S}^T(\mathbf{x}) & \mathbf{R}(\mathbf{x}) \end{bmatrix} \quad (3.28)$$

be a block matrix. Then,

$$\mathbf{F}(\mathbf{x}) \succ 0 \iff \mathbf{R}(\mathbf{x}) \succ 0 \text{ and } \mathbf{Q}(\mathbf{x}) - \mathbf{S}(\mathbf{x})\mathbf{R}^{-1}(\mathbf{x})\mathbf{S}^T(\mathbf{x}) \succ 0 \quad (3.29)$$

3.2 Linear Matrix Inequalities

Furthermore,

$$\mathbf{F}(\mathbf{x}) \succ 0 \iff \mathbf{Q}(\mathbf{x}) \succ 0 \text{ and } \mathbf{R}(\mathbf{x}) - \mathbf{S}^T(\mathbf{x})\mathbf{Q}^{-1}(\mathbf{x})\mathbf{S}(\mathbf{x}) \succ 0 \quad (3.30)$$

△

The following proof of the *Schur* complement consists of applying a congruence transformation as suggested in (Scherer & Weiland, 1999). Although the proof is relatively simple, it is presented here to illustrate the use of this tool.

Proof (Necessity): Consider the congruence transformation with

$$\mathbf{T} = \begin{bmatrix} \mathbf{I} & 0 \\ -(\mathbf{R}^T(\mathbf{x}))^{-1}\mathbf{S}^T(\mathbf{x}) & \mathbf{I} \end{bmatrix} \quad (3.31)$$

and $\mathbf{F}(\mathbf{x})$ given by (3.28). Then,

$$\mathbf{T}^T\mathbf{F}(\mathbf{x})\mathbf{T} = \begin{bmatrix} \mathbf{Q}(\mathbf{x}) - \mathbf{S}(\mathbf{x})\mathbf{R}^{-1}(\mathbf{x})\mathbf{S}^T(\mathbf{x}) & 0 \\ 0 & \mathbf{R}(\mathbf{x}) \end{bmatrix} \succ 0 \quad (3.32)$$

(Sufficiency): Consider

$$\begin{aligned} \mathbf{R}(\mathbf{x}) &\succ 0 \\ \mathbf{Q}(\mathbf{x}) - \mathbf{S}(\mathbf{x})\mathbf{R}^{-1}(\mathbf{x})\mathbf{S}^T(\mathbf{x}) &\succ 0 \end{aligned} \quad (3.33)$$

Since a system of LMIs can be written as a single LMI, then (3.33) can be recast as the right hand side form of (3.32). Define a p.d. matrix \mathbf{W} as follows

$$\mathbf{W} = \begin{bmatrix} \mathbf{Q}(\mathbf{x}) - \mathbf{S}(\mathbf{x})\mathbf{R}^{-1}(\mathbf{x})\mathbf{S}^T(\mathbf{x}) & 0 \\ 0 & \mathbf{R}(\mathbf{x}) \end{bmatrix} \succ 0 \quad (3.34)$$

Therefore,

$$(\mathbf{T}^T)^{-1}\mathbf{W}\mathbf{T}^{-1} = \mathbf{F}(\mathbf{x}) = \begin{bmatrix} \mathbf{Q}(\mathbf{x}) & \mathbf{S}(\mathbf{x}) \\ \mathbf{S}^T(\mathbf{x}) & \mathbf{R}(\mathbf{x}) \end{bmatrix} \quad (3.35)$$

A similar procedure is applied for proving sufficiency and necessity in (3.30). In such a case the transformation matrix to be considered is

$$\mathbf{T} = \begin{bmatrix} \mathbf{I} & -(\mathbf{Q}^T(\mathbf{x}))^{-1}\mathbf{S}(\mathbf{x}) \\ 0 & \mathbf{I} \end{bmatrix} \quad (3.36)$$

Q.E.D.

3.2 Linear Matrix Inequalities

Other LMI tools, which can be found in parts of the technical literature regarding LMI-based approaches (not described here because they are not used directly in this thesis), are the S-procedure (Boyd *et al.*, 1994), the projection Lemma (Gahinet & Apkarian, 1994) and the *Finsler* Lemma (Finsler, 1937)(Boyd *et al.*, 1994). For details, readers are referred to the given references.

3.2.6 LMI Regions

An LMI region \mathcal{D} is a convex sub-set of the complex plane \mathbb{C} defined as

$$\mathcal{D} = \{s \in \mathbb{C} : \mathbf{f}_{\mathcal{D}}(s) = \Xi + s\Phi + \bar{s}\Phi^T \prec 0\} \quad (3.37)$$

where \bar{s} is the complex conjugate of s , $\Xi = \Xi^T$ and Φ are appropriately dimensioned real matrices and the matrix valued function $\mathbf{f}_{\mathcal{D}}$ is said to be the characteristic function of \mathcal{D} .

Theorem 3.2 (Chilali & Gahinet, 1996): *A matrix $\mathbf{M} \in \mathbb{R}^{n \times n}$ has all its eigenvalues in the LMI region \mathcal{D} and is called \mathcal{D} -stable, if and only if there exists a s.p.d. matrix $\mathbf{X} \in \mathbb{R}^{n \times n}$ such that*

$$\mathcal{M}_{\mathcal{D}}(\mathbf{M}, \mathbf{X}) = \Xi \otimes \mathbf{X} + \Phi \otimes (\mathbf{M}\mathbf{X}) + \Phi^T \otimes (\mathbf{M}\mathbf{X})^T \prec 0 \quad (3.38)$$

△

Proof See (Chilali & Gahinet, 1996).

Clearly, the relationship between the characteristic function $\mathbf{f}_{\mathcal{D}}$ in (3.37) and the matrix inequality $\mathcal{M}_{\mathcal{D}}(\mathbf{M}, \mathbf{X})$ in (3.38) is given by

$$(1, s, \bar{s}) \longleftrightarrow (\mathbf{X}, \mathbf{M}\mathbf{X}, \mathbf{X}\mathbf{M}^T) \quad (3.39)$$

which is useful when defining LMI regions as constraints in either feasibility or optimisation problems.

Remark 3.6 *Theorem 3.2 can be interpreted as a generalisation of the Lyapunov Theorem regarding quadratic stability (Chilali et al., 1999). This can be seen by considering the characteristic function*

$$\mathbf{f}_{\mathcal{D}} = s + \bar{s} < 0 \quad (3.40)$$

which describes the open left-half complex plane. Then, it follows using (3.39) that (3.40) yields

$$\mathcal{M}_{\mathcal{D}}(\mathbf{M}, \mathbf{X}) = 1 \otimes (\mathbf{M}\mathbf{X}) + 1 \otimes (\mathbf{X}\mathbf{M}^T) = \mathbf{M}\mathbf{X} + \mathbf{X}\mathbf{M}^T \prec 0 \text{ with } \mathbf{X} = \mathbf{X}^T \succ 0 \quad (3.41)$$

By defining the change of matrix variables $\mathbf{P} = \mathbf{X}^{-1}$, it is easy to obtain the so-called Lyapunov Inequality:

$$\mathbf{M}^T \mathbf{P} + \mathbf{P} \mathbf{M} \prec 0 \quad \text{with } \mathbf{P} = \mathbf{P}^T \succ 0 \quad (3.42)$$

The class of LMI regions considered in control systems are symmetric convex sets with respect to the real axis. Furthermore, an LMI region can be obtained by intersections of elementary LMI regions (recall that convexity is closed under the set operation of intersection) such as a half-plane stability region, disks, conic sectors, vertical and horizontal strips. In the sequel, the most used fundamental LMI regions are formally defined and shown graphically. The mathematical definition of each LMI region has been drawn from (Chilali & Gahinet, 1996) and Chilali *et al.* (1999).

1. Let $\mathcal{H}(h)$ be a half-plane stability region delimited by a vertical line at $(-h, 0)$ in the complex plane, *i.e.* $\text{Re}(s) < -h$, as shown in Figure 3.5.

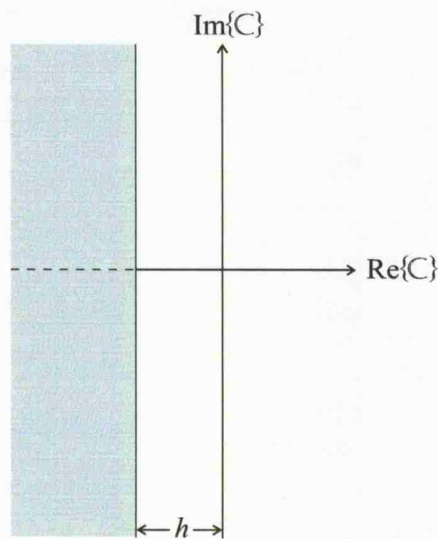


Figure 3.5: Elementary LMI Region: Half-plane $\mathcal{H}(h)$

This convex region is characterised by

$$\mathbf{f}_{\mathcal{D}}(s) = s + \bar{s} + 2h \quad (3.43)$$

Then, from Theorem 3.2, the spectrum of a square matrix \mathbf{M} , denoted by $\lambda(\mathbf{M})$, lies in $\mathcal{H}(h)$ if and only if

$$\mathcal{M}_{\mathcal{D}}(\mathbf{M}, \mathbf{X}) = \mathbf{M}\mathbf{X} + \mathbf{X}\mathbf{M}^T + 2h\mathbf{X} \prec 0 \quad (3.44)$$

2. Let $\mathcal{C}((0,0)_c, \alpha)$ be a conic region centered at the origin of the complex plane \mathbb{C} and at an angle α with respect to the real axis of the complex left half-plane as shown in Figure 3.6. A conic region is characterised by the function

$$\mathbf{f}_{\mathcal{D}}(s) = \begin{bmatrix} \sin(\alpha)(s + \bar{s}) & \cos(\alpha)(s - \bar{s}) \\ \cos(\alpha)(\bar{s} - s) & \sin(\alpha)(s + \bar{s}) \end{bmatrix} \quad (3.45)$$

By considering Theorem 3.2, it follows that the eigenvalues of \mathbf{M} lie within $\mathcal{C}((0,0)_c, \alpha)$ if and only if the matrix inequality

$$\mathcal{M}_{\mathcal{D}}(\mathbf{M}, \mathbf{X}) = \begin{bmatrix} \sin(\alpha)(\mathbf{M}\mathbf{X} + \mathbf{X}\mathbf{M}^T) & \cos(\alpha)(\mathbf{M}\mathbf{X} - \mathbf{X}\mathbf{M}^T) \\ \cos(\alpha)(\mathbf{X}\mathbf{M}^T - \mathbf{M}\mathbf{X}) & \sin(\alpha)(\mathbf{M}\mathbf{X} + \mathbf{X}\mathbf{M}^T) \end{bmatrix} \prec 0 \quad (3.46)$$

is satisfied for a s.p.d. matrix \mathbf{X} .

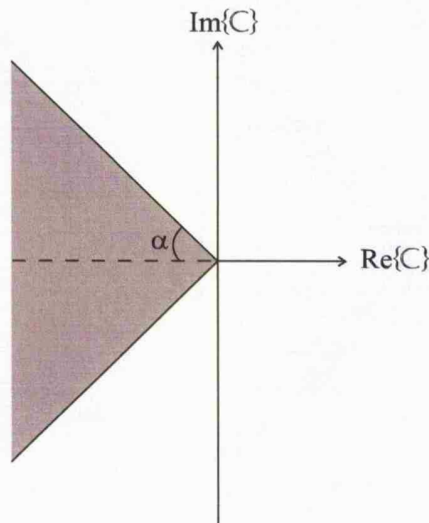
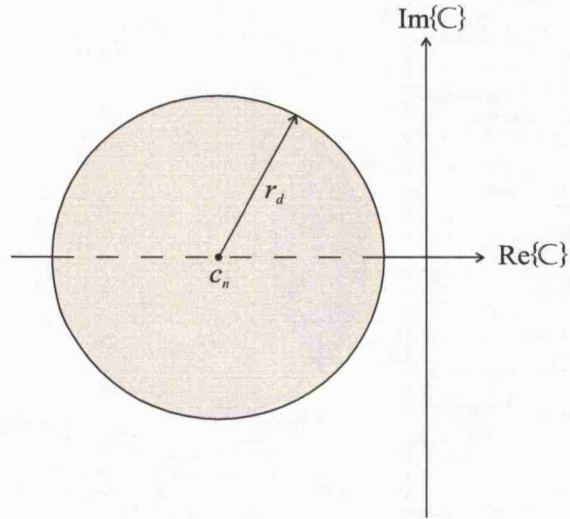


Figure 3.6: Elementary LMI Region: Cone $\mathcal{C}((0,0)_c, \alpha)$

3. Let $\mathcal{D}(c_n, r_d)$ be a disk centered at $(-c_n, 0)$ in the complex plane \mathbb{C} with radius r_d as shown in Figure 3.7.

A disk $\mathcal{D}(c_n, r_d)$ is described mathematically by the following function

$$\mathbf{f}_{\mathcal{D}}(s) = \begin{bmatrix} -r_d & s + c_n \\ \bar{s} + c_n & -r_d \end{bmatrix} \quad (3.47)$$


 Figure 3.7: Elementary LMI Region: Disk $\mathcal{D}(c_n, r_d)$

The corresponding matrix inequality $\mathcal{M}_{\mathcal{D}}(\mathbf{M}, \mathbf{X})$ is given by

$$\mathcal{M}_{\mathcal{D}}(\mathbf{M}, \mathbf{X}) = \begin{bmatrix} -r_d \mathbf{X} & \mathbf{M}\mathbf{X} + c_n \mathbf{X} \\ \mathbf{X}\mathbf{M}^T + c_n \mathbf{X} & -r_d \mathbf{X} \end{bmatrix} \prec 0 \quad (3.48)$$

Then, from Theorem 3.2, it follows that $\lambda(\mathbf{M}) \subset \mathcal{D}(c_n, r_d)$ if and only if the matrix inequality above is satisfied for a s.p.d. matrix \mathbf{X} .

4. Let $\mathcal{V}_s(h_1, h_2)$ be a vertical strip defined by

$$\mathcal{V}_s(h_1, h_2) = \{s \in \mathbb{C} : -h_2 < \text{Re}(s) < -h_1 < 0\} \quad (3.49)$$

where $h_1, h_2 \in \mathfrak{R}_+$. A graphical representation of this region is given in Figure 3.8.

A vertical strip is described by means of the following characteristic functions

$$\mathbf{f}_{\mathcal{D}_1}(s) = s + \bar{s} + 2h_1 \quad (3.50)$$

$$\mathbf{f}_{\mathcal{D}_2}(s) = -s - \bar{s} - 2h_2 \quad (3.51)$$

In turn, two matrix inequalities can be established based upon Theorem 3.2 and using (3.39) as follows

$$\mathcal{M}_{\mathcal{D}_1}(\mathbf{M}, \mathbf{X}) = \mathbf{M}\mathbf{X} + \mathbf{X}\mathbf{M}^T + 2h_1\mathbf{X} \prec 0 \quad (3.52)$$

$$\mathcal{M}_{\mathcal{D}_2}(\mathbf{M}, \mathbf{X}) = \mathbf{M}\mathbf{X} + \mathbf{X}\mathbf{M}^T + 2h_2\mathbf{X} \succ 0 \quad (3.53)$$

Hence, $\lambda(\mathbf{M}) \subset \mathcal{V}_s(h_1, h_2)$ if and only if the matrix inequalities (3.52)-(3.53) hold for a single s.p.d. matrix \mathbf{X} .

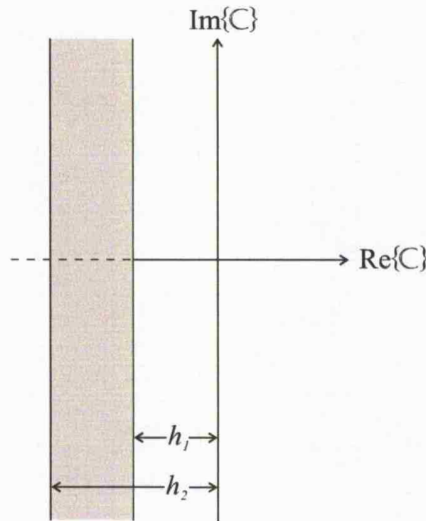


Figure 3.8: Elementary LMI Region: Vertical strip $\mathcal{V}_s(h_1, h_2)$

3.3 Parametric Uncertainty Description: Polytopic Models

A mathematical model is a simplified abstraction of a real world system that considers only a subset of the dynamical characteristics depending on the relevant requirements or available information concerning a particular application. The uncertainties in mathematical models may arise from unknown dynamics, either unknown or approximated numerical values of the parameters in the model, varying parameters, approximate considerations in the modelling process, for example linearisation of nonlinear systems and neglected fast dynamics. Uncertainties can be classified as either internal or external uncertainties. The former is concerned with dynamical phenomena, system parameters and system structure. The latter is related to external stochastic signals called disturbances or perturbations.

Internal uncertainties can be classified as follows:

3.3 Parametric Uncertainty Description: Polytopic Models

1. **Structured Uncertainties:** The structure of the model is known but it has incomplete or unknown information. A common case of structured uncertainty is parametric uncertainty. In this case, the model structure is well known; however, a finite number of parameters are uncertain. Such parameters lie in a bounded interval defined by the lowest and highest possible numerical value.
2. **Non-structured Uncertainties:** This uncertainty arises from unknown causes or structure, *i.e.* there is no information concerned with how the uncertainties affect the system's model. Furthermore, usually only an upper bound is available.

The control and estimation schemes proposed in this thesis are intended for continuous time uncertain systems. In particular, systems with mismatched parametric uncertainties. The lower and upper bounds of the r components of the parameter vector, which are constant and known, define a convex set in the parameter space. Furthermore, if the system matrix (denoted by $\mathbb{S} \in \mathfrak{R}^{(n+p) \times (n+m)}$ and composed of the state, input, output and transmission matrices) is affine with respect to the vector of uncertain parameters, then $N = 2^r$ system matrices can be established by considering all possible combinations of the parameters' bounds. Each one of these matrices corresponds to a vertex of a closed convex polyhedron. The convex combination of such N vertices defines a polytope in the system matrices space. This mathematical representation of parametric uncertainties is referred to in this thesis as a *polytopic model* and is described in this section.

Consider the following linear time-varying system represented in state-space form by

$$\dot{\mathbf{x}}(t) = \mathbf{A}(t)\mathbf{x}(t) + \mathbf{B}(t)\mathbf{u}(t) \quad (3.54)$$

$$\mathbf{y}(t) = \mathbf{C}(t)\mathbf{x}(t) + \mathbf{D}(t)\mathbf{u}(t) \quad (3.55)$$

where $\mathbf{x} \in \mathfrak{R}^n$ is the state vector, $\mathbf{u} \in \mathfrak{R}^m$ is the input vector, $\mathbf{y} \in \mathfrak{R}^p$ is the output vector. The time-varying matrices $\mathbf{A}(t)$, $\mathbf{B}(t)$, $\mathbf{C}(t)$ and $\mathbf{D}(t)$ have appropriate dimensions.

The concepts of convex combination and convex hull stated in definitions (3.3) and (3.4) were established for points within a convex set. These concepts can straightforwardly be extended by considering system matrices, instead of points, as the objects in a closed convex polyhedron, *i.e.* in a polytope. In this thesis, the system matrix of (3.54)-(3.55), is defined as

$$\mathbb{S}(t) \triangleq \left[\begin{array}{c|c} \mathbf{A}(t) & \mathbf{B}(t) \\ \hline \mathbf{C}(t) & \mathbf{D}(t) \end{array} \right] \quad (3.56)$$

3.3 Parametric Uncertainty Description: Polytopic Models

A polytope \mathcal{P} is the set of all convex combinations of N system matrices \mathbb{S}_j of the form

$$\mathbb{S}_j \triangleq \left[\begin{array}{c|c} \mathbf{A}_j & \mathbf{B}_j \\ \hline \mathbf{C}_j & \mathbf{D}_j \end{array} \right] \text{ for } j \in I(1, N) \quad (3.57)$$

That is, the convex hull of $\{\mathbb{S}_1, \mathbb{S}_2, \dots, \mathbb{S}_N\}$. These N system matrices are generated for each vertex of the polytope \mathcal{P} . A polytope \mathcal{P} is defined formally as follows

$$\mathcal{P} = \text{Co}\{\mathbb{S}_1, \mathbb{S}_2, \dots, \mathbb{S}_N\} = \left\{ \sum_{j=1}^N \mu_j \mathbb{S}_j : \sum_{j=1}^N \mu_j = 1, \mu_j \geq 0 \text{ for } j \in I(1, N) \right\} \quad (3.58)$$

where N is the number of vertices of \mathcal{P} . The scalars μ_j with $j \in I(1, N)$ are said to be the polytopic coordinates of $\mathbb{S}(t)$. From (3.58), it follows that the system matrix $\mathbb{S}(t)$ belongs to a polytope \mathcal{P} contained in the space of system matrices (in (Gahinet *et al.*, 1995) this polytope is called a fixed polytope of matrices).

Remark 3.7 *Although the structure of the system matrix $\mathbb{S}(t)$ in (3.56) is perfectly known, the components of the matrix $\mathbb{S}(t)$ might not be precisely known. However, the system matrix belongs to a polytopic uncertain domain \mathcal{P} , i.e. $\mathbb{S}(t) \in \mathcal{P}$, where the matrices \mathbb{S}_j for $j \in I(1, N)$ are known constant matrices and constitutes the vertices of the polytope \mathcal{P} .*

The class of uncertain systems with affine uncertain parameters is studied and represented using polytopic models in the remainder of this section. This study is of practical relevance since such kinds of parametric uncertainty affect real world plants. It is pertinent to draw to the attention of the reader that, in this dissertation, the analysis and design frameworks proposed for synthesising sliding mode controllers and observers consider systems with mismatched parametric uncertainties.

Let $\Theta \subseteq \mathbb{R}^r$ be the parameter space and let $\boldsymbol{\theta} = [\theta_1 \ \theta_2 \ \dots \ \theta_r]^T$ be a vector of real uncertain parameters where the uncertain parameter bounds

$$\underline{\theta}_i \leq \theta_i \leq \bar{\theta}_i \text{ for } i \in I(1, r) \quad (3.59)$$

define a *hyper-rectangle* in Θ . This convex set is also called *parameter box*. The uncertain parameter vector $\boldsymbol{\theta}$ can describe two kinds of uncertainties: time-invariant parametric uncertainties where $\boldsymbol{\theta}$ may correspond to physical parameters which are constant but unknown and for which only extreme values are known up to some accuracy, or time-varying parametric uncertainties where $\boldsymbol{\theta}$ represents a continuous

3.3 Parametric Uncertainty Description: Polytopic Models

time real vector-valued function, *i.e.* $\boldsymbol{\theta}(t) : \mathfrak{R}_+ \rightarrow \Theta$, whose upper and lower component bounds are known. For the sake of generality, uncertain time-varying parameters $\theta_i(t)$ with $i \in I(1, r)$ are considered. This consideration can be made since time-invariant uncertain parameters can be seen as a particular case of time-varying parameters in which $\theta(t)$ is constant $\forall t$.

Consider a dynamical system with parametric uncertainties described in state-space form by

$$\dot{\mathbf{x}}(t) = \mathbf{A}(\boldsymbol{\theta}(t))\mathbf{x}(t) + \mathbf{B}(\boldsymbol{\theta}(t))\mathbf{u}(t) \quad (3.60)$$

$$\mathbf{y}(t) = \mathbf{C}(\boldsymbol{\theta}(t))\mathbf{x}(t) + \mathbf{D}(\boldsymbol{\theta}(t))\mathbf{u}(t) \quad (3.61)$$

where $\mathbf{x} \in \mathfrak{R}^n$ is the state vector, $\mathbf{u} \in \mathfrak{R}^m$ is the input vector, and $\mathbf{y} \in \mathfrak{R}^p$ is the output vector. The uncertain matrices $\mathbf{A}(\boldsymbol{\theta}(t))$, $\mathbf{B}(\boldsymbol{\theta}(t))$, $\mathbf{C}(\boldsymbol{\theta}(t))$ and $\mathbf{D}(\boldsymbol{\theta}(t))$ are matrices of appropriate dimension and are assumed to be affine with respect to the vector of uncertain parameters $\boldsymbol{\theta}(t)$.

The system matrix for the uncertain system (3.60)-(3.61) is given by

$$\mathbb{S}(\boldsymbol{\theta}(t)) = \left[\begin{array}{c|c} \mathbf{A}(\boldsymbol{\theta}(t)) & \mathbf{B}(\boldsymbol{\theta}(t)) \\ \hline \mathbf{C}(\boldsymbol{\theta}(t)) & \mathbf{D}(\boldsymbol{\theta}(t)) \end{array} \right] \quad (3.62)$$

A polytope \mathcal{P} so that $\mathbb{S}(\boldsymbol{\theta}(t)) \in \mathcal{P}$ can be defined by calculating $N = 2^r$ system matrices \mathbb{S}_j generated for each vertex of \mathcal{P} and constructing the set of all convex combinations of such system matrices as follows

$$\mathcal{P} = \text{Co}\{\mathbb{S}_1, \mathbb{S}_2, \dots, \mathbb{S}_N\} = \left\{ \sum_{j=1}^{N=2^r} \mu_j \mathbb{S}_j : \sum_{j=1}^{N=2^r} \mu_j = 1, \mu_j \geq 0 \text{ for } j \in I(1, N) \right\} \quad (3.63)$$

where r is the number of uncertain parameters, and

$$\mathbb{S}_j = \left[\begin{array}{c|c} \mathbf{A}_j & \mathbf{B}_j \\ \hline \mathbf{C}_j & \mathbf{D}_j \end{array} \right] \text{ for } j \in I(1, N = 2^r) \quad (3.64)$$

The system matrices \mathbb{S}_j for $j \in I(1, N)$ are obtained by considering all combinations of the upper and lower bounds of the uncertain parameters. Figure 3.9 illustrates a parameter box for $\boldsymbol{\theta} \in \mathfrak{R}^3$ and the associated polytope of system matrices \mathbb{S}_j for $j \in I(1, 8)$.

3.3 Parametric Uncertainty Description: Polytopic Models

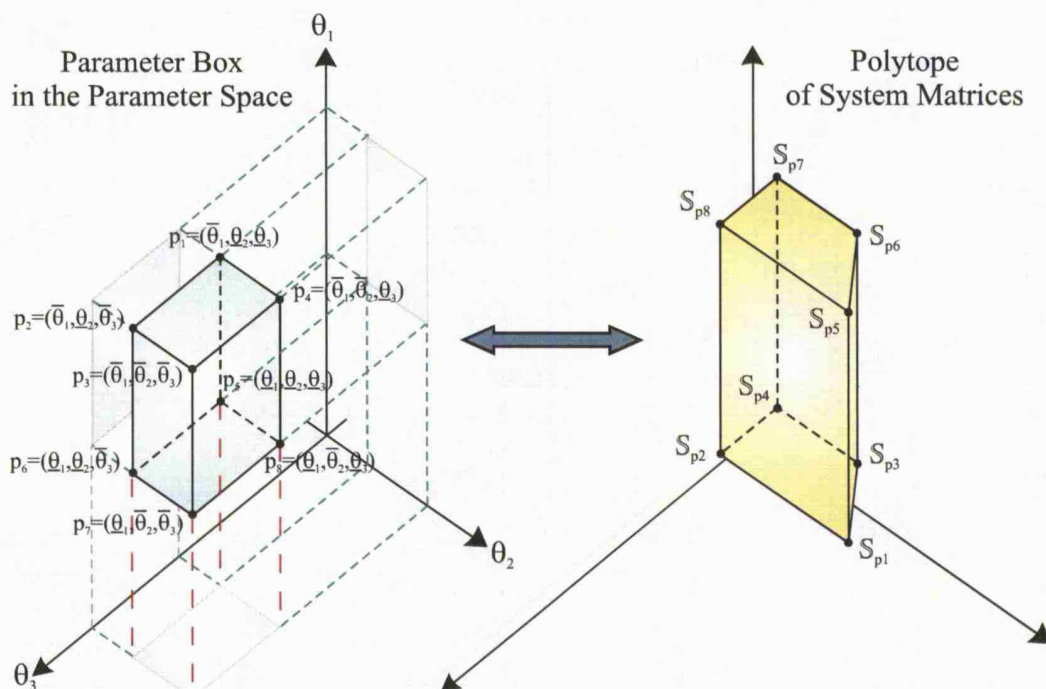


Figure 3.9: Mapping of a Parameter Box in a Polytope of System Matrices.

The uncertain matrices of the system given in (3.60)-(3.61) can be decomposed into nominal matrices and uncertain matrices depending affinely on the components of the uncertain vector $\boldsymbol{\theta}(t)$ as follows

$$\dot{\mathbf{x}}(t) = (\mathbf{A} + \Delta\mathbf{A}(\boldsymbol{\theta}(t)))\mathbf{x}(t) + (\mathbf{B} + \Delta\mathbf{B}(\boldsymbol{\theta}(t)))\mathbf{u}(t) \quad (3.65)$$

$$\mathbf{y}(t) = (\mathbf{C} + \Delta\mathbf{C}(\boldsymbol{\theta}(t)))\mathbf{x}(t) + (\mathbf{D} + \Delta\mathbf{D}(\boldsymbol{\theta}(t)))\mathbf{u}(t) \quad (3.66)$$

It has been shown that polytopic models describe affine parameter dependent systems for which upper and lower bounds are known up to some degree of accuracy. Note that uncertain systems of the form (3.65)-(3.66) can be interpreted as linear time-varying systems which can be represented using polytopic models as described at the beginning of this section. Hence, for the sake of simplicity in the notation, the following representation is considered

$$\dot{\mathbf{x}}(t) = (\mathbf{A} + \Delta\mathbf{A}(t))\mathbf{x}(t) + (\mathbf{B} + \Delta\mathbf{B}(t))\mathbf{u}(t) \quad (3.67)$$

$$\mathbf{y}(t) = (\mathbf{C} + \Delta\mathbf{C}(t))\mathbf{x}(t) + (\mathbf{D} + \Delta\mathbf{D}(t))\mathbf{u}(t) \quad (3.68)$$

3.4 Summary

More precisely, in this thesis, the following particular case of (3.67)-(3.68) is considered

$$\dot{\mathbf{x}}(t) = (\mathbf{A} + \Delta\mathbf{A}(t))\mathbf{x}(t) + \mathbf{B}(\mathbf{u}(t) + \xi(t, \mathbf{x}, \mathbf{u})) \quad (3.69)$$

$$\mathbf{y}(t) = \mathbf{C}\mathbf{x}(t) \quad (3.70)$$

where $\mathbf{x} \in \mathfrak{R}^n$ is the state vector, $\mathbf{u} \in \mathfrak{R}^m$ is the input vector, and $\mathbf{y} \in \mathfrak{R}^p$ is the output vector. The uncertain vector function $\xi(t, \mathbf{x}, \mathbf{u}) : \mathfrak{R}_+ \times \mathfrak{R}^n \times \mathfrak{R}^m \rightarrow \mathfrak{R}^m$ represents the lumped sum of matched nonlinearities and/or uncertainties. It is assumed to be norm bounded.

Remark 3.8 *If all components of the vector of uncertain parameters are constant for all instants of time, then the independent variable $t \in [0, \infty)$ is dropped in the uncertain matrices in (3.67)-(3.68) or (3.69).*

3.4 Summary

A mathematical tool which is applied throughout this thesis, so-called Linear Matrix Inequalities, has been described in this chapter. In this thesis, performance specifications and design constraints are formulated as LMI-based problems. LMI methods are significant, for many reasons, but most importantly because problems that cannot be analytically solved, may be numerically tractable via LMI methods. There are several computational software tools (free and commercial software) to solve efficiently feasibility and optimisation problems involving LMIs, *e.g.* LMI toolbox of MATLAB ¹ and SeDuMi ².

The main definitions associated with convexity of sets and functions have been presented. Furthermore, canonical and other forms of LMI formulations were formally reviewed. Mathematical operations on LMIs applied in the subsequent chapters of this thesis were presented. Concepts concerned with LMI regions (convex sets in the open left-half complex plane defining stability regions) were given and elementary LMI regions were defined in detail. These convex regions are employed in the synthesis approaches proposed in the sequel.

In this chapter, different sources of uncertainty in mathematical models were studied. Here, uncertainties were classified into structured (for example, parametric uncertainties) and non-structured uncertainties. Polytopic models, built on the concept of convexity (convex sets, convex combination, convex hull), have been presented for describing uncertain systems. It was shown in detail how general linear time-varying and affine uncertain parameter dependent systems can be described using polytopic models.

¹Commercial add on toolbox from The Mathworks.

²Free software, which runs under the MATLAB platform, developed by J. F. Sturm (Sturm, 1999).

3.4 Summary

Parametric uncertainties are of practical interest since such kinds of uncertainty affect real world plants. Finally, it has been highlighted that parametric uncertain systems represented by polytopic models are completely tractable via LMI methods. This is relevant because mismatched parametric uncertainties are considered throughout this thesis.

"...to regard old problems from a new angle, requires creative imagination and marks real advances in science."

Albert Einstein (1879 - 1955)

4

State Feedback SMC for Systems With Mismatched Uncertainties

4.1 Introduction

The invariance property (Draženović, 1969) of VSC systems with a sliding mode, as demonstrated in Section 2.4, is one of the most attractive characteristics of this nonlinear control scheme. This invariance can be guaranteed with respect to a class of uncertainty and exogenous disturbances during the sliding motion, if the so-called matching condition is satisfied, *i.e.* the uncertainties and/or disturbances lie within the range space of the input distribution matrix. Although some systems can be categorised as uncertain plants with matched uncertainty, there are many practical systems affected by mismatched uncertainty.

In this chapter, a synthesis methodology is proposed for the design of sliding mode controllers considering parametric mismatched uncertainties in the state matrix. The proposed approach employs robust pole clustering in convex regions of the complex left-half plane using LMI methods. The sliding mode existence problem is then formulated as a state feedback problem for the reduced-order system using a polytopic description considering the mismatched uncertainty affecting the state matrix. The control law is made up of linear and nonlinear parts as established in Section 2.5.3. The linear part is synthesised via LMI methods and a polytopic description of the design problem, whilst the nonlinear component is of the form (2.91), and is synthesised in such a way that the matched uncertainties, nonlinearities and/or exogenous disturbances are rejected completely.

The structure of this chapter is as follows: Section 4.2 defines the class of systems considered and describes the problem formulation. A design framework based on LMI

4.2 System Description and Problem Formulation

methods and polytopic models is presented in Section 4.3 for synthesising sliding surfaces and control laws considering full state information. A design example involving angular position control of a DC motor with parametric uncertainties is discussed in order to illustrate the proposed methodology and its efficacy. Then, Section 4.4 presents some concluding remarks.

4.2 System Description and Problem Formulation

Consider an uncertain dynamical system represented in state-space form $\forall t \geq 0$ by

$$\dot{\mathbf{x}}(t) = (\mathbf{A} + \Delta\mathbf{A}(t))\mathbf{x}(t) + \mathbf{B}(\mathbf{u}(t) + \xi(t, \mathbf{x}, \mathbf{u})) \quad (4.1)$$

where $\mathbf{x} \in \mathfrak{R}^n$ is the state vector and $\mathbf{u} \in \mathfrak{R}^m$ is the input vector. The uncertain vector function $\xi(t, \mathbf{x}, \mathbf{u}) : \mathfrak{R}_+ \times \mathfrak{R}^n \times \mathfrak{R}^m \rightarrow \mathfrak{R}^m$ represents the lumped sum of matched nonlinearities and/or uncertainties. It is assumed to be norm bounded.

Throughout this chapter, the following are assumed:

A-4.1 All state variables are available for measurement.

A-4.2 The input distribution matrix \mathbf{B} is full rank.

Since $\text{rank}(\mathbf{B}) = m$, there exists a similarity transformation $\mathbf{x}(t) \mapsto \mathbf{T}_R\mathbf{x}(t) = \tilde{\mathbf{x}}(t)$ such that the system nominal pair (\mathbf{A}, \mathbf{B}) can be written in regular form. That is,

$$\tilde{\mathbf{A}} = \begin{bmatrix} \tilde{\mathbf{A}}_{11} & \tilde{\mathbf{A}}_{12} \\ \tilde{\mathbf{A}}_{21} & \tilde{\mathbf{A}}_{22} \end{bmatrix}, \quad \tilde{\mathbf{B}} = \begin{bmatrix} \mathbf{0} \\ \tilde{\mathbf{B}}_2 \end{bmatrix} \quad (4.2)$$

where $\tilde{\mathbf{A}}_{11} \in \mathfrak{R}^{(n-m) \times (n-m)}$, $\tilde{\mathbf{A}}_{12} \in \mathfrak{R}^{(n-m) \times m}$, $\tilde{\mathbf{A}}_{21} \in \mathfrak{R}^{m \times (n-m)}$, $\tilde{\mathbf{A}}_{22} \in \mathfrak{R}^{m \times m}$, and $\tilde{\mathbf{B}}_2 \in \mathfrak{R}^{m \times m}$ are known constant matrices. Moreover, the input matrix sub-block $\tilde{\mathbf{B}}_2$ is such that $\det(\tilde{\mathbf{B}}_2) \neq 0$.

In this thesis, for the sake of generality, uncertain time-varying parameters $\theta_i(t)$ with $i \in I(1, r)$ are considered. Furthermore, $\Delta\mathbf{A}(t)$ is assumed to be affine in $\theta(t)$. The uncertain term $\xi(t, \mathbf{x}, \mathbf{u})$ and all matched components of the uncertainty associated with the state matrix, in the new coordinates, have been merged into $\tilde{\xi}_\Delta(t, \tilde{\mathbf{x}}, \mathbf{u})$.

It is assumed that:

A-4.3 The matched uncertainty is bounded by

$$\|\tilde{\xi}_\Delta(t, \tilde{\mathbf{x}}, \mathbf{u})\| \leq k_1\|\mathbf{u}(t)\| + \tilde{\varphi}(t, \tilde{\mathbf{x}}) + k_2 \quad (4.3)$$

4.3 State Feedback SMC Design Framework

where $\tilde{\varphi} : \mathfrak{R}_+ \times \mathfrak{R}^n \rightarrow \mathfrak{R}_+$ is a known function. Furthermore, $0 \leq k_1 < 1$ and $k_2 \geq 0$ are known constant scalars.

The uncertain system matrix $\tilde{\mathbf{A}}_\Delta(t) = \tilde{\mathbf{A}} + \Delta\tilde{\mathbf{A}}(t)$ in the new coordinate system therefore has the structure

$$\tilde{\mathbf{A}}_\Delta(t) = \begin{bmatrix} \tilde{\mathbf{A}}_{11} & \tilde{\mathbf{A}}_{12} \\ \tilde{\mathbf{A}}_{21} & \tilde{\mathbf{A}}_{22} \end{bmatrix} + \begin{bmatrix} \Delta\tilde{\mathbf{A}}_{11}(t) & \Delta\tilde{\mathbf{A}}_{12}(t) \\ 0 & 0 \end{bmatrix} \quad (4.4)$$

The design problem to be addressed can be broken down into two stages: firstly, design a sliding surface so that the sliding mode dynamics are stable despite the uncertainties. Secondly, synthesise a control law which induces a sliding motion on the sliding surface in finite time from any initial point in spite of the matched and mismatched uncertainties in the plant.

4.3 State Feedback SMC Design Framework

The design framework proposed in this section starts from a polytopic representation of the mismatched uncertainty associated with the system matrix. Subsequently, it makes use of LMI methods for synthesising the switching gain matrix $\mathbf{\Gamma}$. With regard to the control law, both matched and mismatched uncertainties are taken into account in the synthesis process.

4.3.1 Sliding Surface Design

Consider the sliding surface \mathcal{S}_{SF} defined as follows

$$\mathcal{S}_{SF} = \{ \mathbf{x} \in \mathfrak{R}^n : \boldsymbol{\sigma}(t) = \mathbf{\Gamma}\mathbf{x}(t) = \mathbf{0} \} \quad (4.5)$$

where $\boldsymbol{\sigma} \in \mathfrak{R}^m$ and the switching gain matrix is given by (Edwards & Spurgeon, 1998b):

$$\mathbf{\Gamma} = \mathbf{\Gamma}_2 \begin{bmatrix} \mathbf{K}_{SF} & \mathbf{I}_m \end{bmatrix} \mathbf{T}_R \quad (4.6)$$

The switching function $\boldsymbol{\sigma}(t)$ and its derivative are identically equal to zero during a sliding mode (Utkin, 1992). Hence

$$\tilde{\mathbf{x}}_2(t) = -\mathbf{K}_{SF}\tilde{\mathbf{x}}_1(t) \quad (4.7)$$

Consequently, the null space $\mathcal{N}(\mathbf{\Gamma})$ dynamics satisfy

$$\dot{\tilde{\mathbf{x}}}_1(t) = \left((\tilde{\mathbf{A}}_{11} + \Delta\tilde{\mathbf{A}}_{11}(t)) - (\tilde{\mathbf{A}}_{12} + \Delta\tilde{\mathbf{A}}_{12}(t))\mathbf{K}_{SF} \right) \tilde{\mathbf{x}}_1(t) \quad (4.8)$$

4.3 State Feedback SMC Design Framework

Writing

$$\tilde{\mathbf{A}}_{\Delta 11}(t) = (\tilde{\mathbf{A}}_{11} + \Delta \tilde{\mathbf{A}}_{11}(t)) \quad (4.9)$$

and

$$\tilde{\mathbf{A}}_{\Delta 12}(t) = (\tilde{\mathbf{A}}_{12} + \Delta \tilde{\mathbf{A}}_{12}(t)) \quad (4.10)$$

implies the reduced-order dynamics involving mismatched uncertainties are given by

$$\dot{\tilde{\mathbf{x}}}_1(t) = (\tilde{\mathbf{A}}_{\Delta 11}(t) - \tilde{\mathbf{A}}_{\Delta 12}(t)\mathbf{K}_{SF})\tilde{\mathbf{x}}_1(t) \quad (4.11)$$

Remark 4.1 Notice that the reduced-order system above does not exhibit the invariance property as in the case of systems with only matched uncertainties.

Remark 4.2 The matrix $\Gamma_2 \in \mathfrak{R}^{m \times m}$ has no direct effect on the sliding mode dynamics since it represents a scaling term of the switching matrix $\Gamma \in \mathfrak{R}^{m \times n}$.

Let $\mathbb{S}(t)$ be the pair $(\tilde{\mathbf{A}}_{\Delta 11}(t), \tilde{\mathbf{A}}_{\Delta 12}(t))$ given in block matrix form as

$$\mathbb{S}(t) := \left[\tilde{\mathbf{A}}_{\Delta 11}(t) \mid \tilde{\mathbf{A}}_{\Delta 12}(t) \right] \quad (4.12)$$

As $\boldsymbol{\theta}(t) \in \Theta$, and $\Delta \tilde{\mathbf{A}}(t)$ is affine in $\boldsymbol{\theta}(t)$, in the sliding mode existence problem, a polytope \mathcal{P}_{SF}^σ for $\mathbb{S}(t)$ can be constructed as follows

$$\mathcal{P}_{SF}^\sigma = \left\{ \sum_{j=1}^N \mu_j \mathbb{S}_j : \sum_{j=1}^N \mu_j = 1, \mu_j \geq 0 \text{ for } j \in I(1, N) \right\} \quad (4.13)$$

where N is the number of vertices of \mathcal{P}_{SF}^σ and

$$\mathbb{S}_j := \left[\tilde{\mathbf{A}}_{\Delta 11j} \mid \tilde{\mathbf{A}}_{\Delta 12j} \right] \quad (4.14)$$

The following is assumed:

A-4.4 the pairs $(\tilde{\mathbf{A}}_{\Delta 11j}, \tilde{\mathbf{A}}_{\Delta 12j})$ for $j \in I(1, N)$ are stabilisable for all admissible uncertainties in the hyper-rectangle contained in Θ .

Proposition 4.1 Let $\mathbf{Q}_1 \in \mathfrak{R}^{(n-m) \times (n-m)}$ be a symmetric positive definite (s.p.d.) matrix and $\mathbf{L}_{RO_1} \in \mathfrak{R}^{m \times (n-m)}$ such that $\mathbf{K}_{SF} = \mathbf{L}_{RO_1} \mathbf{Q}_1^{-1}$. The reduced-order system (4.11) is then quadratically stable if and only if

$$\mathbf{Q}_1 \tilde{\mathbf{A}}_{\Delta 11j}^T + \tilde{\mathbf{A}}_{\Delta 11j} \mathbf{Q}_1 - \mathbf{L}_{RO_1}^T \tilde{\mathbf{A}}_{\Delta 12j}^T - \tilde{\mathbf{A}}_{\Delta 12j} \mathbf{L}_{RO_1} < 0 \quad (4.15)$$

is satisfied for all $j \in I(1, N)$.

△

4.3 State Feedback SMC Design Framework

Proof Necessity (\implies) Quadratic stability of the reduced-order system (4.11) means that for a stabilising gain matrix \mathbf{K}_{SF} there exists a *Lyapunov* function

$$V_1(t) = \tilde{\mathbf{x}}_1^T(t) \mathbf{P}_1 \tilde{\mathbf{x}}_1(t) > 0 \quad (4.16)$$

where $\mathbf{P}_1 \in \mathfrak{R}^{(n-m) \times (n-m)}$ is a s.p.d. matrix. Computing the time derivative of (4.16) along the reduced-order system's trajectories gives

$$\dot{V}_1(t) = \dot{\tilde{\mathbf{x}}}_1^T(t) \mathbf{P}_1 \tilde{\mathbf{x}}_1(t) + \tilde{\mathbf{x}}_1^T(t) \mathbf{P}_1 \dot{\tilde{\mathbf{x}}}_1(t) < 0 \quad \forall \tilde{\mathbf{x}}_1(t) \in \mathfrak{R}^{(n-m)} \neq \mathbf{0} \quad (4.17)$$

Substituting (4.11) into (4.17), and manipulating algebraically yields

$$\dot{V}_1(t) = \tilde{\mathbf{x}}_1^T \left((\tilde{\mathbf{A}}_{\Delta 11}(t) - \tilde{\mathbf{A}}_{\Delta 12}(t) \mathbf{K}_{SF})^T \mathbf{P}_1 + \mathbf{P}_1 (\tilde{\mathbf{A}}_{\Delta 11}(t) - \tilde{\mathbf{A}}_{\Delta 12}(t) \mathbf{K}_{SF}) \right) \tilde{\mathbf{x}}_1 < 0 \quad (4.18)$$

for all $\tilde{\mathbf{x}}_1(t) \in \mathfrak{R}^{(n-m)} \neq \mathbf{0}$, and hence the following Bilinear Matrix Inequality (BMI) holds

$$\mathcal{A}_{RO}^T(t) \mathbf{P}_1 + \mathbf{P}_1 \mathcal{A}_{RO}(t) \prec 0 \quad (4.19)$$

where

$$\mathcal{A}_{RO}(t) = \tilde{\mathbf{A}}_{\Delta 11}(t) - \tilde{\mathbf{A}}_{\Delta 12}(t) \mathbf{K}_{SF} \quad (4.20)$$

Since the hyper-rectangle is a convex set defined by the extreme values of $\theta_i(t) \in \Theta$ for $i \in I(1, r)$, and the uncertain matrix $\Delta \tilde{\mathbf{A}}(t)$ is affine in $\theta(t)$, the vertex matrices for the reduced-order system (4.11), considering the definition of the polytope \mathcal{P}_{SF}^σ in (4.13) along with (4.14), are given by

$$\mathcal{A}_{RO_j} = \tilde{\mathbf{A}}_{\Delta 11j} - \tilde{\mathbf{A}}_{\Delta 12j} \mathbf{K}_{SF} \quad \text{for } j \in I(1, N) \quad (4.21)$$

The quadratic inequality (4.18) can be written as

$$\dot{V}_1(t) = \tilde{\mathbf{x}}_1^T \left(\sum_{j=1}^N \mu_j \mathcal{A}_{RO_j}^T \mathbf{P}_1 + \mathbf{P}_1 \sum_{j=1}^N \mu_j \mathcal{A}_{RO_j} \right) \tilde{\mathbf{x}}_1 < 0 \quad (4.22)$$

or

$$\sum_{j=1}^N \mu_j \left(\mathcal{A}_{RO_j}^T \mathbf{P}_1 + \mathbf{P}_1 \mathcal{A}_{RO_j} \right) \prec 0 \quad (4.23)$$

Consequently

$$\mathcal{A}_{RO_j}^T \mathbf{P}_1 + \mathbf{P}_1 \mathcal{A}_{RO_j} \prec 0 \quad \text{for } j \in I(1, N) \quad (4.24)$$

since $\mu_j \geq 0$ for $j \in I(1, N)$. This inequality is a BMI for each vertex of the polytope \mathcal{P}_{SF}^σ .

Pre and post-multiplying the set of BMIs given above by $\mathbf{Q}_1 \triangleq \mathbf{P}_1^{-1}$, *i.e.* applying

4.3 State Feedback SMC Design Framework

a congruence transformation, yields

$$\mathbf{Q}_1 \tilde{\mathbf{A}}_{\Delta 11j}^T + \tilde{\mathbf{A}}_{\Delta 11j} \mathbf{Q}_1 - \mathbf{Q}_1 \mathbf{K}_{SF}^T \tilde{\mathbf{A}}_{\Delta 12j}^T - \tilde{\mathbf{A}}_{\Delta 12j} \mathbf{K}_{SF} \mathbf{Q}_1 \prec 0 \quad (4.25)$$

for $j \in I(1, N)$. Defining a new decision variable $\mathbf{L}_{RO1} = \mathbf{K}_{SF} \mathbf{Q}_1$ converts the BMIs above into the LMIs defined in (4.15).

Sufficiency (\Leftarrow) Suppose the LMIs in (4.15) feasible. Hence, there exist matrices \mathbf{P}_1 and \mathbf{K}_{SF} which can be straightforwardly computed as follows $\mathbf{P}_1 = \mathbf{Q}_1^{-1}$ and $\mathbf{K}_{SF} = \mathbf{L}_{RO1} \mathbf{Q}_1^{-1}$. Then, after algebraic manipulation, it follows that

$$\mathcal{A}_{RO}^T(t) \mathbf{P}_1 + \mathbf{P}_1 \mathcal{A}_{RO}(t) \prec 0$$

holds. Therefore, there exists a *Lyapunov* function $V_1(t) = \tilde{\mathbf{x}}_1^T(t) \mathbf{P}_1 \tilde{\mathbf{x}}_1(t) > 0$ for the reduced-order (4.11) such that $\dot{V}_1(t) < 0 \quad \forall \tilde{\mathbf{x}}_1(t) \neq \mathbf{0}$. This, means that the reduced-order system (4.11) is quadratically stable.

Q.E.D.

In addition to the quadratic stability guaranteed when (4.15) is feasible, pole placement constraints can be imposed through an LMI region (Chilali *et al.*, 1999) established by the designer.

Let $\mathcal{H}(h)$ be a half-plane stability region delimited by a vertical line at $(-h, 0)$; let $\mathcal{D}(c_n, r_d)$ be a disk centered at $(-c_n, 0)$ with radius r_d ; and let $\mathcal{C}((0, 0), \alpha)$ be a conic sector centered at the origin of \mathbb{C} at an angle α with respect to the negative real axis of the complex left half-plane. The LMI region

$$\mathcal{D}(h, c_n, r_d, \alpha) = \mathcal{H}(h) \cap \mathcal{D}(c_n, r_d) \cap \mathcal{C}((0, 0), \alpha) \quad (4.26)$$

shown in Figure 4.1 will be considered in this chapter.

Proposition 4.2 *Let $\mathbf{Q}_1 \in \mathfrak{R}^{(n-m) \times (n-m)}$ be a s.p.d. matrix and $\mathbf{L}_{RO1} \in \mathfrak{R}^{m \times (n-m)}$ be such that $\mathbf{K}_{SF} = \mathbf{L}_{RO1} \mathbf{Q}_1^{-1}$. The reduced-order system (4.11) is quadratically stable and $\lambda(\tilde{\mathbf{A}}_{\Delta 11j} - \tilde{\mathbf{A}}_{\Delta 12j} \mathbf{K}_{SF}) \in \mathcal{D}(h, c_n, r_d, \alpha)$ for $j \in I(1, N)$ if and only if the following LMIs are satisfied*

$$\Psi_j + 2h\mathbf{Q}_1 \prec 0 \quad (4.27)$$

$$\begin{bmatrix} -r_d \mathbf{Q}_1 & \tilde{\mathbf{A}}_{\Delta 11j} \mathbf{Q}_1 - \tilde{\mathbf{A}}_{\Delta 12j} \mathbf{L}_{RO1} + c_n \mathbf{Q}_1 \\ * & -r_d \mathbf{Q}_1 \end{bmatrix} \prec 0 \quad (4.28)$$

$$\begin{bmatrix} \sin(\alpha) \Psi_j & \cos(\alpha) \Upsilon_j \\ * & \sin(\alpha) \Psi_j \end{bmatrix} \prec 0 \quad (4.29)$$

where

$$\Psi_j = \mathbf{Q}_1 \tilde{\mathbf{A}}_{\Delta 11j}^T + \tilde{\mathbf{A}}_{\Delta 11j} \mathbf{Q}_1 - \mathbf{L}_{RO_1}^T \tilde{\mathbf{A}}_{\Delta 12j}^T - \tilde{\mathbf{A}}_{\Delta 12j} \mathbf{L}_{RO_1} \quad (4.30)$$

and

$$\Upsilon_j = \tilde{\mathbf{A}}_{\Delta 11j} \mathbf{Q}_1 - \mathbf{Q}_1 \tilde{\mathbf{A}}_{\Delta 11j}^T - \tilde{\mathbf{A}}_{\Delta 12j} \mathbf{L}_{RO_1} + \mathbf{L}_{RO_1}^T \tilde{\mathbf{A}}_{\Delta 12j}^T \quad (4.31)$$

△

Proof This follows from Theorem 3.2 and similar arguments applied in Proposition 4.1.

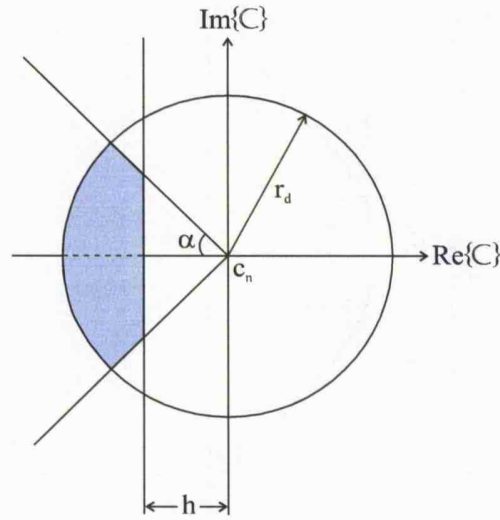


Figure 4.1: LMI Region $\mathcal{D}(h, c_n, r_d, \alpha)$

Remark 4.3 Notice that the LMIs (4.27)-(4.29) correspond to the half-plane stability region $\mathcal{H}(h)$, the disk $\mathcal{D}(c_n, r_d)$, and the conic sector $\mathcal{C}((0,0), \alpha)$ respectively.

Remark 4.4 Propositions 4.1 and 4.2 are constructive since if the associated LMIs are feasible, then the gain matrix \mathbf{K}_{SF} can be calculated, and hence a switching gain matrix of the form given in (4.6) can be designed.

4.3.2 Control Law Synthesis

Assume that an appropriate switching gain matrix $\mathbf{\Gamma}$ has been designed and define the nonsingular transformation matrix

$$\mathbf{T}_u = \begin{bmatrix} \mathbf{I}_{(n-m)} & \mathbf{0} \\ \mathbf{\Gamma}_1 & \mathbf{\Gamma}_2 \end{bmatrix} \quad (4.32)$$

4.3 State Feedback SMC Design Framework

The change of coordinates $\tilde{\mathbf{x}}(t) \mapsto \mathbf{T}_u \tilde{\mathbf{x}}(t) = \bar{\mathbf{x}}(t)$ yields

$$\dot{\tilde{\mathbf{x}}}_1(t) = \bar{\mathbf{A}}_{\Delta 11}(t)\tilde{\mathbf{x}}_1(t) + \tilde{\mathbf{A}}_{\Delta 12}(t)\Gamma_2^{-1}\tilde{\mathbf{x}}_2(t) \quad (4.33)$$

$$\dot{\tilde{\mathbf{x}}}_2(t) = \Gamma_2\bar{\mathbf{A}}_{\Delta 21}(t)\tilde{\mathbf{x}}_1(t) + \Gamma_2\bar{\mathbf{A}}_{\Delta 22}(t)\Gamma_2^{-1}\tilde{\mathbf{x}}_2(t) + \Gamma_2\tilde{\mathbf{B}}_2(\mathbf{u}(t) + \bar{\xi}_\Delta(t, \bar{\mathbf{x}}, \mathbf{u})) \quad (4.34)$$

where

$$\bar{\mathbf{A}}_{\Delta 11}(t) = \tilde{\mathbf{A}}_{\Delta 11}(t) - \tilde{\mathbf{A}}_{\Delta 12}(t)\mathbf{K}_{SF} \quad (4.35)$$

$$\bar{\mathbf{A}}_{\Delta 21}(t) = \mathbf{K}_{SF}\tilde{\mathbf{A}}_{\Delta 11}(t) + \tilde{\mathbf{A}}_{21} - \tilde{\mathbf{A}}_{22}\mathbf{K}_{SF} \quad (4.36)$$

$$\bar{\mathbf{A}}_{\Delta 22}(t) = \mathbf{K}_{SF}\tilde{\mathbf{A}}_{\Delta 12}(t) + \tilde{\mathbf{A}}_{22} \quad (4.37)$$

The transformed system (4.33)-(4.34) can be written in the compact form

$$\dot{\tilde{\mathbf{x}}}(t) = \mathcal{A}(t)\tilde{\mathbf{x}}(t) + \mathcal{B}(\mathbf{u}(t) + \bar{\xi}_\Delta(t, \bar{\mathbf{x}}, \mathbf{u})) \quad (4.38)$$

where

$$\begin{bmatrix} \dot{\tilde{\mathbf{x}}}_1(t) \\ \dot{\tilde{\mathbf{x}}}_2(t) \end{bmatrix} = \begin{bmatrix} \bar{\mathbf{A}}_{\Delta 11}(t) & \tilde{\mathbf{A}}_{\Delta 12}(t)\Gamma_2^{-1} \\ \Gamma_2\bar{\mathbf{A}}_{\Delta 21}(t) & \Gamma_2\bar{\mathbf{A}}_{\Delta 22}(t)\Gamma_2^{-1} \end{bmatrix} \begin{bmatrix} \tilde{\mathbf{x}}_1(t) \\ \tilde{\mathbf{x}}_2(t) \end{bmatrix} + \begin{bmatrix} \mathbf{0} \\ \Gamma_2\tilde{\mathbf{B}}_2 \end{bmatrix} (\mathbf{u}(t) + \bar{\xi}_\Delta(t, \bar{\mathbf{x}}, \mathbf{u})) \quad (4.39)$$

$$= \begin{bmatrix} \mathcal{A}_{11}(t) & \mathcal{A}_{12}(t) \\ \mathcal{A}_{21}(t) & \mathcal{A}_{22}(t) \end{bmatrix} \begin{bmatrix} \tilde{\mathbf{x}}_1(t) \\ \tilde{\mathbf{x}}_2(t) \end{bmatrix} + \begin{bmatrix} \mathbf{0} \\ \mathcal{B}_2 \end{bmatrix} (\mathbf{u}(t) + \bar{\xi}_\Delta(t, \bar{\mathbf{x}}, \mathbf{u})) \quad (4.40)$$

Let \mathbf{P} be a *Lyapunov* matrix partitioned as follows

$$\mathbf{P} \triangleq \begin{bmatrix} \mathbf{P}_1 & \mathbf{0} \\ \mathbf{0} & \mathbf{P}_2 \end{bmatrix} \succ 0 \quad (4.41)$$

such that $\mathbf{P}_1 \in \mathfrak{R}^{(n-m) \times (n-m)}$ is associated with the BMI (4.19) where $\mathcal{A}_{RO}(t) = \mathcal{A}_{11}(t)$. The component $\mathbf{P}_2 \in \mathfrak{R}^{m \times m}$ will be designed in the sequel.

The control law consists of two components

$$\mathbf{u}(t) = \mathbf{u}_L(t) + \mathbf{u}_{NL}(t) \quad (4.42)$$

where \mathbf{u}_L is the linear full-state feedback component and $\mathbf{u}_{NL}(t)$ is the nonlinear part. Although the control law above could potentially have only the nonlinear component, the linear term has an important effect in that the gain of the nonlinear component can be of a smaller magnitude.

The linear component $\mathbf{u}_L(t)$ is taken to have the form

$$\mathbf{u}_L(t) = -\mathcal{F}\tilde{\mathbf{x}}(t) \quad (4.43)$$

4.3 State Feedback SMC Design Framework

where $\mathcal{F} \in \mathfrak{R}^{m \times n}$, and the nonlinear component is given by

$$\mathbf{u}_{NL}(t) = \begin{cases} -\bar{\rho}(t, \bar{\mathbf{x}}, \mathbf{u}) \mathcal{B}_2^{-1} \frac{\mathbf{P}_2 \bar{\mathbf{x}}_2(t)}{\|\mathbf{P}_2 \bar{\mathbf{x}}_2(t)\|} & \text{if } \bar{\mathbf{x}}_2(t) \neq \mathbf{0} \\ 0 & \text{otherwise} \end{cases} \quad (4.44)$$

where the scalar function $\bar{\rho}(t, \bar{\mathbf{x}}, \mathbf{u})$ is such that

$$\bar{\rho}(t, \bar{\mathbf{x}}, \mathbf{u}) \geq \frac{\|\mathcal{B}_2\| (k_1 \|\mathbf{u}_L(t)\| + \bar{\varphi}(t, \bar{\mathbf{x}}) + k_2) + \eta}{1 - k_1 \kappa(\mathcal{B}_2)} \quad (4.45)$$

where

$$0 \leq k_1 \kappa(\mathcal{B}_2) < 1 \quad (4.46)$$

with

$$\kappa(\mathcal{B}_2) := \|\mathcal{B}_2^{-1}\| \|\mathcal{B}_2\| \quad (4.47)$$

and $\eta \in \mathfrak{R}_+$. Note also that by construction $\bar{\mathbf{x}}_2(t) = \sigma(t)$.

Assume the matched uncertainty in (4.38) is equal to zero, and there exists a gain matrix \mathcal{F} in (4.43) such that

$$(\mathcal{A}(t) - \mathcal{B}\mathcal{F})^T \mathbf{P} + \mathbf{P}(\mathcal{A}(t) - \mathcal{B}\mathcal{F}) \prec 0 \quad (4.48)$$

is satisfied.

Since the parameter box in Θ is a convex set and the uncertain system matrix $\mathcal{A}(t)$ is assumed to be affine in $\boldsymbol{\theta}(t)$, a polytope \mathcal{P}_{SF}^u can be constructed considering the pair $(\mathcal{A}(t), \mathcal{B})$ as follows

$$\mathcal{P}_{SF}^u = \left\{ \sum_{j=1}^N \mu_j \mathbb{S}_{u_j} : \sum_{j=1}^N \mu_j = 1, \mu_j \geq 0 \text{ for } j \in I(1, N) \right\} \quad (4.49)$$

where N is the number of vertices of \mathcal{P}_{SF}^u , and

$$\mathbb{S}_{u_j} := [\mathcal{A}_j \mid \mathcal{B}] \text{ for } j \in I(1, N) \quad (4.50)$$

Consequently, using the polytopic description given above, the matrix inequality (4.48) can be written as

$$\sum_{j=1}^N \mu_j (\mathcal{A}_j - \mathcal{B}\mathcal{F})^T \mathbf{P} + \mathbf{P} \sum_{j=1}^N \mu_j (\mathcal{A}_j - \mathcal{B}\mathcal{F}) \prec 0 \quad (4.51)$$

4.3 State Feedback SMC Design Framework

with $\sum_{j=1}^N \mu_j = 1$ and $\mu_j \geq 0$ for $j \in I(1, N)$, or equivalently as

$$\sum_{j=1}^N \mu_j \left((\mathcal{A}_j - \mathcal{B}\mathcal{F})^T \mathbf{P} + \mathbf{P}(\mathcal{A}_j - \mathcal{B}\mathcal{F}) \right) \prec 0 \quad (4.52)$$

Since $\mu_j \geq 0$ for $j \in I(1, N)$ a necessary and sufficient condition for (4.52) to hold is that

$$(\mathcal{A}_j - \mathcal{B}\mathcal{F})^T \mathbf{P} + \mathbf{P}(\mathcal{A}_j - \mathcal{B}\mathcal{F}) \prec 0 \quad \text{for } j \in I(1, N) \quad (4.53)$$

Write this matrix inequality conformably with (4.40) and partition the gain matrix

$$\mathcal{F} = \begin{bmatrix} F_1 & F_2 \end{bmatrix} \quad (4.54)$$

then, (4.53) is equivalent to

$$\begin{bmatrix} \mathcal{A}_{11j}^T \mathbf{P}_1 + \mathbf{P}_1 \mathcal{A}_{11j} & (\mathcal{A}_{21j} - \mathcal{B}_2 \mathcal{F}_1)^T \mathbf{P}_2 + \mathbf{P}_1 \mathcal{A}_{12j} \\ * & (\mathcal{A}_{22j} - \mathcal{B}_2 \mathcal{F}_2)^T \mathbf{P}_2 + \mathbf{P}_2 (\mathcal{A}_{22j} - \mathcal{B}_2 \mathcal{F}_2) \end{bmatrix} \prec 0 \quad (4.55)$$

for $j \in I(1, N)$.

Introducing a change of variable $\mathbf{Q} = \mathbf{P}^{-1}$, *i.e.*

$$\begin{bmatrix} \mathbf{Q}_1 & \mathbf{0} \\ \mathbf{0} & \mathbf{Q}_2 \end{bmatrix} = \begin{bmatrix} \mathbf{P}_1^{-1} & \mathbf{0} \\ \mathbf{0} & \mathbf{P}_2^{-1} \end{bmatrix} \quad (4.56)$$

and applying a congruence transformation, (4.55) is equivalent to

$$\begin{bmatrix} \mathbf{Q}_1 \mathcal{A}_{11j}^T + \mathcal{A}_{11j} \mathbf{Q}_1 & \mathbf{Q}_1 (\mathcal{A}_{21j} - \mathcal{B}_2 \mathcal{F}_1)^T + \mathcal{A}_{12j} \mathbf{Q}_2 \\ * & \mathbf{Q}_2 (\mathcal{A}_{22j} - \mathcal{B}_2 \mathcal{F}_2)^T + (\mathcal{A}_{22j} - \mathcal{B}_2 \mathcal{F}_2) \mathbf{Q}_2 \end{bmatrix} \prec 0 \quad (4.57)$$

for $j \in I(1, N)$.

Defining further matrix variables

$$\mathbf{L}_1 \triangleq \mathcal{F}_1 \mathbf{Q}_1 \quad \text{and} \quad \mathbf{L}_2 \triangleq \mathcal{F}_2 \mathbf{Q}_2 \quad (4.58)$$

yields

$$\begin{bmatrix} \mathbf{Q}_1 \mathcal{A}_{11j}^T + \mathcal{A}_{11j} \mathbf{Q}_1 & \mathbf{Q}_1 \mathcal{A}_{21j}^T - \mathbf{L}_1^T \mathcal{B}_2^T + \mathcal{A}_{12j} \mathbf{Q}_2 \\ * & \mathbf{Q}_2 \mathcal{A}_{22j}^T - \mathbf{L}_2^T \mathcal{B}_2^T + \mathcal{A}_{22j} \mathbf{Q}_2 - \mathcal{B}_2 \mathbf{L}_2 \end{bmatrix} \prec 0 \quad (4.59)$$

for $j \in I(1, N)$.

4.3 State Feedback SMC Design Framework

These are LMIs with \mathbf{Q}_1 , \mathbf{Q}_2 , \mathbf{L}_1 and \mathbf{L}_2 as matrix decision variables. The gain matrix \mathcal{F} in terms of these matrix variables is given by

$$\mathcal{F} = \begin{bmatrix} \mathcal{F}_1 & \mathcal{F}_2 \end{bmatrix} = \begin{bmatrix} \mathbf{L}_1 \mathbf{Q}_1^{-1} & \mathbf{L}_2 \mathbf{Q}_2^{-1} \end{bmatrix} \quad (4.60)$$

Proposition 4.3 *The control law (4.42) with linear state feedback (4.43) and nonlinear component (4.44) guarantees that a sliding motion takes place in finite time on the sliding surface \mathcal{S} defined in (2.3) inside the sliding patch*

$$\Omega_{SF} = \{ \bar{\mathbf{x}}_1 \in \mathbb{R}^{n-m}, \bar{\mathbf{x}}_2 \in \mathbb{R}^m : \|\bar{\mathbf{x}}_1\| < \eta \gamma^{-1} \} \quad (4.61)$$

where

$$\gamma = \max_{j \in I(1,n)} \{ \|\mathcal{A}_{21j} - \mathcal{B}_2 \mathcal{F}_1\| \} \quad (4.62)$$

and $\eta \in \mathbb{R}_+$.

△

Proof Using

$$\mathbf{u}(t) = -\mathcal{F}\bar{\mathbf{x}}(t) - \bar{\rho}(t, \bar{\mathbf{x}}, \mathbf{u}) \mathcal{B}_2^{-1} \frac{\mathbf{P}_2 \bar{\mathbf{x}}_2(t)}{\|\mathbf{P}_2 \bar{\mathbf{x}}_2(t)\|} \quad (4.63)$$

in (4.40) produces the following expression associated with the vector $\bar{\mathbf{x}}_2$

$$\dot{\bar{\mathbf{x}}}_2(t) = \mathcal{A}_{21}(t)\bar{\mathbf{x}}_1(t) + \mathcal{A}_{22}(t)\bar{\mathbf{x}}_2(t) - \bar{\rho}(t, \bar{\mathbf{x}}, \mathbf{u}) \frac{\mathbf{P}_2 \bar{\mathbf{x}}_2(t)}{\|\mathbf{P}_2 \bar{\mathbf{x}}_2(t)\|} + \mathcal{B}_2 \bar{\xi}_\Delta(t, \bar{\mathbf{x}}, \mathbf{u}) \quad (4.64)$$

where

$$\mathcal{A}_{21}(t) = \mathcal{A}_{21}(t) - \mathcal{B}_2 \mathcal{F}_1 \quad (4.65)$$

$$\mathcal{A}_{22}(t) = \mathcal{A}_{22}(t) - \mathcal{B}_2 \mathcal{F}_2 \quad (4.66)$$

Consider the *Lyapunov* function

$$\bar{V}_2(t) := \bar{\mathbf{x}}_2^T(t) \mathbf{P}_2 \bar{\mathbf{x}}_2(t) \quad (4.67)$$

Using the polytopic description of the pair $(\mathcal{A}_{21}(t), \mathcal{A}_{22}(t))$ defined in (4.49) along with the time derivative of (4.67) yields

4.3 State Feedback SMC Design Framework

$$\begin{aligned} \dot{\hat{V}}_2(t) = & \sum_{j=1}^N \mu_j \left(\mathcal{A}_{21j} \bar{\mathbf{x}}_1(t) + \mathcal{A}_{22j} \bar{\mathbf{x}}_2(t) - \bar{\rho}(t, \bar{\mathbf{x}}, \mathbf{u}) \frac{\mathbf{P}_2 \bar{\mathbf{x}}_2(t)}{\|\mathbf{P}_2 \bar{\mathbf{x}}_2(t)\|} + \mathcal{B}_2 \bar{\xi}_\Delta(t, \bar{\mathbf{x}}, \mathbf{u}) \right)^\top \mathbf{P}_2 \bar{\mathbf{x}}_2(t) \\ & + \bar{\mathbf{x}}_2^\top(t) \mathbf{P}_2 \sum_{j=1}^N \mu_j \left(\mathcal{A}_{21j} \bar{\mathbf{x}}_1(t) + \mathcal{A}_{22j} \bar{\mathbf{x}}_2(t) - \bar{\rho}(t, \bar{\mathbf{x}}, \mathbf{u}) \frac{\mathbf{P}_2 \bar{\mathbf{x}}_2(t)}{\|\mathbf{P}_2 \bar{\mathbf{x}}_2(t)\|} + \mathcal{B}_2 \bar{\xi}_\Delta(t, \bar{\mathbf{x}}, \mathbf{u}) \right) \end{aligned} \quad (4.68)$$

where

$$\mathcal{A}_{21j} = \mathcal{A}_{21j} - \mathcal{B}_2 \mathcal{F}_1 \quad (4.69)$$

$$\mathcal{A}_{22j} = \mathcal{A}_{22j} - \mathcal{B}_2 \mathcal{F}_2 \quad (4.70)$$

Define

$$\mathcal{M}_j \triangleq \mathcal{A}_{22j}^\top \mathbf{P}_2 + \mathbf{P}_2 \mathcal{A}_{22j} \quad (4.71)$$

which is negative definite (n.d.) by design. This follows from (4.55) and a *Schur* complement argument since (4.55) is equivalent to

$$(\mathcal{A}_{22j} - \mathcal{B}_2 \mathcal{F}_2)^\top \mathbf{P}_2 + \mathbf{P}_2 (\mathcal{A}_{22j} - \mathcal{B}_2 \mathcal{F}_2) \prec 0 \quad (4.72)$$

Replacing \mathcal{M}_j in (4.68) and using the fact that

$$\|\bar{\mathbf{x}}_2^\top \mathbf{P}_2 \mathcal{B}_2 \bar{\xi}_\Delta(t, \bar{\mathbf{x}}, \mathbf{u})\| \leq \|\mathbf{P}_2 \bar{\mathbf{x}}_2\| \|\mathcal{B}_2\| \|\bar{\xi}_\Delta(t, \bar{\mathbf{x}}, \mathbf{u})\| \quad (4.73)$$

produces

$$\begin{aligned} \dot{\hat{V}}_2(t) \leq & 2 \bar{\mathbf{x}}_2^\top(t) \mathbf{P}_2 \sum_{j=1}^N \mu_j \mathcal{A}_{21j} \bar{\mathbf{x}}_1(t) + \bar{\mathbf{x}}_2^\top(t) \sum_{j=1}^N \mu_j \mathcal{M}_j \bar{\mathbf{x}}_2(t) \\ & - 2 \|\mathbf{P}_2 \bar{\mathbf{x}}_2(t)\| (\bar{\rho}(t, \bar{\mathbf{x}}, \mathbf{u}) - \|\mathcal{B}_2\| \|\bar{\xi}_\Delta(t, \bar{\mathbf{x}}, \mathbf{u})\|) \end{aligned} \quad (4.74)$$

From (4.45)-(4.47), it follows

$$\bar{\rho}(t, \bar{\mathbf{x}}, \mathbf{u}) \geq \|\mathcal{B}_2\| (k_1 \|\mathbf{u}_L(t)\| + \bar{\varphi}(t, \bar{\mathbf{x}}) + k_2) + \eta + \bar{\rho}(t, \bar{\mathbf{x}}, \mathbf{u}) k_1 \|\mathcal{B}_2^{-1}\| \|\mathcal{B}_2\| \quad (4.75)$$

By rearrangement, inequality (4.75) becomes

$$\bar{\rho}(t, \bar{\mathbf{x}}, \mathbf{u}) \geq \|\mathcal{B}_2\| (k_1 (\|\mathbf{u}_L(t)\| + \bar{\rho}(t, \bar{\mathbf{x}}, \mathbf{u}) \|\mathcal{B}_2^{-1}\|) + \bar{\varphi}(t, \bar{\mathbf{x}}) + k_2) + \eta \quad (4.76)$$

and consequently

$$\bar{\rho}(t, \bar{\mathbf{x}}, \mathbf{u}) \geq \|\mathcal{B}_2\| (k_1 \|\mathbf{u}(t)\| + \bar{\varphi}(t, \bar{\mathbf{x}}) + k_2) + \eta \quad (4.77)$$

4.3 State Feedback SMC Design Framework

because

$$\|\mathbf{u}(t)\| = \|\mathbf{u}_L(t) + \mathbf{u}_{NL}(t)\| \leq \|\mathbf{u}_L(t)\| + \|\mathbf{u}_{NL}(t)\| \leq \|\mathbf{u}_L(t)\| + \bar{\rho}(t, \bar{\mathbf{x}}, \mathbf{u}) \|\mathcal{B}_2^{-1}\| \quad (4.78)$$

Considering (4.3), in the new coordinates, inequality (4.77) can straightforwardly be written as

$$\bar{\rho}(t, \bar{\mathbf{x}}, \mathbf{u}) \geq \|\mathcal{B}_2\| \|\bar{\xi}_\Delta(t, \bar{\mathbf{x}}, \mathbf{u})\| + \eta \quad (4.79)$$

and hence

$$\dot{V}_2(t) \leq 2\bar{\mathbf{x}}_2^\top(t) \mathbf{P}_2 \sum_{j=1}^N \mu_j \mathcal{A}_{21j} \bar{\mathbf{x}}_1(t) + \bar{\mathbf{x}}_2^\top(t) \sum_{j=1}^N \mu_j \mathcal{M}_j \bar{\mathbf{x}}_2(t) - 2\|\mathbf{P}_2 \bar{\mathbf{x}}_2(t)\| \eta \quad (4.80)$$

Finally, inside the sliding patch $\|\bar{\mathbf{x}}_1(t)\| < \eta\gamma^{-1}$, so

$$\dot{V}_2(t) < 2\|\mathbf{P}_2 \bar{\mathbf{x}}_2(t)\| \left(\sum_{j=1}^N \mu_j \|\mathcal{A}_{21j}\| \eta\gamma^{-1} - \eta \right) + \bar{\mathbf{x}}_2^\top(t) \sum_{j=1}^N \mu_j \mathcal{M}_j \bar{\mathbf{x}}_2(t) < 0 \quad (4.81)$$

since

$$\sum_{j=1}^N \mu_j \|\mathcal{A}_{21j}\| \gamma^{-1} \leq 1 \quad (4.82)$$

with

$$\gamma = \max_{j \in I(1,n)} \{\|\mathcal{A}_{21j}\|\} = \max_{j \in I(1,n)} \{\|\mathcal{A}_{21j} - \mathcal{B}_2 \mathcal{F}_1\|\} \quad (4.83)$$

and

$$\sum_{j=1}^N \mu_j = 1 \quad \text{and} \quad \mu_j \geq 0 \quad \text{for } j \in I(1, N) \quad (4.84)$$

Therefore, the sliding motion occurs in finite time, provided $\bar{\mathbf{x}}_1(t)$ remains in Ω_{SF} .

Q.E.D.

The design of the gain matrix \mathbf{F} in (4.85) consists of finding a solution, if there exists, to the LMI feasibility problem in (4.59).

Note, moreover, that the linear part of the control law in the original coordinates is given by

$$\mathbf{u}_L(t) = -\mathcal{F} \mathbf{T}_u \mathbf{T}_R \mathbf{x}(t) = -\mathbf{F} \mathbf{x}(t) \quad (4.85)$$

Since, $\bar{\rho}(t, \bar{\mathbf{x}}, \mathbf{u}) \xrightarrow{\bar{\mathbf{x}} = \mathbf{T}_u \mathbf{T}_R \mathbf{x}} \rho(t, \mathbf{x}, \mathbf{u})$ and $\bar{\mathbf{x}}_2(t) = \boldsymbol{\sigma}(t)$, the nonlinear component is given by

$$\mathbf{u}_{NL}(t) = \begin{cases} -\rho(t, \mathbf{x}, \mathbf{u}) \mathcal{B}_2^{-1} \frac{\mathbf{P}_2 \boldsymbol{\sigma}(t)}{\|\mathbf{P}_2 \boldsymbol{\sigma}(t)\|} & \text{if } \boldsymbol{\sigma}(t) \neq \mathbf{0} \\ \mathbf{0} & \text{otherwise} \end{cases} \quad (4.86)$$

4.3.3 Design Example

Conversion of electromechanical energy using rotating electric machines involves converting electrical energy into mechanical energy or vice versa. These machines can be classified depending on its energy conversion function as generators or motors. The former converts mechanical energy into electrical energy, and the latter absorbs energy in electric form and converts it into mechanical energy. In turn, electric rotating machines can be divided into Direct Current (DC) machines and Alternating Current (AC) machines.

DC motors are commonly used as electromechanical actuators in control systems. These kinds of motors can be found in many engineering applications, *e.g.* robotics, machine tools, aircraft actuators, valve actuators, the automotive industry, etc.

In (Chapman, 2005) DC motors are classified according to the field and armature connection into four main categories: (1) Separately excited DC motors, (2) shunt wound DC motors, (3) series wound DC motors, (4) permanent-magnet DC motors, and (4) compounded DC motors which can be cumulatively or differentially compounded DC motors.

A DC motor as other rotating electric machines are made up of two main components: the stator is the stationary or fixed part of the motor, whilst the rotor provides a mechanical rotary motion. Figure 4.2 shows a detailed schematic representation of a DC motor. The electromechanical diagram of a DC motor is presented in Figure 4.3.

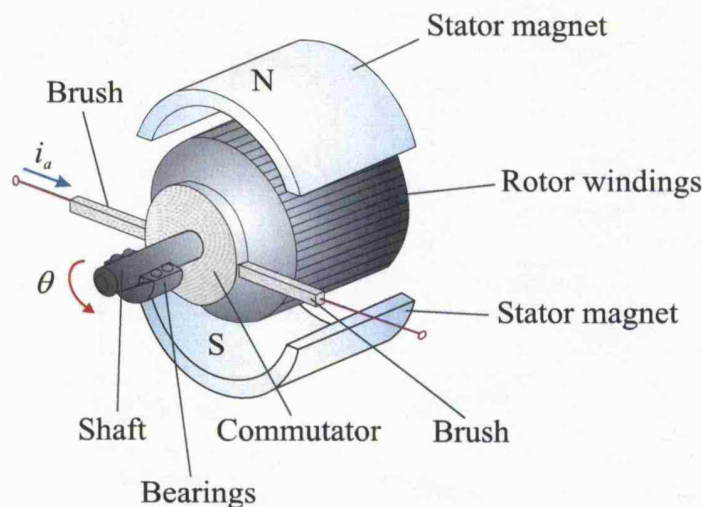


Figure 4.2: Schematic Diagram of a DC Motor (Figure adapted from (Franklin *et al.*, 2002) page 55)

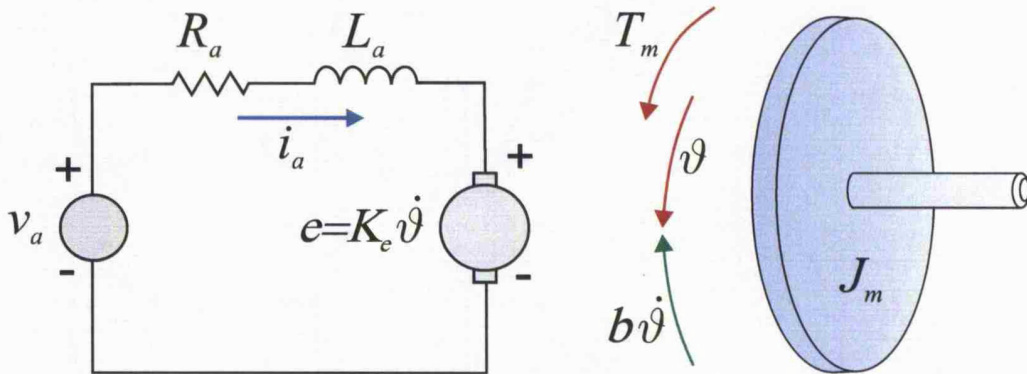


Figure 4.3: Electric and Mechanical Diagram of a DC Motor (Figure adapted from (Franklin *et al.*, 2002) page 54)

From a control viewpoint, DC motors can be either armature or field controlled. Since in this section an armature controlled DC motor is considered, only this scheme is described. In this case, the field current i_f is constant.

A mathematical model of an armature controlled DC motor can be constructed following the concepts presented in (Franklin *et al.*, 2002) (Ogata, 2002). This model comprises differential equations describing the electrical and mechanical dynamics of the system. The torque generated at the motor shaft is given by

$$T_m(t) = K_T i_a(t) \quad (4.87)$$

where K_T [Nm/A] is a torque constant or electromotive force (emf) constant, and $i_a(t)$ is the armature current [A]. The back emf voltage $e(t)$ induced in the armature is given by

$$e(t) = K_e \frac{d\vartheta(t)}{dt} \quad (4.88)$$

where K_e [Vsec/rad] is the electric constant, and $\vartheta(t)$ [rad] is the shaft angular position. By applying the *Kirchhoff's Voltage Law* (KVL), the following differential equation can be written

$$L_a \frac{di_a(t)}{dt} + R_a i_a(t) = v_a(t) - K_e \frac{d\vartheta(t)}{dt} \quad (4.89)$$

4.3 State Feedback SMC Design Framework

where L_a [H] is the armature inductance, R_a [Ω] is the armature resistance, and $v_a(t)$ [V] is the armature voltage.

In order to obtain the differential equation governing the mechanical dynamics of the DC motor, *Newton's* second law for rotations is applied producing

$$J_m \frac{d^2\vartheta(t)}{dt^2} + b \frac{d\vartheta(t)}{dt} = K_T i_a(t) \quad (4.90)$$

By defining state variables as

$$x_1(t) = \vartheta(t) \text{ [rad]} \quad , \quad x_2(t) = \frac{d\vartheta(t)}{dt} \text{ [rad/sec]} \quad , \quad x_3(t) = i_a(t) \text{ [A]} \quad (4.91)$$

and considering the armature voltage $v_a(t)$ as the input signal of the system, the following state-space representation of a DC motor results from differential equations (4.89)-(4.90):

$$\dot{\mathbf{x}}(t) = \begin{bmatrix} 0 & 1 & 0 \\ 0 & -\frac{b}{J_m} & \frac{K_T}{J_m} \\ 0 & -\frac{K_e}{L_a} & -\frac{R_a}{L_a} \end{bmatrix} \mathbf{x}(t) + \begin{bmatrix} 0 \\ 0 \\ \frac{1}{L_a} \end{bmatrix} u(t) \quad (4.92)$$

The constant parameters are: the viscous friction coefficient b [Nmsec], the motor torque constant K_T [Nm/A], the back emf constant K_e [V/(rad/sec)], and the armature resistance R_a [Ω]. Here, the moment of inertia J_m [kgm²] and the armature inductance L_a [H] are assumed to be uncertain parameters. The uncertain moment of inertia J_m can be written as

$$\frac{1}{J_m} = \frac{1}{J_{m_0}} + \delta_{J_m} \quad (4.93)$$

where J_{m_0} stands for the nominal inertia and the term δ_{J_m} is uncertain but bounded.

Define the error ratio $\delta_{L_a} \triangleq (L_{a_0} + L_a)/L_a$. This allows the uncertain armature inductance to be modelled as

$$\frac{1}{L_a} = \frac{1}{L_{a_0}} (1 + \delta_{L_a}) \quad (4.94)$$

where L_{a_0} denotes the nominal inductance.

The nominal parameter values of the DC motor under study are given in Table 4.1.

4.3 State Feedback SMC Design Framework

R_a [Ω]	L_{a0} [H]	J_{m0} [kgm ²]	K_T [Nm/A]	K_e [V/(rad/sec)]
1.20	0.05	0.135	0.60	0.60

Table 4.1: DC motor nominal parameters (Edwards & Spurgeon, 1998b)

It is assumed that the nominal viscous friction coefficient is $b = 0.01$ [Nmsec]. The uncertain terms δ_{J_m} and δ_{L_a} , are assumed to be $-2.41 \leq \delta_{J_m} \leq 2.60$ for $0.20 \geq J_m \geq 0.10$ and $|\delta_{L_a}| < 0.10$ (which means that the armature inductance is known up to an accuracy of 90 %).

A convex LMI region is defined so that the damping ratio is $\zeta = 0.95$ and the natural frequency $w_n = 2.0$. To this end, let $h = 1.9$, $c_n = 0$, $r_d = 13.0$ and $\alpha = 0.3176$. The design framework proposed in this chapter yields the following switching gain matrix

$$\Gamma = \begin{bmatrix} 4.1534 & 2.4110 & 1.0000 \end{bmatrix} \quad (4.95)$$

where $\Gamma_2 = 1$.

The eigenvalues of $\lambda(\tilde{\mathbf{A}}_{\Delta 11j} - \tilde{\mathbf{A}}_{\Delta 12j} \mathbf{K}_{SF})$ for $j \in I(1, 2)$ are $\{-2.7468, -4.5362\}$ and $\{-1.9800, -12.5861\}$.

The linear component of the control law (4.85) is

$$u_L(t) = \begin{bmatrix} -4.5011 & -2.2175 & -0.4021 \end{bmatrix} \mathbf{x}(t) \quad (4.96)$$

The eigenvalues of the closed loop using (4.96) are $\{-25.9069, -3.0924 \pm 0.9283i\}$ and $\{-1.9036, -15.1190 \pm 7.4268i\}$.

The nonlinear part of the control law has been designed considering the scalar gain $k_1 = 0.1$. The known function $\varphi(t, \mathbf{x})$ in (4.3) is given by

$$\varphi(t, \mathbf{x}) = 0.06|x_2(t)| + 0.12|x_3(t)| \quad (4.97)$$

and $k_2 = 0$.

The following cases were considered: (1) the nominal plant; (2) the uncertain plant with $L = 0.046$ [H] and $J = 0.10$ [kgm²]; (3) the uncertain plant with $L = 0.046$ [H] and $J = 0.20$ [kgm²]. The initial condition considered in all the computer simulations was $\begin{bmatrix} 1 & 0 & 0 \end{bmatrix}^T$. The time evolution of the state variables are shown in Figures 4.4, 4.5 and 4.6 for the three cases described above. Figure 4.7 depicts the control signals. The switching function for each simulation case is shown in Figure 4.8.

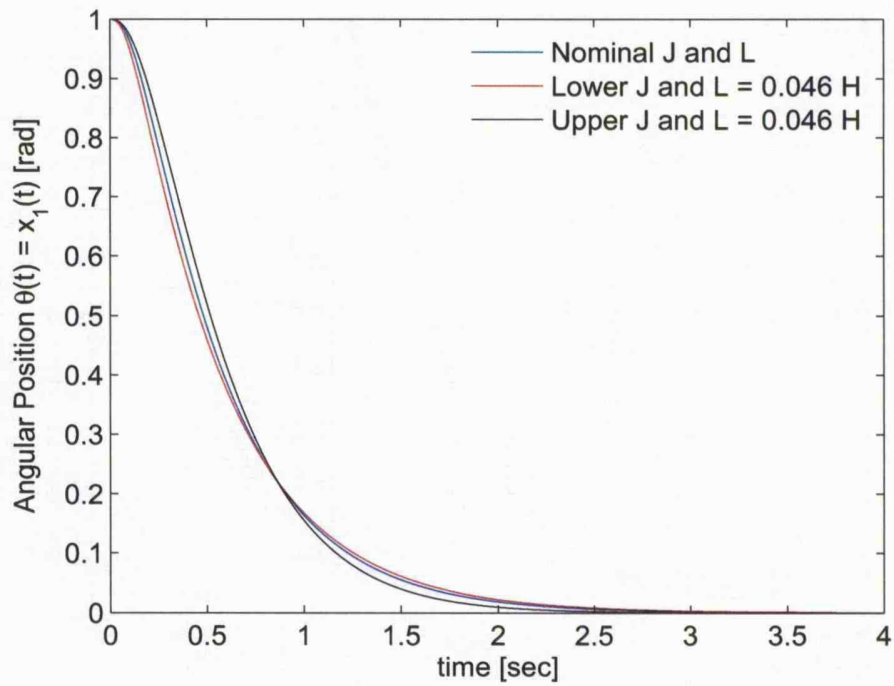


Figure 4.4: Angular position $\vartheta(t)$ [rad].

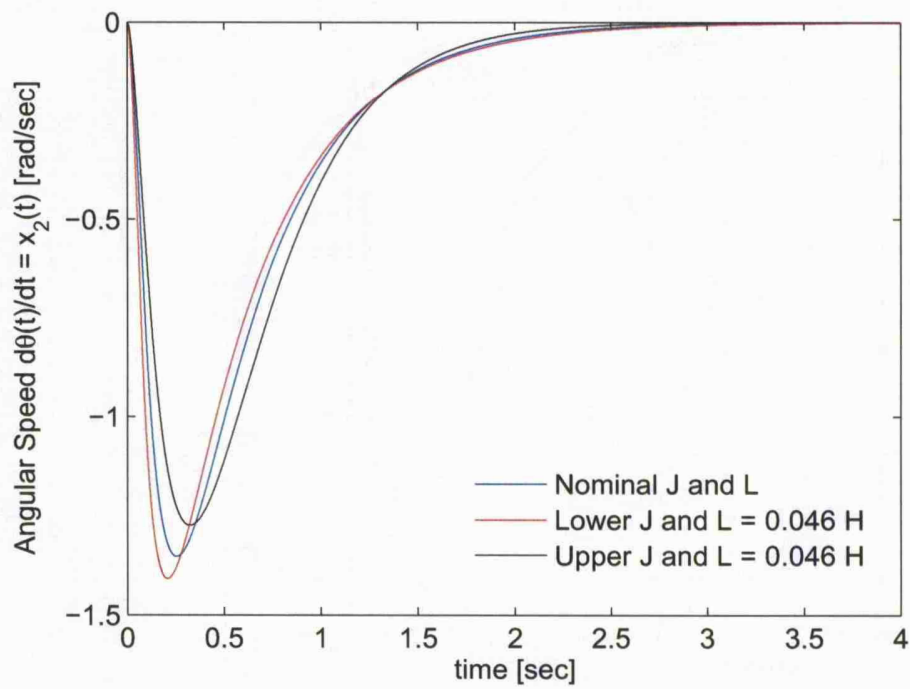


Figure 4.5: Angular speed $d\vartheta(t)/dt$ [rad/sec].

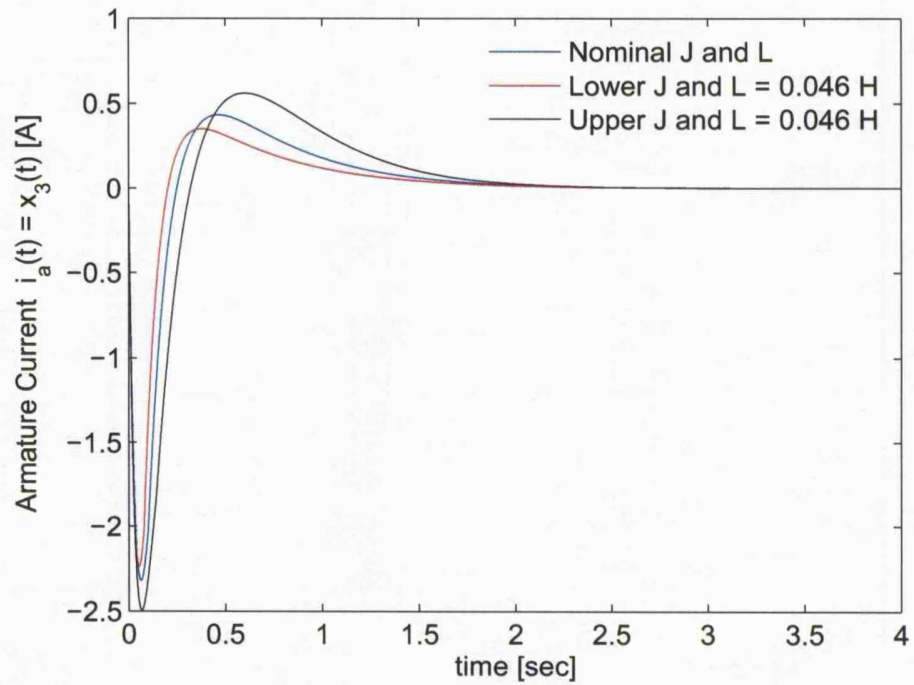


Figure 4.6: Armature current i_a [A].

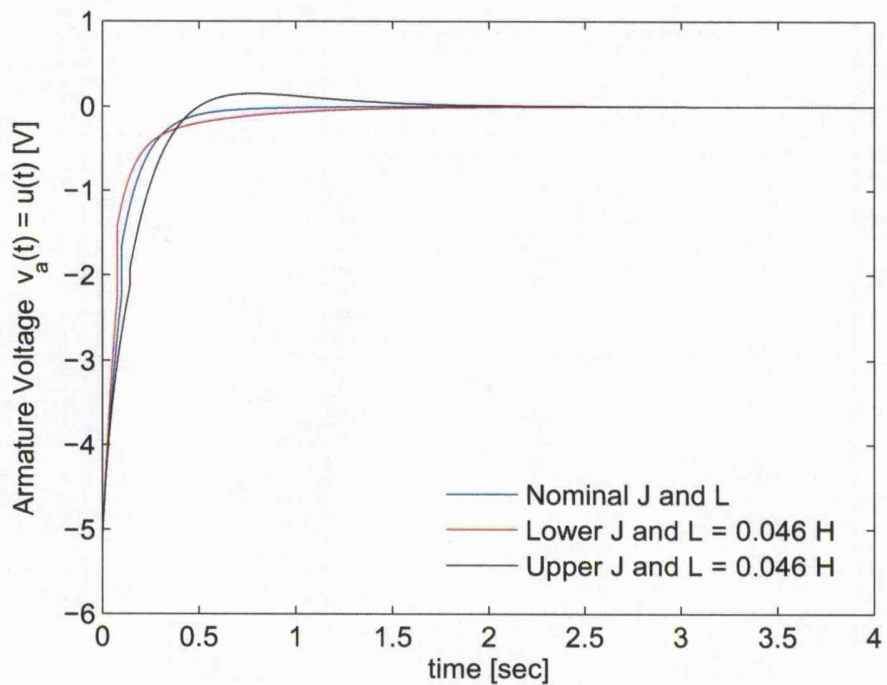


Figure 4.7: Armature voltage $v_a(t)$ [V].

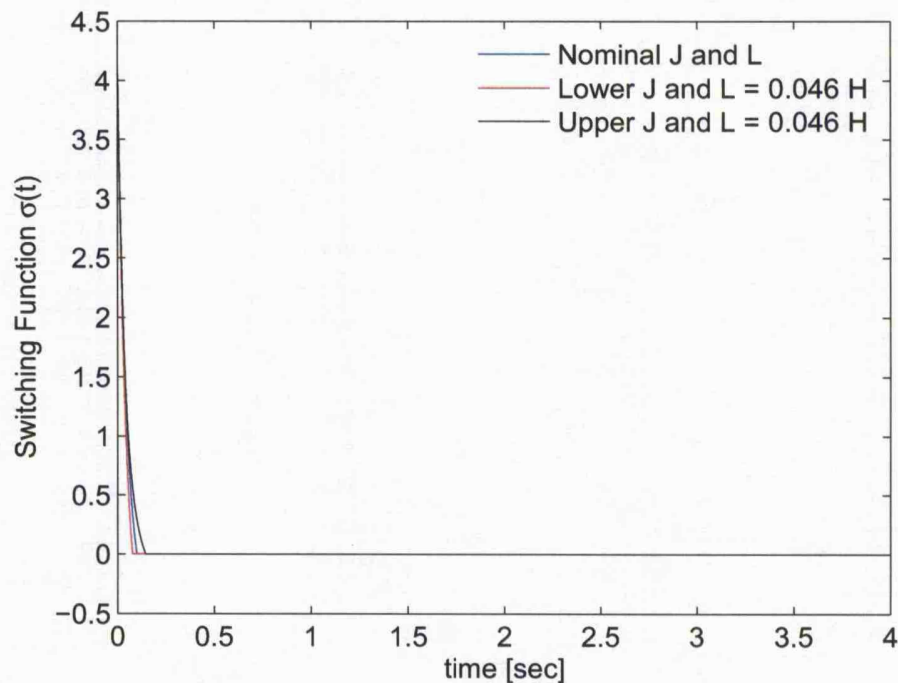


Figure 4.8: Switching functions.

Figures 4.4, 4.5 and 4.6 show that the designed sliding mode controller stabilises the DC motor in spite of the uncertain parameters J and L . After 2.5 sec, all state variables are essentially at the origin in the state space. The control effort shown in Figure 4.7 is smooth and from a practical viewpoint it is within an admissible range. It can be seen in Figure 4.8 that a sliding mode occurs between about 0.1 and 0.2 sec which can be considered fast enough for several engineering applications.

4.4 Summary

The effect of mismatched uncertainties on the reduced-order sliding mode dynamics has been studied. A sliding mode controller design approach based on LMI methods and a polytopic description of mismatched parametric uncertainties has been presented. This class of uncertainties is of practical interest in real world applications.

The switching function and control law use full state information. Although this assumption might be restrictive in some practical engineering problems, an argument supporting the use of full state feedback is the existence of estimation approaches which can reconstruct state variables.

The sliding mode existence and reachability problems have been dealt with using polytopic models. Robust pole clustering in LMI regions, considering mismatched

4.4 Summary

parametric uncertainties, has been employed for synthesising a parameterised sliding surface. The control law consists of two components and its design also takes into account both types of uncertainties. The gain matrix in the linear component of the control law is obtained by solving an LMI feasibility problem. The design of the nonlinear part is dependent on one of the matrix variables obtained when synthesising the linear component.

An example, considering angular position control of a DC motor involving matched and mismatched uncertainties, has illustrated the proposed synthesis framework and demonstrated its efficacy through computer simulations.

"A mathematical problem should be difficult in order to entice us, yet not completely inaccessible, lest it mock at our efforts. It should be to us a guide post on the mazy paths to hidden truths, and ultimately a reminder of our pleasure in the successful solution"

David Hilbert (1862 - 1943)

5

Sliding Mode Output Feedback Control: A Polytopic Approach

5.1 Introduction

Many of the early SMC approaches assumed that the state vector is accessible, and hence all state variables are available to the control law. This was the most limiting assumption made in the previous chapter. Although this assumption has allowed real applications to be tackled, it is quite restrictive, as in many applications only a subset of the state variables are physically measurable. Sometimes the state vector cannot be measured because some state variables do not have physical meaning, or perhaps software and hardware overhead costs to measure them may be high. There are two main ways of overcoming this problem: (1) static output feedback control, and (2) dynamic output feedback control. In this chapter, a design framework based on LMIs is presented for synthesising static and compensator-based output feedback sliding mode controllers. The existence and reachability problems are formulated using a polytopic description. The sliding surface and sliding mode control law design is based on LMIs. In this chapter, both matched and mismatched uncertainties are considered when synthesising the output feedback sliding mode controllers.

This chapter is organised as follows: firstly, the class of systems considered, and the formulation of the problems to be dealt with, are described in Section 5.2. Then, in Section 5.3, a static output feedback sliding mode controller design methodology is presented and design examples (a numerical example and one involving lateral control of an aircraft) illustrate the proposed approach. In Section 5.4, dynamic compensation is considered in such a way that compensator-based output feedback sliding mode controllers can be synthesised. A numerical example, involving a system which is not

5.2 System Description and Statement of Problems

stabilisable via sliding mode static output feedback control, demonstrates the effectiveness of the proposed methodology. Finally, some concluding remarks are drawn in Section 5.5.

5.2 System Description and Statement of Problems

Consider an uncertain dynamical system described in state-space form $\forall t \geq 0$ by

$$\left. \begin{aligned} \dot{\mathbf{x}}(t) &= (\mathbf{A} + \Delta\mathbf{A}(t))\mathbf{x}(t) + \mathbf{B}(\mathbf{u}(t) + \xi(t, \mathbf{x}, \mathbf{u})) \\ \mathbf{y}(t) &= \mathbf{C}\mathbf{x}(t) \end{aligned} \right\} \quad (5.1)$$

where $\mathbf{x} \in \mathfrak{R}^n$ is the state vector, $\mathbf{u} \in \mathfrak{R}^m$ is the input vector, and $\mathbf{y} \in \mathfrak{R}^p$ is the output vector. The uncertain function $\xi(t, \mathbf{x}, \mathbf{u}) : \mathfrak{R}_+ \times \mathfrak{R}^n \times \mathfrak{R}^m \rightarrow \mathfrak{R}^m$ represents the lumped sum of matched nonlinearities and/or uncertainties.

The following assumptions are postulated:

A-5.1 The order of the system and the number of output and input signals satisfy $n > p > m$.

A-5.2 The input and output matrices are both full rank, *i.e.* $rank(\mathbf{B}) = m$ and $rank(\mathbf{C}) = p$.

A-5.3 In the nominal triple $(\mathbf{A}, \mathbf{B}, \mathbf{C})$, $rank(\mathbf{CB}) = m$.

As discussed in Section 2.3.2, from assumption **A-5.3** there exists a similarity transformation in which the nominal triple $(\mathbf{A}, \mathbf{B}, \mathbf{C})$ of the system (5.1) can be written in the output feedback canonical form (Edwards & Spurgeon, 1995):

$$\bar{\mathbf{A}} = \begin{bmatrix} \bar{\mathbf{A}}_{11} & \bar{\mathbf{A}}_{12} \\ \bar{\mathbf{A}}_{21} & \bar{\mathbf{A}}_{22} \end{bmatrix}, \quad \bar{\mathbf{B}} = \begin{bmatrix} \mathbf{0} \\ \bar{\mathbf{B}}_2 \end{bmatrix}, \quad \bar{\mathbf{C}} = \begin{bmatrix} \mathbf{0} & \mathbf{T} \end{bmatrix} \quad (5.2)$$

where $\bar{\mathbf{A}}_{11} \in \mathfrak{R}^{(n-m) \times (n-m)}$, $\bar{\mathbf{A}}_{12} \in \mathfrak{R}^{(n-m) \times m}$, $\bar{\mathbf{A}}_{21} \in \mathfrak{R}^{m \times (n-m)}$, $\bar{\mathbf{A}}_{22} \in \mathfrak{R}^{m \times m}$, and $\bar{\mathbf{B}}_2 \in \mathfrak{R}^{m \times m}$ are known constant matrices. The state vector $\bar{\mathbf{x}}$ is partitioned conformably with (5.2) as follows

$$\bar{\mathbf{x}}(t) = \begin{bmatrix} \bar{\mathbf{x}}_1^T(t) & \bar{\mathbf{x}}_2^T(t) \end{bmatrix}^T \quad (5.3)$$

Assuming all matched components of the parametric uncertainty associated with the system matrix and $\xi(t, \mathbf{x}, \mathbf{u})$ have been incorporated into $\bar{\xi}_\Delta(t, \bar{\mathbf{x}}, \mathbf{u})$, the system matrix

$$\mathbf{A}_\Delta(t) = \mathbf{A} + \Delta\mathbf{A}(t) \quad (5.4)$$

5.2 System Description and Statement of Problems

in the new coordinates, has the structure

$$\bar{\mathbf{A}}_{\Delta}(t) = \bar{\mathbf{A}} + \Delta\bar{\mathbf{A}}(t) = \begin{bmatrix} \bar{\mathbf{A}}_{11} & \bar{\mathbf{A}}_{12} \\ \bar{\mathbf{A}}_{21} & \bar{\mathbf{A}}_{22} \end{bmatrix} + \begin{bmatrix} \Delta\bar{\mathbf{A}}_{11}(t) & \Delta\bar{\mathbf{A}}_{12}(t) \\ \mathbf{0} & \mathbf{0} \end{bmatrix} \quad (5.5)$$

Throughout this chapter the following assumptions are considered:

A-5.4 The matched uncertainty term $\bar{\xi}_{\Delta}(t, \bar{\mathbf{x}}, \mathbf{u})$ is bounded by

$$\|\bar{\xi}_{\Delta}(t, \bar{\mathbf{x}}, \mathbf{u})\| \leq k_1 \|\mathbf{u}(t)\| + \varphi(t, \mathbf{y}(t)) + k_2 \quad (5.6)$$

where $\varphi : \mathfrak{R}_+ \times \mathfrak{R}^p \rightarrow \mathfrak{R}_+$ is a known function. Furthermore, $0 \leq k_1 < 1$ and $k_2 \geq 0$ are known constant scalars.

A-5.5 The uncertain matrix $\Delta\bar{\mathbf{A}}(t)$ in (5.5) is affine with respect to the parameter vector $\boldsymbol{\theta}(t) \in \Theta$.

The *sliding surface* \mathcal{S}_{OF} is defined as follows

$$\mathcal{S}_{OF} = \{\mathbf{x} \in \mathfrak{R}^n : \boldsymbol{\sigma}(t) = \boldsymbol{\Gamma}\mathbf{y}(t) = \boldsymbol{\Gamma}\mathbf{C}\mathbf{x}(t) = \mathbf{0}\} \quad (5.7)$$

where $\boldsymbol{\sigma}(t) \in \mathfrak{R}^m$ and $\boldsymbol{\Gamma} \in \mathfrak{R}^{m \times p}$. The switching gain matrix $\boldsymbol{\Gamma}$ is parameterised as

$$\boldsymbol{\Gamma} = \boldsymbol{\Gamma}_2 \begin{bmatrix} \mathbf{K}_{OF} & \mathbf{I}_m \end{bmatrix} \mathbf{T}^T \quad (5.8)$$

where $\boldsymbol{\Gamma}_2 \in \mathfrak{R}^{m \times m}$ is nonsingular and $\mathbf{K}_{OF} \in \mathfrak{R}^{m \times (p-m)}$.

Using similar arguments to those presented in Section 2.3.2, but now considering the uncertain system (5.1) yields the following reduced-order system

$$\dot{\bar{\mathbf{x}}}_1(t) = (\bar{\mathbf{A}}_{\Delta 11}(t) - \bar{\mathbf{A}}_{\Delta 12}(t)\mathbf{K}_{OF}\mathbf{C}_1)\bar{\mathbf{x}}_1(t) \quad (5.9)$$

where

$$\bar{\mathbf{A}}_{\Delta 11}(t) = (\bar{\mathbf{A}}_{11} + \Delta\bar{\mathbf{A}}_{11}(t)) \quad (5.10)$$

$$\bar{\mathbf{A}}_{\Delta 12}(t) = (\bar{\mathbf{A}}_{12} + \Delta\bar{\mathbf{A}}_{12}(t)) \quad (5.11)$$

and \mathbf{C}_1 is defined in 2.43.

The reduced-order dynamics (5.9) correspond to an output feedback problem involving mismatched uncertainties.

SMSOF Control Problem: Design a switching gain matrix $\boldsymbol{\Gamma}$ of the form (5.8) such that the sliding dynamics (5.9) are stable. Furthermore, synthesise a SMC law which guarantees a finite time reaching phase from any initial point $\mathbf{x}(t_0) = \mathbf{x}_0 \notin \mathcal{S}_{OF}$ in the state space \mathcal{X} to the sliding surface.

△

5.2 System Description and Statement of Problems

In some particular cases, the existence problem for systems given by (5.1) with matched and mismatched uncertainties cannot be solved, as the following *bilinear matrix inequality* (BMI) is not feasible (*i.e.* the uncertain reduced-order system (5.9) is not static output feedback stabilisable):

$$(\bar{\mathbf{A}}_{\Delta 11}(t) - \bar{\mathbf{A}}_{\Delta 12}(t)\mathbf{K}_{oF}\mathbf{C}_1)^T \mathbf{P}_1 + \mathbf{P}_1(\bar{\mathbf{A}}_{\Delta 11}(t) - \bar{\mathbf{A}}_{\Delta 12}(t)\mathbf{K}_{oF}\mathbf{C}_1) \prec 0 \quad (5.12)$$

where $\bar{\mathbf{A}}_{\Delta 11}(t)$ and $\bar{\mathbf{A}}_{\Delta 12}(t)$ have been defined in (5.10) and (5.11) respectively.

This problem can be addressed by adding extra dynamics through a compensator providing further degrees of freedom for synthesising a sliding surface. Consider a dynamic compensator of the same form as in (Edwards & Spurgeon, 2003) described by

$$\dot{\mathbf{x}}_c(t) = \mathbf{\Xi}\mathbf{x}_c(t) + \mathbf{\Psi}\mathbf{y}(t) \quad (5.13)$$

where $\mathbf{\Xi} \in \mathfrak{R}^{q \times q}$ and $\mathbf{\Psi} \in \mathfrak{R}^{q \times p}$, and a sliding surface in the augmented state space $\mathcal{X}_a \subseteq \mathfrak{R}^{n+q}$ defined as

$$\mathcal{S}_{oF_a} = \{\mathbf{x}_a \in \mathfrak{R}^{n+q} : \boldsymbol{\sigma}_a(t) = \mathbf{\Gamma}_c \mathbf{x}_c(t) + \mathbf{\Gamma} \mathbf{C} \mathbf{x}(t) = \mathbf{0}\} \quad (5.14)$$

where $\mathbf{x}_a = [\mathbf{x}_c^T \quad \mathbf{x}^T]^T$ is the augmented state vector, $\boldsymbol{\sigma}_a(t) \in \mathfrak{R}^m$ is the *augmented switching function*, whilst $\mathbf{\Gamma}_c \in \mathfrak{R}^{m \times q}$ and $\mathbf{\Gamma} \in \mathfrak{R}^{m \times p}$ are components of the *augmented switching gain matrix* $\mathbf{\Gamma}_a = [\mathbf{\Gamma}_c \quad \mathbf{\Gamma}]$ to be synthesised.

Let

$$\mathbf{\Psi} \mathbf{T} = [\mathbf{\Psi}_1 \quad \mathbf{\Psi}_2] \quad (5.15)$$

where $\mathbf{\Psi}_1 \in \mathfrak{R}^{q \times (p-m)}$ and $\mathbf{\Psi}_2 \in \mathfrak{R}^{q \times m}$.

Consequently, the dynamic compensator (5.13), considering $\mathbf{y}(t) = \bar{\mathbf{C}}\bar{\mathbf{x}}(t) = [\mathbf{0} \quad \mathbf{T}] \bar{\mathbf{x}}(t)$ and the state vector partition (5.3), can be written as follows

$$\dot{\mathbf{x}}_c(t) = \mathbf{\Xi}\mathbf{x}_c(t) + \mathbf{\Psi}_1 \mathbf{C}_1 \bar{\mathbf{x}}_1(t) + \mathbf{\Psi}_2 \bar{\mathbf{x}}_2(t) \quad (5.16)$$

where

$$\mathbf{C}_1 = [\mathbf{0}_{(p-m) \times (n-p)} \quad \mathbf{I}_{(p-m)}] \quad (5.17)$$

During the sliding mode,

$$\boldsymbol{\sigma}_a = \mathbf{\Gamma}_1 \mathbf{C}_1 \bar{\mathbf{x}}_1 + \mathbf{\Gamma}_2 \bar{\mathbf{x}}_2 + \mathbf{\Gamma}_c \mathbf{x}_c = \mathbf{0} \quad (5.18)$$

Since $\mathbf{\Gamma}_2$ is nonsingular, equation (5.18) can be multiplied by $\mathbf{\Gamma}_2^{-1}$ producing

$$\mathbf{K}_{oF} \mathbf{C}_1 \bar{\mathbf{x}}_1 + \bar{\mathbf{x}}_2 + \mathbf{K}_c \mathbf{x}_c = \mathbf{0} \quad (5.19)$$

5.3 Sliding Mode Static Output Feedback Control

where $\mathbf{K}_{OF} \in \mathfrak{R}^{m \times (p-m)}$ and $\mathbf{K}_c \in \mathfrak{R}^{m \times q}$ are defined as

$$\mathbf{K}_{OF} \triangleq \Gamma_2^{-1} \Gamma_1 \quad (5.20)$$

$$\mathbf{K}_c \triangleq \Gamma_2^{-1} \Gamma_c \quad (5.21)$$

Now, consider the following set of first order differential equations describing the dynamics of the null space $\mathcal{N}(\Gamma_a)$ of the uncertain system (5.1) given by

$$\dot{\bar{\mathbf{x}}}_1(t) = \bar{\mathbf{A}}_{\Delta 11}(t) \bar{\mathbf{x}}_1(t) + \bar{\mathbf{A}}_{\Delta 12}(t) \bar{\mathbf{x}}_2(t) \quad (5.22)$$

Then, substituting for $\bar{\mathbf{x}}_2(t)$ from (5.19) in (5.22) and (5.16), yields the following reduced-order sliding mode system

$$\dot{\bar{\mathbf{x}}}_1(t) = (\bar{\mathbf{A}}_{\Delta 11}(t) - \bar{\mathbf{A}}_{\Delta 12}(t) \mathbf{K}_{OF} \mathbf{C}_1) \bar{\mathbf{x}}_1(t) - \bar{\mathbf{A}}_{\Delta 12}(t) \mathbf{K}_c \mathbf{x}_c(t) \quad (5.23)$$

$$\dot{\mathbf{x}}_c(t) = (\Psi_1 - \Psi_2 \mathbf{K}_{OF}) \mathbf{C}_1 \bar{\mathbf{x}}_1(t) + (\Xi - \Psi_2 \mathbf{K}_c) \mathbf{x}_c(t) \quad (5.24)$$

SMDOF Control Problem: Find Ξ , Ψ_1 , Ψ_2 , \mathbf{K}_{OF} and \mathbf{K}_c so that

$$\Upsilon(t) = \begin{bmatrix} (\bar{\mathbf{A}}_{\Delta 11}(t) - \bar{\mathbf{A}}_{\Delta 12}(t) \mathbf{K}_{OF} \mathbf{C}_1) & -\bar{\mathbf{A}}_{\Delta 12}(t) \mathbf{K}_c \\ (\Psi_1 - \Psi_2 \mathbf{K}_{OF}) \mathbf{C}_1 & (\Xi - \Psi_2 \mathbf{K}_c) \end{bmatrix} \quad (5.25)$$

is stable. This defines both the compensator and the augmented sliding surface (to be discussed in Section 5.4). Furthermore, design a sliding mode control law such that the sliding surface \mathcal{S}_{OF_a} is reached in finite time from any initial point $\mathbf{x}_a(t_0) \notin \mathcal{S}_{OF_a}$ in the augmented state space \mathcal{X}_a and a sliding motion takes place thereafter.

△

5.3 Sliding Mode Static Output Feedback Control

In the sequel, the existence and reachability sliding mode control problems are formulated from a polytopic perspective via LMIs.

5.3.1 Sliding Surface Design

Let $\mathbb{S}(t)$ be the block matrix form of the triple $(\bar{\mathbf{A}}_{\Delta 11}(t), \bar{\mathbf{A}}_{\Delta 12}(t), \mathbf{C}_1)$ given by

$$\mathbb{S}(t) = \left[\begin{array}{c|c} \bar{\mathbf{A}}_{\Delta 11}(t) & \bar{\mathbf{A}}_{\Delta 12}(t) \\ \hline \mathbf{C}_1 & \mathbf{0} \end{array} \right] \quad (5.26)$$

5.3 Sliding Mode Static Output Feedback Control

and let \mathbb{S}_j be the block matrix form of the triple $(\bar{\mathbf{A}}_{\Delta_{11j}}, \bar{\mathbf{A}}_{\Delta_{12j}}, \mathbf{C}_1)$ given by

$$\mathbb{S}_j = \left[\begin{array}{c|c} \bar{\mathbf{A}}_{\Delta_{11j}} & \bar{\mathbf{A}}_{\Delta_{12j}} \\ \hline \mathbf{C}_1 & \mathbf{0} \end{array} \right] \quad (5.27)$$

then a polytope can be constructed as follows

$$\mathcal{P}_{O_F}^\sigma = \left\{ \sum_{j=1}^N \mu_j \mathbb{S}_j : \sum_{j=1}^N \mu_j = 1, \mu_j \geq 0 \text{ for } j \in I(1, N) \right\} \quad (5.28)$$

where N is the number of vertices of $\mathcal{P}_{O_F}^\sigma$. These vertices can be computed using

$$\bar{\mathbf{A}}_{\Delta_{1kj}} = \bar{\mathbf{A}}_{1k} + \Delta \bar{\mathbf{A}}_{1kj} = \bar{\mathbf{A}}_{1k} + \sum_{i=1}^r \theta_i \Delta \mathbf{A}_{1ki} \Big|_{\theta_i = \{\underline{\theta}_i, \bar{\theta}_i\}} \quad (5.29)$$

for $k \in I(1, 2)$ and $j \in I(1, N = 2^r)$ and \mathbf{C}_1 is defined in (5.17). Note that permutation of the uncertain parameters θ_i for $i \in I(1, r)$, considering the upper and lower bounds, is applied in order to calculate $\bar{\mathbf{A}}_{\Delta_{1kj}}$ defined in (5.29).

The following is assumed:

A-5.6 The system triples $(\bar{\mathbf{A}}_{\Delta_{11j}}, \bar{\mathbf{A}}_{\Delta_{12j}}, \mathbf{C}_1)$ for $j \in I(1, N)$ are stabilisable and detectable.

The vertices of the polytope $\mathcal{P}_{O_F}^\sigma$ are said to be simultaneously stabilised by the gain matrix \mathbf{K}_{O_F} if there exists a s.p.d *Lyapunov* matrix $\mathbf{P}_1 \in \mathbb{R}^{(n-m) \times (n-m)}$ such that

$$\left(\bar{\mathbf{A}}_{\Delta_{11j}} - \bar{\mathbf{A}}_{\Delta_{12j}} \mathbf{K}_{O_F} \mathbf{C}_1 \right)^T \mathbf{P}_1 + \mathbf{P}_1 \left(\bar{\mathbf{A}}_{\Delta_{11j}} - \bar{\mathbf{A}}_{\Delta_{12j}} \mathbf{K}_{O_F} \mathbf{C}_1 \right) \prec 0 \quad (5.30)$$

for all $j \in I(1, N)$.

As the synthesis of the gain \mathbf{K}_{O_F} corresponds to a static output feedback problem for the system triple $(\bar{\mathbf{A}}_{\Delta_{11}}(t), \bar{\mathbf{A}}_{\Delta_{12}}(t), \mathbf{C}_1)$ any available LMI approach for polytopic models could be employed. Here the non-iterative LMI-based algorithm proposed in (Benton & Smith, 1999) is applied. An important feature of *Benton & Smith's* approach is its simplicity, but the main drawback is the difficulty in finding a suitable state feedback gain \mathbf{K}_{S_F} such that the system is *Simultaneously K-Stabilisable and Detectable* (Benton & Smith, 1999).

The *Benton & Smith* algorithm is now formulated for the SMSOFC existence problem as follows:

Step 1) Define the N vertices of the polytopic model.

5.3 Sliding Mode Static Output Feedback Control

Step 2) Define a degree of stability such that

$$\bar{\mathbf{A}}_{\Delta_{11\alpha j}} = \bar{\mathbf{A}}_{\Delta_{11j}} + \alpha \mathbf{I}_{(n-m)} \quad \text{for } j \in I(1, N)$$

Step 3) Solve the following optimisation problem

$$\begin{aligned} \min \quad & \text{trace}(\mathbf{Q}_{SF}) \\ \text{s.t.} \quad & \end{aligned}$$

$$\begin{aligned} \mathbf{Q}_{SF} & \succ \mathbf{I}_{(n-m)} \\ \mathbf{Q}_{SF} \bar{\mathbf{A}}_{\Delta_{11\alpha j}}^T + \bar{\mathbf{A}}_{\Delta_{11\alpha j}} \mathbf{Q}_{SF} + \mathbf{Y}_{SF}^T \bar{\mathbf{A}}_{\Delta_{12j}}^T + \bar{\mathbf{A}}_{\Delta_{12j}} \mathbf{Y}_{SF} & \prec 0 \\ \text{for } j & \in I(1, N) \end{aligned}$$

Step 4) Set $\mathbf{K}_{SF} = \mathbf{Y}_{SF} \mathbf{Q}_{SF}^{-1}$.

Step 5) Solve the LMI feasibility problem

$$\begin{aligned} \text{find } \epsilon \text{ and } \mathbf{P}_1 \\ \text{s.t.} \end{aligned}$$

$$\begin{aligned} \mathbf{P}_1 & \succ \mathbf{I}_{(n-m)}, \quad \epsilon > 0 \\ (\bar{\mathbf{A}}_{\Delta_{11\alpha j}} + \bar{\mathbf{A}}_{\Delta_{12j}} \mathbf{K}_{SF})^T \mathbf{P}_1 + \mathbf{P}_1 (\bar{\mathbf{A}}_{\Delta_{11\alpha j}} + \bar{\mathbf{A}}_{\Delta_{12j}} \mathbf{K}_{SF}) & \prec 0 \\ \bar{\mathbf{A}}_{\Delta_{11\alpha j}}^T \mathbf{P}_1 + \mathbf{P}_1 \bar{\mathbf{A}}_{\Delta_{11\alpha j}} - \epsilon \mathbf{C}_1^T \mathbf{C}_1 & \prec 0 \\ \text{for } j & \in I(1, N) \end{aligned}$$

Step 6) Solve the following LMI problem

$$\begin{aligned} \text{find } \mathbf{K}_{OF} \\ \text{s.t.} \end{aligned}$$

$$\begin{aligned} (\bar{\mathbf{A}}_{\Delta_{11\alpha j}} - \bar{\mathbf{A}}_{\Delta_{12j}} \mathbf{K}_{OF} \mathbf{C}_1)^T \mathbf{P}_1 + \mathbf{P}_1 (\bar{\mathbf{A}}_{\Delta_{11\alpha j}} - \bar{\mathbf{A}}_{\Delta_{12j}} \mathbf{K}_{OF} \mathbf{C}_1) & \prec 0 \\ \text{for } j & \in I(1, N) \end{aligned}$$

Remark 5.1 *The feasibility problem formulated in step 6 can be replaced by an optimisation problem involving the minimization of a norm defined by the designer. Specifically*

$$\begin{aligned} \min \quad & \rho \\ \text{s.t.} \quad & \end{aligned}$$

$$\begin{aligned} \begin{bmatrix} \rho & \mathbf{k}^T \\ \mathbf{k} & \mathbf{M} \end{bmatrix} & \succ 0 \\ (\bar{\mathbf{A}}_{\Delta_{11\alpha j}} - \bar{\mathbf{A}}_{\Delta_{12j}} \mathbf{K}_{OF} \mathbf{C}_1)^T \mathbf{P}_1 + \mathbf{P}_1 (\bar{\mathbf{A}}_{\Delta_{11\alpha j}} - \bar{\mathbf{A}}_{\Delta_{12j}} \mathbf{K}_{OF} \mathbf{C}_1) & \prec 0 \\ \text{for } j & \in I(1, N) \end{aligned}$$

where \mathbf{k} = vector(\mathbf{K}_{OF}) and \mathbf{M} is a p.d. matrix chosen by the designer. Thus, if $\mathbf{M} = \mathbf{I}$ the optimisation problem corresponds to a minimisation of the Frobenius norm (Benton & Smith, 1999).

5.3.2 Control Law Synthesis

If a switching gain matrix Γ given in (5.8) exists such that (5.9) is stable, then a nonsingular change of coordinates $\bar{\mathbf{x}} \mapsto \hat{\mathbf{T}}\bar{\mathbf{x}} = \hat{\mathbf{x}}$ exists where

$$\hat{\mathbf{T}} = \begin{bmatrix} \mathbf{I}_{(n-m)} & \mathbf{0} \\ \bar{\mathbf{B}}_2^{-1}\mathbf{K}_{OF}\mathbf{C}_1 & \bar{\mathbf{B}}_2^{-1} \end{bmatrix} \quad (5.31)$$

such that the triple $(\bar{\mathbf{A}}_\Delta(t), \bar{\mathbf{B}}, \bar{\mathbf{C}})$ from (5.5) and (5.2) can be transformed into

$$\hat{\mathbf{A}}_\Delta(t) = \hat{\mathbf{A}} + \Delta\hat{\mathbf{A}}(t) = \begin{bmatrix} \hat{\mathbf{A}}_{\Delta 11}(t) & \hat{\mathbf{A}}_{\Delta 12}(t) \\ \hat{\mathbf{A}}_{\Delta 21}(t) & \hat{\mathbf{A}}_{\Delta 22}(t) \end{bmatrix} \quad (5.32)$$

$$\hat{\mathbf{B}} = \begin{bmatrix} \mathbf{0} & \mathbf{I}_m \end{bmatrix}^T \quad (5.33)$$

$$\Gamma\hat{\mathbf{C}} = \begin{bmatrix} \mathbf{0} & \mathbf{I}_m \end{bmatrix} \quad \text{where} \quad \hat{\mathbf{C}} = \begin{bmatrix} \mathbf{0} & \bar{\mathbf{T}} \end{bmatrix} \quad (5.34)$$

with $\bar{\mathbf{T}} \in \mathbb{R}^{p \times p}$ such that $\det\{\bar{\mathbf{T}}\} \neq 0$. Noting the form of (5.31) it is evident that equation (5.33) holds. The structure of $\Gamma\hat{\mathbf{C}}$ in (5.34), follows straightforwardly since $\bar{\mathbf{B}}_2^{-1} = \Gamma_2$.

Let $\mathbb{S}(t)$ be the block matrix form of the triple $(\hat{\mathbf{A}}_\Delta(t), \hat{\mathbf{B}}, \hat{\mathbf{C}})$ given by

$$\mathbb{S}(t) = \left[\begin{array}{c|c} \hat{\mathbf{A}}_\Delta(t) & \hat{\mathbf{B}} \\ \hline \hat{\mathbf{C}} & \mathbf{0} \end{array} \right] \quad (5.35)$$

and let \mathbb{S}_j be the block matrix form of the triple $(\hat{\mathbf{A}}_{\Delta j}, \hat{\mathbf{B}}, \hat{\mathbf{C}})$ given by

$$\mathbb{S}_j = \left[\begin{array}{c|c} \hat{\mathbf{A}}_{\Delta j} & \hat{\mathbf{B}} \\ \hline \hat{\mathbf{C}} & \mathbf{0} \end{array} \right] \quad \text{for } j \in I(1, N) \quad (5.36)$$

Thus, a polytope can be defined as follows

$$\mathcal{P}_{OF}^u = \left\{ \sum_{j=1}^N \mu_j \mathbb{S}_j : \sum_{j=1}^N \mu_j = 1, \mu_j \geq 0 \text{ for } j \in I(1, N) \right\} \quad (5.37)$$

where N is the number of vertices of \mathcal{P}_{OF}^u . These vertices can be calculated using

$$\hat{\mathbf{A}}_{\Delta j} = \hat{\mathbf{A}} + \sum_{i=1}^r \theta_i \Delta \hat{\mathbf{A}}_i \Big|_{\theta_i = \{\underline{\theta}_i, \bar{\theta}_i\}} = \begin{bmatrix} \hat{\mathbf{A}}_{\Delta 11j} & \hat{\mathbf{A}}_{\Delta 12j} \\ \hat{\mathbf{A}}_{\Delta 21j} & \hat{\mathbf{A}}_{\Delta 22j} \end{bmatrix} \quad (5.38)$$

where $\hat{\mathbf{B}}$ and $\hat{\mathbf{C}}$ are defined in (5.33) and (5.34) respectively.

5.3 Sliding Mode Static Output Feedback Control

The sliding mode dynamics are associated with

$$\hat{\mathbf{A}}_{\Delta 11j} = \bar{\mathbf{A}}_{\Delta 11j} - \bar{\mathbf{A}}_{\Delta 12j} \mathbf{K}_{OF} \mathbf{C}_1 \text{ for } j \in I(1, N) \quad (5.39)$$

which are stable by design, and in turn

$$\hat{\mathbf{A}}_{\Delta 11}(t) = \bar{\mathbf{A}}_{\Delta 11}(t) - \bar{\mathbf{A}}_{\Delta 12}(t) \mathbf{K}_{OF} \mathbf{C}_1 \quad (5.40)$$

is stable by the convexity property of the polytope \mathcal{P}_{OF}^u .

Let $\mathbf{P} \in \mathfrak{R}^{n \times n}$ be a *Lyapunov* matrix partitioned as follows

$$\mathbf{P} = \begin{bmatrix} \mathbf{P}_1 & \mathbf{0} \\ \mathbf{0} & \mathbf{P}_2 \end{bmatrix} \succ \mathbf{I}_n \quad (5.41)$$

where $\mathbf{P}_1 \in \mathfrak{R}^{(n-m) \times (n-m)}$ and $\mathbf{P}_2 \in \mathfrak{R}^{m \times m}$.

Consider the control law

$$\mathbf{u}(t) = \mathbf{u}_L(t) + \mathbf{u}_{NL}(t) \quad (5.42)$$

with the linear component $\mathbf{u}_L(t)$ of the form

$$\mathbf{u}_L(t) = -\mathbf{G}\mathbf{y}(t) \quad (5.43)$$

and the nonlinear part $\mathbf{u}_{NL}(t)$ given by

$$\mathbf{u}_{NL}(t) = \begin{cases} -\rho(t, \mathbf{y}, \mathbf{u}) \mathbf{P}_2^{-1} \frac{\mathbf{\Gamma}\mathbf{y}(t)}{\|\mathbf{\Gamma}\mathbf{y}(t)\|} & \text{if } \mathbf{\Gamma}\mathbf{y}(t) \neq \mathbf{0} \\ \mathbf{0} & \text{otherwise} \end{cases} \quad (5.44)$$

where

$$\rho(t, \mathbf{y}, \mathbf{u}) \geq \frac{\|\mathbf{P}_2\| (k_1 \|\mathbf{u}_L(t)\| + \varphi(t, \mathbf{y}) + k_2) + \eta}{(1 - \|\mathbf{P}_2\| k_1)} \quad (5.45)$$

with $\eta > 0$ as a design parameter.

The gain matrix \mathbf{G} , in (5.43), is parameterised conformably with the output matrix $\hat{\mathbf{C}}$ defined in (5.34) and the partition of \mathbf{P} given in (5.41), as follows

$$\mathbf{G} = \begin{bmatrix} \mathbf{G}_1 & \mathbf{G}_2 \end{bmatrix} \bar{\mathbf{T}}^{-1} \quad (5.46)$$

where $\mathbf{G}_1 \in \mathfrak{R}^{m \times (p-m)}$ and $\mathbf{G}_2 \in \mathfrak{R}^{m \times m}$ are such that the following matrix inequality holds

$$\mathcal{A}_j^T \mathbf{P} + \mathbf{P} \mathcal{A}_j \prec 0 \text{ for } j \in I(1, N) \quad (5.47)$$

5.3 Sliding Mode Static Output Feedback Control

where

$$\mathcal{A}_j = \begin{bmatrix} \hat{\mathbf{A}}_{\Delta 11j} & \hat{\mathbf{A}}_{\Delta 12j} \\ \hat{\mathbf{A}}_{\Delta 21j} - \mathbf{G}_1 \mathbf{C}_1 & \hat{\mathbf{A}}_{\Delta 22j} - \mathbf{G}_2 \end{bmatrix} \quad (5.48)$$

for $j \in I(1, N)$.

Let Ω be a *sliding patch* defined as

$$\Omega = \left\{ (\hat{\mathbf{x}}_1 \in \mathbb{R}^{(n-m)}, \hat{\mathbf{x}}_2 \in \mathbb{R}^m) : \|\hat{\mathbf{x}}_1\| < \eta\gamma^{-1} \right\} \quad (5.49)$$

where

$$\gamma = \max_{j \in I(1, N)} \left\{ \|\mathbf{P}_2(\hat{\mathbf{A}}_{\Delta 21j} - \mathbf{G}_1 \mathbf{C}_1)\| \right\} \quad (5.50)$$

Proposition 5.1 *The control law (5.42)-(5.45) guarantees that the sliding patch Ω is reached in finite time and a sliding motion takes place on the sliding surface \mathcal{S}_{OF} within Ω .*

△

Proof Consider the *Lyapunov* function

$$V(t) := \hat{\mathbf{x}}^T(t) \mathbf{P} \hat{\mathbf{x}}(t) \quad (5.51)$$

The time derivative of $V(t)$ along the closed-loop system's trajectories satisfies

$$\begin{aligned} \dot{V}(t) &= \sum_{j=1}^N \mu_j (\hat{\mathbf{A}}_{\Delta j} \hat{\mathbf{x}}(t) + \hat{\mathbf{B}}(\mathbf{u}(t) + \hat{\xi}_{\Delta}(\cdot)))^T \mathbf{P} \hat{\mathbf{x}}(t) \\ &\quad + \hat{\mathbf{x}}^T(t) \mathbf{P} \sum_{j=1}^N \mu_j (\hat{\mathbf{A}}_{\Delta j} \hat{\mathbf{x}}(t) + \hat{\mathbf{B}}(\mathbf{u}(t) + \hat{\xi}_{\Delta}(\cdot))) \end{aligned} \quad (5.52)$$

$$\begin{aligned} &= \hat{\mathbf{x}}^T(t) \sum_{j=1}^N \mu_j (\hat{\mathbf{A}}_{\Delta j} - \hat{\mathbf{B}} \mathbf{G} \hat{\mathbf{C}})^T \mathbf{P} \hat{\mathbf{x}}(t) + (\hat{\mathbf{B}}(\mathbf{u}_{NL}(t) + \hat{\xi}_{\Delta}(\cdot)))^T \mathbf{P} \hat{\mathbf{x}}(t) \\ &\quad + \hat{\mathbf{x}}^T(t) \mathbf{P} \sum_{j=1}^N \mu_j (\hat{\mathbf{A}}_{\Delta j} - \hat{\mathbf{B}} \mathbf{G} \hat{\mathbf{C}}) \hat{\mathbf{x}}(t) + \hat{\mathbf{x}}^T(t) \mathbf{P} \hat{\mathbf{B}}(\mathbf{u}_{NL}(t) + \hat{\xi}_{\Delta}(\cdot)) \end{aligned} \quad (5.53)$$

$$\begin{aligned} &= \hat{\mathbf{x}}^T(t) \left(\sum_{j=1}^N \mu_j (\hat{\mathbf{A}}_{\Delta j} - \hat{\mathbf{B}} \mathbf{G} \hat{\mathbf{C}})^T \mathbf{P} + \mathbf{P} \sum_{j=1}^N \mu_j (\hat{\mathbf{A}}_{\Delta j} - \hat{\mathbf{B}} \mathbf{G} \hat{\mathbf{C}}) \right) \hat{\mathbf{x}}(t) \\ &\quad - 2\hat{\mathbf{x}}^T(t) \mathbf{P} \hat{\mathbf{B}} \rho(\cdot) \mathbf{P}_2^{-1} \frac{\mathbf{F} \hat{\mathbf{C}} \hat{\mathbf{x}}(t)}{\|\mathbf{F} \hat{\mathbf{C}} \hat{\mathbf{x}}(t)\|} + 2\hat{\mathbf{x}}^T(t) \mathbf{P} \hat{\mathbf{B}} \hat{\xi}_{\Delta}(\cdot) \end{aligned} \quad (5.54)$$

5.3 Sliding Mode Static Output Feedback Control

Let

$$\hat{\mathbf{M}} \triangleq \sum_{j=1}^N \mu_j \left(\hat{\mathbf{A}}_{\Delta j} - \hat{\mathbf{B}}\mathbf{G}\hat{\mathbf{C}} \right)^T \mathbf{P} + \mathbf{P} \sum_{j=1}^N \mu_j \left(\hat{\mathbf{A}}_{\Delta j} - \hat{\mathbf{B}}\mathbf{G}\hat{\mathbf{C}} \right) \quad (5.55)$$

which is a negative definite matrix by design.

$$\dot{V}(t) = \hat{\mathbf{x}}^T(t) \hat{\mathbf{M}} \hat{\mathbf{x}}(t) - 2\hat{\mathbf{x}}^T(t) \mathbf{P} \hat{\mathbf{B}} \rho(\cdot) \mathbf{P}_2^{-1} \frac{\Gamma \hat{\mathbf{C}} \hat{\mathbf{x}}(t)}{\|\Gamma \hat{\mathbf{C}} \hat{\mathbf{x}}(t)\|} + 2\hat{\mathbf{x}}^T(t) \mathbf{P} \hat{\mathbf{B}} \hat{\xi}_{\Delta}(\cdot) \quad (5.56)$$

From the partition of \mathbf{P} in (5.41) and the input matrix $\hat{\mathbf{B}}$ defined in (5.33), it follows straightforwardly that the structural property

$$\mathbf{P} \hat{\mathbf{B}} = (\Gamma \hat{\mathbf{C}})^T \mathbf{P}_2 \quad (5.57)$$

holds. Then, (5.56) can be written as

$$\dot{V}(\hat{\mathbf{x}}) = \hat{\mathbf{x}}^T(t) \hat{\mathbf{M}} \hat{\mathbf{x}}(t) - 2\rho(\cdot) (\Gamma \hat{\mathbf{C}} \hat{\mathbf{x}}(t))^T \frac{(\Gamma \hat{\mathbf{C}} \hat{\mathbf{x}}(t))}{\|\Gamma \hat{\mathbf{C}} \hat{\mathbf{x}}(t)\|} + 2\hat{\mathbf{x}}^T(t) (\Gamma \hat{\mathbf{C}})^T \mathbf{P}_2 \hat{\xi}_{\Delta}(\cdot) \quad (5.58)$$

$$= \hat{\mathbf{x}}^T(t) \hat{\mathbf{M}} \hat{\mathbf{x}}(t) - 2\rho(\cdot) \|\Gamma \hat{\mathbf{C}} \hat{\mathbf{x}}(t)\| + 2(\Gamma \hat{\mathbf{C}} \hat{\mathbf{x}})^T \mathbf{P}_2 \hat{\xi}_{\Delta}(\cdot) \quad (5.59)$$

$$\leq \hat{\mathbf{x}}^T(t) \hat{\mathbf{M}} \hat{\mathbf{x}}(t) - 2\|\Gamma \hat{\mathbf{C}} \hat{\mathbf{x}}(t)\| \left(\rho(\cdot) - \|\mathbf{P}_2\| \|\hat{\xi}_{\Delta}(\cdot)\| \right) \quad (5.60)$$

$$\leq \hat{\mathbf{x}}^T(t) \hat{\mathbf{M}} \hat{\mathbf{x}}(t) - 2\|\Gamma \hat{\mathbf{C}} \hat{\mathbf{x}}(t)\| \left(\rho(\cdot) - \|\mathbf{P}_2\| (k_1 \|\mathbf{u}(t)\| + \varphi(\cdot) + k_2) \right) \quad (5.61)$$

Noting that

$$\begin{aligned} \|\mathbf{u}(t)\| &= \|\mathbf{u}_L(t) + \mathbf{u}_{NL}(t)\| \leq \|\mathbf{u}_L(t)\| + \|\mathbf{u}_{NL}(t)\| \leq \|\mathbf{u}_L(t)\| + \rho(\cdot) \|\mathbf{P}_2^{-1}\| \\ &< \|\mathbf{u}_L(t)\| + \rho(\cdot) \end{aligned} \quad (5.62)$$

since $\|\mathbf{P}_2^{-1}\| < 1$ because $\mathbf{P}_2 \succ \mathbf{I}_m$. Then, from (5.45) and (5.62), it follows

$$\|\mathbf{P}_2\| (k_1 \|\mathbf{u}(t)\| + \varphi(\cdot) + k_2) < \|\mathbf{P}_2\| \left(k_1 (\|\mathbf{u}_L(t)\| + \rho(\cdot)) + \varphi(\cdot) + k_2 \right) \leq \rho(\cdot) - \eta \quad (5.63)$$

and, this in turn implies

$$\rho(\cdot) \geq \|\mathbf{P}_2\| (k_1 \|\mathbf{u}(t)\| + \varphi(\cdot) + k_2) + \eta \quad (5.64)$$

Thus, (5.61) becomes

$$\dot{V}(t) \leq \hat{\mathbf{x}}^T(t) \hat{\mathbf{M}} \hat{\mathbf{x}}(t) - 2\|\Gamma \hat{\mathbf{C}} \hat{\mathbf{x}}(t)\| \eta < 0 \quad \forall \hat{\mathbf{x}}(t) \neq \mathbf{0} \quad (5.65)$$

and the system is said to be quadratically stable.

5.3 Sliding Mode Static Output Feedback Control

Partition the state vector $\hat{\mathbf{x}} = \begin{bmatrix} \hat{\mathbf{x}}_1^T & \hat{\mathbf{x}}_2^T \end{bmatrix}^T$. Consequently

$$\Gamma \mathbf{y}(t) = \Gamma \hat{\mathbf{C}} \hat{\mathbf{x}}(t) = \hat{\mathbf{x}}_2(t) \quad (5.66)$$

Now consider the *Lyapunov* function

$$V_\sigma(t) = \hat{\mathbf{x}}_2^T(t) \mathbf{P}_2 \hat{\mathbf{x}}_2(t) \quad (5.67)$$

Computing the time derivative along the closed-loop trajectories gives

$$\begin{aligned} \dot{V}_\sigma(t) = & \sum_{j=1}^N \mu_j \left(2\hat{\mathbf{x}}_2^T(t) \mathbf{P}_2 (\hat{\mathbf{A}}_{\Delta 21j} - \mathbf{G}_1 \mathbf{C}_1) \hat{\mathbf{x}}_1(t) + 2\hat{\mathbf{x}}_2^T \mathbf{P}_2 (\mathbf{u}_{NL}(t) + \hat{\xi}_\Delta(\cdot)) \right. \\ & \left. + \hat{\mathbf{x}}_2^T(t) \left((\hat{\mathbf{A}}_{\Delta 22j} - \mathbf{G}_2)^T \mathbf{P}_2 + \mathbf{P}_2 (\hat{\mathbf{A}}_{\Delta 22j} - \mathbf{G}_2) \right) \hat{\mathbf{x}}_2(t) \right) \end{aligned} \quad (5.68)$$

From the matrix inequality (5.47), it follows that

$$\hat{\mathbf{x}}_2^T(t) \hat{\mathbf{H}}_\sigma \hat{\mathbf{x}}_2(t) < 0 \quad (5.69)$$

where

$$\hat{\mathbf{H}}_\sigma = \sum_{j=1}^N \mu_j (\hat{\mathbf{A}}_{\Delta 22j} - \mathbf{G}_2)^T \mathbf{P}_2 + \mathbf{P}_2 \sum_{j=1}^N \mu_j (\hat{\mathbf{A}}_{\Delta 22j} - \mathbf{G}_2) < 0 \quad (5.70)$$

Furthermore, using (5.44) and re-writing (5.68) produces

$$\begin{aligned} \dot{V}_\sigma(t) \leq & \hat{\mathbf{x}}_2^T(t) \hat{\mathbf{H}}_\sigma \hat{\mathbf{x}}_2(t) + \sum_{j=1}^N \mu_j \left(2\|\hat{\mathbf{x}}_2(t)\| \|\mathbf{P}_2 (\hat{\mathbf{A}}_{\Delta 21j} - \mathbf{G}_1 \mathbf{C}_1)\| \|\hat{\mathbf{x}}_1(t)\| \right. \\ & \left. - 2\|\hat{\mathbf{x}}_2(t)\| (\rho(\cdot) - \|\mathbf{P}_2\| (k_1 \|\mathbf{u}(t)\| + \varphi(\cdot) + k_2)) \right) \end{aligned} \quad (5.71)$$

Since

$$\rho(\cdot) \geq \|\mathbf{P}_2\| (k_1 \|\mathbf{u}(t)\| + \varphi(\cdot) + k_2) + \eta \quad (5.72)$$

then

$$\dot{V}_\sigma(t) \leq \hat{\mathbf{x}}_2^T(t) \hat{\mathbf{H}}_\sigma \hat{\mathbf{x}}_2(t) + 2\|\hat{\mathbf{x}}_2(t)\| \sum_{j=1}^N \mu_j \left(\|\mathbf{P}_2 (\hat{\mathbf{A}}_{\Delta 21j} - \mathbf{G}_1 \mathbf{C}_1)\| \|\hat{\mathbf{x}}_1(t)\| - \eta \right) \quad (5.73)$$

5.3 Sliding Mode Static Output Feedback Control

Inside the sliding patch defined in (5.49) along with (5.50) yields

$$\dot{V}_\sigma(t) < 2\|\hat{\mathbf{x}}_2(t)\| \sum_{j=1}^N \mu_j (\|\mathbf{P}_2(\hat{\mathbf{A}}_{\Delta 21j} - \mathbf{G}_1 \mathbf{C}_1)\| \eta \gamma^{-1} - \eta) < 0 \quad (5.74)$$

which means that a sliding motion occurs inside the invariant set Ω defined in (5.49). Therefore, a sliding motion occurs in finite time since the system is quadratically stable.

Q.E.D.

From (5.33)–(5.38) and (5.46), the matrix \mathcal{A}_j given in (5.48) can be expressed as

$$\mathcal{A}_j \triangleq \hat{\mathbf{A}}_{\Delta j} - \hat{\mathbf{B}}\mathbf{G}\hat{\mathbf{C}} \quad (5.75)$$

then it follows that

$$\mathcal{A}_j^T \mathbf{P} + \mathbf{P} \mathcal{A}_j = \begin{bmatrix} \hat{\mathbf{A}}_{\Delta 11j}^T \mathbf{P}_1 + \mathbf{P}_1 \hat{\mathbf{A}}_{\Delta 11j} & \mathbf{P}_1 \hat{\mathbf{A}}_{\Delta 12j} + \hat{\mathbf{A}}_{\Delta 21j}^T \mathbf{P}_2 - \mathbf{C}_1^T \mathbf{L}_1^T \\ * & \mathbf{P}_2 \hat{\mathbf{A}}_{\Delta 22j} - \mathbf{L}_2 + \hat{\mathbf{A}}_{\Delta 22j}^T \mathbf{P}_2 - \mathbf{L}_2^T \end{bmatrix} < 0 \quad (5.76)$$

for $j \in I(1, N)$ with

$$\mathbf{L}_1 \triangleq \mathbf{P}_2 \mathbf{G}_1 \quad \text{and} \quad \mathbf{L}_2 \triangleq \mathbf{P}_2 \mathbf{G}_2 \quad (5.77)$$

The *Lyapunov* inequality (5.76) depends affinely on the matrix variables \mathbf{P}_1 , \mathbf{P}_2 , \mathbf{L}_1 and \mathbf{L}_2 . Therefore, an LMI problem can be formulated in order to design a gain matrix \mathbf{G} such that

$$\|\mathbf{G}\| < \psi \quad (5.78)$$

and

$$\|\mathbf{P}_2 \hat{\mathbf{A}}_{\Delta 21j} - \mathbf{L}_1 \mathbf{C}_1\| < \gamma \quad (5.79)$$

However, the firstly inequality (5.78) has to be formulated in terms of the matrix decision variables \mathbf{L}_1 and \mathbf{L}_2 defined in (5.77). This inequality can be expressed more conveniently considering \mathbf{P}_2 from (5.41) and the parameterisation of \mathbf{G} given in (5.46). As shown in the sequel

$$\|\mathbf{G}\| = \|\mathbf{P}_2^{-1} [\mathbf{L}_1 \quad \mathbf{L}_2] \bar{\mathbf{T}}^{-1}\| \leq \|\mathbf{P}_2^{-1}\| \| [\mathbf{L}_1 \quad \mathbf{L}_2] \bar{\mathbf{T}}^{-1} \|$$

since $\mathbf{P}_2 \succ \mathbf{I}_m$ by definition in (5.41). Then, it follows that

$$\|\mathbf{G}\| < \left\| [\mathbf{L}_1 \quad \mathbf{L}_2] \bar{\mathbf{T}}^{-1} \right\| \quad (5.80)$$

and therefore by ensuring

$$\left\| \begin{bmatrix} \mathbf{L}_1 & \mathbf{L}_2 \end{bmatrix} \overline{\mathbf{T}}^{-1} \right\| < \psi \quad (5.81)$$

inequality (5.78) is satisfied.

The poles of \mathcal{A}_j for $j \in I(1, N)$ can be placed in an LMI region (Chilali *et al.*, 1999) of the complex plane \mathbb{C} established by the designer as discussed in Section 3.2.6. Without any loss of generality, an LMI region characterised by the intersection of the disk $\mathcal{D}(c_n, r_d)$ centered at $(-c_n, 0)$ with radius r_d and a half-plane $\mathcal{H}(h)$ delimited by a vertical line at $(-h, 0)$ is considered. That is, $\mathcal{D}(h, c_n, r_d) = \mathcal{D}(c_n, r_d) \cap \mathcal{H}(h)$. Figure 5.1 depicts the LMI region $\mathcal{D}(h, c_n, r_d)$ under consideration

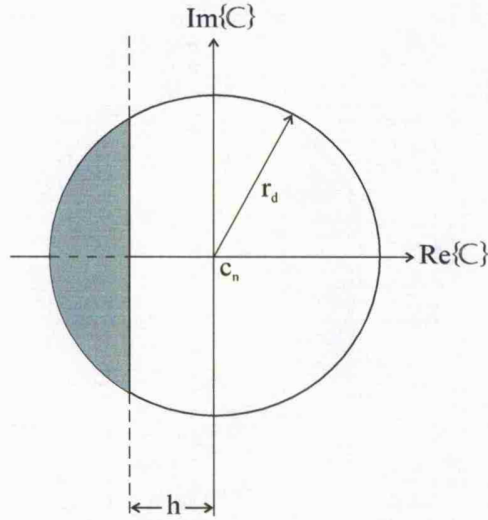


Figure 5.1: LMI Region $\mathcal{D}(h, c_n, r_d)$

In order to formulate an optimisation problem for synthesising the gain matrix \mathbf{G} , consider a partition of

$$\hat{\mathbf{A}}_{\Delta 21j} = \begin{bmatrix} \hat{\mathbf{A}}_{\Delta 211j} & \hat{\mathbf{A}}_{\Delta 212j} \end{bmatrix} \quad \text{for } j \in I(1, N) \quad (5.82)$$

where $\hat{\mathbf{A}}_{\Delta 211j} \in \mathbb{R}^{m \times (n-p)}$ and $\hat{\mathbf{A}}_{\Delta 212j} \in \mathbb{R}^{m \times (p-m)}$.

Then, choose any

$$\gamma > \max_{j \in I(1, N)} \left\{ \|\hat{\mathbf{A}}_{\Delta 211j}\| \right\} \quad (5.83)$$

5.3 Sliding Mode Static Output Feedback Control

and solve the following LMI problem

$$\left. \begin{array}{l}
 \min \psi \\
 \text{s.t.} \\
 \left[\begin{array}{cc} -\psi \mathbf{I}_m & \left[\mathbf{L}_1 \quad \mathbf{L}_2 \right] \overline{\mathbf{T}}^{-1} \\ \left(\left[\mathbf{L}_1 \quad \mathbf{L}_2 \right] \overline{\mathbf{T}}^{-1} \right)^{\text{T}} & -\psi \mathbf{I}_p \end{array} \right] \prec 0 \\
 \left[\begin{array}{cc} -\gamma \mathbf{I}_m & \mathbf{P}_2 \hat{\mathbf{A}}_{\Delta 21j} - \mathbf{L}_1 \mathbf{C}_1 \\ \hat{\mathbf{A}}_{\Delta 21j}^{\text{T}} \mathbf{P}_2 - \mathbf{C}_1^{\text{T}} \mathbf{L}_1^{\text{T}} & -\gamma \mathbf{I}_{(n-m)} \end{array} \right] \prec 0 \\
 \left[\begin{array}{cc} -r_d \mathbf{P} & \mathbf{P} \mathcal{A}_j + c_n \mathbf{P} \\ c_n \mathbf{P} + \mathcal{A}_j^{\text{T}} \mathbf{P} & -r_d \mathbf{P} \end{array} \right] \prec 0 \\
 \mathcal{A}_j^{\text{T}} \mathbf{P} + \mathbf{P} \mathcal{A}_j + 2h \mathbf{P} \prec 0 \\
 \mathbf{P} \succ \mathbf{I}_n
 \end{array} \right\} \quad (5.84)$$

for $j \in I(1, N)$ in terms of the variables \mathbf{L}_1 , \mathbf{L}_2 , \mathbf{P}_1 and \mathbf{P}_2 .

If there exists a feasible solution to the optimisation problem (5.84) then choose

$$\mathbf{G}_1 = \mathbf{P}_2^{-1} \mathbf{L}_1 \quad \text{and} \quad \mathbf{G}_2 = \mathbf{P}_2^{-1} \mathbf{L}_2 \quad (5.85)$$

and the proposed control law (5.42) with (5.84) guarantees that a sliding mode takes place inside the sliding patch. Furthermore, the state trajectories will reach the sliding patch in finite time and will remain within it.

Remark 5.2 Condition (5.78) imposes a minimum norm constraint in (5.84) with respect to the decision variables \mathbf{L}_1 and \mathbf{L}_2 .

Remark 5.3 In some cases, the LMI region in (5.84) may have to be redefined in order to find a feasible solution. In addition, the designer can set the parameters of the LMI solvers (e.g. relative accuracy required on the optimal value, maximum number of iterations, feasibility radius, etc.) more conveniently for the same purpose.

5.3.3 Design and Computer Simulation Examples: SMSOFC

Example 5.1 The system considered in this example is taken from (Xiang *et al.*, 2006). Such a system belongs to the class of uncertain systems with mismatched uncertainties. Another feature of this plant is that only a subset of the state variables is available for measurement. The mathematical representation of the plant is given

5.3 Sliding Mode Static Output Feedback Control

by

$$\dot{\mathbf{x}}(t) = \begin{bmatrix} -3 + \sin(t) & 0 & 1 + \sin(2t) \\ 1 & 2 & \sin(4t) \\ 0 & 1 + \sin(3t) & -2 \end{bmatrix} \mathbf{x}(t) + \begin{bmatrix} 0 \\ 1 \\ 0 \end{bmatrix} (u(t) + \sin(5t)) \quad (5.86)$$

$$\mathbf{y}(t) = \begin{bmatrix} 0 & 1 & 0 \\ 1 & 1 & 0 \end{bmatrix} \mathbf{x}(t) \quad (5.87)$$

The initial condition considered is the same as in (Xiang *et al.*, 2006), *i.e.* $\mathbf{x}(t)|_{t=t_0} = \mathbf{x}_0 = [1 \ 0 \ -1]^T$.

Since $\text{rank}(\mathbf{CB}) = m$, the system in (5.86)-(5.87) can be written in the regular form (5.2) and consequently (5.5). Using the polytopic approach proposed in Section 5.3, the following switching gain matrix is obtained

$$\mathbf{\Gamma} = \begin{bmatrix} 0.7327 & 0.2673 \end{bmatrix} \quad (5.88)$$

and the gain matrix of the linear component of the control law (5.43) corresponds to

$$\mathbf{G} = \begin{bmatrix} 1.8829 & 1.1597 \end{bmatrix} \quad (5.89)$$

The closed-loop eigenvalues of \mathcal{A}_j for $j = 1, \dots, 8$ (*i.e.* the poles of the closed-loop system when only the linear component of the control law is considered) are shown in Figure 5.2 and the numerical values are the following $\{-2, -1.0425, -4\}$, $\{-0.4126, -2.6299, -4\}$, $\{-4, -2, -1.0425\}$, $\{-3.7656, -1.6385 \pm 0.4807j\}$, $\{-1.0425, -2, -2\}$, $\{-0.4126, -2.6300, -2\}$, $\{-2.0036, -1.9964, -1.0426\}$, and $\{-2.9440, -1.0492 \pm 1.3752j\}$.

The nonlinear component (5.44) with (5.45) is designed such that

$$\rho(t, \mathbf{y}, u) = 3.1213|y_1(t)| + 2.1213|y_2(t)| + 1.4242 \quad (5.90)$$

Furthermore, $\mathbf{P}_2 = 1.0030$. In order to avoid high frequency oscillations in the control signal, the nonlinear component (5.44) has been replaced by

$$u_{NL}(t) = \begin{cases} -\rho(\cdot)\mathbf{P}_2^{-1} \frac{\mathbf{\Gamma}\mathbf{y}(t)}{\|\mathbf{\Gamma}\mathbf{y}(t)\| + \epsilon} & \text{if } \mathbf{\Gamma}\mathbf{y}(t) \neq 0 \\ 0 & \text{otherwise} \end{cases} \quad (5.91)$$

and ϵ has been chosen as $\epsilon = 0.00001$.

The closed-loop time response is shown in Figure 5.3. The control effort and the time evolution of the switching function $\sigma(t)$ is shown in Figure 5.4. As expected there is no high frequency switching in the control signal because of the smoothed unit vector control structure considered in (5.91). The results obtained demonstrate the efficacy of the proposed sliding mode static output feedback control system.

5.3 Sliding Mode Static Output Feedback Control

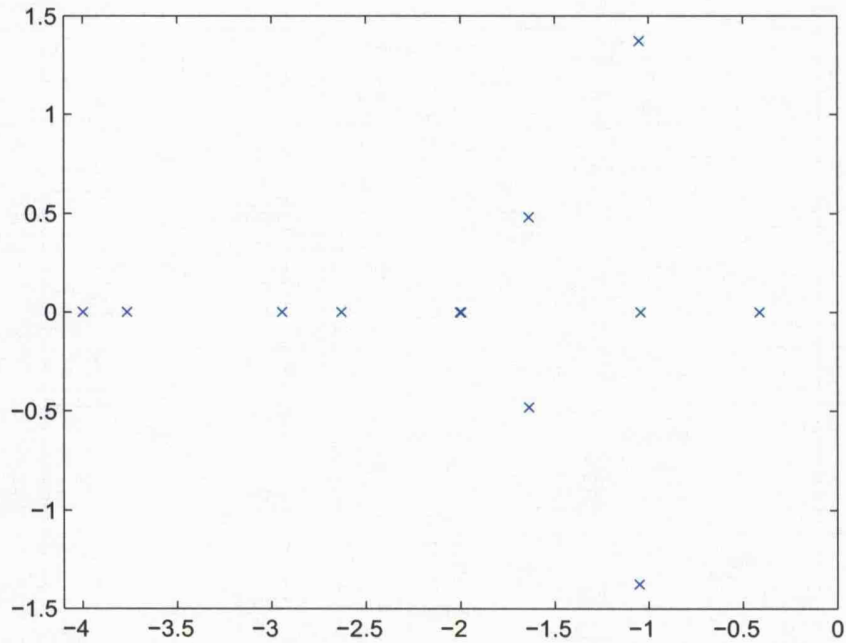


Figure 5.2: Closed-loop poles obtained when using only the linear part of the control law

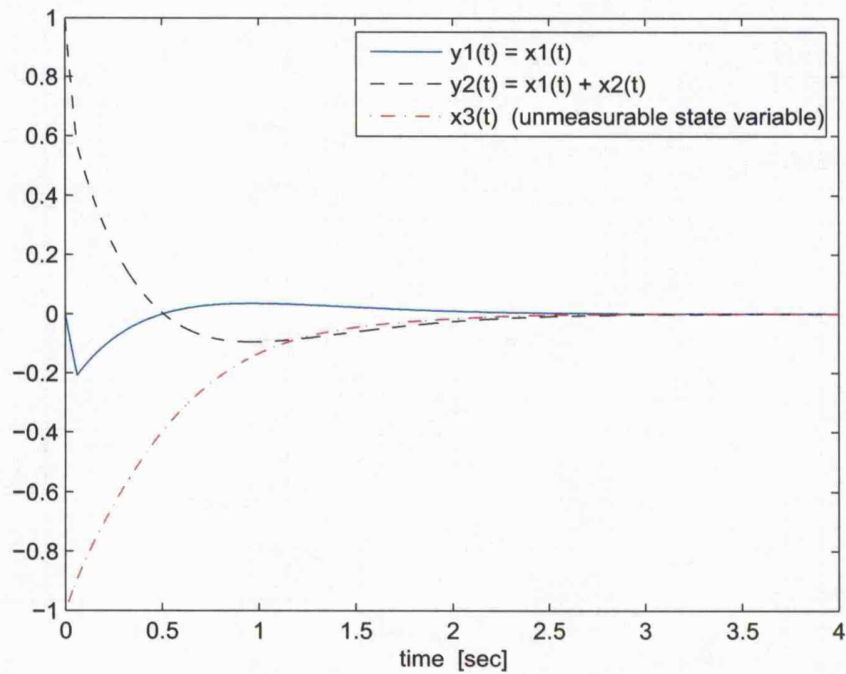
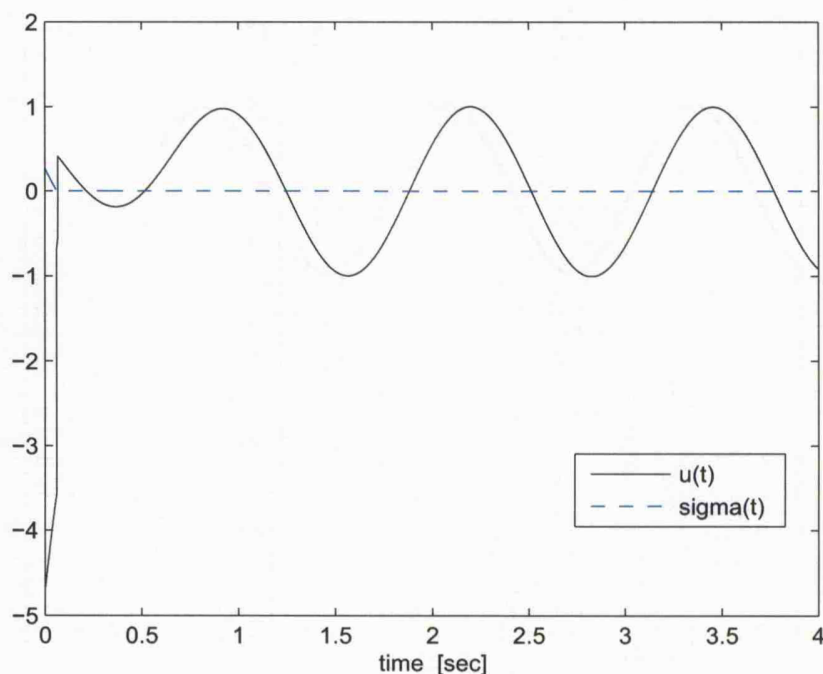


Figure 5.3: Closed-loop response


 Figure 5.4: Control signal $u(t)$ and switching function $\sigma(t)$

Example 5.2 Consider the following lateral model of an aircraft (Anderson & Moore, 2007):

$$\begin{bmatrix} \dot{\phi}(t) \\ \ddot{\phi}(t) \\ \dot{\beta}(t) \\ \dot{r}(t) \end{bmatrix} = \begin{bmatrix} 0 & 1 & 0 & 0 \\ 0 & L_p & L_\beta & L_r \\ \frac{g}{V} & 0 & Y_\beta & -1 \\ N_{\dot{\beta}\frac{g}{V}} & N_p & N_{\beta\dot{\beta}} & N_{r\dot{\beta}} \end{bmatrix} \begin{bmatrix} \phi(t) \\ \dot{\phi}(t) \\ \beta(t) \\ r(t) \end{bmatrix} + \begin{bmatrix} 0 & 0 \\ L_{\delta_r} & L_{\delta_a} \\ Y_{\delta_r} & 0 \\ N_{\delta_r\dot{\beta}} & N_{\delta_a} \end{bmatrix} \begin{bmatrix} \delta_r(t) \\ \delta_a(t) \end{bmatrix} \quad (5.92)$$

where $\phi(t)$ is the bank angle [rad], $\beta(t)$ is the sideslip angle [rad], $r(t)$ is the yaw rate [rad/sec], $\delta_r(t)$ is the rudder deflection [rad], $\delta_a(t)$ is the aileron deflection [rad], $N_{\beta\dot{\beta}} = (N_\beta + N_{\dot{\beta}}Y_\beta)$, $N_{r\dot{\beta}} = (N_r - N_{\dot{\beta}})$ and $N_{\delta_r\dot{\beta}} = (N_{\delta_r} + N_{\dot{\beta}}Y_{\delta_r})$. It is assumed that $\dot{\phi}(t)$, $\beta(t)$ and $r(t)$ are the output signals. The nominal parameter values of (5.92) are given in Table 5.1.

L_{p_0}	L_{β_0}	L_{r_0}	N_{p_0}	N_{β_0}	N_{r_0}	$\frac{g_0}{V_0}$
-2.39	-4.75	0.78	-0.042	2.59	-0.39	0.086
Y_{β_0}	$N_{\dot{\beta}_0}$	$L_{\delta_{r_0}}$	$L_{\delta_{a_0}}$	$Y_{\delta_{r_0}}$	$N_{\delta_{r_0}}$	$N_{\delta_{a_0}}$
-0.11	0	0	-3.91	0.035	-2.53	0.31

Table 5.1: Aircraft nominal parameters

5.3 Sliding Mode Static Output Feedback Control

Here, only Y_β , L_{δ_a} and N_{δ_a} are considered uncertain. These parameters are assumed to be

$$Y_\beta(t) = 0.50|Y_{\beta_0}|\sin(10\pi t) \quad (5.93)$$

$$L_{\delta_a}(t) = 0.25|L_{\delta_{a0}}|\sin(4\pi t) \quad (5.94)$$

$$N_{\delta_a}(t) = 0.25|N_{\delta_{a0}}|\sin(2\pi t) \quad (5.95)$$

The gain matrix \mathbf{K}_{OF} has been designed such that the poles of the reduced-order motion for each vertex are $\{-0.1518, -1.5186\}$ and $\{-0.1650, -1.3975\}$. The associated switching gain matrix is given by

$$\mathbf{\Gamma} = \begin{bmatrix} -0.0308 & 0.5243 & -0.3880 \\ -0.2565 & -0.6857 & -0.0095 \end{bmatrix} \quad (5.96)$$

The LMI region is given by the intersection of the disk $D(c_n, r_d)$ and the left half-plane $H(h)$ regions defined by $c_n = 0$, $r_d = 5$ and $h = 0.02$. The gain matrix \mathbf{G} is

$$\mathbf{G} = \begin{bmatrix} 0.1242 & 0.7743 & -1.3628 \\ -0.2871 & -0.9447 & 0.4470 \end{bmatrix} \quad (5.97)$$

The nonlinear component (5.44) has been smoothed as in (5.91). The scalar valued function $\rho(t, \mathbf{y}, \mathbf{u})$ has been designed as follows

$$\rho(\cdot) = 0.35\|\mathbf{u}_L\| + 0.14(|y_1(t)| + \|\mathbf{x}_2(t)\|) + 0.0014 \quad (5.98)$$

The *Lyapunov* matrix \mathbf{P}_2 is given by

$$\mathbf{P}_2 = \begin{bmatrix} 304.7039 & 231.4102 \\ 231.4102 & 177.5499 \end{bmatrix} \quad (5.99)$$

and $\varepsilon = 0.1 \times 10^{-3}$.

Figure 5.5 shows the bank angle rate $y_1(t) = \dot{\phi}(t)$, the sideslip angle $y_2(t) = \beta(t)$ and the yaw rate $y_3(t) = r(t)$. It can be seen that the proposed SMSOF controller regulates all output signals to zero and robustness is maintained in the presence of the unmatched parameter variations. The associated control efforts $u_1(t) = \delta_r(t)$ and $u_2(t) = \delta_a(t)$ are shown in Figure 5.6. The rudder and aileron input signals do not exhibit high frequency oscillations and are within reasonable practical ranges. The switching functions $\sigma_1(t)$ and $\sigma_2(t)$ are depicted in Figure 5.7. The sliding motion occurs after approximately 0.6 sec and the system maintains the sliding mode thereafter.

5.3 Sliding Mode Static Output Feedback Control

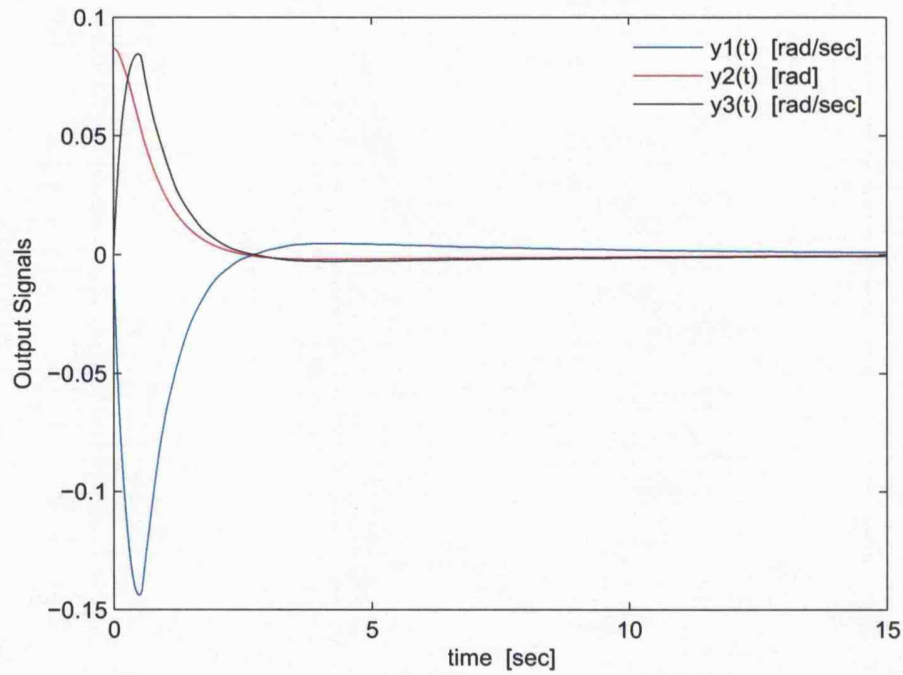


Figure 5.5: Time evolution of the output signals $y_1(t)$, $y_2(t)$ and $y_3(t)$.

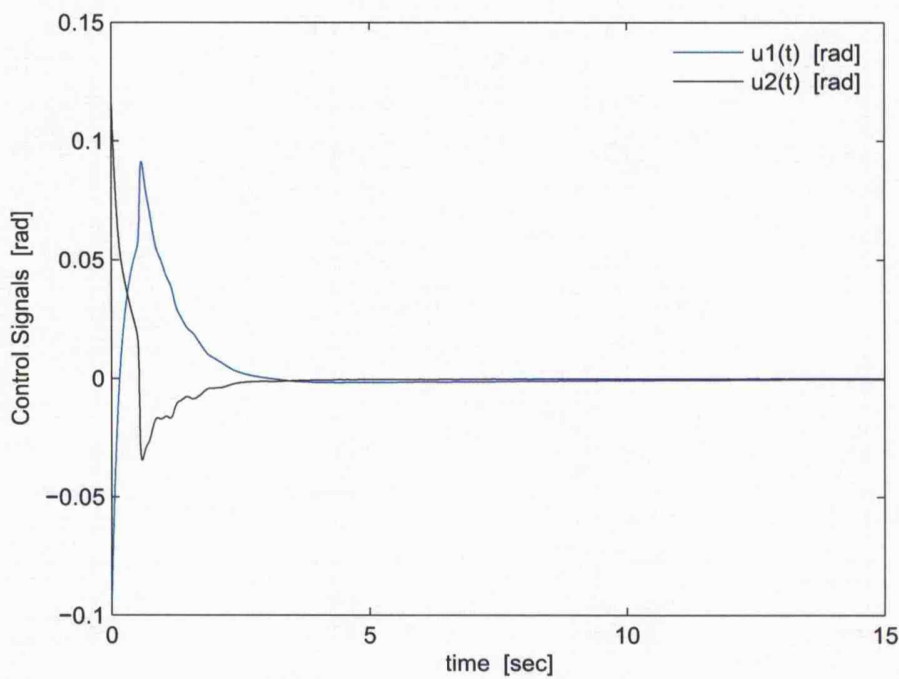


Figure 5.6: Control signals $u_1(t) = \delta_r(t)$ and $u_2(t) = \delta_a(t)$.

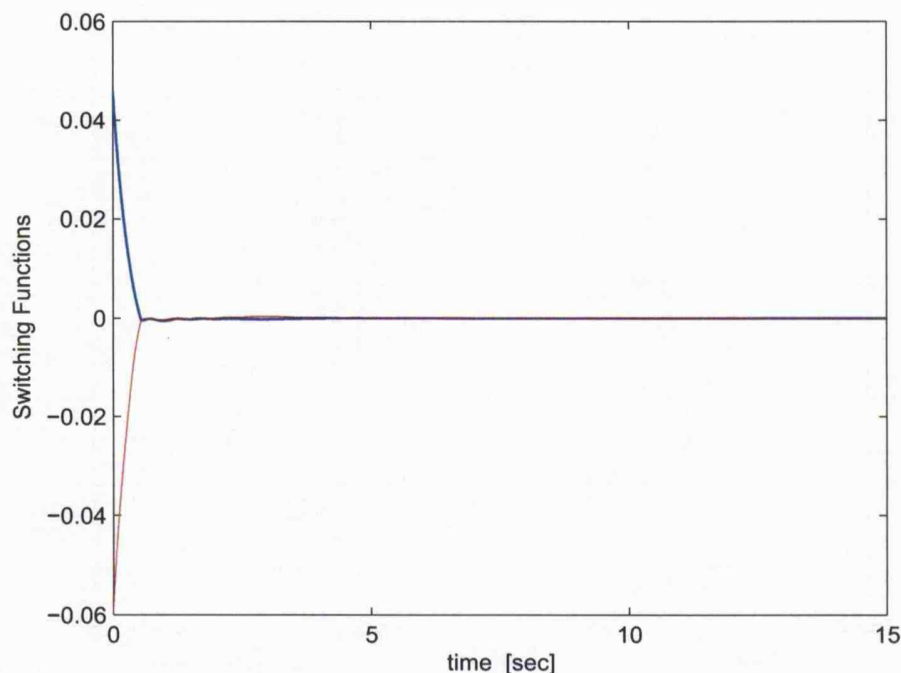


Figure 5.7: Time evolution of switching functions $\sigma_1(t)$ and $\sigma_2(t)$.

5.4 Sliding Mode Dynamic Output Feedback Control

The Sliding Mode Dynamic Output Feedback Control (SMDOFC) design approach developed in this section considers a polytopic formulation for the existence and reachability problems and employs LMI methods. The sliding surface defined in (5.14) and the dynamic compensator given in (5.16) are considered in this section. Moreover, recall that the corresponding reduced-order sliding mode dynamics are governed by (5.23)-(5.24).

5.4.1 Compensator-based Sliding Surface Design

The problem of designing the compensator gains Ψ_1 , Ψ_2 , and Ξ as well as the gain matrices \mathbf{K} and \mathbf{K}_c can be written, using arguments similar to those in (Edwards & Spurgeon, 2003), in a static output feedback fashion as follows:

$$\dot{\bar{\mathbf{x}}}_{a1}(t) = (\mathbf{A}(t) - \mathbf{B}(t)\mathbf{K}\mathbf{C})\bar{\mathbf{x}}_{a1}(t) \quad (5.100)$$

where

$$\bar{\mathbf{x}}_{a1}(t) = \begin{bmatrix} \bar{\mathbf{x}}_1^T(t) & \mathbf{x}_c^T(t) \end{bmatrix}^T \quad (5.101)$$

5.4 Sliding Mode Dynamic Output Feedback Control

$$\mathcal{A}(t) = \begin{bmatrix} \bar{\mathbf{A}}_{\Delta 11}(t) & \mathbf{0} \\ \mathbf{0} & \mathbf{0} \end{bmatrix} \quad \mathcal{B}(t) = \begin{bmatrix} \bar{\mathbf{A}}_{\Delta 12}(t) & \mathbf{0} \\ \Psi_2 & -\mathbf{I}_q \end{bmatrix} \quad \mathcal{C} = \begin{bmatrix} \mathbf{C}_1 & \mathbf{0} \\ \mathbf{0} & \mathbf{I}_q \end{bmatrix} \quad (5.102)$$

$$\mathcal{K} = \begin{bmatrix} \mathbf{K}_{OF} & \mathbf{K}_c \\ \Psi_1 & \Xi \end{bmatrix} \quad (5.103)$$

Let $\Phi(t)$ be the block matrix form of the triple $(\mathcal{A}(t), \mathcal{B}(t), \mathcal{C})$, and let Φ_j be the block matrix form of the triple $(\mathcal{A}_j, \mathcal{B}_j, \mathcal{C})$. That is

$$\mathbb{S}(t) = \left[\begin{array}{c|c} \mathcal{A}(t) & \mathcal{B}(t) \\ \hline \mathcal{C} & \mathbf{0} \end{array} \right] \quad (5.104)$$

and

$$\mathbb{S}_j = \left[\begin{array}{c|c} \mathcal{A}_j & \mathcal{B}_j \\ \hline \mathcal{C} & \mathbf{0} \end{array} \right] \quad (5.105)$$

Then, $\mathbb{S}_j \in \mathcal{P}_{OFa}^\sigma$, where the polyhedral closed convex sub-set

$$\mathcal{P}_{OFa}^\sigma = \left\{ \sum_{j=1}^N \mu_j \mathbb{S}_j : \sum_{j=1}^N \mu_j = 1, \mu_j \geq 0 \text{ for } j \in I(1, N) \right\} \quad (5.106)$$

whose N vertices are given by sub-matrices from (5.105) made up of the matrix \mathcal{C} defined in (5.102) and

$$\mathcal{A}_j = \mathcal{A}_0 + \sum_{i=1}^r \theta_i \Delta \mathcal{A}_j \Big|_{\theta_i = \{\underline{\theta}_i, \bar{\theta}_i\}} \quad \text{for } j \in I(1, N = 2^r) \quad (5.107)$$

$$\mathcal{B}_j = \mathcal{B}_0 + \sum_{i=1}^r \theta_i \Delta \mathcal{B}_j \Big|_{\theta_i = \{\underline{\theta}_i, \bar{\theta}_i\}} \quad \text{for } j \in I(1, N = 2^r) \quad (5.108)$$

where

$$\mathcal{A}_0 \triangleq \begin{bmatrix} \bar{\mathbf{A}}_{11} & \mathbf{0} \\ \mathbf{0} & \mathbf{0} \end{bmatrix}, \quad \Delta \mathcal{A}_j \triangleq \begin{bmatrix} \Delta \bar{\mathbf{A}}_{11j} & \mathbf{0} \\ \mathbf{0} & \mathbf{0} \end{bmatrix} \quad (5.109)$$

$$\mathcal{B}_0 \triangleq \begin{bmatrix} \bar{\mathbf{A}}_{12} & \mathbf{0} \\ \Psi_2 & -\mathbf{I}_q \end{bmatrix}, \quad \Delta \mathcal{B}_j \triangleq \begin{bmatrix} \Delta \bar{\mathbf{A}}_{12j} & \mathbf{0} \\ \mathbf{0} & \mathbf{0} \end{bmatrix} \quad (5.110)$$

5.4 Sliding Mode Dynamic Output Feedback Control

The following is assumed:

A-5.4) The system triples $(\mathcal{A}_j, \mathcal{B}_j, \mathcal{C})$ for $j \in I(1, N)$, whose matrices have been defined in (5.107)-(5.108) and (5.102), are stabilisable and detectable.

The reduced-order system (5.23)-(5.24) is output feedback stabilisable if there exists a *Lyapunov* matrix $\mathbf{P}_{a1} = \mathbf{P}_{a1}^T \in \mathfrak{R}^{(n+q-m) \times (n+q-m)}$ and a gain matrix \mathcal{K} such that the following N bilinear matrix inequalities are satisfied

$$\left(\mathcal{A}_j - \mathcal{B}_j \mathcal{K} \mathcal{C}\right)^T \mathbf{P}_{a1} + \mathbf{P}_{a1} \left(\mathcal{A}_j - \mathcal{B}_j \mathcal{K} \mathcal{C}\right) \prec 0 \quad (5.111)$$

for $j \in I(1, N)$.

As in the SMSOF control framework proposed in Section 5.3, if the matrix inequalities (5.111) hold, then the vertices of the polytope $\mathscr{P}_{\mathcal{O}_{F_a}}^\sigma$ are simultaneously stabilised by the gain matrix \mathcal{K} . The adapted Benton and Smith algorithm (Benton & Smith, 1999) presented in Section 5.3.1 can be formulated in terms of the triples $(\mathcal{A}_j, \mathcal{B}_j, \mathcal{C})$ for $j \in (1, N)$ and \mathbf{P}_{a1} in order to design the gain matrix \mathcal{K} as follows:

Step 1) Define the N vertices of the polytope $\mathscr{P}_{\mathcal{O}_{F_a}}^\sigma$.

Step 2) Define a degree of stability such that

$$\mathcal{A}_{\alpha j} = \mathcal{A}_j + \alpha \mathbf{I}_{(n+q-m)} \quad \text{for } j \in I(1, N)$$

Step 3) Solve the following optimisation problem

$$\begin{aligned} \min \quad & \text{trace}(\mathbf{Q}_{SF_a}) \\ \text{s.t.} \quad & \end{aligned}$$

$$\begin{aligned} & \mathbf{Q}_{SF_a} \succ \mathbf{I}_{(n+q-m)} \\ & \mathbf{Q}_{SF_a} \mathcal{A}_{\alpha j}^T + \mathcal{A}_{\alpha j} \mathbf{Q}_{SF_a} + \mathbf{Y}_{SF_a}^T \mathcal{B}_j^T + \mathcal{B}_j \mathbf{Y}_{SF_a} \prec 0 \\ & \text{for } j \in I(1, N) \end{aligned}$$

Step 4) Set $\mathbf{K}_{SF_a} = \mathbf{Y}_{SF_a} \mathbf{Q}_{SF_a}^{-1}$.

Step 5) Solve the LMI feasibility problem

$$\begin{aligned} \text{find } & \epsilon \text{ and } \mathbf{P}_{a1} \\ \text{s.t.} \quad & \end{aligned}$$

$$\begin{aligned} & \mathbf{P}_{a1} \succ \mathbf{I}_{(n+q-m)}, \quad \epsilon > 0 \\ & \left(\mathcal{A}_{\alpha j} + \mathcal{B}_j \mathbf{K}_{SF_a}\right)^T \mathbf{P}_{a1} + \mathbf{P}_{a1} \left(\mathcal{A}_{\alpha j} + \mathcal{B}_j \mathbf{K}_{SF_a}\right) \prec 0 \\ & \mathcal{A}_{\alpha j}^T \mathbf{P}_{a1} + \mathbf{P}_{a1} \mathcal{A}_{\alpha j} - \epsilon \mathcal{C}^T \mathcal{C} \prec 0 \\ & \text{for } j \in I(1, N) \end{aligned}$$

5.4 Sliding Mode Dynamic Output Feedback Control

Step 6) Solve the following LMI problem

find \mathcal{K}

s.t.

$$\begin{aligned} & \left(\mathcal{A}_{\alpha j} - \mathcal{B}_j \mathcal{K} \mathcal{C} \right)^T \mathbf{P}_{\alpha 1} + \mathbf{P}_{\alpha 1} \left(\mathcal{A}_{\alpha j} - \mathcal{B}_j \mathcal{K} \mathcal{C} \right) \prec 0 \\ & \text{for } j \in I(1, N) \end{aligned}$$

Remark 5.4 An optimisation problem involving the minimization of a norm, chosen by the designer, may take place in the step 6 of the adapted Benton & Smith Algorithm. For further details, see Remark 5.1.

5.4.2 Compensator-based Control Law Synthesis

Consider the following augmented matrices

$$\mathcal{A}_{a\Delta}(t) = \begin{bmatrix} \Xi & \Psi \mathbf{C} \\ \mathbf{0} & \bar{\mathbf{A}}_{\Delta}(t) \end{bmatrix} \quad \mathcal{B}_a = \begin{bmatrix} \mathbf{0} \\ \bar{\mathbf{B}} \end{bmatrix} \quad \mathcal{C}_a = \begin{bmatrix} \mathbf{I}_q & \mathbf{0} \\ \mathbf{0} & \bar{\mathbf{C}} \end{bmatrix} \quad (5.112)$$

If a switching gain matrix $\mathbf{\Gamma}_a = [\mathbf{\Gamma}_c \quad \mathbf{\Gamma}]$ exists such that the sliding dynamics in (5.23) and (5.24) are stable, then a nonsingular change of coordinates $\mathbf{x} \mapsto \hat{\mathbf{T}}_a \mathbf{x}$ exists such that the triple $(\mathcal{A}_{a\Delta}(t), \mathcal{B}_a, \mathcal{C}_a)$ can be transformed into

$$\hat{\mathcal{A}}_{a\Delta}(t) = \hat{\mathcal{A}}_a + \Delta \hat{\mathcal{A}}_a(t) = \begin{bmatrix} \hat{\mathcal{A}}_{a\Delta 11}(t) & \hat{\mathcal{A}}_{a\Delta 12}(t) \\ \hat{\mathcal{A}}_{a\Delta 21}(t) & \hat{\mathcal{A}}_{a\Delta 22}(t) \end{bmatrix} \quad (5.113)$$

$$\hat{\mathcal{B}}_a = \begin{bmatrix} \mathbf{0} & \mathbf{I}_m \end{bmatrix}^T \quad (5.114)$$

$$\mathbf{\Gamma}_a \hat{\mathcal{C}}_a = \begin{bmatrix} \mathbf{0} & \mathbf{I}_m \end{bmatrix} \quad \text{where } \hat{\mathcal{C}}_a = \begin{bmatrix} \mathbf{0} & \bar{\mathbf{T}}_a \end{bmatrix} \quad (5.115)$$

with $\bar{\mathbf{T}}_a \in \mathbb{R}^{(p+q) \times (p+q)}$ such that $\det\{\bar{\mathbf{T}}_a\} \neq 0$. As in the SMSOF approach in Section 5.3.2, the structure of $\mathbf{\Gamma}_a \hat{\mathcal{C}}_a$ follows since, by construction, $\mathbf{\Gamma}_a \hat{\mathcal{C}}_a \hat{\mathcal{B}}_a = \mathbf{\Gamma} \bar{\mathbf{C}} \bar{\mathbf{B}} = \mathbf{I}_m$.

Let

$$\mathbb{S}(t) = \left[\begin{array}{c|c} \hat{\mathcal{A}}_{a\Delta}(t) & \hat{\mathcal{B}}_a \\ \hline \hat{\mathcal{C}}_a & \mathbf{0} \end{array} \right] \quad (5.116)$$

The corresponding polytope $\mathcal{P}_{SF_a}^u$ is constructed by defining

$$\mathbb{S}_j = \left[\begin{array}{c|c} \hat{\mathcal{A}}_{a\Delta j} & \hat{\mathcal{B}}_a \\ \hline \hat{\mathcal{C}}_a & \mathbf{0} \end{array} \right] \quad (5.117)$$

i.e.

$$\mathcal{P}_{SF_a}^u = \left\{ \sum_{j=1}^N \mu_j \mathbb{S}_j : \sum_{j=1}^N \mu_j = 1, \mu_j \geq 0 \text{ for } j \in I(1, N) \right\} \quad (5.118)$$

5.4 Sliding Mode Dynamic Output Feedback Control

where the vertices are given by

$$\hat{\mathcal{A}}_{a\Delta j} = \hat{\mathcal{A}}_a + \sum_{i=1}^r \theta_i \Delta \hat{\mathcal{A}}_{ai} \Big|_{\theta_i = \{\underline{\theta}_i, \bar{\theta}_i\}} = \begin{bmatrix} \hat{\mathcal{A}}_{a\Delta 11j} & \hat{\mathcal{A}}_{a\Delta 12j} \\ \hat{\mathcal{A}}_{a\Delta 21j} & \hat{\mathcal{A}}_{a\Delta 22j} \end{bmatrix} \quad (5.119)$$

for $j \in I(1, N = 2^r)$, and $\hat{\mathcal{B}}_a$ and $\hat{\mathcal{C}}_a$ are defined in (5.114) and (5.115) respectively. The sliding mode dynamics are represented as a convex combination of

$$\hat{\mathcal{A}}_{a\Delta 11j} = \mathcal{A}_j - \mathcal{B}_j \mathcal{K} \mathcal{C} \quad \text{for } j \in I(1, N) \quad (5.120)$$

which are *Hurwitz* by design, and in turn

$$\hat{\mathcal{A}}_{a\Delta 11}(t) = \mathcal{A}(t) - \mathcal{B}(t) \mathcal{K} \mathcal{C} \quad (5.121)$$

is stable by the convexity property of the polytope \mathcal{P}_{OFA}^u .

Let \mathbf{P}_a be a Lyapunov matrix partitioned as follows

$$\mathbf{P}_a = \begin{bmatrix} \mathbf{P}_{a1} & \mathbf{0} \\ \mathbf{0} & \mathbf{P}_{a2} \end{bmatrix} \succ \mathbf{I}_{(n+q)} \quad (5.122)$$

where $\mathbf{P}_{a1} \in \mathfrak{R}^{(n+q-m) \times (n+q-m)}$ is the Lyapunov matrix in (5.111) calculated by means of the *Benton & Smith* algorithm, and $\mathbf{P}_{a2} \in \mathfrak{R}^{m \times m}$.

Consider the control law

$$\mathbf{u}(t) = \mathbf{u}_L(t) + \mathbf{u}_{NL}(t) \quad (5.123)$$

with a linear part $\mathbf{u}_L(t)$ of the form

$$\mathbf{u}_L(t) = -\mathbf{G}_a \mathbf{y}_a(t) \quad (5.124)$$

where $\mathbf{G}_a \in \mathfrak{R}^{m \times (p+q)}$. In (5.124), $\mathbf{y}_a(t) = [\mathbf{x}_c^T(t) \quad \mathbf{y}^T(t)]^T \in \mathfrak{R}^{(p+q)}$ is the augmented output vector. The nonlinear component $\mathbf{u}_{NL}(t)$ is given by

$$\mathbf{u}_{NL}(t) = \begin{cases} -\rho(t, \mathbf{y}, \mathbf{u}) \mathbf{P}_{a2}^{-1} \frac{\mathbf{\Gamma}_a \mathbf{y}_a(t)}{\|\mathbf{\Gamma}_a \mathbf{y}_a(t)\|} & \text{if } \mathbf{\Gamma}_a \mathbf{y}_a(t) \neq \mathbf{0} \\ \mathbf{0} & \text{otherwise} \end{cases} \quad (5.125)$$

where $\rho(t, \mathbf{y}, \mathbf{u})$ is of the form defined in (5.45).

The gain matrix \mathbf{G}_a in (5.124) is parameterized as follows

$$\mathbf{G}_a = \begin{bmatrix} \mathbf{G}_{a1} & \mathbf{G}_{a2} \end{bmatrix} \bar{\mathbf{T}}_a^{-1} \quad (5.126)$$

where $\mathbf{G}_{a1} \in \mathfrak{R}^{m \times (p+q-m)}$ and $\mathbf{G}_{a2} \in \mathfrak{R}^{m \times m}$. Suppose \mathbf{G}_a is chosen such that the

5.4 Sliding Mode Dynamic Output Feedback Control

following matrix inequality is satisfied

$$\mathcal{A}_j^T \mathbf{P}_a + \mathbf{P}_a \mathcal{A}_j \prec 0 \quad \text{for } j \in I(1, N) \quad (5.127)$$

where

$$\mathcal{A}_j = \begin{bmatrix} \hat{\mathcal{A}}_{a\Delta 11j} & \hat{\mathcal{A}}_{a\Delta 12j} \\ \hat{\mathcal{A}}_{a\Delta 21j} - \mathbf{G}_{a1}\mathcal{C} & \hat{\mathcal{A}}_{a\Delta 22j} - \mathbf{G}_{a2} \end{bmatrix} \quad (5.128)$$

Proposition 5.2 *The control law (5.123) along with (5.124) and (5.125) guarantees that the augmented sliding patch*

$$\Omega_a = \left\{ (\hat{\mathbf{x}}_{a1} \in \mathfrak{R}^{n+q-m}, \hat{\mathbf{x}}_{a2} \in \mathfrak{R}^m) : \|\hat{\mathbf{x}}_{a1}\| < \eta\gamma^{-1} \right\} \quad (5.129)$$

where $\eta > 0$ is a design scalar and

$$\gamma = \max_{j \in I(1, N)} \left\{ \|\mathbf{P}_{a2}(\hat{\mathcal{A}}_{a\Delta 21j} - \mathbf{G}_{a1}\mathcal{C})\| \right\}, \quad (5.130)$$

is reached in finite time, and a sliding motion on the surface $\mathcal{S}_{\mathcal{O}_{F_a}} \subset \Omega_a$ occurs.

△

Proof This follows straightforwardly from similar arguments as those applied when proving Proposition 5.1.

Q.E.D.

The LMI-based controller synthesis approach described in sub-section 5.3 can be applied to the augmented system triple $(\hat{\mathcal{A}}_{a\Delta j}, \hat{\mathcal{B}}_a, \hat{\mathcal{C}}_a)$ defined in (5.119), (5.114) and (5.115) respectively. To this end, partition $\hat{\mathcal{A}}_{a\Delta 21j}$ as follows

$$\hat{\mathcal{A}}_{a\Delta 21j} = \begin{bmatrix} \hat{\mathcal{A}}_{a\Delta 211j} & \hat{\mathcal{A}}_{a\Delta 212j} \end{bmatrix} \quad \text{for } j \in I(1, N) \quad (5.131)$$

where $\hat{\mathcal{A}}_{a\Delta 211j} \in \mathfrak{R}^{m \times (n+q-p)}$ and $\hat{\mathcal{A}}_{a\Delta 212j} \in \mathfrak{R}^{m \times (p-m)}$. Then, choose any

$$\gamma > \max_{j \in I(1, N)} \left\{ \|\hat{\mathcal{A}}_{a\Delta 211j}\| \right\} \quad (5.132)$$

and solve the following LMI problem:

5.4 Sliding Mode Dynamic Output Feedback Control

$$\begin{array}{l}
 \min \psi \\
 \text{s.t.} \\
 \left. \begin{array}{l}
 \left[\begin{array}{cc} -\psi \mathbf{I}_m & \left[\mathbf{L}_{a_1} \ \mathbf{L}_{a_2} \right] \bar{\mathbf{T}}_a^{-1} \\ \left(\left[\mathbf{L}_{a_1} \ \mathbf{L}_{a_2} \right] \bar{\mathbf{T}}_a^{-1} \right)^T & -\psi \mathbf{I}_{(p+q)} \end{array} \right] \prec 0 \\
 \left[\begin{array}{cc} -\gamma \mathbf{I}_m & \mathbf{P}_{a_2} \hat{\mathbf{A}}_{a\Delta 21j} - \mathbf{L}_{a_1} \mathbf{C} \\ \hat{\mathbf{A}}_{a\Delta 21j}^T \mathbf{P}_{a_2} - \mathbf{C}^T \mathbf{L}_{a_1}^T & -\gamma \mathbf{I}_{(n+q-m)} \end{array} \right] \prec 0 \\
 \left[\begin{array}{cc} -r_d \mathbf{P}_a & \mathbf{P}_a \mathcal{A}_j + c_n \mathbf{P}_a \\ c_n \mathbf{P}_a + \mathcal{A}_j^T \mathbf{P}_a & -r_d \mathbf{P}_a \end{array} \right] \prec 0 \\
 \mathcal{A}_j^T \mathbf{P}_a + \mathbf{P}_a \mathcal{A}_j + 2h \mathbf{P}_a \prec 0 \\
 \mathbf{P}_a \succ \mathbf{I}_{(n+q)}
 \end{array} \right\} \quad (5.133)
 \end{array}$$

for $j \in I(1, N)$ where \mathbf{L}_{a_1} , \mathbf{L}_{a_2} , \mathbf{P}_{a_1} and \mathbf{P}_{a_2} are the decision variables.

The block matrices of interest \mathbf{G}_{a_1} and \mathbf{G}_{a_2} can be recovered, if the optimisation problem (5.133) has a solution, as follows

$$\mathbf{G}_{a_1} = \mathbf{P}_{a_2}^{-1} \mathbf{L}_{a_1} \quad \text{and} \quad \mathbf{G}_{a_2} = \mathbf{P}_{a_2}^{-1} \mathbf{L}_{a_2} \quad (5.134)$$

5.4.3 Design and Computer Simulation Examples: SMDOFC

Example 5.3 Consider the uncertain dynamical plant

$$\left. \begin{array}{l}
 \dot{\mathbf{x}}(t) = \left[\begin{array}{ccc} -1 + \theta(t) & 1 & -1 \\ 1 & -1 & 0 \\ 4 & 0 & 2 \end{array} \right] \mathbf{x}(t) + \left[\begin{array}{c} 0 \\ 0 \\ 1 \end{array} \right] (u(t) + \xi(t, \mathbf{x}, u)) \\
 \mathbf{y}(t) = \left[\begin{array}{ccc} 0 & 1 & 0 \\ 0 & 0 & 1 \end{array} \right] \mathbf{x}(t)
 \end{array} \right\} \quad (5.135)$$

where $\xi(t, \mathbf{x}, u) = 0.5(\sin(2\pi t)x_2(t) + \sin(4\pi t)x_3(t))$ corresponds to the matched uncertainty, and $\theta(t) = 0.2\sin(t)$ is the mismatched uncertain parameter.

The root loci of $(\tilde{\mathbf{A}}_{11j}, \tilde{\mathbf{A}}_{12j}, \mathbf{C}_{1j})$ for $j \in I(1, 2)$, considering the extreme values of the mismatched parameter $\theta(t)$, are shown in Figure 5.8 and Figure 5.9 respectively. Figure 5.9 demonstrates that the reduced-order system is not static output feedback stabilisable. Therefore, a dynamical compensator is required to solve the SMC problem.

Defining $\Psi_2 = 1$ and $\Gamma_2 = 1$, the LMI approach proposed in Section 5.4.1 generates the following matrix

$$\mathcal{K} = \begin{bmatrix} -5.8603 & 4.6965 \\ -4.7174 & 3.0759 \end{bmatrix} \quad (5.136)$$

5.4 Sliding Mode Dynamic Output Feedback Control

which determines the compensator and the switching gain matrix Γ .

The convex region is defined through $c_n = 0$, $r_d = 5$ and $h = 0.10$. The gain matrix \mathbf{G} designed using the LMI method developed in this paper is given by

$$\mathbf{G}_a = \begin{bmatrix} 25.3915 & -23.5923 & 6.8839 \end{bmatrix} \quad (5.137)$$

The nonlinear part of the control law is smoothed as

$$u_{NL}(t) = \begin{cases} -\rho(t, \mathbf{y}, u) \mathbf{P}_{a_2}^{-1} \frac{\Gamma_a \mathbf{y}_a(t)}{\|\Gamma_a \mathbf{y}_a(t)\| + \varepsilon} & \text{if } \Gamma_a \mathbf{y}_a(t) \neq 0 \\ 0 & \text{otherwise} \end{cases} \quad (5.138)$$

which can be straightforwardly computed from the matched uncertainty $\xi(t, \mathbf{x}, u)$.

Computer simulations were carried out using the initial condition $\mathbf{x}_0 = [1 \ -1 \ 0]^T$. The time evolution of the output signals $\mathbf{y}(t)$ and the unmeasurable state variable $x_1(t)$ is shown in Figure 5.10. The designed SMDOFC stabilises the plant (5.135) in spite of the mismatched uncertain parameter $\theta(t)$. Figure 5.11 depicts the corresponding control signal whilst Figure 5.12 shows the switching function.

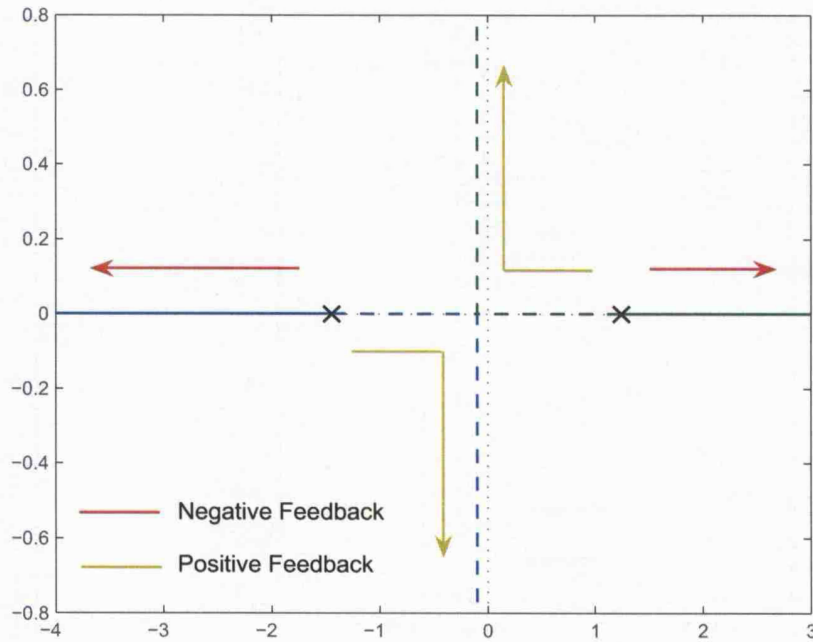


Figure 5.8: Root locus for the system triple $(\tilde{\mathbf{A}}_{111}, \tilde{\mathbf{A}}_{121}, \mathbf{C}_{11})$ for $\theta = \underline{\theta} = -0.2$

5.4 Sliding Mode Dynamic Output Feedback Control

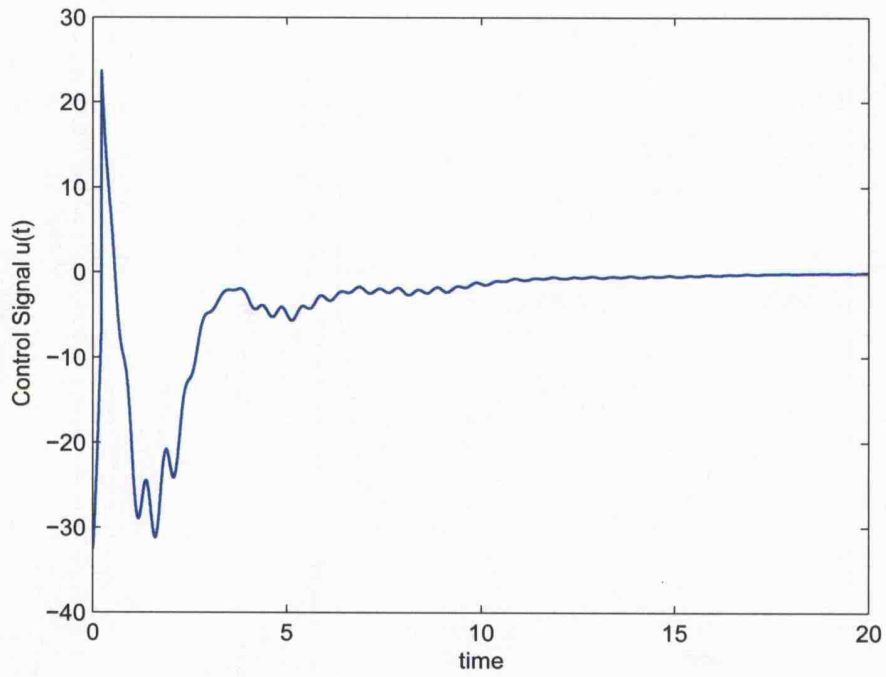


Figure 5.11: Control signal $u(t)$

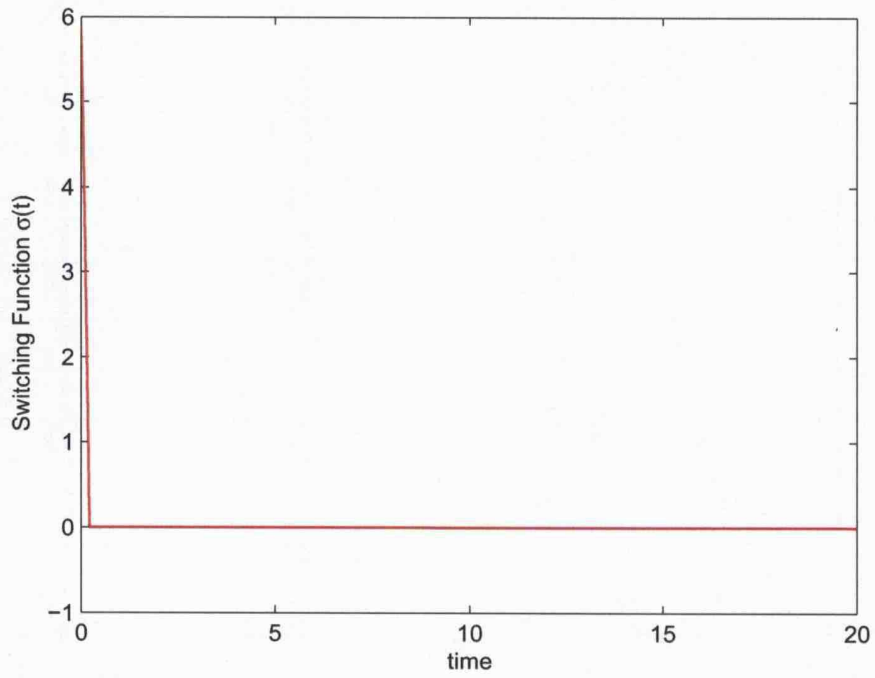


Figure 5.12: Time evolution of the switching function $\sigma(t)$

5.5 Summary

A new sliding mode static output feedback controller (SMSOFC) based on LMIs for systems with matched and mismatched uncertainties has been proposed in this chapter. The existence problem and the reaching problem have been formulated using a polytopic description. Once the existence problem has been formulated as a static output feedback (SOF) problem using a polytopic description, the switching gain matrix can be designed using a numerical algorithm. In this thesis, the non-iterative algorithm proposed in (Benton & Smith, 1999) has been adapted to tackle the sliding surface design. The control law is made up of linear and nonlinear (switched) components. The linear gains of the control law are numerically synthesised after formulating the reaching problem from a polytopic perspective as in the existence problem. The design methodology can be implemented in a straightforward way. Computer simulations have shown the efficacy of the newly proposed SMSOFC.

A sliding mode dynamic output feedback controller (SMDOFC) for uncertain plants with matched and mismatched uncertainties has been also proposed in this chapter. This control scheme represents an alternative when sliding mode static output feedback cannot be applied. An augmented uncertain system is constructed in order to design a compensator-based sliding surface. The existence problem is formulated as an SOF problem. The adapted algorithm applied for synthesising a sliding surface for the sliding mode static output feedback control scheme was re-adapted in order to deal with an augmented polytopic model. It should be noted that other algorithms available for polytopic models could be applied after carrying out a reformulation consistent with the sliding surface design. As in the sliding mode static output feedback control approach, the control law consists of two components. The linear part of the control law is designed using LMI methods through an optimisation problem similar to that used in the static output feedback case. The nonlinear part deals with the matched uncertainty and is not independent of the linear component gain matrix.

The control laws in both proposed control schemes do not incur high control effort, and do not induce chattering. The latter has been achieved by smoothing the discontinuous term in the nonlinear control component (see the nonlinear control parts defined in (5.91) and (5.138)). Study designs and computer simulations have illustrated the proposed approaches and have demonstrated their efficacy.

"The important thing in science is not so much to obtain new facts as to discover new ways of thinking about them"

Sir William Lawrence Bragg (1890 - 1971)

6

Sliding Mode Output Feedback Control: Simultaneous Stabilisation

6.1 Introduction

In this chapter, a sliding mode controller using only measured output signals for the simultaneous stabilisation of a finite set of uncertain systems is proposed. The proposed controller belongs to the class of output feedback controllers (static and dynamic). The synthesis methodology involves solving LMI problems. A noteworthy feature of the approaches presented in this chapter is that both matched and mismatched uncertainties can be considered. Furthermore, these control schemes can be also applied in the context of fault tolerant control (FTC), as discussed in Chapter 1, where the operating conditions are regarded as the fault-free and various fault affected plant models. Thus, a single output feedback sliding mode controller, if one exists, simultaneously stabilises a plant when there are faults affecting the dynamics of the system and in normal operating conditions. Here the class of faults considered affect the state matrix, whilst faults associated with actuators (that is, faults in the input-channel) can be interpreted as matched uncertainties.

This chapter is structured as follows: Section 6.2 describes the class of systems considered and problems to be addressed. A sliding mode static output feedback (SMSOF) controller design framework for the problem of simultaneous stabilisation is proposed in Section 6.3. This comprises sliding surface and control law synthesis for a finite set of plant models. Section 6.4 illustrates the SMSOF control strategy applied to a lateral motion autopilot for a remotely piloted vehicle when different flight conditions are considered. Then, as in Chapter 5, a dynamic output feedback sliding mode control scheme is presented in Section 6.5 as an option for cases in which the

6.2 System Description and Statement of Problems

collection of models is not simultaneous stabilisable by a single static output feedback sliding mode controller or the plant considered necessitates improvement of the closed-loop response for all its conditions of operation. The design methodology consists of synthesising a sliding surface and a control law considering a finite set of augmented models involving further dynamics provided by a compensator. Two design examples are presented in Section 6.6 to illustrate the proposed methodology. The first one consists of a finite set of systems which are not static output feedback stabilisable. This numerical example is presented in the context of robust FTC by considering fault-free and faulty operation modes. The second example considers a six-plate gas absorber whose operating conditions change depending on the load requirements. Finally, some conclusions are drawn in Section 6.7.

6.2 System Description and Statement of Problems

Consider the following finite set of N LTI uncertain plant models

$$\left. \begin{aligned} \dot{\mathbf{x}}(t) &= \mathbf{A}_i \mathbf{x}(t) + \mathbf{B}(\mathbf{u}(t) + \xi_i(t, \mathbf{x}, \mathbf{u})) \\ \mathbf{y}(t) &= \mathbf{C} \mathbf{x}(t) \quad , \quad \mathbf{x}_0 = \mathbf{x}(0) \end{aligned} \right\} \quad (6.1)$$

where $\mathbf{x}(t) \in \mathbb{R}^n$ is the state vector, $\mathbf{u}(t) \in \mathbb{R}^m$ is the input vector, and $\mathbf{y}(t) \in \mathbb{R}^p$ is the measurable output vector. The state matrices \mathbf{A}_i for $i \in I(1, N)$, the input matrix \mathbf{B} and the output matrix \mathbf{C} are constant matrices of appropriate dimensions. The vector valued-functions $\xi_i(t, \mathbf{x}, \mathbf{u})$ for $i \in I(1, N)$ represent the lumped sum of matched nonlinearities and/or uncertainties respectively.

Remark 6.1 *The finite set of plant models (6.1) may represent an uncertain linear system of the form $\dot{\mathbf{x}}(t) = (\mathbf{A} + \Delta \mathbf{A})\mathbf{x}(t) + \mathbf{B}(\mathbf{u}(t) + \xi(t, \mathbf{x}, \mathbf{u}))$, $\mathbf{y}(t) = \mathbf{C}\mathbf{x}(t)$ in which extreme values of the uncertain parameters in $\Delta \mathbf{A}$ are known up to some accuracy. This allows matched and mismatched uncertainties to be considered straightforwardly. Furthermore, in the context of fault tolerant control (FTC) where the operating conditions are regarded as the fault-free and various fault affected plant models.*

In this chapter the following are assumed:

- A-5.1** The N models of the plant have state matrices of the same order n .
- A-5.2** The order of the system (6.1) and the number of output and input signals satisfy $n > p > m$.
- A-5.3** The input and output matrices are both full rank, *i.e.* $rank(\mathbf{B}) = m$ and $rank(\mathbf{C}) = p$.

6.2 System Description and Statement of Problems

A-5.4 In the nominal triples $(\mathbf{A}_i, \mathbf{B}, \mathbf{C})$, $\text{rank}(\mathbf{CB}) = m$ for all $i \in I(1, N)$.

A-5.5 The matched uncertainty is bounded by

$$\max_{i \in I(1, N)} \{ \|\xi_i(t, \mathbf{x}, \mathbf{u})\| \} \leq k_1 \|\mathbf{u}(t)\| + \varphi(t, \mathbf{y}(t)) + k_2 \quad (6.2)$$

where $\varphi : \mathfrak{R}_+ \times \mathfrak{R}^p \rightarrow \mathfrak{R}_+$ is a known function, whilst $0 \leq k_1 < 1$ and $k_2 \geq 0$ are known constant scalars.

As discussed in Chapter 2 and Chapter 5, the assumption $\text{rank}(\mathbf{CB}) = m$ guarantees a similarity transformation exists such that the system triples $(\mathbf{A}_i, \mathbf{B}, \mathbf{C})$ for $i \in I(1, N)$ have the output feedback canonical form (Edwards & Spurgeon, 1995):

$$\left. \begin{aligned} \bar{\mathbf{A}}_i &= \begin{bmatrix} \bar{\mathbf{A}}_{11_i} & \bar{\mathbf{A}}_{12_i} \\ \bar{\mathbf{A}}_{21_i} & \bar{\mathbf{A}}_{22_i} \end{bmatrix} \quad \text{for } i \in I(1, N) \\ \bar{\mathbf{B}} &= \begin{bmatrix} \mathbf{0} \\ \bar{\mathbf{B}}_2 \end{bmatrix}, \quad \bar{\mathbf{C}} = \begin{bmatrix} \mathbf{0} & \mathbf{T} \end{bmatrix} \end{aligned} \right\} \quad (6.3)$$

where $\bar{\mathbf{A}}_{11_i} \in \mathfrak{R}^{(n-m) \times (n-m)}$, $\bar{\mathbf{A}}_{12_i} \in \mathfrak{R}^{(n-m) \times m}$, $\bar{\mathbf{A}}_{21_i} \in \mathfrak{R}^{m \times (n-m)}$, $\bar{\mathbf{A}}_{22_i} \in \mathfrak{R}^{m \times m}$, and the sub-matrix $\bar{\mathbf{B}}_2 \in \mathfrak{R}^{m \times m}$ is non-singular and $\mathbf{T} \in \mathfrak{R}^{p \times p}$ is an orthogonal matrix. Partition the states conformably with the structure of $\bar{\mathbf{A}}_i$ given in (6.3) so that $\bar{\mathbf{x}} = [\bar{\mathbf{x}}_1^T \quad \bar{\mathbf{x}}_2^T]^T$ where $\bar{\mathbf{x}}_2(t) \in \mathfrak{R}^m$.

Consider the sliding surface

$$\mathcal{S}_{OF} = \{ \mathbf{x} \in \mathfrak{R}^n : \boldsymbol{\sigma}(t) = \boldsymbol{\Gamma} \mathbf{y}(t) = \mathbf{0} \} \quad (6.4)$$

where $\boldsymbol{\sigma} \in \mathfrak{R}^m$, and the switching gain matrix is parameterised as in (Edwards & Spurgeon, 1995):

$$\boldsymbol{\Gamma} = \boldsymbol{\Gamma}_2 [\mathbf{K}_{OF} \quad \mathbf{I}_m] \mathbf{T}^T \quad (6.5)$$

where $\boldsymbol{\Gamma}_2 \in \mathfrak{R}^{m \times m}$ is nonsingular and $\mathbf{K}_{OF} \in \mathfrak{R}^{m \times (p-m)}$.

As in the previous chapter, for each of the models, the reduced-order sliding mode dynamics are governed by

$$\dot{\bar{\mathbf{x}}}_1(t) = (\bar{\mathbf{A}}_{11_i} - \bar{\mathbf{A}}_{12_i} \mathbf{K}_{OF} \mathbf{C}_1) \bar{\mathbf{x}}_1(t) \quad (6.6)$$

which corresponds to an output feedback problem. The sliding mode static output feedback simultaneous stabilisation (SMSOFSS) control problem is stated as follows:

SMSOFSS Control Problem: Design a switching gain matrix $\boldsymbol{\Gamma}$ of the form in (6.5) which defines the sliding surface \mathcal{S}_{OF} in (6.4), such that the sliding dynamics (6.6) are stable for all $i \in I(1, N)$. Furthermore, synthesise a sliding mode control law which

6.2 System Description and Statement of Problems

guarantees a finite time reaching phase from any initial point $\mathbf{x}(t_0) = \mathbf{x}_0 \notin \mathcal{S}_{OF}$ in the state space \mathcal{X} .

△

As discussed previously in Sections 5.2 and 5.4, in some particular cases, the sliding mode existence problem for systems given by (6.1) cannot be solved using static output feedback sliding mode. In this situation, as discussed in Chapter 5, the problem can be addressed by introducing further degrees of freedom through a dynamic compensator, given by

$$\dot{\mathbf{x}}_c(t) = \mathbf{\Xi}\mathbf{x}_c(t) + \mathbf{\Psi}_1\mathbf{C}_1\bar{\mathbf{x}}_1(t) + \mathbf{\Psi}_2\bar{\mathbf{x}}_2(t) \quad (6.7)$$

where $\mathbf{\Xi} \in \mathfrak{R}^{q \times q}$, $\mathbf{\Psi}_1 \in \mathfrak{R}^{q \times (p-m)}$ and $\mathbf{\Psi}_2 \in \mathfrak{R}^{q \times m}$. A sliding surface in the augmented state space $\mathcal{X}_a \subseteq \mathfrak{R}^{n+q}$ can be defined as

$$\mathcal{S}_{OF_a} = \{\mathbf{x}_a \in \mathfrak{R}^{n+q} : \boldsymbol{\sigma}_a(t) = \mathbf{\Gamma}_c\mathbf{x}_c(t) + \mathbf{\Gamma}\mathbf{C}\mathbf{x}(t) = \mathbf{0}\} \quad (6.8)$$

where $\mathbf{x}_a = [\mathbf{x}_c^T \quad \mathbf{x}^T]^T$ is the augmented state vector, and $\boldsymbol{\sigma}_a(t) \in \mathfrak{R}^m$ is the augmented switching function. The matrices $\mathbf{\Gamma}_c \in \mathfrak{R}^{m \times q}$ and $\mathbf{\Gamma} \in \mathfrak{R}^{m \times p}$ can be viewed as components of the augmented switching gain matrix

$$\mathbf{\Gamma}_a = \begin{bmatrix} \mathbf{\Gamma}_c & \mathbf{\Gamma} \end{bmatrix} \quad (6.9)$$

where $\mathbf{\Gamma}_c \in \mathfrak{R}^{m \times q}$ and $\mathbf{\Gamma} \in \mathfrak{R}^{m \times p}$.

The matrix $\mathbf{\Gamma}$ is parameterised as in (6.5). In what follows the matrix $\mathbf{\Gamma}_c$ is decomposed as

$$\mathbf{\Gamma}_c = \mathbf{\Gamma}_2\mathbf{K}_c \quad (6.10)$$

where $\mathbf{K}_c \in \mathfrak{R}^{m \times q}$.

It can be demonstrated that the compensator-based reduced-order sliding mode dynamics are governed by

$$\dot{\bar{\mathbf{x}}}_1(t) = (\bar{\mathbf{A}}_{11_i} - \bar{\mathbf{A}}_{12_i}\mathbf{K}_{OF}\mathbf{C}_1)\bar{\mathbf{x}}_1(t) - \bar{\mathbf{A}}_{12_i}\mathbf{K}_c\mathbf{x}_c(t) \quad (6.11)$$

$$\dot{\mathbf{x}}_c(t) = (\mathbf{\Psi}_1 - \mathbf{\Psi}_2\mathbf{K}_{OF})\mathbf{C}_1\bar{\mathbf{x}}_1(t) + (\mathbf{\Xi} - \mathbf{\Psi}_2\mathbf{K}_c)\mathbf{x}_c(t) \quad (6.12)$$

As in Chapter 5, the gain matrices \mathbf{K}_c and \mathbf{K}_{OF} must be synthesised such that (6.11)-(6.12) is stable, then the augmented switching gain matrix (6.9) can be calculated. The sliding mode dynamic output feedback simultaneous stabilisation (SMD-OFSS) control problem can be stated as:

6.3 SMSOFSS: Synthesis Framework

SMDOFSS Control Problem: The SMDOF controller design problem consists of finding Ξ , Ψ_1 , Ψ_2 , \mathbf{K}_{OF} and \mathbf{K}_c so that the

$$\Upsilon_i = \begin{bmatrix} (\bar{\mathbf{A}}_{11i} - \bar{\mathbf{A}}_{12i}\mathbf{K}_{OF}\mathbf{C}_1) & -\bar{\mathbf{A}}_{12i}\mathbf{K}_c \\ (\Psi_1 - \Psi_2\mathbf{K}_{OF})\mathbf{C}_1 & (\Xi - \Psi_2\mathbf{K}_c) \end{bmatrix} \quad (6.13)$$

are *Hurwitz* for $i \in I(1, N)$. This defines both the compensator and the augmented sliding hyperplane. In addition, a sliding mode control law for the collection of uncertain dynamical models (6.1) has to be designed such that the sliding surface \mathcal{S}_{OF_a} is reached in finite time from any initial point $\mathbf{x}_a(t_0) \notin \mathcal{S}_{OF_a}$ in the augmented state space $\mathcal{X}_a \subseteq \mathfrak{R}^{n+q}$. Once the sliding hyperplane is reached, the system trajectory is governed by the reduced-order sliding motion (6.11)-(6.12).

△

6.3 SMSOFSS: Synthesis Framework

The design methodology proposed in this section breaks down into two phases. The first one is concerned with synthesising the sliding surface by formulating a special static output feedback problem for the finite set of plant models (6.1). In this section, the LMI-based algorithm proposed in (Cao & Sun, 1998) has been adapted for finding, if there exists, a gain matrix \mathbf{K}_{OF} . The second phase corresponds to designing a control law using LMIs to ensure sliding is achieved.

6.3.1 Switching Surface Design

Consider a family of LTI uncertain plant models (6.1) and the corresponding finite set of reduced-order subsystems given by the triple $(\bar{\mathbf{A}}_{11i}, \bar{\mathbf{A}}_{12i}, \mathbf{C}_1)$ defined in (6.3) and (2.43) for $i \in I(1, N)$.

In this section, two results from (Cao & Sun, 1998) are reformulated in the context of the sliding mode existence problem.

Theorem 6.1 *The system triples $(\bar{\mathbf{A}}_{11i}, \bar{\mathbf{A}}_{12i}, \mathbf{C}_1)$ for $i \in I(1, N)$ are static output feedback stabilisable if and only if there exist N Lyapunov matrices $\mathbf{P}_{1i} \in \mathfrak{R}^{(n-m) \times (n-m)}$ and a gain matrix $\mathbf{K}_{OF} \in \mathfrak{R}^{m \times (p-m)}$ such that the following Quadratic Matrix Inequalities (QMIs) are satisfied*

$$\begin{aligned} & \bar{\mathbf{A}}_{11i}^T \mathbf{P}_{1i} + \mathbf{P}_{1i} \bar{\mathbf{A}}_{11i} - \mathbf{P}_{1i} \bar{\mathbf{A}}_{12i} \bar{\mathbf{A}}_{12i}^T \mathbf{P}_{1i} \\ & + (\bar{\mathbf{A}}_{12i}^T \mathbf{P}_{1i} + \mathbf{K}_{OF} \mathbf{C}_1)^T (\bar{\mathbf{A}}_{12i}^T \mathbf{P}_{1i} + \mathbf{K}_{OF} \mathbf{C}_1) \prec 0 \end{aligned} \quad (6.14)$$

for $i \in I(1, N)$.

△

6.3 SMSOFSS: Synthesis Framework

Proof Follows from the same arguments in (Cao & Sun, 1998) adapted to the reduced-order system (6.6).

The matrix variables in the QMIs above are \mathbf{P}_{1_i} and \mathbf{K}_{OF} . These QMIs can be written more conveniently by introducing additional variables \mathbf{X}_{1_i} of the same dimension as \mathbf{P}_{1_i} for $i \in I(1, N)$ such that

$$(\mathbf{X}_{1_i} - \mathbf{P}_{1_i})^T \bar{\mathbf{A}}_{12_i} \bar{\mathbf{A}}_{12_i}^T (\mathbf{X}_{1_i} - \mathbf{P}_{1_i}) \succeq 0 \quad (6.15)$$

As a consequence of using the matrix inequalities (6.15) in (6.14) and the *Schur* Complement, the following theorem is obtained.

Theorem 6.2 *The system triples $(\bar{\mathbf{A}}_{11_i}, \bar{\mathbf{A}}_{12_i}, \mathbf{C}_1)$ for $i \in I(1, N)$ are static output feedback stabilisable if and only if there exist N Lyapunov matrices $\mathbf{P}_{1_i} \in \mathfrak{R}^{(n-m) \times (n-m)}$, N matrices $\mathbf{X}_{1_i} \in \mathfrak{R}^{(n-m) \times (n-m)}$ and a gain matrix $\mathbf{K}_{OF} \in \mathfrak{R}^{m \times (p-m)}$ such that the following QMIs are satisfied*

$$\begin{bmatrix} \Sigma_i & (\bar{\mathbf{A}}_{12_i}^T \mathbf{P}_{1_i} + \mathbf{K}_{OF} \mathbf{C}_1)^T \\ (\bar{\mathbf{A}}_{12_i}^T \mathbf{P}_{1_i} + \mathbf{K}_{OF} \mathbf{C}_1) & -\mathbf{I}_m \end{bmatrix} \prec 0 \quad (6.16)$$

where

$$\Sigma_i := \bar{\mathbf{A}}_{11_i}^T \mathbf{P}_{1_i} + \mathbf{P}_{1_i} \bar{\mathbf{A}}_{11_i} - \mathbf{X}_{1_i} \bar{\mathbf{A}}_{12_i} \bar{\mathbf{A}}_{12_i}^T \mathbf{P}_{1_i} - \mathbf{P}_{1_i} \bar{\mathbf{A}}_{12_i} \bar{\mathbf{A}}_{12_i}^T \mathbf{X}_{1_i} + \mathbf{X}_{1_i} \bar{\mathbf{A}}_{12_i} \bar{\mathbf{A}}_{12_i}^T \mathbf{X}_{1_i} \quad (6.17)$$

for $i \in I(1, N)$.

△

Proof Follows from the same arguments in (Cao & Sun, 1998) adapted to the reduced-order system (6.6).

Note that if \mathbf{X}_{1_i} are fixed, then the QMIs in (6.16) become LMIs with respect to the matrix variables \mathbf{P}_{1_i} and \mathbf{K}_{OF} . This represent a sufficient condition.

The iterative algorithm proposed in (Cao & Sun, 1998) has been adapted to synthesise the gain matrix \mathbf{K}_{OF} as follows:

STEP 1) Set $j = 1$.

Select $\mathbf{Q}_i \succ 0$ and solve the following algebraic *Riccati* equations (AREs):

$$\bar{\mathbf{A}}_{11_i}^T \mathbf{P}_{1_i} + \mathbf{P}_{1_i} \bar{\mathbf{A}}_{11_i} - \mathbf{P}_{1_i} \bar{\mathbf{A}}_{12_i} \bar{\mathbf{A}}_{12_i}^T \mathbf{P}_{1_i} + \mathbf{Q}_i = 0 \quad (6.18)$$

Assume $\mathbf{X}_{1_{ij}} = \mathbf{P}_{1_i}$ with $i \in I(1, N)$ as the solution.

6.3 SMSOFSS: Synthesis Framework

STEP 2) Solve the following optimisation problem with respect to α_j , \mathbf{P}_{1ij} and \mathbf{K}_{OF} :

$$\begin{aligned} \min \quad & \alpha_j \\ \text{s.t.} \quad & \\ & \begin{bmatrix} \Sigma_{ij} - \alpha_j \mathbf{P}_{1ij} & (\bar{\mathbf{A}}_{12i}^T \mathbf{P}_{1ij} + \mathbf{K}_{OF} \mathbf{C}_1)^T \\ (\bar{\mathbf{A}}_{12i}^T \mathbf{P}_{1ij} + \mathbf{K}_{OF} \mathbf{C}_1) & -\mathbf{I}_m \end{bmatrix} \prec 0 \end{aligned} \quad (6.19)$$

$$\mathbf{P}_{1ij} = \mathbf{P}_{1ij}^T \succ 0 \quad (6.20)$$

where

$$\Sigma_{ij} \triangleq \bar{\mathbf{A}}_{11i}^T \mathbf{P}_{1ij} + \mathbf{P}_{1ij} \bar{\mathbf{A}}_{11i} - \mathbf{X}_{1ij} \bar{\mathbf{A}}_{12i} \bar{\mathbf{A}}_{12i}^T \mathbf{P}_{1ij} - \mathbf{P}_{1ij} \bar{\mathbf{A}}_{12i} \bar{\mathbf{A}}_{12i}^T \mathbf{X}_{1ij} + \mathbf{X}_{1ij} \bar{\mathbf{A}}_{12i} \bar{\mathbf{A}}_{12i}^T \mathbf{X}_{1ij} \quad (6.21)$$

for $i \in I(1, N)$.

STEP 3) If $\alpha_j < 0$ then the static output feedback gain \mathbf{K}_{OF} simultaneously stabilises (6.6). In which case STOP the algorithm.

STEP 4) Solve the following optimisation problem with respect to \mathbf{P}_{1ij} and \mathbf{K}_{OF} :

$$\begin{aligned} \min \quad & \sum_{i=1}^N \text{trace}(\mathbf{P}_{1ij}) \\ \text{s.t.} \quad & \end{aligned}$$

LMI given in (6.19)

$$\mathbf{P}_{1ij} = \mathbf{P}_{1ij}^T \succ 0$$

STEP 5) If $\sum_{i=1}^N \|\mathbf{X}_{1ij} - \mathbf{P}_{1ij}\| < \delta$ then go to step 6, else set $\mathbf{X}_{1ij} = \mathbf{P}_{1ij}$ and $j = j + 1$ then go to step 2. Notice that δ represents a tolerance level defined by the designer.

STEP 6) The finite set of reduced-order systems (6.6) may not be static output feedback simultaneously stabilisable. Therefore, STOP.

6.3.2 Control Law Design

If there exists a switching gain matrix Γ given in (6.5) so that the sliding dynamics defined in (6.6) are stable for $i \in I(1, N)$, then there exists a similarity transformation $\bar{\mathbf{x}} \mapsto \hat{\mathbf{T}}\bar{\mathbf{x}} = \hat{\mathbf{x}}$ which induces the following structure in the triple $(\bar{\mathbf{A}}_i, \bar{\mathbf{B}}, \bar{\mathbf{C}})$ from (6.3):

6.3 SMSOFSS: Synthesis Framework

$$\hat{\mathbf{A}}_i = \begin{bmatrix} \hat{\mathbf{A}}_{11i} & \hat{\mathbf{A}}_{12i} \\ \hat{\mathbf{A}}_{21i} & \hat{\mathbf{A}}_{22i} \end{bmatrix} \quad (6.22)$$

$$\hat{\mathbf{B}} = \begin{bmatrix} \mathbf{0} & \mathbf{I}_m \end{bmatrix}^T \quad (6.23)$$

$$\Gamma \hat{\mathbf{C}} = \begin{bmatrix} \mathbf{0} & \mathbf{I}_m \end{bmatrix} \quad \text{where} \quad \hat{\mathbf{C}} = \begin{bmatrix} \mathbf{0} & \bar{\mathbf{T}} \end{bmatrix} \quad (6.24)$$

with $\bar{\mathbf{T}} \in \mathfrak{R}^{(p \times p)}$ such that $\det\{\bar{\mathbf{T}}\} \neq 0$.

The sliding mode dynamics are given by

$$\hat{\mathbf{A}}_{11i} = \bar{\mathbf{A}}_{11i} - \bar{\mathbf{A}}_{12i} \mathbf{K}_{OF} \mathbf{C}_1 \quad \text{for } i \in (1, N) \quad (6.25)$$

which are *Hurwitz* by design.

Let \mathbf{P}_i for $i \in (1, N)$ be a finite set of *Lyapunov* block matrices satisfying

$$\mathbf{P}_i = \begin{bmatrix} \mathbf{P}_{1i} & \mathbf{0} \\ \mathbf{0} & \mathbf{P}_2 \end{bmatrix} \quad \text{for } i \in I(1, N) \quad (6.26)$$

where the $\mathbf{P}_{1i} \in \mathfrak{R}^{(n-m) \times (n-m)}$ are obtained from Section 6.3.1 for $i \in I(1, N)$, whilst the matrix $\mathbf{P}_2 \in \mathfrak{R}^{m \times m} \succ \mathbf{I}_m$ will be calculated when designing the control law. From the partition of \mathbf{P}_i in (6.26), and the input matrix $\hat{\mathbf{B}}$ defined in (6.23), it follows that the structural property

$$\mathbf{P}_i \hat{\mathbf{B}} = (\Gamma \hat{\mathbf{C}})^T \mathbf{P}_2 \quad \text{for } i \in I(1, N) \quad (6.27)$$

is satisfied.

The control law to be considered is made up of two components

$$\mathbf{u}(t) = \mathbf{u}_L(t) + \mathbf{u}_{NL}(t) \quad (6.28)$$

where $\mathbf{u}_L(t)$ is the linear output feedback component and $\mathbf{u}_{NL}(t)$ is the nonlinear part.

The linear component $\mathbf{u}_L(t)$ has the form

$$\mathbf{u}_L(t) = -\mathbf{G}\mathbf{y}(t) \quad (6.29)$$

where $\mathbf{G} \in \mathfrak{R}^{m \times p}$ is parameterised, conformably with the output matrix $\hat{\mathbf{C}}$ defined in (6.24) and the partition of \mathbf{P}_i given in (6.26), as

$$\mathbf{G} = \begin{bmatrix} \mathbf{G}_1 & \mathbf{G}_2 \end{bmatrix} \bar{\mathbf{T}}^{-1} \quad (6.30)$$

where $\mathbf{G}_1 \in \mathfrak{R}^{m \times (p-m)}$ and $\mathbf{G}_2 \in \mathfrak{R}^{m \times m}$.

6.3 SMSOFSS: Synthesis Framework

The nonlinear component is given by

$$\mathbf{u}_{NL}(t) = \begin{cases} -\rho(t, \mathbf{y}, \mathbf{u}) \mathbf{P}_2^{-1} \frac{\Gamma \mathbf{y}(t)}{\|\Gamma \mathbf{y}(t)\|} & \text{if } \Gamma \mathbf{y}(t) \neq \mathbf{0} \\ \mathbf{0} & \text{otherwise} \end{cases} \quad (6.31)$$

where the scalar function $\rho(t, \mathbf{y}, \mathbf{u})$ is such that

$$\rho(t, \mathbf{y}, \mathbf{u}) \geq \frac{\|\mathbf{P}_2\| (k_1 \|\mathbf{u}_L(t)\| + \varphi(t, \mathbf{y}) + k_2) + \eta}{(1 - \|\mathbf{P}_2\| k_1)} \quad (6.32)$$

with $\eta \in \mathfrak{R}_+$ a design parameter.

The following closed-loop matrix stems from applying (6.29) with (6.30) to the family of plants in the new coordinate system given in (6.22)-(6.24):

$$\mathcal{A}_i = \hat{\mathbf{A}}_i - \hat{\mathbf{B}} \mathbf{G} \hat{\mathbf{C}} = \begin{bmatrix} \hat{\mathbf{A}}_{11i} & \hat{\mathbf{A}}_{12i} \\ \hat{\mathbf{A}}_{21i} - \mathbf{G}_1 \mathbf{C}_1 & \hat{\mathbf{A}}_{22i} - \mathbf{G}_2 \end{bmatrix} \quad (6.33)$$

Suppose, the following matrix inequalities hold

$$\mathcal{A}_i^T \mathbf{P}_i + \mathbf{P}_i \mathcal{A}_i \prec 0 \quad \text{for } i \in I(1, N) \quad (6.34)$$

where \mathbf{P}_i has been defined in (6.26), then the following can be proved:

Proposition 6.1 *The control law (6.28)-(6.32) guarantees that the sliding patch*

$$\Omega = \left\{ (\hat{\mathbf{x}}_1 \in \mathfrak{R}^{(n-m)}, \hat{\mathbf{x}}_2 \in \mathfrak{R}^m) : \|\hat{\mathbf{x}}_1\| < \eta \gamma^{-1} \right\} \quad (6.35)$$

where $\eta > 0$ is a design scalar and

$$\gamma = \max_{i \in (1, N)} \left\{ \|\mathbf{P}_2 (\hat{\mathbf{A}}_{21i} - \mathbf{G}_1 \mathbf{C}_1)\| \right\} \quad (6.36)$$

is reached in finite time and a sliding motion takes place on the sliding surface \mathcal{S}_{OF} contained in the domain Ω .

△

Proof Consider the collection of *Lyapunov* functions

$$V_i(t) := \hat{\mathbf{x}}^T(t) \mathbf{P}_i \hat{\mathbf{x}}(t) \quad \text{for } i \in I(1, N) \quad (6.37)$$

6.3 SMSOFSS: Synthesis Framework

Their time derivatives along the closed-loop system's trajectories are given by

$$\begin{aligned} \dot{V}_i(t) &= ((\hat{\mathbf{A}}_i - \hat{\mathbf{B}}\mathbf{G}\hat{\mathbf{C}})\hat{\mathbf{x}}(t) + \hat{\mathbf{B}}(\mathbf{u}_{NL}(t) + \hat{\xi}_i(\cdot)))^T \mathbf{P}_i \hat{\mathbf{x}}(t) \\ &\quad + \hat{\mathbf{x}}^T(t) \mathbf{P}_i ((\hat{\mathbf{A}}_i - \hat{\mathbf{B}}\mathbf{G}\hat{\mathbf{C}})\hat{\mathbf{x}}(t) + \hat{\mathbf{B}}(\mathbf{u}_{NL}(t) + \hat{\xi}_i(\cdot))) \end{aligned} \quad (6.38)$$

$$\begin{aligned} &= \hat{\mathbf{x}}^T(t) ((\hat{\mathbf{A}}_i - \hat{\mathbf{B}}\mathbf{G}\hat{\mathbf{C}})^T \mathbf{P}_i + \mathbf{P}_i (\hat{\mathbf{A}}_i - \hat{\mathbf{B}}\mathbf{G}\hat{\mathbf{C}})) \hat{\mathbf{x}}(t) \\ &\quad - 2\hat{\mathbf{x}}^T \mathbf{P}_i \hat{\mathbf{B}} \rho(\cdot) \mathbf{P}_2^{-1} \frac{\Gamma \mathbf{y}(t)}{\|\Gamma \mathbf{y}(t)\|} + 2\hat{\mathbf{x}}^T(t) \mathbf{P}_i \hat{\mathbf{B}} \hat{\xi}_i(\cdot) \end{aligned} \quad (6.39)$$

Define

$$\hat{\mathbf{M}}_i \triangleq (\hat{\mathbf{A}}_i - \hat{\mathbf{B}}\mathbf{G}\hat{\mathbf{C}})^T \mathbf{P}_i + \mathbf{P}_i (\hat{\mathbf{A}}_i - \hat{\mathbf{B}}\mathbf{G}\hat{\mathbf{C}}) \quad \text{for } i \in I(1, N) \quad (6.40)$$

which are negative definite by assumption. Hence, the expression (6.39) can be written as

$$\dot{V}_i(t) = \hat{\mathbf{x}}^T(t) \hat{\mathbf{M}}_i \hat{\mathbf{x}}(t) - 2\hat{\mathbf{x}}^T(t) \mathbf{P}_i \hat{\mathbf{B}} \rho(\cdot) \mathbf{P}_2^{-1} \frac{\Gamma \mathbf{y}(t)}{\|\Gamma \mathbf{y}(t)\|} + 2\hat{\mathbf{x}}^T(t) \mathbf{P}_i \hat{\mathbf{B}} \hat{\xi}_i(\cdot) \quad (6.41)$$

By using the structural property (6.27), it follows

$$\dot{V}_i(t) = \hat{\mathbf{x}}^T(t) \hat{\mathbf{M}}_i \hat{\mathbf{x}}(t) - 2\rho(\cdot) \|\Gamma \hat{\mathbf{C}} \hat{\mathbf{x}}(t)\| + 2(\Gamma \hat{\mathbf{C}} \hat{\mathbf{x}}(t))^T \mathbf{P}_2 \hat{\xi}_i(\cdot) \quad (6.42)$$

$$\leq \hat{\mathbf{x}}^T(t) \hat{\mathbf{M}}_i \hat{\mathbf{x}}(t) - 2\rho(\cdot) \|\Gamma \hat{\mathbf{C}} \hat{\mathbf{x}}(t)\| + 2\|\Gamma \hat{\mathbf{C}} \hat{\mathbf{x}}(t)\| \|\mathbf{P}_2\| \|\hat{\xi}_i(\cdot)\| \quad (6.43)$$

$$\leq \hat{\mathbf{x}}^T(t) \hat{\mathbf{M}}_i \hat{\mathbf{x}}(t) - 2\|\Gamma \hat{\mathbf{C}} \hat{\mathbf{x}}(t)\| (\rho(\cdot) - \|\mathbf{P}_2\| (k_1 \|\mathbf{u}(t)\| + \varphi(\cdot) + k_2)) \quad (6.44)$$

From (6.2) and (6.32), the following has already been proved in Section 5.3.2:

$$\rho(t, \mathbf{y}, \mathbf{u}) \geq \|\mathbf{P}_2\| (k_1 \|\mathbf{u}(t)\| + \varphi(t, \mathbf{y}) + k_2) + \eta \quad (6.45)$$

Thus, (6.44) can be written as

$$\dot{V}_i(t) \leq \hat{\mathbf{x}}^T(t) \hat{\mathbf{M}}_i \hat{\mathbf{x}}(t) - 2\|\Gamma \hat{\mathbf{C}} \hat{\mathbf{x}}(t)\| \eta < 0 \quad \forall \hat{\mathbf{x}}(t) \neq 0 \quad \text{and } i \in I(1, N) \quad (6.46)$$

Therefore, the finite set of N uncertain systems is quadratically stable.

Partition the state vector $\hat{\mathbf{x}}(t)$ conformably with the structure of (6.26), so that $\hat{\mathbf{x}}(t) = [\hat{\mathbf{x}}_1^T(t) \quad \hat{\mathbf{x}}_2^T(t)]^T$ where $\hat{\mathbf{x}}_1 \in \mathfrak{R}^{(n-m)}$ and $\hat{\mathbf{x}}_2 \in \mathfrak{R}^m$. As a consequence of (6.24), it follows that

$$\Gamma \mathbf{y}(t) = \Gamma \hat{\mathbf{C}} \hat{\mathbf{x}}(t) = \hat{\mathbf{x}}_2(t) \quad (6.47)$$

6.3 SMSOFSS: Synthesis Framework

Define a finite set of *Lyapunov* functions

$$V_{\sigma_i}(t) := \hat{\mathbf{x}}_2^T(t) \mathbf{P}_2 \hat{\mathbf{x}}_2(t) \quad \text{for } i \in I(1, N) \quad (6.48)$$

Computation of their time derivatives along the trajectories results in

$$\begin{aligned} \dot{V}_{\sigma_i}(t) &= 2\hat{\mathbf{x}}_2^T(t) \mathbf{P}_2 (\hat{\mathbf{A}}_{21_i} - \mathbf{G}_1 \mathbf{C}_1) \hat{\mathbf{x}}_1(t) + \hat{\mathbf{x}}_2^T(t) \left((\hat{\mathbf{A}}_{22_i} - \mathbf{G}_2)^T \mathbf{P}_2 \right. \\ &\quad \left. + \mathbf{P}_2 (\hat{\mathbf{A}}_{22_i} - \mathbf{G}_2) \right) \hat{\mathbf{x}}_2(t) + 2\hat{\mathbf{x}}_2^T(t) \mathbf{P}_2 (\mathbf{u}_{NL}(t) + \hat{\xi}_i(\cdot)) \end{aligned} \quad (6.49)$$

Let

$$\hat{\mathbf{H}}_{\sigma_i} \triangleq (\hat{\mathbf{A}}_{22_i} - \mathbf{G}_2)^T \mathbf{P}_2 + \mathbf{P}_2 (\hat{\mathbf{A}}_{22_i} - \mathbf{G}_2) \quad (6.50)$$

which is negative definite as a consequence of (6.34). Therefore

$$\begin{aligned} \dot{V}_{\sigma_i}(t) &= \hat{\mathbf{x}}_2^T(t) \hat{\mathbf{H}}_{\sigma_i} \hat{\mathbf{x}}_2(t) + 2\hat{\mathbf{x}}_2^T(t) \mathbf{P}_2 (\hat{\mathbf{A}}_{21_i} - \mathbf{G}_1 \mathbf{C}_1) \hat{\mathbf{x}}_1(t) \\ &\quad + 2\hat{\mathbf{x}}_2^T(t) \mathbf{P}_2 (\mathbf{u}_{NL}(t) + \hat{\xi}_i(\cdot)) \end{aligned} \quad (6.51)$$

From (6.31)

$$\begin{aligned} \dot{V}_{\sigma_i}(t) &\leq \hat{\mathbf{x}}_2^T(t) \hat{\mathbf{H}}_{\sigma_i} \hat{\mathbf{x}}_2(t) + 2\|\hat{\mathbf{x}}_2(t)\| \|\mathbf{P}_2 (\hat{\mathbf{A}}_{21_i} - \mathbf{G}_1 \mathbf{C}_1)\| \|\hat{\mathbf{x}}_1(t)\| \\ &\quad - 2\|\hat{\mathbf{x}}_2(t)\| (\rho(\cdot) - \|\mathbf{P}_2\| \|\hat{\xi}_i(\cdot)\|) \end{aligned} \quad (6.52)$$

Since

$$\rho(\cdot) \geq \|\mathbf{P}_2\| (k_1 \|\mathbf{u}(t)\| + \varphi(\cdot) + k_2) + \eta \quad (6.53)$$

then

$$\begin{aligned} \dot{V}_{\sigma_i}(t) &\leq \hat{\mathbf{x}}_2^T(t) \hat{\mathbf{H}}_{\sigma_i} \hat{\mathbf{x}}_2(t) + 2\|\hat{\mathbf{x}}_2(t)\| \|\mathbf{P}_2 (\hat{\mathbf{A}}_{21_i} - \mathbf{G}_1 \mathbf{C}_1)\| \|\hat{\mathbf{x}}_1(t)\| - 2\eta \|\hat{\mathbf{x}}_2(t)\| \\ &< \hat{\mathbf{x}}_2^T(t) \hat{\mathbf{H}}_{\sigma_i} \hat{\mathbf{x}}_2(t) + 2\eta \gamma^{-1} \|\hat{\mathbf{x}}_2(t)\| \|\mathbf{P}_2 (\hat{\mathbf{A}}_{21_i} - \mathbf{G}_1 \mathbf{C}_1)\| - 2\eta \|\hat{\mathbf{x}}_2(t)\| < 0 \end{aligned} \quad (6.54)$$

which means that a sliding motion occurs inside the sliding patch Ω defined in (6.35) with (6.36). Since the system is quadratically stable, the system trajectories enter the domain Ω in finite time, and hence sliding occurs in finite time.

Q.E.D.

Remark 6.2 *The Lyapunov sub-matrices \mathbf{P}_{1_i} for $i \in I(1, N)$ in (6.26) are computed when solving the sliding mode existence problem using the approach presented in Section 6.3.1.*

In what follows, the control law design problem is addressed using similar arguments to those presented in Section 5.3.2. To this end, consider the expression in (6.34):

$$\mathcal{A}_i^T \mathbf{P}_i + \mathbf{P}_i \mathcal{A}_i = \begin{bmatrix} \hat{\mathbf{A}}_{11i}^T \mathbf{P}_{1i} + \mathbf{P}_{1i} \hat{\mathbf{A}}_{11i} & \mathbf{P}_{1i} \hat{\mathbf{A}}_{12i} + \hat{\mathbf{A}}_{21i}^T \mathbf{P}_2 - \mathbf{C}_1^T \mathbf{L}_1^T \\ * & \mathbf{P}_2 \hat{\mathbf{A}}_{22i} - \mathbf{L}_2 + \hat{\mathbf{A}}_{22i}^T \mathbf{P}_2 - \mathbf{L}_2^T \end{bmatrix} \quad (6.55)$$

Since (6.55) depends affinely on the matrix variables \mathbf{P}_{1i} , \mathbf{P}_2 , \mathbf{L}_1 and \mathbf{L}_2 ; an optimisation problem based on LMIs for synthesising a norm bounded gain matrix \mathbf{G} to ensure (6.34) holds can be formulated considering an LMI region. Here such a convex subset of the complex left-half plane \mathbb{C} is characterised by the intersection of the disk $D(c_n, r_d)$ centered at $(-c_n, 0)$ with radius r_d , and a half-plane $H(h)$ delimited by a vertical line at $(-h, 0)$ as shown in Figure 6.1.

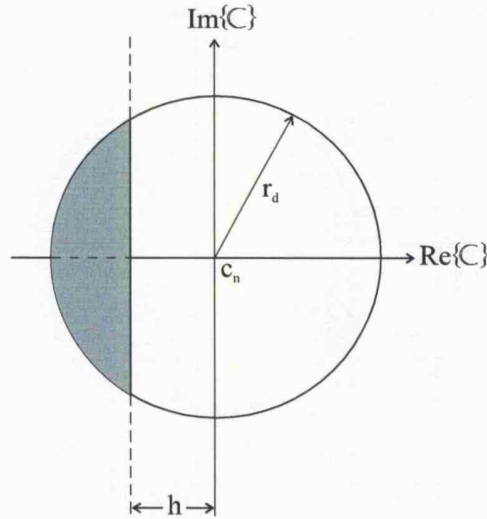


Figure 6.1: LMI Region $\mathcal{D}(h, c_n, r_d)$

The formulation of an optimisation problem for designing \mathbf{G} requires the partition

$$\hat{\mathbf{A}}_{21i} = \begin{bmatrix} \hat{\mathbf{A}}_{211i} & \hat{\mathbf{A}}_{212i} \end{bmatrix} \quad \text{for } i \in (1, N) \quad (6.56)$$

where $\hat{\mathbf{A}}_{211i} \in \mathbb{R}^{m \times (n-p)}$ and $\hat{\mathbf{A}}_{212i} \in \mathbb{R}^{m \times (p-m)}$.

Choose any

$$\gamma > \max_{i \in I(1, N)} \left\{ \|\hat{\mathbf{A}}_{211i}\| \right\} \quad (6.57)$$

6.4 Design and Computer Simulation Example

and solve the following LMI problem:

$$\begin{array}{l}
 \min \psi \\
 \text{s.t.} \\
 \left. \begin{array}{l}
 \left[\begin{array}{cc} -\psi \mathbf{I}_m & \left[\mathbf{L}_1 \quad \mathbf{L}_2 \right] \bar{\mathbf{T}}^{-1} \\ \left(\left[\mathbf{L}_1 \quad \mathbf{L}_2 \right] \bar{\mathbf{T}}^{-1} \right)^T & -\psi \mathbf{I}_p \end{array} \right] \prec 0 \\
 \left[\begin{array}{cc} -\gamma \mathbf{I}_m & \mathbf{P}_2 \hat{\mathbf{A}}_{21_i} - \mathbf{L}_1 \mathbf{C}_1 \\ \hat{\mathbf{A}}_{21_i}^T \mathbf{P}_2 - \mathbf{C}_1^T \mathbf{L}_1^T & -\gamma \mathbf{I}_{(n-m)} \end{array} \right] \prec 0 \\
 \left[\begin{array}{cc} -r_d \mathbf{P}_i & \mathbf{P}_i \mathcal{A}_i + c_n \mathbf{P}_i \\ c_n \mathbf{P}_i + \mathcal{A}_i^T \mathbf{P}_i & -r_d \mathbf{P}_i \end{array} \right] \prec 0 \\
 \mathcal{A}_i^T \mathbf{P}_i + \mathbf{P}_i \mathcal{A}_i + 2h \mathbf{P}_i \prec 0 \\
 \mathbf{P}_{1_i} \succ 0 \\
 \mathbf{P}_2 \succ \mathbf{I}_m
 \end{array} \right\} \quad (6.58)
 \end{array}$$

for $i \in (1, N)$ in terms of the matrix variables \mathbf{L}_1 , \mathbf{L}_2 , \mathbf{P}_{1_i} and \mathbf{P}_2 . If there exists a feasible solution to the optimisation problem formulated above, then the gain matrix \mathbf{G} can be calculated using

$$\mathbf{G}_1 = \mathbf{P}_2^{-1} \mathbf{L}_1 \quad \text{and} \quad \mathbf{G}_2 = \mathbf{P}_2^{-1} \mathbf{L}_2 \quad (6.59)$$

and the proposed controller guarantees a sliding mode takes place in finite time inside the sliding patch Ω .

6.4 Design and Computer Simulation Example

Consider the lateral motion autopilot for a remotely piloted vehicle presented in (White, 1990). The nonlinear aircraft system has been linearised around two operating conditions. In this design example, the actuators' dynamics have been neglected. The state and input matrices corresponding to each flight condition are:

$$\mathbf{A}_0 = \begin{bmatrix} 0 & 1 & 0 & 0 \\ 0 & -7.867 & -0.00939 & 3.58 \\ 9.80 & 0 & -0.255 & -30.35 \\ 0 & 0 & 0.3366 & -0.304 \end{bmatrix} \quad \mathbf{B}_0 = \begin{bmatrix} 0 & 0 \\ -24.40 & 0 \\ 0 & -4.69 \\ 0 & -8.02 \end{bmatrix} \quad (6.60)$$

$$\mathbf{A}_1 = \begin{bmatrix} 0.0079 & 1 & 0 & -0.0025 \\ 0 & -7.76 & -0.122 & 3.94 \\ 9.80 & -0.0018 & -0.267 & -29.08 \\ 0 & -0.215 & 0.332 & -0.288 \end{bmatrix} \quad \mathbf{B}_1 = \begin{bmatrix} 0 & 0 \\ -23.76 & 0 \\ 0 & -4.50 \\ 0 & -7.812 \end{bmatrix} \quad (6.61)$$

6.4 Design and Computer Simulation Example

$$\mathbf{C}_0 = \mathbf{C}_1 = \begin{bmatrix} 0 & 1 & 0 & 0 \\ 0 & 0 & 1 & 0 \\ 0 & 0 & 0 & 1 \end{bmatrix} \quad (6.62)$$

The state variables are the roll angle ϕ_{lc} ¹ [rad], the roll rate p_{lc} [rad/sec], the sideslip velocity v_{lc} [m/sec] and the yaw rate r_{lc} [rad/sec]. The control signals are the aileron angle $\zeta_{lc}(t)$ [rad] and the rudder angle $\tau_{lc}(t)$ [rad]. It has been assumed, without any loss of generality, the following matched vector-valued function

$$\xi_0(t, \mathbf{x}, \mathbf{u}) = \xi_1(t, \mathbf{x}, \mathbf{u}) = 0.5 \begin{bmatrix} \sin(t) \\ \sin(2t) \end{bmatrix} x_4(t) \quad (6.63)$$

impacts on the system.

In this example, there are two different input matrices \mathbf{B}_0 and \mathbf{B}_1 . The nominal input matrix has been considered as a common design input distribution matrix in the approach presented in this work. This argument will be justified in the sequel. Let \mathbf{B}_{ik} with $i \in I(0, 1)$, $k \in (1, 2)$, and $i \neq k$ be the k -th column vector of the i -th input distribution matrix. Let θ_{ijk} be the angle between the k -th column vector of the i -th and j -th input matrices. It can be verified that $\theta_{011} = 0^\circ$, and $\theta_{012} = 0.3751^\circ$. Since this angle is sufficiently small, it can be assumed $\mathbf{B}_{12} \approx \mathbf{B}_{02}\delta$. Therefore, it can be assumed $\mathbf{B}_1 \approx \mathbf{B}_0\delta$ where $\delta \in \mathfrak{R}$ is a scaling factor satisfying $0 < |\delta| < 1$. Notice that

$$\begin{bmatrix} 0 & 0 \\ -24.40 & 0 \\ 0 & -4.69 \\ 0 & -8.02 \end{bmatrix} \delta = \begin{bmatrix} 0 & 0 \\ -23.76 & 0 \\ 0 & -4.5510 \\ 0 & -7.7824 \end{bmatrix} \quad (6.64)$$

when $\delta = 0.9738$. The matrix on the R.H.S. of (6.64) is the same as \mathbf{B}_1 in (6.61) to 2 dps.

The gain matrix \mathbf{K}_{OP} has been designed using the approach described in Section 6.3. The corresponding iterative LMI algorithm generates

$$\mathbf{\Gamma} = \begin{bmatrix} -0.0753 & -0.0410 & 0 \\ 0.0384 & 0 & -0.1247 \end{bmatrix} \quad (6.65)$$

The convex LMI region associated with the control law has been defined using $c_n = 0$, $r_d = 20$ and $h = 0.10$. The following gain matrix has been obtained

$$\mathbf{G} = \begin{bmatrix} -0.5171 & -0.0223 & -0.0565 \\ 0.0297 & -0.0432 & -0.6491 \end{bmatrix} \quad (6.66)$$

¹Subscript *lc* stands for 'lateral control'.

6.4 Design and Computer Simulation Example

This, in turn, results in $\lambda(\hat{\mathbf{A}}_i - \mathbf{G}\hat{\mathbf{C}})$ for $i \in I(1, 2)$ as:

$$\{-6.1097, -1.7741, -3.1461 \pm 2.0421j\} \quad \{-5.8569, -1.7416, -3.1546 \pm 2.0466j\}$$

The nonlinear component in (6.28) has been designed as

$$\mathbf{u}_{NL} = - \begin{bmatrix} 0.1538 & 0.0062 \\ 0.0062 & 0.1765 \end{bmatrix} \frac{\mathbf{\Gamma}\mathbf{y}(t)}{\|\mathbf{\Gamma}\mathbf{y}(t)\| + \varepsilon} \quad (6.67)$$

where $\varepsilon = 1 \times 10^{-3}$ smooths the discontinuous term in order to obtain a chatter free control signal.

Computer simulations were performed using the initial condition

$$\mathbf{x}(0) = [0.4 \quad 0.4 \quad 0.8 \quad 0.4]^T \quad (6.68)$$

The response of each model in terms of the output signals $\mathbf{y}(t) = [p_{lc}(t) \quad v_{lc}(t) \quad r_{lc}(t)]^T$ is shown in Figure 6.2. This figure demonstrates that the designed sliding mode output feedback controller simultaneously stabilises the plant at the considered operating conditions. Figure 6.3 depicts the control signals which are within the permissible physical range. The time evolution of the switching functions is shown in Figure 6.4.

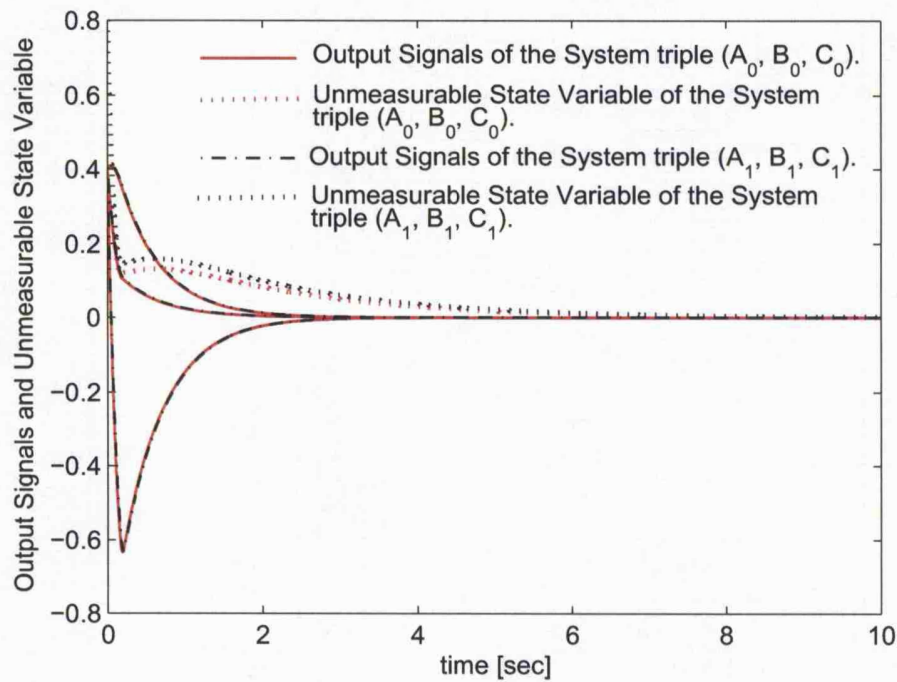


Figure 6.2: Time evolution of the output signals using the designed sliding mode output feedback controller.

6.4 Design and Computer Simulation Example

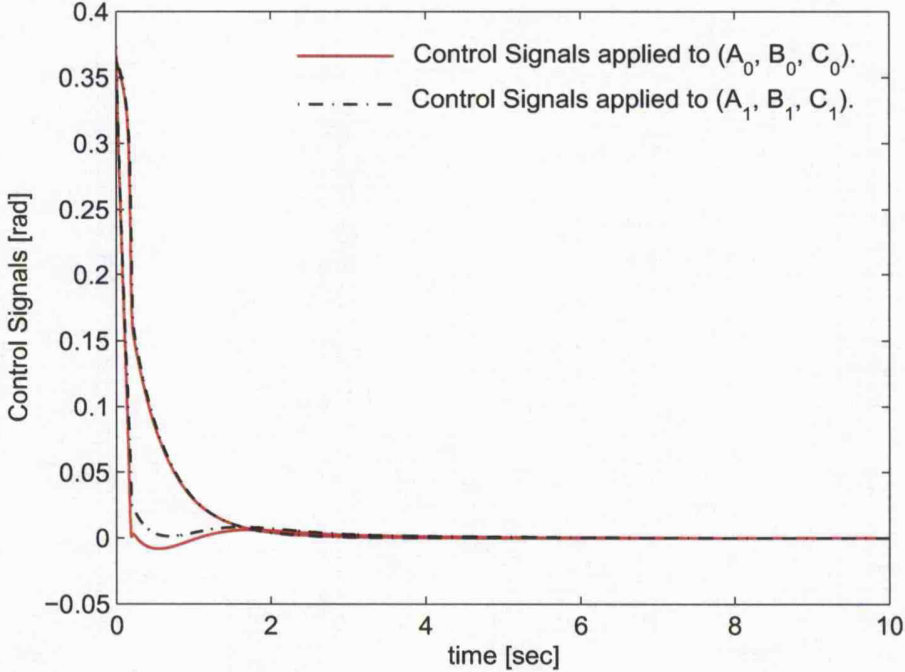


Figure 6.3: Control signals $\zeta(t)$ and $\tau(t)$.

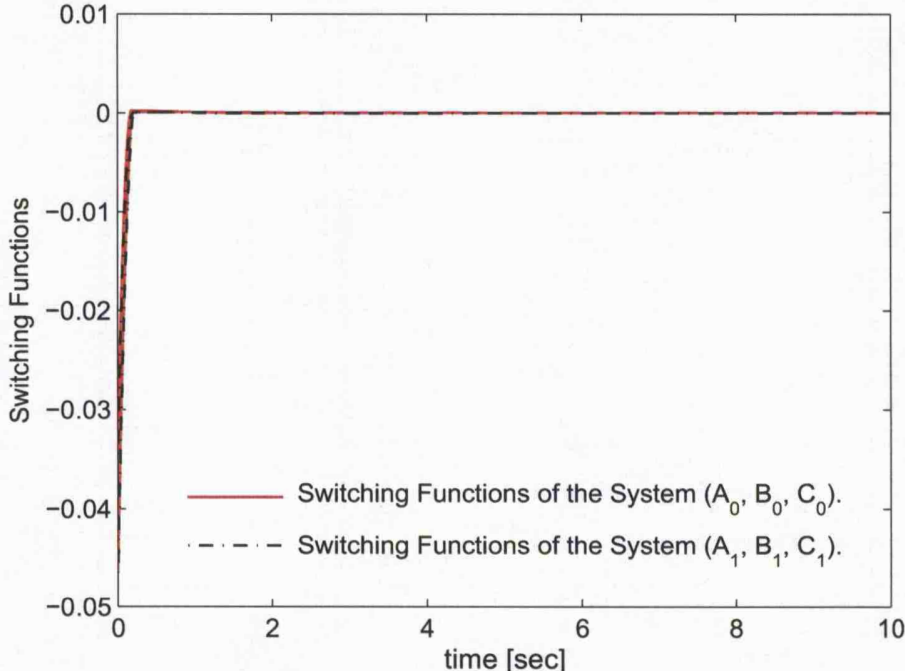


Figure 6.4: Switching functions vs time.

6.5 SMDOFSS: Synthesis Framework

6.5.1 Compensator-based Sliding Hyperplane Design

If it is not possible to stabilise the set of plants using static output feedback, a compensator must be introduced. As in Section 5.4, the problem of designing a dynamical compensator and a sliding surface is formulated in static output feedback form as follows:

$$\dot{\mathbf{z}}(t) = (\mathcal{A}_i - \mathcal{B}_i \mathcal{K} \mathcal{C}) \mathbf{z}(t) \quad (6.69)$$

where

$$\mathbf{z}(t) := \begin{bmatrix} \bar{\mathbf{x}}_1^T(t) & \mathbf{x}_c^T(t) \end{bmatrix}^T \quad (6.70)$$

$$\mathcal{A}_i := \begin{bmatrix} \bar{\mathbf{A}}_{11i} & \mathbf{0} \\ \mathbf{0} & \mathbf{0} \end{bmatrix} \quad \mathcal{B}_i := \begin{bmatrix} \bar{\mathbf{A}}_{12i} & \mathbf{0} \\ \boldsymbol{\Psi}_2 & -\mathbf{I}_q \end{bmatrix} \quad \mathcal{C} := \begin{bmatrix} \mathbf{C}_1 & \mathbf{0} \\ \mathbf{0} & \mathbf{I}_q \end{bmatrix} \quad (6.71)$$

$$\mathcal{K} := \begin{bmatrix} \mathbf{K}_{OF} & \mathbf{K}_c \\ \boldsymbol{\Psi}_1 & \boldsymbol{\Xi} \end{bmatrix} \quad (6.72)$$

Consider a finite set of reduced-order subsystems given by the triples $(\mathcal{A}_i, \mathcal{B}_i, \mathcal{C})$ defined in (6.71) for $i \in I(1, N)$. In the sequel, Theorems 6.1 and 6.2, as well as the algorithm presented in Section 6.3, are re-formulated in terms of the system matrices (6.70)-(6.72) in order to design a compensator-based sliding hyperplane.

Theorem 6.3 *The system triples $(\mathcal{A}_i, \mathcal{B}_i, \mathcal{C})$ for $i \in I(1, N)$ are static output feedback stabilisable if and only if there exist N Lyapunov matrices $\mathbf{P}_{a1_i} \in \mathfrak{R}^{(n+q-m) \times (n+q-m)}$ and a gain matrix $\mathcal{K} \in \mathfrak{R}^{(m+q) \times (p+q-m)}$ such that the following QMIs*

$$\mathcal{A}_i^T \mathbf{P}_{a1_i} + \mathbf{P}_{a1_i} \mathcal{A}_i - \mathbf{P}_{a1_i} \mathcal{B}_i \mathcal{B}_i^T \mathbf{P}_{a1_i} + (\mathcal{B}_i^T \mathbf{P}_{a1_i} + \mathcal{K} \mathcal{C})^T (\mathcal{B}_i^T \mathbf{P}_{a1_i} + \mathcal{K} \mathcal{C}) \prec 0 \quad (6.73)$$

for $i \in I(1, N)$ hold.

△

Proof This follows from the arguments in (Cao & Sun, 1998) adapted to the reduced-order system (6.11)-(6.12).

Theorem 6.4 *The system triples $(\mathcal{A}_i, \mathcal{B}_i, \mathcal{C})$ for $i \in I(1, N)$ are static output feedback stabilisable if and only if there exist N Lyapunov matrices $\mathbf{P}_{a1_i} \in \mathfrak{R}^{(n+q-m) \times (n+q-m)}$,*

6.5 SMDOFSS: Synthesis Framework

N matrices $\mathbf{X}_{a1_i} \in \mathfrak{R}^{(n+q-m) \times (n+q-m)}$ and a gain matrix $\mathcal{K} \in \mathfrak{R}^{(m+q) \times (p+q-m)}$ such that the following LMI

$$\begin{bmatrix} \Sigma_i & (\mathcal{B}_i^T \mathbf{P}_{a1_i} + \mathcal{K}\mathcal{C})^T \\ (\mathcal{B}_i^T \mathbf{P}_{a1_i} + \mathcal{K}\mathcal{C}) & -\mathbf{I}_{(m+q)} \end{bmatrix} \prec 0 \quad (6.74)$$

where

$$\Sigma_i = \mathcal{A}_i^T \mathbf{P}_{a1_i} + \mathbf{P}_{a1_i} \mathcal{A}_i - \mathbf{X}_{a1_i} \mathcal{B}_i \mathcal{B}_i^T \mathbf{P}_{a1_i} - \mathbf{P}_{a1_i} \mathcal{B}_i \mathcal{B}_i^T \mathbf{X}_{a1_i} + \mathbf{X}_{a1_i} \mathcal{B}_i \mathcal{B}_i^T \mathbf{X}_{a1_i} \quad (6.75)$$

holds for $i \in I(1, N)$.

△

Proof This follows from the arguments in (Cao & Sun, 1998) adapted to the reduced-order system (6.11)-(6.12).

In order to synthesise the gain matrix \mathcal{K} , the iterative algorithm proposed in (Cao & Sun, 1998) adapted in Section 6.3.1, is recast in terms of the system matrices (6.71) as follows:

STEP 1) Set $j = 1$.

Select $\mathbf{Q}_{a_i} \succ 0$ and solve the following algebraic *Riccati* equation (ARE):

$$\mathcal{A}_i^T \mathbf{P}_{a1_i} + \mathbf{P}_{a1_i} \mathcal{A}_i - \mathbf{P}_{a1_i} \mathcal{B}_i \mathcal{B}_i^T \mathbf{P}_{a1_i} + \mathbf{Q}_i = 0 \quad (6.76)$$

Define $\mathbf{X}_{a1_{ij}} = \mathbf{P}_{a1_i}$ with $i \in I(1, N)$ as the solution.

STEP 2) Solve the following optimisation problem with respect to α_j and $\mathbf{P}_{a1_{ij}}$:

min α_j
s.t.

$$\begin{bmatrix} \Sigma_{ij} - \alpha_j \mathbf{P}_{a1_{ij}} & (\mathcal{B}_i^T \mathbf{P}_{a1_{ij}} + \mathcal{K}\mathcal{C})^T \\ (\mathcal{B}_i^T \mathbf{P}_{a1_{ij}} + \mathcal{K}\mathcal{C}) & -\mathbf{I}_{(m+q)} \end{bmatrix} \prec 0 \quad (6.77)$$

$$\mathbf{P}_{a1_{ij}} = \mathbf{P}_{a1_{ij}}^T \succ 0 \quad (6.78)$$

where

$$\begin{aligned} \Sigma_{ij} := & \mathcal{A}_i^T \mathbf{P}_{a1_{ij}} + \mathbf{P}_{a1_{ij}} \mathcal{A}_i - \mathbf{X}_{a1_{ij}} \mathcal{B}_i \mathcal{B}_i^T \mathbf{P}_{a1_{ij}} \\ & - \mathbf{P}_{a1_{ij}} \mathcal{B}_i \mathcal{B}_i^T \mathbf{X}_{a1_{ij}} + \mathbf{X}_{a1_{ij}} \mathcal{B}_i \mathcal{B}_i^T \mathbf{X}_{a1_{ij}} \end{aligned} \quad (6.79)$$

for $i \in I(1, N)$.

6.5 SMDOFSS: Synthesis Framework

STEP 3) If $\alpha_j < 0$ then the SOF gain \mathcal{K} simultaneously stabilises (6.11)-(6.12).

In such a case, STOP the algorithm and set $\mathbf{P}_{a1_i} = \mathbf{P}_{a1_{ij}}$.

STEP 4) Solve the following optimisation problem:

$$\begin{aligned} \min \quad & \sum_{i=1}^N \text{trace}(\mathbf{P}_{a1_{ij}}) \\ \text{s.t.} \quad & \\ & \text{LMI given in (6.77)} \\ & \mathbf{P}_{a1_{ij}} = \mathbf{P}_{a1_{ij}}^T \succ 0 \end{aligned}$$

STEP 5) If $\sum_{i=1}^N \|\mathbf{X}_{a1_{ij}} - \mathbf{P}_{a1_{ij}}\| < \delta$, then go to step 6, else set $\mathbf{X}_{a1_{ij}} = \mathbf{P}_{a1_{ij}}$ and $j = j + 1$ then go to step 2.

STEP 6) The finite set of reduced-order systems (6.11)-(6.12) may not be static output feedback simultaneously stabilisable. Hence, STOP.

6.5.2 Control Law Design

Consider the following system of augmented matrices:

$$\mathcal{A}_{a_i} = \begin{bmatrix} \Xi & \Psi \mathbf{C} \\ \mathbf{0} & \bar{\mathbf{A}}_i \end{bmatrix} \quad \mathcal{B}_a = \begin{bmatrix} \mathbf{0} \\ \bar{\mathbf{B}} \end{bmatrix} \quad \mathcal{C}_a = \begin{bmatrix} \mathbf{I}_q & \mathbf{0} \\ \mathbf{0} & \bar{\mathbf{C}} \end{bmatrix} \quad (6.80)$$

The existence of a switching gain matrix $\Gamma_a = [\Gamma_c \quad \Gamma]$ such that the sliding dynamics (6.11)-(6.12) are stable, is of crucial importance for establishing a nonsingular change of coordinates $\bar{\mathbf{x}}_a \mapsto \hat{\Gamma}_a \bar{\mathbf{x}}_a = \hat{\mathbf{x}}_a$ which brings about the following form for the triples $(\mathcal{A}_{a_i}, \mathcal{B}_a, \mathcal{C}_a)$:

$$\hat{\mathcal{A}}_{a_i} = \begin{bmatrix} \hat{\mathcal{A}}_{a11i} & \hat{\mathcal{A}}_{a12i} \\ \hat{\mathcal{A}}_{a21i} & \hat{\mathcal{A}}_{a22i} \end{bmatrix} \quad (6.81)$$

$$\hat{\mathcal{B}}_a = \begin{bmatrix} \mathbf{0} & \mathbf{I}_m \end{bmatrix}^T \quad (6.82)$$

$$\Gamma_a \hat{\mathcal{C}}_a = \begin{bmatrix} \mathbf{0} & \mathbf{I}_m \end{bmatrix} \quad \text{where} \quad \hat{\mathcal{C}}_a = \begin{bmatrix} \mathbf{0} & \bar{\mathbf{T}}_a \end{bmatrix} \quad (6.83)$$

with $\bar{\mathbf{T}}_a \in \mathfrak{R}^{(p+q) \times (p+q)}$ such that $\det\{\bar{\mathbf{T}}_a\} \neq 0$. It is easy to see that the structure of $\Gamma_a \hat{\mathcal{C}}_a$ follows since by construction $\Gamma_a \hat{\mathcal{C}}_a \hat{\mathcal{B}}_a = \Gamma \bar{\mathbf{C}} \bar{\mathbf{B}} = \mathbf{I}_m$.

Let $\mathbf{P}_{a_i} \in \mathfrak{R}^{(n+q) \times (n+q)}$ for $i \in (1, N)$ be a finite set of *Lyapunov* sub-matrices of

6.5 SMDOFSS: Synthesis Framework

the form:

$$\mathbf{P}_{a_i} = \begin{bmatrix} \mathbf{P}_{a_{1i}} & \mathbf{0} \\ \mathbf{0} & \mathbf{P}_{a_2} \end{bmatrix} \quad \text{for } i \in I(1, N) \quad (6.84)$$

where the $\mathbf{P}_{a_{1i}} \in \mathfrak{R}^{(n+q-m) \times (n+q-m)}$ are obtained from the adapted algorithm formulated in Section 6.5.1 for $i \in I(1, N)$.

The control law to be considered is of the form

$$\mathbf{u}(t) = \mathbf{u}_L(t) + \mathbf{u}_{NL}(t) \quad (6.85)$$

The linear output feedback component is given by

$$\mathbf{u}_L(t) = -\mathbf{G}_a \mathbf{y}_a(t) \quad (6.86)$$

where $\mathbf{G}_a \in \mathfrak{R}^{m \times (p+q)}$ is so that

$$\mathbf{G}_a = \begin{bmatrix} \mathbf{G}_{a_1} & \mathbf{G}_{a_2} \end{bmatrix} \overline{\mathbf{T}}_a^{-1} \quad (6.87)$$

with $\mathbf{G}_{a_1} \in \mathfrak{R}^{m \times (p+q-m)}$ and $\mathbf{G}_{a_2} \in \mathfrak{R}^{m \times m}$.

The nonlinear component is given by

$$\mathbf{u}_{NL}(t) = \begin{cases} -\rho(t, \mathbf{y}, \mathbf{u}) \mathbf{P}_{a_2}^{-1} \frac{\Gamma_a \mathbf{y}_a(t)}{\|\Gamma_a \mathbf{y}_a(t)\|} & \text{if } \Gamma_a \mathbf{y}_a(t) \neq \mathbf{0} \\ \mathbf{0} & \text{otherwise} \end{cases} \quad (6.88)$$

where

$$\rho(t, \mathbf{y}, \mathbf{u}) \geq \frac{\|\mathbf{P}_2\| (k_1 \|\mathbf{u}_L(t)\| + \varphi(t, \mathbf{y}) + k_2) + \eta}{(1 - \|\mathbf{P}_2\| k_1)} \quad (6.89)$$

with $\eta \in \mathfrak{R}_+$. In addition, the augmented output vector $\mathbf{y}_a(t) \in \mathfrak{R}^{(p+q)}$ is given by

$$\mathbf{y}_a(t) = \begin{bmatrix} \mathbf{x}_c^T(t) & \mathbf{y}^T(t) \end{bmatrix}^T \quad (6.90)$$

Suppose the following inequality holds

$$\mathcal{A}_{a_i}^T \mathbf{P}_{a_i} + \mathbf{P}_{a_i} \mathcal{A}_{a_i} < 0 \quad \text{for } i \in I(1, N) \quad (6.91)$$

where \mathbf{P}_{a_i} is given in (6.84) and

$$\mathcal{A}_{a_i} := \begin{bmatrix} \hat{\mathcal{A}}_{a_{11i}} & \hat{\mathcal{A}}_{a_{12i}} \\ \hat{\mathcal{A}}_{a_{21i}} - \mathbf{G}_{a_1} \mathbf{C} & \hat{\mathcal{A}}_{a_{22i}} - \mathbf{G}_{a_2} \end{bmatrix} \quad (6.92)$$

6.5 SMDOFSS: Synthesis Framework

Proposition 6.2 *The control law (6.85) along with (6.86)-(6.88) guarantees that the sliding patch:*

$$\Omega_a = \left\{ (\hat{\mathbf{x}}_{a1} \in \mathfrak{R}^{(n+q-m)}, \hat{\mathbf{x}}_{a2} \in \mathfrak{R}^m) : \|\hat{\mathbf{x}}_{a1}\| < \eta\gamma^{-1} \right\} \quad (6.93)$$

where $\eta > 0$ is a design scalar and

$$\gamma = \max_{i \in (1, N)} \left\{ \|\mathbf{P}_{a2}(\hat{\mathcal{A}}_{a21i} - \mathbf{G}_{a1}\mathcal{C})\| \right\} \quad (6.94)$$

is reached in finite time and a sliding motion takes place on the sliding surface $\mathcal{S}_{OF_a} \subset \Omega_a$ defined in (6.8).

△

Proof This follows straightforwardly by using similar arguments to those applied when proving Proposition 6.1.

In the remainder of this section, an optimisation problem is formulated using LMI methods, following a similar methodology as used in previous sections. Note that the matrix \mathcal{A}_{a_i} in (6.92) can be written in compact form as

$$\mathcal{A}_{a_i} \triangleq \hat{\mathcal{A}}_{a_i} - \hat{\mathbf{B}}_a \mathbf{G}_a \hat{\mathcal{C}}_a \quad (6.95)$$

In addition, by defining matrix variables

$$\mathbf{L}_{a1} \triangleq \mathbf{P}_{a2} \mathbf{G}_{a1} \quad \text{and} \quad \mathbf{L}_{a2} \triangleq \mathbf{P}_{a2} \mathbf{G}_{a2} \quad (6.96)$$

it follows that

$$\mathcal{A}_{a_i}^T \mathbf{P}_{a_i} + \mathbf{P}_{a_i} \mathcal{A}_{a_i} = \begin{bmatrix} \hat{\mathcal{A}}_{a11i}^T \mathbf{P}_{a1i} + \mathbf{P}_{a1i} \hat{\mathcal{A}}_{a11i} & \mathbf{P}_{a1i} \hat{\mathcal{A}}_{a12i} + \hat{\mathcal{A}}_{a21i}^T \mathbf{P}_{a2} - \mathcal{C}^T \mathbf{L}_{a1}^T \\ * & \mathbf{P}_{a2} \hat{\mathcal{A}}_{a22i} - \mathbf{L}_{a2} + \hat{\mathcal{A}}_{a22i}^T \mathbf{P}_{a2} - \mathbf{L}_{a2}^T \end{bmatrix} \quad (6.97)$$

for $i \in I(1, N)$.

Using (6.97) the *Lyapunov* inequalities (6.91) are affine in the matrix variables \mathbf{P}_{a1i} , \mathbf{P}_{a2} , \mathbf{L}_{a1} and \mathbf{L}_{a2} . An LMI problem can be formulated in order to design a norm bounded gain matrix \mathbf{G}_a such that

$$\|\mathbf{G}_a\| < \psi \quad (6.98)$$

and

6.5 SMDOFSS: Synthesis Framework

$$\|\mathbf{P}_{a_2}\hat{\mathcal{A}}_{a_{21i}} - \mathbf{L}_{a_1}\mathcal{C}\| < \gamma \quad (6.99)$$

Inequality (6.98) has to be formulated in terms of the matrix variables \mathbf{L}_{a_1} and \mathbf{L}_{a_2} . It can be straightforwardly proved that

$$\|\mathbf{G}_a\| < \left\| \begin{bmatrix} \mathbf{L}_{a_1} & \mathbf{L}_{a_2} \end{bmatrix} \overline{\mathbf{T}}_a^{-1} \right\| \quad (6.100)$$

Consequently, by ensuring by design

$$\left\| \begin{bmatrix} \mathbf{L}_{a_1} & \mathbf{L}_{a_2} \end{bmatrix} \overline{\mathbf{T}}_a^{-1} \right\| < \psi \quad (6.101)$$

then inequality (6.98) is guaranteed to hold.

The LMI region to be considered is a convex region of the left half complex plane characterised by the intersection of the disk $D(c_n, r_d)$ centered at $(-c_n, 0)$ with radius r_d , and a half-plane $H(h)$ delimited by a vertical line at $(-h, 0)$ as shown in Figure 6.1.

The formulation of an LMI problem for synthesising the gain matrix \mathbf{G}_a requires the partition

$$\hat{\mathcal{A}}_{a_{21i}} = \begin{bmatrix} \hat{\mathcal{A}}_{a_{211i}} & \hat{\mathcal{A}}_{a_{212i}} \end{bmatrix} \text{ for } i \in (1, N) \quad (6.102)$$

where $\hat{\mathcal{A}}_{a_{211i}} \in \Re^{m \times (n+q-p)}$ and $\hat{\mathcal{A}}_{a_{212i}} \in \Re^{m \times (p-m)}$. To this end, choose any

$$\gamma > \max_{i \in I(1, N)} \left\{ \|\hat{\mathcal{A}}_{a_{211i}}\| \right\} \quad (6.103)$$

and solve the following LMI problem:

$$\left. \begin{array}{l} \min \psi \\ \text{s.t.} \\ \left[\begin{array}{cc} -\psi \mathbf{I}_m & \begin{bmatrix} \mathbf{L}_{a_1} & \mathbf{L}_{a_2} \end{bmatrix} \overline{\mathbf{T}}_a^{-1} \\ \left(\begin{bmatrix} \mathbf{L}_{a_1} & \mathbf{L}_{a_2} \end{bmatrix} \overline{\mathbf{T}}_a^{-1} \right)^T & -\psi \mathbf{I}_{(p+q)} \end{array} \right] \prec 0 \\ \left[\begin{array}{cc} -\gamma \mathbf{I}_m & \mathbf{P}_{a_2} \hat{\mathcal{A}}_{a_{21i}} - \mathbf{L}_{a_1} \mathcal{C} \\ \hat{\mathcal{A}}_{a_{21i}}^T \mathbf{P}_{a_2} - \mathcal{C}^T \mathbf{L}_{a_1}^T & -\gamma \mathbf{I}_{(n+q-m)} \end{array} \right] \prec 0 \\ \left[\begin{array}{cc} -r_d \mathbf{P}_{a_i} & \mathbf{P}_{a_i} \mathcal{A}_{a_i} + c_n \mathbf{P}_{a_i} \\ c_n \mathbf{P}_{a_i} + \mathcal{A}_{a_i}^T \mathbf{P}_{a_i} & -r_d \mathbf{P}_{a_i} \end{array} \right] \prec 0 \\ \mathcal{A}_{a_i}^T \mathbf{P}_{a_i} + \mathbf{P}_{a_i} \mathcal{A}_{a_i} + 2h \mathbf{P}_{a_i} \prec 0 \\ \mathbf{P}_{a_{1i}} \succ 0 \\ \mathbf{P}_{a_2} \succ \mathbf{I}_m \end{array} \right\} \quad (6.104)$$

6.6 Design and Computer Simulation Examples

for $i \in (1, N)$ in terms of the matrix variables \mathbf{L}_{a_1} , \mathbf{L}_{a_2} , \mathbf{P}_{a_1} and \mathbf{P}_{a_2} .

If a feasible solution exists to the LMI problem formulated above then the gain matrix \mathbf{G}_a can be built from

$$\mathbf{G}_{a_1} = \mathbf{P}_{a_2}^{-1} \mathbf{L}_{a_1} \quad \text{and} \quad \mathbf{G}_{a_2} = \mathbf{P}_{a_2}^{-1} \mathbf{L}_{a_2} \quad (6.105)$$

and the proposed control law (6.85) with (6.86)-(6.88) guarantees that a sliding mode takes place in finite time inside the sliding patch. Furthermore, the state trajectories will reach the sliding patch in finite time and will remain within it.

6.6 Design and Computer Simulation Examples

In this section two examples illustrate the sliding mode dynamic output feedback controller design approach proposed in the preceding two sections. The first example corresponds to a system which is not static output feedback stabilisable. In this case, a compensator-based sliding mode controller using only output information is employed.

In order to assess the proposed synthesis methodology in a plant with physical interpretation, a process engineering application corresponding to a gas absorber is considered as the second example. It is worth mentioning that another feature of the compensator-based control scheme is to improve the system's performance by introducing further dynamics.

Example 6.1 Consider the following system whose operation modes are determined by the values of the parameter θ_i for $i \in I(1, 2)$:

$$\mathbf{A}_i = \begin{bmatrix} 1 & 1 & -1 \\ 1 & -\theta_i & 0 \\ 4 & 0 & 2 \end{bmatrix} \quad \mathbf{B} = \begin{bmatrix} 0 \\ 0 \\ 1 \end{bmatrix} \quad \mathbf{C} = \begin{bmatrix} 0 & 1 & 0 \\ 0 & 0 & 1 \end{bmatrix} \quad (6.106)$$

$$\xi(\cdot)_1 = \xi(\cdot)_2 = 0.50(\sin(2\pi t)x_2(t) + \sin(4\pi t)x_3(t)) \quad (6.107)$$

Here two operating conditions are considered. It is assumed that $\theta_1 = 0.8$ corresponds to a fault-free mode, whilst $\theta_2 = 1.2$ represents a faulty operating condition.

It can be shown using root locus arguments that the sliding mode reduced-order dynamics corresponding to the set of models above are not static output feedback stabilisable. However, the sliding mode dynamic output feedback controller proposed in Section 6.5 can be applied.

6.6 Design and Computer Simulation Examples

Define $\Psi_2 = 1$ and $\Gamma_2 = 1$, then the following gain matrix which defines the compensator and the switching gain matrix Γ is given by

$$\mathcal{K} = \begin{bmatrix} -8.6721 & 1.8676 \\ 0.8460 & -1.2326 \end{bmatrix} \quad (6.108)$$

It can be shown this choice gives eigenvalues of the sliding mode reduced-order system at

$$\{ -1.0682 \pm 1.8653j, -0.7638 \}$$

and

$$\{ -1.4585 \pm 1.9615j, -0.3831 \}$$

respectively when $\theta_1 = 0.8$ and $\theta_2 = 1.2$.

An LMI region defined by $c_n = 0$, $r_d = 10$ and $h = 0.1$ has been used when designing the gain matrix \mathbf{G}_a and the *Lyapunov* matrix \mathbf{P}_{a2} via the LMI approach proposed in this chapter. The following gain matrix has been synthesised

$$\mathbf{G}_a = \begin{bmatrix} 3.0566 & -11.4253 & 5.0032 \end{bmatrix} \quad (6.109)$$

The eigenvalues $\lambda(\hat{\mathcal{A}}_{ai} - \hat{\mathcal{B}}_a \mathbf{G}_a \hat{\mathcal{C}}_a)$ for $i \in I(1, 2)$ are $\{ -0.6930 \pm 1.7388j, -0.4192 - 2.2306j \}$ and $\{ -0.7920 \pm 1.9153j, -0.2256, -2.6261 \}$. In the simulations, the non-linear part of the control law has been smoothed in order to obtain a chatter free control signal as follows:

$$u_{NL}(t) = \begin{cases} -\rho(t, \mathbf{y}, u) \mathbf{P}_{a2}^{-1} \frac{\mathbf{\Gamma}_a \mathbf{y}_a(t)}{\|\mathbf{\Gamma}_a \mathbf{y}_a(t)\| + \varepsilon} & \text{if } \mathbf{\Gamma}_a \mathbf{y}_a(t) \neq 0 \\ 0 & \text{otherwise} \end{cases} \quad (6.110)$$

which can be straightforwardly designed considering the matched uncertainty functions. The value of the constant ε has been chosen as 10×10^{-6} .

The initial condition $\mathbf{x}_0 = [-1 \ 1 \ 0]^T$ has been used for the computer simulations. In the sequel, the figures have been plotted considering both operation modes for θ_1 (black colour) and θ_2 (red colour). Figure 6.5 depicts the output signals $\mathbf{y}(t) = [y_1 \ y_2]^T$ and the unmeasurable state $x_1(t)$ for both operation modes. The system response demonstrates that the compensator-based sliding mode controller stabilises the set of models (6.106)-(6.107) using only output information. The corresponding control signals are shown in Figure 6.6 (which do not exhibit high frequency switching). The time evolution of the switching functions $\sigma(t)$ are presented in Figure 6.7. They are indistinguishable in both operating conditions of the system.

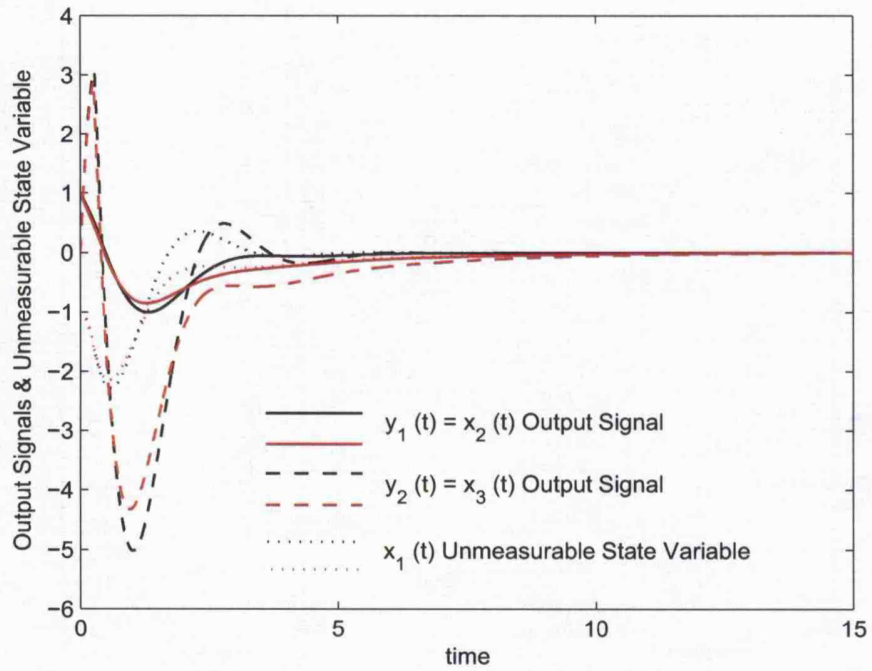


Figure 6.5: Time evolution of the output signals y_1 and y_2 , and the unmeasurable state x_1 for both operation modes of the plant

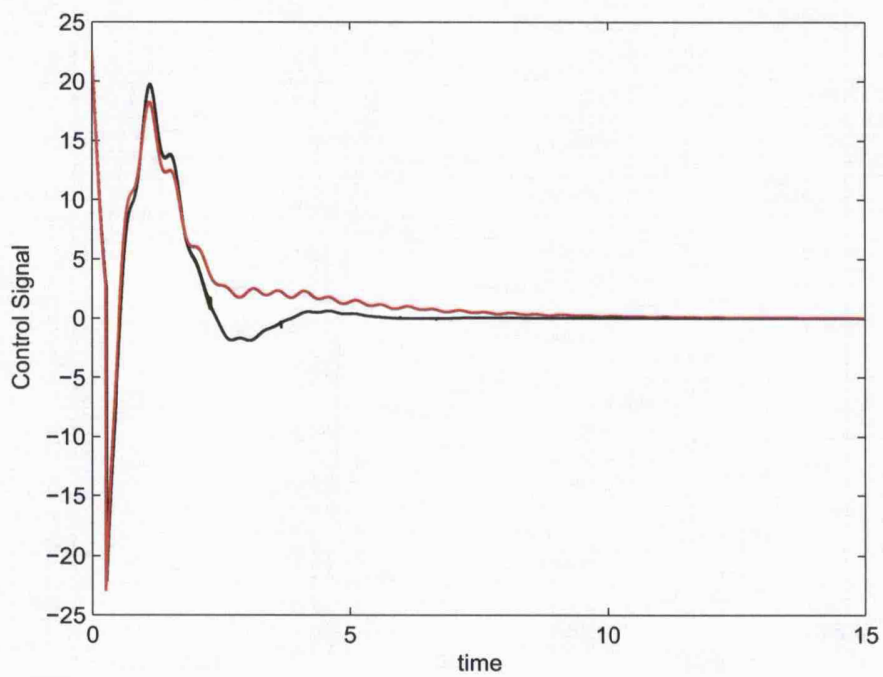


Figure 6.6: Control signal $u(t)$ for both operation modes of the plant

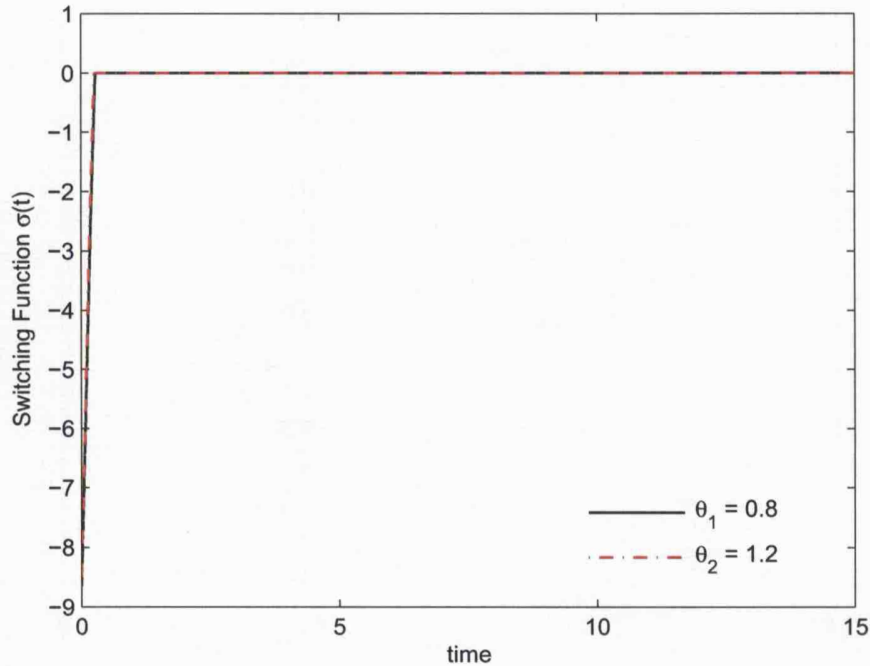


Figure 6.7: Switching function $\sigma(t)$ for both operation modes of the plant

Example 6.2 A gas absorber is a process plant which consists of n plates vertically disposed inside an absorption tower. The dynamical behaviour of the plant depends on the composition of the liquid and the vapor streams. This can be shown through the application of the principle of mass conservation by performing a mass balance study on the m -th plate of the gas absorber as in (Luus, 2000):

$$H_{ga} \dot{y}_m(t) + h_{ga} \dot{x}_m(t) = L_{ga}(x_{m-1}(t) - x_m(t)) + G_{ga}(y_{m+1}(t) - y_m(t)) \quad (6.111)$$

where $x_m(t)$ and $y_m(t)$ for $m \in I(1, n)$ represent the composition of liquid and vapor leaving the m -th plate [kg solute/kg inert], h_{ga} ¹ and H_{ga} are the inert liquid and vapor hold-ups on each plate [kg], L_{ga} is the flow rate of inert liquid absorbent [kg/min], G_{ga} is the flow rate of inert gas stream [kg/min], and time t [min]. As in (Luus, 2000), it is assumed that both h_{ga} and H_{ga} are constant. The flow rates are expressed in terms of the inerts to ensure that L_{ga} and G_{ga} remain constant from stage to stage, although the physical flow rates change because of the absorption process. Also, the following linear relation between the compositions in the liquid and vapor is assumed:

$$y_m(t) = \alpha_{ga} x_m(t) \quad \text{for } m \in I(1, n) \quad (6.112)$$

Substituting equation (6.112) into (6.111) yields

$$\dot{x}_m(t) = \frac{d}{e} x_{m-1}(t) - \left(\frac{d+1}{e} \right) x_{m+1}(t) \quad \text{for } m \in I(1, n) \quad (6.113)$$

¹Subscript *ga* stands for 'gas absorber'.

Figure 6.8 shows a schematic diagram of an n plate gas absorber.

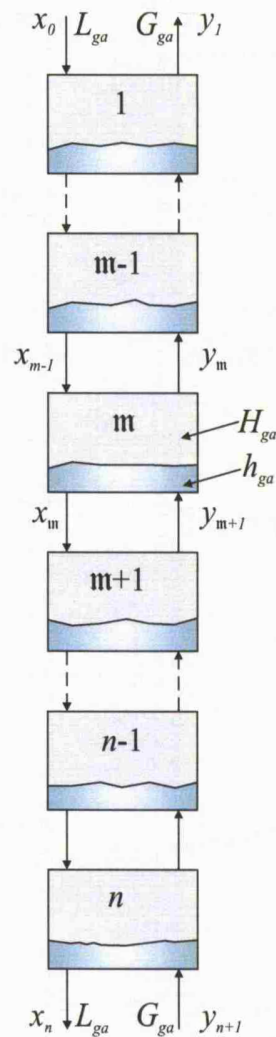


Figure 6.8: Schematic Diagram of an n plates Gas absorber [adapted from (Luus, 2000)]

The state-space description of a sixth-order gas absorber system has been widely used, e.g. (Bashein, 1971) (Howitt & Luus, 1993) and (Luus, 2000). This mathematical model follows from the differential equation (6.113) for $m \in I(1, 6)$ and is given by

$$\mathbf{A} = \begin{bmatrix} -\frac{d+1}{e} & \frac{1}{e} & 0 & 0 & 0 & 0 \\ \frac{d}{e} & -\frac{d+1}{e} & \frac{1}{e} & 0 & 0 & 0 \\ 0 & \frac{d}{e} & -\frac{d+1}{e} & \frac{1}{e} & 0 & 0 \\ 0 & 0 & \frac{d}{e} & -\frac{d+1}{e} & \frac{1}{e} & 0 \\ 0 & 0 & 0 & \frac{d}{e} & -\frac{d+1}{e} & \frac{1}{e} \\ 0 & 0 & 0 & 0 & \frac{d}{e} & -\frac{d+1}{e} \end{bmatrix} \quad (6.114)$$

6.6 Design and Computer Simulation Examples

$$\mathbf{B} = \begin{bmatrix} \frac{d}{e} & 0 & 0 & 0 & 0 & 0 \\ 0 & 0 & 0 & 0 & 0 & \frac{1}{e} \end{bmatrix}^T \quad (6.115)$$

where $d = L_{ga}/G_{ga}\alpha$ and $e = (H_{ga}\alpha_{ga} + h_{ga})/G_{ga}\alpha_{ga}$.

The following output distribution matrix has been considered

$$\mathbf{C} = \begin{bmatrix} 1 & 0 & 0 & 0 & 0 & 0 \\ 0 & 0 & 0 & 1 & 0 & 0 \\ 0 & 0 & 0 & 0 & 0 & 1 \end{bmatrix} \quad (6.116)$$

The nominal parameter values taken from (Luus, 2000) are $L_{ga} = 40.8$ [kg/min], $G_{ga} = 66.7$ [kg/min], $h_{ga} = 75$ [kg], $H_{ga} = 1$ [kg] and $\alpha_{ga} = 0.72$. As argued in (Howitt & Luus, 1993), the flow rates L_{ga} and G_{ga} may change during the operation of the plant depending on the load requirements. Five operating conditions are considered, and the corresponding flow rate values are given in Table 6.1.

k	L_{ga} [kg/min]	G_{ga} [kg/min]
1	40.8	66.7
2	35.8	61.7
3	35.8	71.7
4	45.8	71.7
5	45.8	61.7

Table 6.1: Liquid and gas flow rates for a set of operating conditions (Howitt & Luus, 1993)

The gas absorber plant model can be written straightforwardly in the form (6.1) considering the nominal parameters given above and embedding the changes in the input matrix (6.115) in the matched uncertainty terms $\xi_i(t, \mathbf{x}, \mathbf{u})$ for $i \in I(1, 5)$.

After applying the methodology presented in Section 6.5.1 and choosing $\Psi_2 = \begin{bmatrix} 1.0 & 1.0 \end{bmatrix}$, the following matrix is obtained in only one iteration of the iterative LMI algorithm described in Section 6.5.1.

$$\mathcal{K} = \begin{bmatrix} 1.9634 & 1.8152 \\ -1.7184 & 1.8842 \\ 0.3087 & -2.0785 \end{bmatrix} \quad (6.117)$$

The eigenvalues of the sliding mode reduced-order systems are shown in Figure 6.9. An LMI region defined by $c_n = 0$, $r_d = 10$ and $h = 0.2$ has been used and the following gain matrix has been synthesised as

$$\mathbf{G}_a = \begin{bmatrix} 0.9377 & 1.0612 & 0.6211 & 1.7966 \\ -0.2771 & -0.6510 & 2.2488 & -0.2482 \end{bmatrix} \quad (6.118)$$

6.6 Design and Computer Simulation Examples

The eigenvalues $\lambda(\hat{\mathcal{A}}_{ai} - \hat{\mathcal{B}}_a \mathbf{G}_a \hat{\mathcal{C}}_a) \in \mathbb{C}_-$ for $i \in I(1, 5)$ are depicted in Figure 6.10. As in example 2, the discontinuous component of the control law was straightforwardly designed considering the matched uncertainties $\xi_i(\cdot)$ for $i \in I(1, 5)$, and smoothed as in (6.110). In this example, the scalar ϵ is 10×10^{-3} .

The initial condition, considered in the computer simulations, is

$$\mathbf{x}_0 = \begin{bmatrix} -0.0306 & -0.0568 & -0.0788 & -0.0977 & -0.1138 & -0.1273 \end{bmatrix}^T \quad (6.119)$$

as used in (Howitt & Luus, 1993).

The dynamic response of the gas absorber system, for the set of operating conditions, using the SMDOF controller proposed in this chapter is shown in Figure 6.11. The control signals, as expected without high frequency oscillations, are depicted in Figure 6.12. The switching functions are shown in Figure 6.13. It can be seen that the sliding motion occurs after approximately 2 minutes for all operating conditions. The overshoot in the time evolution of the switching functions reveals the variable structure nature arising from the additional dynamics of the output feedback controller.

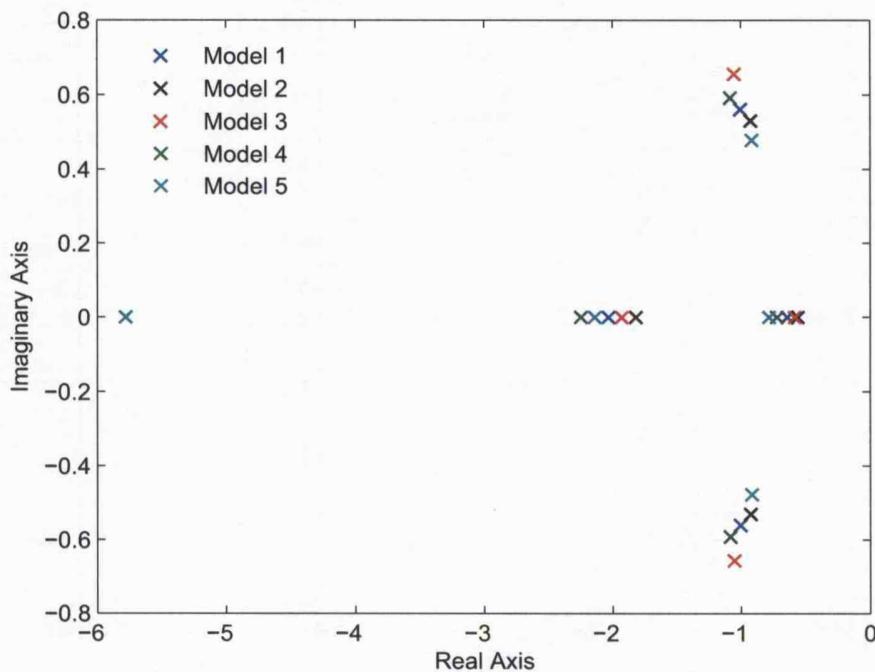


Figure 6.9: Eigenvalues of the sliding mode reduced-order system at each operating condition of the gas absorber plant.

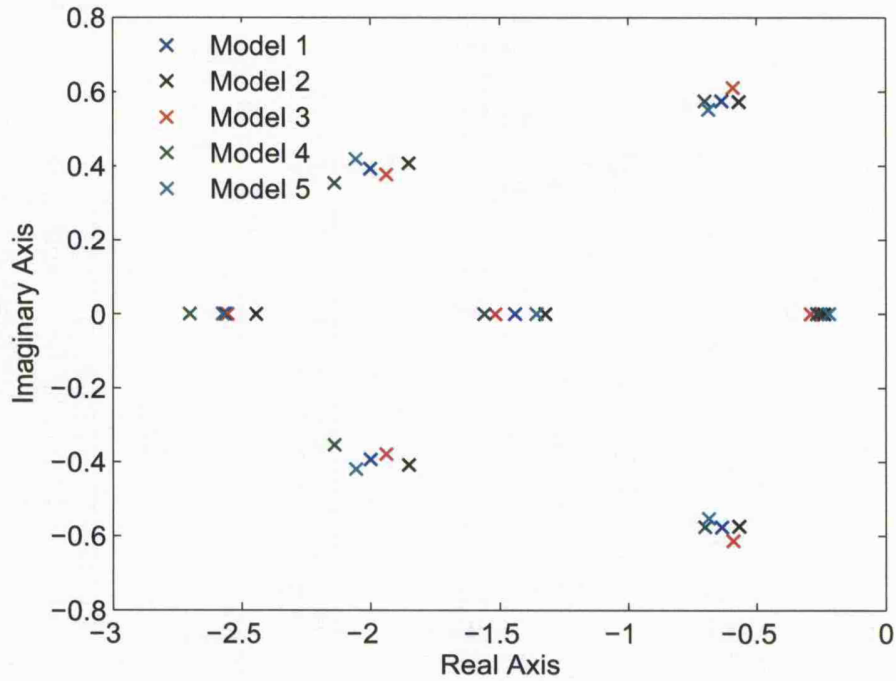


Figure 6.10: Eigenvalues of $(\hat{A}_{ai} - \hat{B}_a \mathbf{G}_a \hat{C}_a)$ for the set of operating conditions of the gas absorber plant.

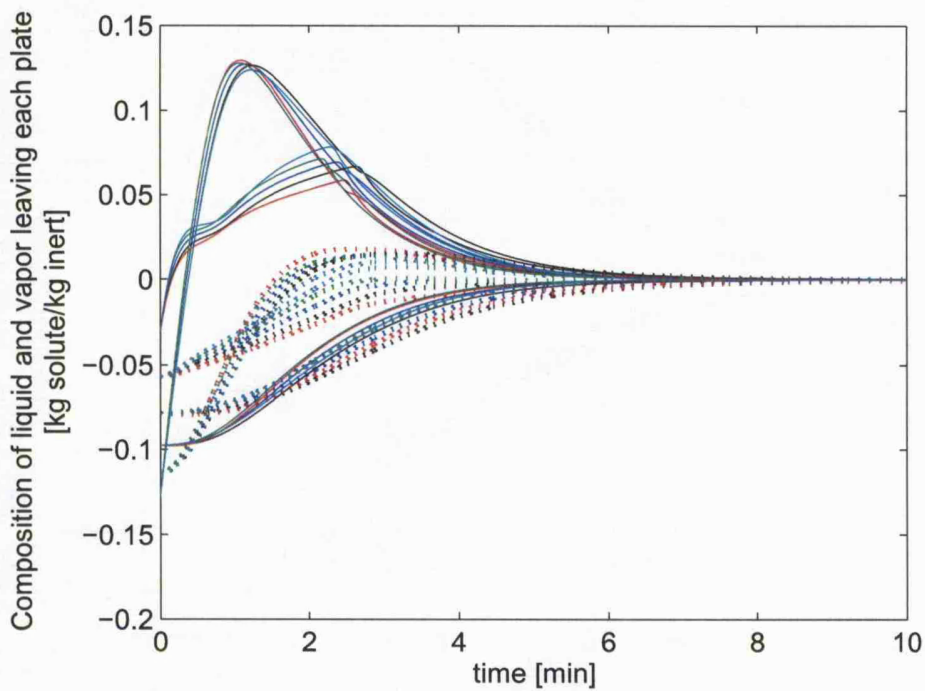


Figure 6.11: Time evolution of the output signals (continuous lines), and the unmeasured state variables (dotted lines) for the set of operating conditions of the gas absorber plant

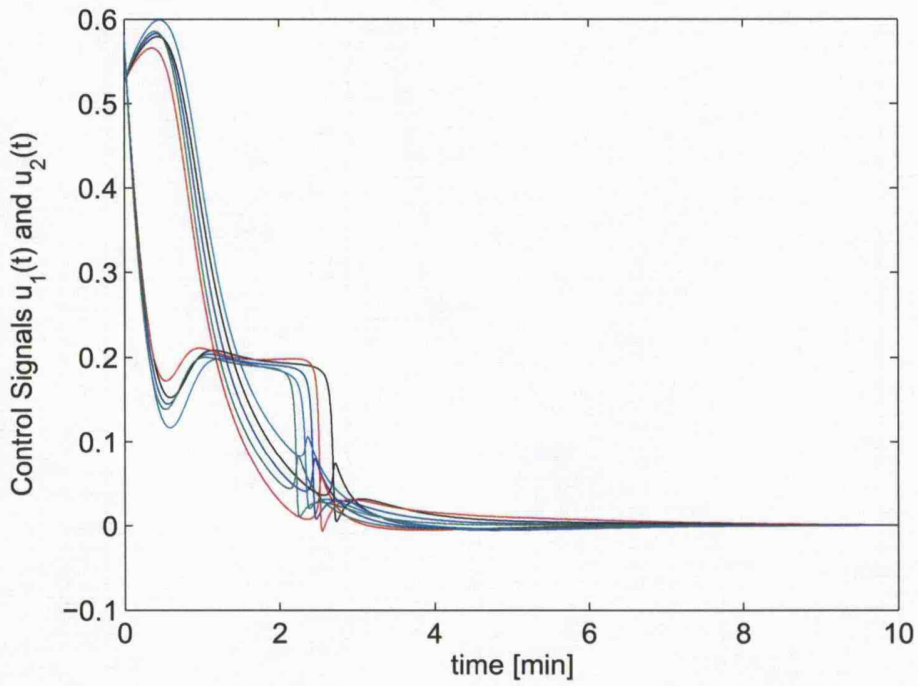


Figure 6.12: Control signals $u_1(t)$ and $u_2(t)$ for the set of operating conditions of the gas absorber plant

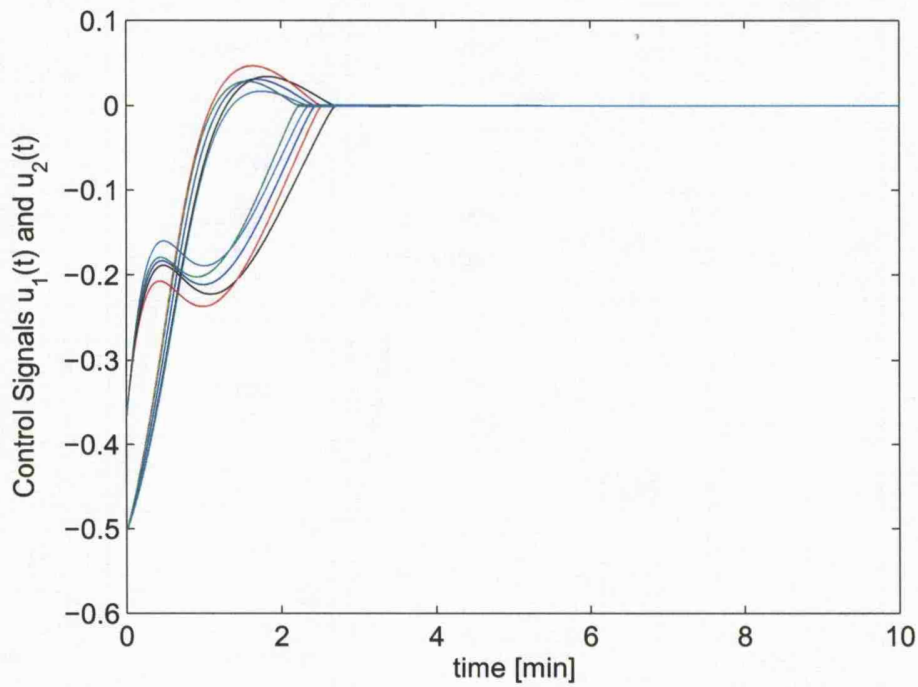


Figure 6.13: Switching functions $\sigma_1(t)$ and $\sigma_2(t)$ for the set of operating conditions of the gas absorber plant

6.7 Summary

An LMI-based design framework for sliding mode static output feedback control systems which simultaneously stabilises a finite set of models has been proposed. This approach can be applied to a set of uncertain linear systems. In both cases matched and mismatched uncertainties can be dealt with. This is a noteworthy feature since most of the existing sliding mode output feedback control approaches only tackle matched uncertainties and a ‘one plant’ model. The existence problem has been formulated as a static output feedback problem for the set of models under study. The LMIs involved in the solution of the existence problems have as many *Lyapunov* matrices as models considered. This reduces the conservatism compared to the case (in Chapter 5 for example) when only one *Lyapunov* matrix is used for all models. The sliding mode controller is static in nature and the control law consists of a linear and a nonlinear component. The design of the linear component is carried out by solving an LMI-based optimisation problem considering the set of models. The proposed sliding mode static output feedback controller has demonstrated, through computer simulations, its efficacy in simultaneously stabilising a lateral motion autopilot for a remotely piloted vehicle when different flight conditions were considered.

A compensator-based sliding mode controller using only output information, which simultaneously stabilises a finite set of models, has also been proposed. This synthesis methodology can be applied when the collection of sliding mode reduced-order systems is not static output feedback stabilisable. As in the sliding mode static output feedback scheme proposed in this chapter, an interpretation of the different state matrices is that they constitute mismatched uncertainty. An example involving a set of plant models which are not static output feedback stabilisable has been stabilised by means of the proposed sliding mode dynamic output feedback controller. A six-order gas absorber operating under different conditions has been considered as a collection of models and a single sliding mode dynamic output feedback controller is shown to stabilise the plant in all the operating conditions considered. These two examples have demonstrated the efficacy of the approach.

"Measure what is measurable, and make measurable what is not so."

Galileo Galilei (1564 - 1642)

7

Sliding Mode Observer

7.1 Introduction

In many practical engineering applications the state vector is not entirely available for use in the control law. There are two ways of overcoming this problem: control schemes using only output information, and state reconstruction. Control schemes considering only measurable output signals have been considered in Chapters 5 and 6. Synthesis frameworks involving LMIs and polytopic models for plants with matched and mismatched uncertainties have been proposed in Chapter 5 (static and dynamic output feedback), whilst the multi-model paradigm along with LMI methods have been considered in Chapter 6 (static and dynamic output feedback). In this chapter, the problem of state estimation using a discontinuous observer with sliding modes, for uncertain systems, is studied. The robust state reconstruction problem for plants with matched and mismatched uncertainties is addressed here. A sliding mode observer of the same structure as proposed in (Edwards & Spurgeon, 1994) is considered. The proposed design framework is based on LMI methods and employs a polytopic description of the mismatched uncertainty for designing the gain matrices of the sliding mode observer. Thus, a wide study of partial state information control engineering problems for the class of uncertain systems referred to above is found throughout this thesis.

Stability of the estimation error system is studied for the nominal error system and the uncertain error system. The concept of uniform ultimate bounded stability (Ryan & Corless, 1984), also known as practical stability (Edwards & Spurgeon, 1998a), corresponds to a relaxation of the notion of asymptotic stability in the sense of *Lyapunov*. Practical stability is useful when considering uncertain dynamical systems, since asymptotic stability might not be achievable in some cases. This concept is exploited in the stability results for the uncertain estimation error system presented formally in this chapter.

7.2 System Description and Statement of Problem

This chapter is structured as follows: Section 7.2 describes the class of systems to be considered and states the problem to be addressed. In this section, the canonical form proposed in (Edwards & Spurgeon, 1994) is recast for the case of plants with matched and mismatched uncertainties. Section 7.3 goes into detail studying the stability of the nominal and uncertain estimation error system as well as the stability of the reduced-order error system. A design methodology based on LMI methods considering a polytopic description of the reduced-order estimation error system is presented in Section 7.4. A design example illustrates the proposed synthesis framework and demonstrates its applicability in Section 7.5. Finally, some concluding remarks are given in Section 7.6.

7.2 System Description and Statement of Problem

Consider an uncertain system described in state-space form by

$$\dot{\mathbf{x}}(t) = (\mathbf{A} + \Delta\mathbf{A}(t))\mathbf{x}(t) + \mathbf{B}(\mathbf{u}(t) + \xi(t, \mathbf{x}, \mathbf{u})) \quad (7.1)$$

$$\mathbf{y}(t) = \mathbf{C}\mathbf{x}(t) \quad (7.2)$$

where $\mathbf{x} \in \mathfrak{R}^n$ is the state vector and $\mathbf{x}_0 = \mathbf{x}(0)$ the initial condition, $\mathbf{u} \in \mathfrak{R}^m$ is the input vector, and $\mathbf{y} \in \mathfrak{R}^p$ is the output vector. The uncertain function $\xi(t, \mathbf{x}, \mathbf{u}) : \mathfrak{R}_+ \times \mathfrak{R}^n \times \mathfrak{R}^m \rightarrow \mathfrak{R}^m$ represents the lumped sum of matched nonlinearities and/or uncertainties. The uncertain system matrix $\Delta\mathbf{A}(t)$ depends upon the time-varying uncertain vector $\boldsymbol{\theta}(t) : \mathfrak{R}_+ \rightarrow \Theta$, where $\Theta \subseteq \mathfrak{R}^r$ is the parameter space.

In this chapter, the following are assumed:

A-7.1 The number of output and input signals are such that $n > p > m$.

A-7.2 The input and output matrices are full rank, *i.e.* $\text{rank}(\mathbf{B}) = m$ and $\text{rank}(\mathbf{C}) = p$. Moreover, $\text{rank}(\mathbf{CB}) = m$.

Define the following sliding mode observer of the same form as in (Edwards & Spurgeon, 1998b):

$$\dot{\hat{\mathbf{x}}}(t) = \mathbf{A}\hat{\mathbf{x}}(t) + \mathbf{B}\mathbf{u}(t) - \mathbf{G}_L\mathbf{e}_y(t) + \mathbf{G}_{NL}\boldsymbol{\nu} \quad (7.3)$$

$$\hat{\mathbf{y}}(t) = \mathbf{C}\hat{\mathbf{x}}(t) \quad (7.4)$$

where $\mathbf{G}_L \in \mathfrak{R}^{n \times p}$ and $\mathbf{G}_{NL} \in \mathfrak{R}^{n \times p}$ are the gain matrices to be designed. The so-called discontinuous output error injection vector $\boldsymbol{\nu} \in \mathfrak{R}^p$, which induces a sliding motion, is given by

7.2 System Description and Statement of Problem

$$\nu = \begin{cases} -\rho(t, \mathbf{y}, \mathbf{u}) \|\mathcal{B}_2\| \frac{\mathbf{P}_2 \mathbf{e}_y(t)}{\|\mathbf{P}_2 \mathbf{e}_y(t)\|} & \text{if } \mathbf{e}_y(t) \neq \mathbf{0} \\ \mathbf{0} & \text{otherwise} \end{cases} \quad (7.5)$$

where $\mathbf{e}_y(t) = \hat{\mathbf{y}}(t) - \mathbf{y}(t)$ is the output error system. The matrix $\mathbf{P}_2 \in \mathfrak{R}^{p \times p}$ is s.p.d., and the matrix $\mathcal{B}_2 \in \mathfrak{R}^{p \times m}$ will be defined later in the section describing the observer synthesis framework. The scalar function $\rho : \mathfrak{R}_+ \times \mathfrak{R}^p \times \mathfrak{R}^m \rightarrow \mathfrak{R}_+$ satisfies

$$\rho(t, \mathbf{y}, \mathbf{u}) \geq k_1 \|\mathbf{u}(t)\| + \varphi(t, \mathbf{y}(t)) + k_2 + \eta \quad (7.6)$$

where k_1 and k_2 are known scalars, $\varphi : \mathfrak{R}_+ \times \mathfrak{R}^p \rightarrow \mathfrak{R}_+$ is a known function, and $\eta \in \mathfrak{R}_+$.

By defining the state estimation error as

$$\mathbf{e}(t) \triangleq \hat{\mathbf{x}}(t) - \mathbf{x}(t) \quad (7.7)$$

it follows from (7.1) and (7.3) that the error system dynamics are governed by

$$\dot{\mathbf{e}}(t) = (\mathbf{A} - \mathbf{G}_L \mathbf{C}) \mathbf{e}(t) - \Delta \mathbf{A}(t) \mathbf{x}(t) + \mathbf{G}_{NL} \nu - \mathbf{B} \xi(t, \mathbf{y}, \mathbf{u}) \quad (7.8)$$

Under certain conditions the matched uncertainty can be completely rejected by the discontinuous term ν when appropriately designed. Nevertheless, the error system dynamics (7.8) are affected by the mismatched uncertainty associated to the matrix $\Delta \mathbf{A}(t)$ which cannot be cancelled.

The problem to be addressed consists of synthesising a sliding mode observer defined in (7.3)-(7.4) which guarantees robust stable error dynamics and the existence of a stable sliding motion in finite time on the sliding hyperplane

$$\mathcal{S}_{obs} = \{\mathbf{e}(t) \in \mathfrak{R}^n : \mathbf{e}_y(t) = \mathbf{C} \mathbf{e}(t) = 0\} \quad (7.9)$$

despite the uncertainties present in the plant (7.1)-(7.2). In this chapter, “robust stable error dynamics” means $\hat{\mathbf{x}}(t) \rightarrow \mathbf{x}(t)$ within a certain domain Ω_{obs} in finite time considering the maximum feasible attenuation level for the mismatched uncertainty effect in the output error $\mathbf{e}_y(t)$.

Lemma 7.1 *Consider the system described in (7.1)-(7.2). Under assumptions A-7.1 and A-7.2, there exists a similarity transformation $\mathbf{x} \mapsto \mathbf{T}_o \mathbf{x} = \bar{\mathbf{x}}$ so that the uncertain dynamical system (7.1)-(7.2) can be written as follows*

$$\dot{\bar{\mathbf{x}}}(t) = (\bar{\mathbf{A}} + \Delta \bar{\mathbf{A}}_u(t)) \bar{\mathbf{x}}(t) + \bar{\mathbf{B}}(\mathbf{u}(t) + \xi_\Delta(t, \bar{\mathbf{x}}, \mathbf{u})) \quad (7.10)$$

$$\mathbf{y}(t) = \bar{\mathbf{C}} \bar{\mathbf{x}}(t) \quad (7.11)$$

7.2 System Description and Statement of Problem

with the nominal system triple $(\bar{\mathbf{A}}, \bar{\mathbf{B}}, \bar{\mathbf{C}})$ in the form

$$\bar{\mathbf{A}} = \begin{bmatrix} \bar{\mathbf{A}}_{11} & \bar{\mathbf{A}}_{12} \\ \bar{\mathbf{A}}_{21} & \bar{\mathbf{A}}_{22} \end{bmatrix} \quad \bar{\mathbf{B}} = \begin{bmatrix} \mathbf{0} \\ \bar{\mathbf{B}}_2 \end{bmatrix} \quad \bar{\mathbf{C}} = \begin{bmatrix} \mathbf{0} & \mathbf{T} \end{bmatrix} \quad (7.12)$$

where

a)- The matrices $\bar{\mathbf{A}}_{11} \in \mathfrak{R}^{(n-p) \times (n-p)}$ and $\bar{\mathbf{A}}_{21} \in \mathfrak{R}^{p \times (n-p)}$ are such that

$$\bar{\mathbf{A}}_{11} = \begin{bmatrix} \bar{\mathbf{A}}_{11}^o & \bar{\mathbf{A}}_{12}^o \\ \mathbf{0} & \bar{\mathbf{A}}_{22}^o \end{bmatrix} \quad (7.13)$$

$$\bar{\mathbf{A}}_{21} = \begin{bmatrix} \bar{\mathbf{A}}_{211} \\ \bar{\mathbf{A}}_{212} \end{bmatrix} \quad \text{and} \quad \bar{\mathbf{A}}_{211} = \begin{bmatrix} \mathbf{0} & \bar{\mathbf{A}}_{21}^o \end{bmatrix} \quad (7.14)$$

with $\bar{\mathbf{A}}_{11}^o \in \mathfrak{R}^{r \times r}$ and $\bar{\mathbf{A}}_{21}^o \in \mathfrak{R}^{(p-m) \times (n-p-r)}$ for some $r \geq 0$.

b)- The pair $(\bar{\mathbf{A}}_{22}^o, \bar{\mathbf{A}}_{21}^o)$ is completely observable by construction.

c)- The eigenvalues of the matrix $\bar{\mathbf{A}}_{11}^o$ are the invariant zeros of the system triple $(\bar{\mathbf{A}}, \bar{\mathbf{B}}, \bar{\mathbf{C}})$.

d)- The matrix $\bar{\mathbf{B}}_2 \in \mathfrak{R}^{p \times m}$ is partitioned as follows

$$\bar{\mathbf{B}}_2 = \begin{bmatrix} \mathbf{0} \\ \tilde{\mathbf{B}}_2 \end{bmatrix} \quad (7.15)$$

with $\tilde{\mathbf{B}}_2 \in \mathfrak{R}^{m \times m}$ a nonsingular matrix. The matrix $\mathbf{T} \in \mathfrak{R}^{p \times p}$, in (7.12), is orthogonal.

e)- The uncertain matrix $\Delta \bar{\mathbf{A}}(t)$ is given by

$$\Delta \bar{\mathbf{A}}(t) = \Delta \bar{\mathbf{A}}_u(t) + \Delta \bar{\mathbf{A}}_m(t) \quad (7.16)$$

where the mismatched component has the structure

$$\Delta \bar{\mathbf{A}}_u(t) = \begin{bmatrix} \Delta \bar{\mathbf{A}}_{11}(t) & \Delta \bar{\mathbf{A}}_{12}(t) \\ \mathbf{0} & \mathbf{0} \end{bmatrix} \quad (7.17)$$

with $\Delta \bar{\mathbf{A}}_{11}(t) \in \mathfrak{R}^{(n-p) \times (n-p)}$ and $\Delta \bar{\mathbf{A}}_{12}(t) \in \mathfrak{R}^{(n-p) \times p}$. The matched component has the form

$$\Delta \bar{\mathbf{A}}_m(t) = \begin{bmatrix} \mathbf{0} & \mathbf{0} \\ \Delta \bar{\mathbf{A}}_{21}(t) & \Delta \bar{\mathbf{A}}_{22}(t) \end{bmatrix} \quad (7.18)$$

with $\Delta \bar{\mathbf{A}}_{22}(t) \in \mathfrak{R}^{p \times (n-p)}$ and $\Delta \bar{\mathbf{A}}_{21}(t) \in \mathfrak{R}^{p \times p}$.

7.2 System Description and Statement of Problem

f)- The matched uncertainty $\xi_\Delta(t, \bar{\mathbf{x}}, \mathbf{u})$ is given by

$$\bar{\xi}_\Delta(t, \bar{\mathbf{x}}, \mathbf{u}) = \Delta \bar{\mathbf{A}}_{mB}(t) \bar{\mathbf{x}}(t) + \bar{\xi}(t, \bar{\mathbf{x}}, \mathbf{u}) \quad (7.19)$$

where $\Delta \bar{\mathbf{A}}_{mB}(t)$ is such that $\Delta \bar{\mathbf{A}}_m = \bar{\mathbf{B}} \Delta \bar{\mathbf{A}}_{mB}(t)$.

△

The proof of the Lemma above is mainly based upon the arguments used in Lemmas 1 and 2 in (Edwards & Spurgeon, 1995).

Proof Firstly, a nonsingular change of coordinates $\mathbf{x} \mapsto \mathbf{T}_C \mathbf{x} = \mathbf{x}_{T_C}$, which forces the last p state variables of the system to be the plant's output signals, is applied by defining the transformation matrix

$$\mathbf{T}_C \triangleq \begin{bmatrix} \mathbf{N}_C^T \\ \mathbf{C} \end{bmatrix} \quad (7.20)$$

where $\mathbf{N}_C \in \mathfrak{R}^{n \times (n-p)}$ is such that its columns span the null space of the output matrix \mathbf{C} . Consequently,

$$\mathbf{A}_{T_C} = \begin{bmatrix} \mathbf{A}_{C_{11}} & \mathbf{A}_{C_{12}} \\ \mathbf{A}_{C_{21}} & \mathbf{A}_{C_{22}} \end{bmatrix} \quad (7.21)$$

where $\mathbf{A}_{C_{11}} \in \mathfrak{R}^{(n-p) \times (n-p)}$ and

$$\mathbf{B}_{T_C} = \begin{bmatrix} \mathbf{B}_{C_1} \\ \mathbf{B}_{C_2} \end{bmatrix} \quad (7.22)$$

where $\mathbf{B}_{C_1} \in \mathfrak{R}^{(n-p) \times m}$ and $\mathbf{B}_{C_2} \in \mathfrak{R}^{p \times m}$. As a result of the transformation

$$\mathbf{C}_{T_C} = \begin{bmatrix} \mathbf{0} & \mathbf{I}_p \end{bmatrix} \quad (7.23)$$

By assumption $\text{rank}(\mathbf{C}\mathbf{B}) = m$, then since $\mathbf{C}_{T_C} \mathbf{B}_{T_C} = \mathbf{B}_{C_2}$, it follows that $\text{rank}(\mathbf{B}_{C_2}) = m$. This implies that an orthogonal matrix $\mathbf{T} \in \mathfrak{R}^{p \times p}$ exists such that

$$\mathbf{T}^T \mathbf{B}_{C_2} = \begin{bmatrix} \mathbf{0} \\ \check{\mathbf{B}}_2 \end{bmatrix} \quad (7.24)$$

7.2 System Description and Statement of Problem

where $\tilde{\mathbf{B}}_2 \in \mathfrak{R}^{m \times m}$ is a nonsingular matrix. Another implication is that a left pseudo-inverse $\mathbf{B}_{C_2}^{\dagger L} \in \mathfrak{R}^{m \times p}$ for \mathbf{B}_{C_2} can be computed given by

$$\mathbf{B}_{C_2}^{\dagger L} = (\mathbf{B}_{C_2}^T \mathbf{B}_{C_2})^{-1} \mathbf{B}_{C_2}^T \quad (7.25)$$

By applying a further nonsingular change of coordinates $\mathbf{x}_{T_C} \mapsto \mathbf{T}_B \mathbf{x}_{T_C} = \mathbf{x}_{T_B}$ to the system triple $(\mathbf{A}_{T_C}, \mathbf{B}_{T_C}, \mathbf{C}_{T_C})$ where

$$\mathbf{T}_B \triangleq \begin{bmatrix} \mathbf{I}_{(n-p)} & -\mathbf{B}_{C_1} \mathbf{B}_{C_2}^{\dagger L} \\ \mathbf{0} & \mathbf{T}^T \end{bmatrix} \quad (7.26)$$

it follows that the system triple $(\mathbf{A}_{T_C}, \mathbf{B}_{T_C}, \mathbf{C}_{T_C})$ in the new coordinates has the form

$$\mathbf{A}_{T_B} = \begin{bmatrix} \mathbf{A}_{B_{11}} & \mathbf{A}_{B_{12}} \\ \mathbf{A}_{B_{21}} & \mathbf{A}_{B_{22}} \end{bmatrix} \quad \mathbf{B}_{T_B} = \begin{bmatrix} \mathbf{0} \\ \tilde{\mathbf{B}}_2 \end{bmatrix} \quad \mathbf{C}_{T_B} = \begin{bmatrix} \mathbf{0} & \mathbf{T} \end{bmatrix} \quad (7.27)$$

Now, the sub-matrix $\mathbf{A}_{B_{11}} \in \mathfrak{R}^{(n-m) \times (n-m)}$ is partitioned as follows

$$\mathbf{A}_{B_{11}} = \begin{bmatrix} \mathbf{A}_{B_{1111}} & \mathbf{A}_{B_{1112}} \\ \mathbf{A}_{B_{1121}} & \mathbf{A}_{B_{1122}} \end{bmatrix} \quad (7.28)$$

where $\mathbf{A}_{B_{1111}} \in \mathfrak{R}^{(n-p) \times (n-p)}$. If the pair $(\mathbf{A}_{B_{1111}}, \mathbf{A}_{B_{1121}})$ is unobservable, then a matrix $\mathbf{T}_{obs} \in \mathfrak{R}^{(n-p) \times (n-p)}$ exists so that

$$\mathbf{T}_{obs} \mathbf{A}_{B_{1111}} \mathbf{T}_{obs}^{-1} = \begin{bmatrix} \bar{\mathbf{A}}_{11}^o & \bar{\mathbf{A}}_{12}^o \\ \mathbf{0} & \bar{\mathbf{A}}_{22}^o \end{bmatrix} \quad (7.29)$$

$$\mathbf{A}_{B_{1121}} \mathbf{T}_{obs}^{-1} = \begin{bmatrix} \mathbf{0} & \bar{\mathbf{A}}_{21}^o \end{bmatrix} \quad (7.30)$$

where $\bar{\mathbf{A}}_{11}^o \in \mathfrak{R}^{r \times r}$, $\bar{\mathbf{A}}_{21}^o \in \mathfrak{R}^{(p-m) \times (n-p-r)}$ and $(\bar{\mathbf{A}}_{22}^o, \bar{\mathbf{A}}_{21}^o)$ is observable (Edwards & Spurgeon, 1995) (Edwards & Spurgeon, 1998a). This means that the pair $(\mathbf{A}_{B_{1111}}, \mathbf{A}_{B_{1121}})$ has been written in observability canonical form where the scalar $r \geq 0$ corresponds to the number of unobservable states of $(\mathbf{A}_{B_{1111}}, \mathbf{A}_{B_{1121}})$.

An additional transformation matrix involving the sub-matrix \mathbf{T}_{obs} can be defined as

$$\mathbf{T}_A \triangleq \begin{bmatrix} \mathbf{T}_{obs} & \mathbf{0} \\ \mathbf{0} & \mathbf{I}_p \end{bmatrix} \quad (7.31)$$

so that the change of coordinates $\mathbf{x}_{T_B} \mapsto \mathbf{T}_A \mathbf{x}_{T_B} = \bar{\mathbf{x}}$ yields

7.2 System Description and Statement of Problem

$$\bar{\mathbf{A}} = \begin{bmatrix} \bar{\mathbf{A}}_{11} & \bar{\mathbf{A}}_{12} \\ \bar{\mathbf{A}}_{21} & \bar{\mathbf{A}}_{22} \end{bmatrix} \quad \bar{\mathbf{B}} = \begin{bmatrix} \mathbf{0} \\ \bar{\mathbf{B}}_2 \end{bmatrix} \quad \bar{\mathbf{C}} = \begin{bmatrix} \mathbf{0} & \mathbf{T} \end{bmatrix} \quad (7.32)$$

where $\bar{\mathbf{A}}_{11} \in \mathfrak{R}^{(n-p) \times (n-p)}$ is given in (7.29), the sub-matrix $\bar{\mathbf{A}}_{21} \in \mathfrak{R}^{p \times (n-p)}$ has the structure

$$\bar{\mathbf{A}}_{21} = \begin{bmatrix} \bar{\mathbf{A}}_{211} \\ \bar{\mathbf{A}}_{212} \end{bmatrix} \quad (7.33)$$

with $\bar{\mathbf{A}}_{211} \in \mathfrak{R}^{(p-m) \times (n-p)}$ given in (7.30), and

$$\bar{\mathbf{B}}_2 = \begin{bmatrix} \mathbf{0} \\ \tilde{\mathbf{B}}_2 \end{bmatrix} \quad (7.34)$$

with $\tilde{\mathbf{B}}_2 \in \mathfrak{R}^{m \times m}$.

The transformation matrix $\mathbf{T}_o \in \mathfrak{R}^{n \times n}$ from the lemma statement is made up of the transformation matrices defined during this proof, *i.e.*

$$\mathbf{T}_o = \mathbf{T}_C \mathbf{T}_B \mathbf{T}_A \quad (7.35)$$

and produces the change of coordinates $\mathbf{x} \mapsto \bar{\mathbf{x}}$.

Now, it will be demonstrated that the $\lambda(\bar{\mathbf{A}}_{11}^o)$ are the invariant zeros of the system triple $(\bar{\mathbf{A}}, \bar{\mathbf{B}}, \bar{\mathbf{C}})$. The invariant zeros of $(\bar{\mathbf{A}}, \bar{\mathbf{B}}, \bar{\mathbf{C}})$ are defined to be the set

$$\{s \in \mathbb{C} : \mathcal{R}(s) \text{ loses normal rank}\} \quad (7.36)$$

where $\mathcal{R}(s)$ is the *Rosenbrock's* system matrix

$$\mathcal{R}(s) = \left[\begin{array}{c|c} (s\mathbf{I} - \bar{\mathbf{A}}) & \bar{\mathbf{B}} \\ \hline \bar{\mathbf{C}} & \mathbf{0} \end{array} \right] \quad (7.37)$$

By considering the system triple $(\bar{\mathbf{A}}, \bar{\mathbf{B}}, \bar{\mathbf{C}})$ given in (7.32) with the matrix $\bar{\mathbf{A}}_{11}$ of the form defined in (7.29), and the matrices (7.33)-(7.34) produce

$$\mathcal{R}(s) = \left[\begin{array}{cc|c|c} \left[\begin{array}{cc} (s\mathbf{I}_r - \bar{\mathbf{A}}_{11}^o) & -\bar{\mathbf{A}}_{12}^o \\ \mathbf{0} & (s\mathbf{I}_{(n-p-r)} - \bar{\mathbf{A}}_{22}^o) \end{array} \right] & -\bar{\mathbf{A}}_{12} & \mathbf{0} & \\ \left[\begin{array}{c} -\bar{\mathbf{A}}_{211} \\ -\bar{\mathbf{A}}_{212} \end{array} \right] & (s\mathbf{I}_p - \bar{\mathbf{A}}_{22}) & \left[\begin{array}{c} \mathbf{0} \\ \tilde{\mathbf{B}}_2 \end{array} \right] & \\ \hline \mathbf{0} & \mathbf{T} & \mathbf{0} & \end{array} \right] \quad (7.38)$$

7.2 System Description and Statement of Problem

Since $\tilde{\mathbf{B}}_2 \in \mathfrak{R}^{m \times m}$ is nonsingular and $\mathbf{T} \in \mathfrak{R}^{p \times p}$, by using $\bar{\mathbf{A}}_{211}$ defined in (7.30),

$$\mathcal{R}(s) \text{ loses normal rank} \iff \mathcal{Q}(s) \text{ loses normal rank} \quad (7.39)$$

where

$$\mathcal{Q}(s) = \begin{bmatrix} (s\mathbf{I}_r - \bar{\mathbf{A}}_{11}^o) & -\bar{\mathbf{A}}_{12}^o \\ \mathbf{0} & (s\mathbf{I}_{(n-p-r)} - \bar{\mathbf{A}}_{22}^o) \\ \mathbf{0} & \bar{\mathbf{A}}_{21}^o \end{bmatrix} \quad (7.40)$$

Moreover, by construction the pair $(\bar{\mathbf{A}}_{22}^o, \bar{\mathbf{A}}_{21}^o)$ is completely observable, then from the *Popov-Belevitch-Hautus* test

$$\text{rank} \begin{bmatrix} (s\mathbf{I}_{(n-p-r)} - \bar{\mathbf{A}}_{22}^o) \\ \bar{\mathbf{A}}_{21}^o \end{bmatrix} = n - p - r \quad (7.41)$$

for all $s \in \mathbb{C}$. Therefore,

$$\mathcal{R}(s) \text{ loses normal rank} \iff \mathcal{Q}(s) \text{ loses normal rank} \iff \det(s\mathbf{I} - \bar{\mathbf{A}}_{11}^o) = 0 \quad (7.42)$$

which means that $\lambda(\bar{\mathbf{A}}_{11}^o)$ are the invariant zeros of the system triple $(\bar{\mathbf{A}}, \bar{\mathbf{B}}, \bar{\mathbf{C}})$.

The uncertain matrix $\Delta\mathbf{A}(t)$, partitioned conformably with (7.32) in the new coordinates $\bar{\mathbf{x}}$, has the structure

$$\Delta\bar{\mathbf{A}}(t) = \begin{bmatrix} \Delta\bar{\mathbf{A}}_{11}(t) & \Delta\bar{\mathbf{A}}_{12}(t) \\ \Delta\bar{\mathbf{A}}_{21}(t) & \Delta\bar{\mathbf{A}}_{22}(t) \end{bmatrix} \quad (7.43)$$

This uncertain matrix can be decomposed into matched and mismatched uncertain matrices, *i.e.* $\Delta\bar{\mathbf{A}}_m(t)$ and $\Delta\bar{\mathbf{A}}_u(t)$, as follows

$$\Delta\bar{\mathbf{A}}(t) = \Delta\bar{\mathbf{A}}_u(t) + \Delta\bar{\mathbf{A}}_m(t) \quad (7.44)$$

where

$$\Delta\bar{\mathbf{A}}_u(t) = \begin{bmatrix} \Delta\bar{\mathbf{A}}_{11}(t) & \Delta\bar{\mathbf{A}}_{12}(t) \\ \mathbf{0} & \mathbf{0} \end{bmatrix} \quad (7.45)$$

$$\Delta\bar{\mathbf{A}}_m(t) = \begin{bmatrix} \mathbf{0} & \mathbf{0} \\ \Delta\bar{\mathbf{A}}_{21}(t) & \Delta\bar{\mathbf{A}}_{22}(t) \end{bmatrix} \quad (7.46)$$

7.3 Stability Analysis

Since $\mathcal{R}(\Delta\bar{\mathbf{A}}_m) \subset \mathcal{R}(\bar{\mathbf{B}})$ the matrix $\Delta\bar{\mathbf{A}}_m(t) = \bar{\mathbf{B}}\Delta\bar{\mathbf{A}}_{mB}(t)$; hence $\bar{\mathbf{A}}_{mB}(t)$ can be embedded into the matched uncertainty $\bar{\xi}_\Delta(t, \bar{\mathbf{x}}, \mathbf{u})$ as follows

$$\bar{\xi}_\Delta(t, \bar{\mathbf{x}}, \mathbf{u}) = \Delta\bar{\mathbf{A}}_{mB}(t)\bar{\mathbf{x}}(t) + \bar{\xi}(t, \bar{\mathbf{x}}, \mathbf{u}) \quad (7.47)$$

Q.E.D.

Remark 7.1 *Stable sliding mode dynamics require that any invariant zeros $\lambda(\bar{\mathbf{A}}_{11}^o) \in \mathbb{C}_-$. In this case, the pair $(\bar{\mathbf{A}}_{11}, \bar{\mathbf{A}}_{211})$ is detectable and its unobservable modes are the invariant zeros of the system triple $(\bar{\mathbf{A}}, \bar{\mathbf{B}}, \bar{\mathbf{C}})$.*

In this chapter, it is assumed that

A-7.3 the matched uncertainty is bounded by

$$\|\bar{\xi}_\Delta(t, \bar{\mathbf{x}}, \mathbf{u})\| \leq k_1\|\mathbf{u}(t)\| + \varphi(t, \mathbf{y}(t)) + k_2 \quad (7.48)$$

where $\varphi : \mathfrak{R}_+ \times \mathfrak{R}^p \rightarrow \mathfrak{R}_+$ is a known function, and k_1 and k_2 are known scalars.

The observer (7.3)-(7.4) in the new coordinates $\bar{\mathbf{x}} \in \mathfrak{R}^n$ is represented by

$$\dot{\hat{\mathbf{x}}}(t) = \bar{\mathbf{A}}\hat{\mathbf{x}}(t) + \bar{\mathbf{B}}\mathbf{u}(t) - \bar{\mathbf{G}}_L\mathbf{e}_y(t) + \bar{\mathbf{G}}_{NL}\nu \quad (7.49)$$

$$\hat{\mathbf{y}}(t) = \bar{\mathbf{C}}\hat{\mathbf{x}}(t) \quad (7.50)$$

whilst the estimation error is defined by $\bar{\mathbf{e}}(t) = \hat{\mathbf{x}}(t) - \bar{\mathbf{x}}(t)$.

Consequently, the estimation error system dynamics are described by

$$\dot{\bar{\mathbf{e}}}(t) = (\bar{\mathbf{A}} - \bar{\mathbf{G}}_L\bar{\mathbf{C}})\bar{\mathbf{e}}(t) - \Delta\bar{\mathbf{A}}_u(t)\bar{\mathbf{x}}(t) + \bar{\mathbf{G}}_{NL}\nu - \bar{\mathbf{B}}\bar{\xi}_\Delta(t, \bar{\mathbf{x}}, \mathbf{u}) \quad (7.51)$$

In this chapter, a novel design framework based upon LMIs is proposed for designing the gain matrices $\bar{\mathbf{G}}_L$ and $\bar{\mathbf{G}}_{NL}$.

7.3 Stability Analysis

This section provides the analytical results concerned with the practical stability of the uncertain error system dynamics in (7.51). The ultimate boundedness stability concept is used in most of the mathematical results in this section. Also, stability of the nominal error system dynamics is studied.

7.3 Stability Analysis

The following lemma establishes a gain matrix $\bar{\mathbf{G}}_L$ ensuring the matrix $(\bar{\mathbf{A}} - \bar{\mathbf{G}}_L \bar{\mathbf{C}})$ is *Hurwitz*. The structure of the associated *Lyapunov* matrix $\bar{\mathbf{P}}$, which satisfies the *Lyapunov* inequality for the nominal error system dynamics, is also defined. The matrix $\bar{\mathbf{P}}$ has the same form as the *Lyapunov* matrix used in (Tan & Edwards, 2001).

Lemma 7.2 *Let $(\bar{\mathbf{A}}, \bar{\mathbf{B}}, \bar{\mathbf{C}})$ be the nominal system triple defined in (7.12) with $\bar{\mathbf{A}}_{21} \in \mathbb{R}^{p \times (n-p)}$ partitioned as follows*

$$\bar{\mathbf{A}}_{21} = \begin{bmatrix} \bar{\mathbf{A}}_{211} \\ \bar{\mathbf{A}}_{212} \end{bmatrix} \quad (7.52)$$

where $\bar{\mathbf{A}}_{211} \in \mathbb{R}^{(p-m) \times (n-p)}$. Let $\mathbf{L} \in \mathbb{R}^{(n-p) \times (p-m)}$ be a design matrix such that $\lambda(\bar{\mathbf{A}}_{11} + \mathbf{L}\bar{\mathbf{A}}_{211}) \in \mathbb{C}_-$ where $\bar{\mathbf{A}}_{11}$ is a submatrix of $\bar{\mathbf{A}}$ defined in (7.12). Let $\bar{\mathbf{G}}_L \in \mathbb{R}^{n \times p}$ be a gain matrix of the form

$$\bar{\mathbf{G}}_L = \begin{bmatrix} \bar{\mathbf{G}}_{L1} \\ \bar{\mathbf{G}}_{L2} \end{bmatrix} = \begin{bmatrix} -\bar{\mathbf{A}}_{11}\bar{\mathbf{L}}\mathbf{T}^T + \bar{\mathbf{A}}_{12}\mathbf{T}^T + \bar{\mathbf{L}}\mathbf{T}^T\mathcal{A}_{22}^{stb} \\ -\bar{\mathbf{A}}_{21}\bar{\mathbf{L}}\mathbf{T}^T + \bar{\mathbf{A}}_{22}\mathbf{T}^T - \mathbf{T}^T\mathcal{A}_{22}^{stb} \end{bmatrix} \quad (7.53)$$

where $\bar{\mathbf{G}}_{L1} \in \mathbb{R}^{(n-p) \times p}$ and $\bar{\mathbf{G}}_{L2} \in \mathbb{R}^{p \times p}$. The sub-matrix $\mathbf{T} \in \mathbb{R}^{p \times p}$ is part of the output matrix $\bar{\mathbf{C}}$, the matrix $\mathcal{A}_{22}^{stb} \in \mathbb{R}^{p \times p}$ is a stable matrix constructed by the designer and $\bar{\mathbf{L}} \in \mathbb{R}^{(n-p) \times p}$ is given by

$$\bar{\mathbf{L}} = \begin{bmatrix} \mathbf{L} & \mathbf{0}_{(n-p) \times m} \end{bmatrix} \quad (7.54)$$

Then, the nominal error system dynamics

$$\dot{\bar{\mathbf{e}}}(t) = (\bar{\mathbf{A}} - \bar{\mathbf{G}}_L \bar{\mathbf{C}})\bar{\mathbf{e}}(t) \quad (7.55)$$

are stable and the following *Lyapunov* matrix inequality holds

$$(\bar{\mathbf{A}} - \bar{\mathbf{G}}_L \bar{\mathbf{C}})^T \bar{\mathbf{P}} + \bar{\mathbf{P}}(\bar{\mathbf{A}} - \bar{\mathbf{G}}_L \bar{\mathbf{C}}) \prec 0 \quad (7.56)$$

where

$$\bar{\mathbf{P}} = \begin{bmatrix} \bar{\mathbf{P}}_1 & \bar{\mathbf{P}}_1 \bar{\mathbf{L}} \\ \bar{\mathbf{L}}^T \bar{\mathbf{P}}_1 & \bar{\mathbf{P}}_2 + \bar{\mathbf{L}}^T \bar{\mathbf{P}}_1 \bar{\mathbf{L}} \end{bmatrix} \succ 0 \quad (7.57)$$

with $\bar{\mathbf{P}}_1 \in \mathbb{R}^{(n-p) \times (n-p)}$ and $\bar{\mathbf{P}}_2 \in \mathbb{R}^{p \times p}$ are appropriately chosen s.p.d. matrices.

Proof Define a nonsingular change of coordinates $\bar{\mathbf{e}} \mapsto \mathbf{T}_L \bar{\mathbf{e}} = \tilde{\mathbf{e}}$ where the transformation matrix $\mathbf{T}_L \in \mathbb{R}^{n \times n}$ is given by

$$\mathbf{T}_L = \begin{bmatrix} \mathbf{I}_{(n-p)} & \bar{\mathbf{L}} \\ \mathbf{0} & \mathbf{T} \end{bmatrix} \quad (7.58)$$

7.3 Stability Analysis

In the new coordinates the nominal error system dynamics are described by

$$\dot{\tilde{\mathbf{e}}}(t) = (\tilde{\mathbf{A}} - \tilde{\mathbf{G}}_L \tilde{\mathbf{C}}) \tilde{\mathbf{e}}(t) \quad (7.59)$$

where

$$\tilde{\mathbf{A}} = \begin{bmatrix} \tilde{\mathbf{A}}_{11} & \tilde{\mathbf{A}}_{12} \\ \tilde{\mathbf{A}}_{21} & \tilde{\mathbf{A}}_{22} \end{bmatrix} = \begin{bmatrix} \bar{\mathbf{A}}_{11} + \bar{\mathbf{L}}\bar{\mathbf{A}}_{21} & -\bar{\mathbf{A}}_{11}\bar{\mathbf{L}}\mathbf{T}^\mathbf{T} - \bar{\mathbf{L}}\bar{\mathbf{A}}_{21}\bar{\mathbf{L}}\mathbf{T}^\mathbf{T} + \bar{\mathbf{A}}_{12}\mathbf{T}^\mathbf{T} + \bar{\mathbf{L}}\bar{\mathbf{A}}_{22}\mathbf{T}^\mathbf{T} \\ \mathbf{T}\bar{\mathbf{A}}_{21} & -\mathbf{T}\bar{\mathbf{A}}_{21}\bar{\mathbf{L}}\mathbf{T}^\mathbf{T} + \mathbf{T}\bar{\mathbf{A}}_{22}\mathbf{T}^\mathbf{T} \end{bmatrix} \quad (7.60)$$

$$\tilde{\mathbf{G}}_L = \begin{bmatrix} -\bar{\mathbf{A}}_{11}\bar{\mathbf{L}}\mathbf{T}^\mathbf{T} - \bar{\mathbf{L}}\bar{\mathbf{A}}_{21}\bar{\mathbf{L}}\mathbf{T}^\mathbf{T} + \bar{\mathbf{A}}_{12}\mathbf{T}^\mathbf{T} + \bar{\mathbf{L}}\bar{\mathbf{A}}_{22}\mathbf{T}^\mathbf{T} \\ -\mathbf{T}\bar{\mathbf{A}}_{21}\bar{\mathbf{L}}\mathbf{T}^\mathbf{T} + \mathbf{T}\bar{\mathbf{A}}_{22}\mathbf{T}^\mathbf{T} - \mathcal{A}_{22}^{stb} \end{bmatrix} \quad (7.61)$$

$$\tilde{\mathbf{C}} = [\mathbf{0} \quad \mathbf{I}_p] \quad (7.62)$$

Algebraic manipulation of (7.60)-(7.62) yields

$$\tilde{\mathbf{A}}_0 = (\tilde{\mathbf{A}} - \tilde{\mathbf{G}}_L \tilde{\mathbf{C}}) = \begin{bmatrix} \bar{\mathbf{A}}_{11} + \bar{\mathbf{L}}\bar{\mathbf{A}}_{21} & \mathbf{0} \\ \mathbf{T}\bar{\mathbf{A}}_{21} & \mathcal{A}_{22}^{stb} \end{bmatrix} \quad (7.63)$$

From the structure of (7.52) and (7.54), it follows

$$\bar{\mathbf{L}}\bar{\mathbf{A}}_{21} = \mathbf{L}\bar{\mathbf{A}}_{211} \quad (7.64)$$

Then, equation (7.63) can be written as

$$\tilde{\mathbf{A}}_0 = \begin{bmatrix} \bar{\mathbf{A}}_{11} + \mathbf{L}\bar{\mathbf{A}}_{211} & \mathbf{0} \\ \mathbf{T}\bar{\mathbf{A}}_{21} & \mathcal{A}_{22}^{stb} \end{bmatrix} \quad (7.65)$$

The *Lyapunov* matrix $\tilde{\mathbf{P}}$ in the new coordinates is given by

$$\tilde{\mathbf{P}} = (\mathbf{T}_L^{-1})^\mathbf{T} \tilde{\mathbf{P}} \mathbf{T}_L^{-1} = \begin{bmatrix} \tilde{\mathbf{P}}_1 & \mathbf{0} \\ \mathbf{0} & \mathbf{P}_2 \end{bmatrix} \succ 0 \quad (7.66)$$

where

$$\mathbf{P}_2 = \mathbf{T}\tilde{\mathbf{P}}_2\mathbf{T}^\mathbf{T} \quad (7.67)$$

Consider the *Lyapunov* function

$$\tilde{V}(t) := \tilde{\mathbf{e}}^\mathbf{T}(t) \tilde{\mathbf{P}} \tilde{\mathbf{e}}(t) \quad (7.68)$$

7.3 Stability Analysis

Taking time derivatives along the nominal error system's trajectories yields

$$\dot{V}(t) = \tilde{\mathbf{e}}^T(t) \begin{bmatrix} \tilde{\mathbf{A}}_{11}^T \tilde{\mathbf{P}}_1 + \tilde{\mathbf{P}}_1 \tilde{\mathbf{A}}_{11} & \tilde{\mathbf{A}}_{21}^T \mathbf{P}_2 \\ \mathbf{P}_2 \tilde{\mathbf{A}}_{21} & (\mathcal{A}_{22}^{stb})^T \mathbf{P}_2 + \mathbf{P}_2 \mathcal{A}_{22}^{stb} \end{bmatrix} \tilde{\mathbf{e}}(t) \quad (7.69)$$

where $\tilde{\mathbf{A}}_{11} = \bar{\mathbf{A}}_{11} + \mathbf{L}\bar{\mathbf{A}}_{211}$ and $\tilde{\mathbf{A}}_{21} = \mathbf{T}\bar{\mathbf{A}}_{21}$. Since by design the matrix $\mathcal{A}_{22}^{stb} \in \mathbb{R}^{p \times p}$ is a stable matrix, for a given s.p.d. matrix $\mathbf{Q}_2 \in \mathbb{R}^{p \times p}$ the following *Lyapunov* equation

$$(\mathcal{A}_{22}^{stb})^T \mathbf{P}_2 + \mathbf{P}_2 \mathcal{A}_{22}^{stb} = -\mathbf{Q}_2 \quad (7.70)$$

has a solution \mathbf{P}_2 . Then, a further *Lyapunov* equation can be written considering the solution of (7.70) as follows

$$\tilde{\mathbf{A}}_{11}^T \tilde{\mathbf{P}}_1 + \tilde{\mathbf{P}}_1 \tilde{\mathbf{A}}_{11} = -(\tilde{\mathbf{Q}}_1 + \tilde{\mathbf{A}}_{21}^T \mathbf{P}_2 \mathbf{Q}_2^{-1} \mathbf{P}_2 \tilde{\mathbf{A}}_{21}) \quad (7.71)$$

where $\tilde{\mathbf{Q}}_1 \in \mathbb{R}^{(n-p) \times (n-p)}$ is a s.p.d. design matrix. Note that by construction

$$\tilde{\mathbf{Q}}_1 + \tilde{\mathbf{A}}_{21}^T \mathbf{P}_2 \mathbf{Q}_2^{-1} \mathbf{P}_2 \tilde{\mathbf{A}}_{21} \succ 0 \quad (7.72)$$

Using (7.70) and (7.71), quadratic equation (7.69) can be written as

$$\dot{V}(t) = \tilde{\mathbf{e}}^T(t) \begin{bmatrix} -(\tilde{\mathbf{Q}}_1 + \tilde{\mathbf{A}}_{21}^T \mathbf{P}_2 \mathbf{Q}_2^{-1} \mathbf{P}_2 \tilde{\mathbf{A}}_{21}) & \tilde{\mathbf{A}}_{21}^T \mathbf{P}_2 \\ \mathbf{P}_2 \tilde{\mathbf{A}}_{21} & -\mathbf{Q}_2 \end{bmatrix} \tilde{\mathbf{e}}(t) \quad (7.73)$$

From the *Schur* complement, the expression on the R.H.S. of (7.73) is negative definite.

Hence, the nominal error system in the new coordinates given in (7.59) is stable. Moreover, stability of the error system in the original coordinates follows from the properties of similarity transformations. Finally, since the nominal error system is quadratically stable, the following matrix inequality holds

$$(\bar{\mathbf{A}} - \bar{\mathbf{G}}_L \bar{\mathbf{C}})^T \bar{\mathbf{P}} + \bar{\mathbf{P}} (\bar{\mathbf{A}} - \bar{\mathbf{G}}_L \bar{\mathbf{C}}) \prec 0 \quad (7.74)$$

for $\bar{\mathbf{G}}_L$ and $\bar{\mathbf{P}}$ defined in (7.53) and (7.57).

Q.E.D.

Now consider the uncertain error system dynamics governed by

$$\dot{\mathbf{e}}(t) = (\bar{\mathbf{A}} - \bar{\mathbf{G}}_L \bar{\mathbf{C}}) \bar{\mathbf{e}}(t) - \Delta \bar{\mathbf{A}}_u(t) \bar{\mathbf{x}}(t) + \bar{\mathbf{G}}_{NL} \nu - \bar{\mathbf{B}} \bar{\xi}_\Delta(t, \bar{\mathbf{x}}, \mathbf{u}) \quad (7.75)$$

where the matrix $\bar{\mathbf{G}}_L \in \mathbb{R}^{n \times p}$ is defined in (7.53) whilst the matrix $\bar{\mathbf{G}}_{NL} \in \mathbb{R}^{n \times p}$ has

7.3 Stability Analysis

the same structure as in (Tan & Edwards, 2001):

$$\tilde{\mathbf{G}}_{NL} = \begin{bmatrix} \tilde{\mathbf{G}}_{NL1} \\ \tilde{\mathbf{G}}_{NL2} \end{bmatrix} = \begin{bmatrix} -\bar{\mathbf{L}}\mathbf{T}^T \\ \mathbf{T}^T \end{bmatrix} \quad (7.76)$$

with $\bar{\mathbf{L}} \in \mathfrak{R}^{(n-p) \times p}$ given in (7.54).

Note that both gain matrices $\tilde{\mathbf{G}}_L$ and $\tilde{\mathbf{G}}_{NL}$ are parameterised in terms of the sub-matrix $\bar{\mathbf{L}}$ which in turn depends only on \mathbf{L} . The rest of the sub-matrices involved in these two gain matrices are obtained directly from the state and output matrices in the canonical form stated in Lemma 7.1. Notice that only the sub-matrix \mathbf{L} has to be designed. To this end, a synthesis framework, which considers the mismatched uncertainties, is proposed in next section.

The form of the reduced-order uncertain error system is a consequence of applying some of the statements and proof arguments of Lemma 7.2 to the uncertain error system (7.75). Such a form is introduced in the following corollary.

Corollary 7.1 *The sliding mode dynamics are governed by the reduced-order system*

$$\dot{\tilde{\mathbf{e}}}_1(t) = (\bar{\mathbf{A}}_{11} + \mathbf{L}\bar{\mathbf{A}}_{211})\tilde{\mathbf{e}}_1(t) - \Delta\bar{\mathbf{A}}_{11}(t)\bar{\mathbf{x}}_1(t) - \Delta\bar{\mathbf{A}}_{12}(t)\bar{\mathbf{x}}_2(t) \quad (7.77)$$

where $\mathbf{L} \in \mathfrak{R}^{(n-p) \times (p-m)}$ and $\bar{\mathbf{A}}_{211} \in \mathfrak{R}^{(p-m) \times (n-p)}$ are defined in Lemma 7.2.

Proof By applying the similarity transformation $\bar{\mathbf{e}}(t) \mapsto \mathbf{T}_L\bar{\mathbf{e}}(t) = \tilde{\mathbf{e}}(t)$ used in Lemma 7.2, it is easy to show that the uncertain error system dynamics are governed by

$$\dot{\tilde{\mathbf{e}}}_1(t) = \tilde{\mathbf{A}}_{11}\tilde{\mathbf{e}}_1(t) - \Delta\tilde{\mathbf{A}}_{11}(t)\bar{\mathbf{x}}_1(t) - \Delta\tilde{\mathbf{A}}_{12}(t)\bar{\mathbf{x}}_2(t) \quad (7.78)$$

$$\dot{\tilde{\mathbf{e}}}_y(t) = \tilde{\mathbf{A}}_{21}\tilde{\mathbf{e}}_1(t) + \mathcal{A}_{22}^{stb}\mathbf{e}_y(t) + \nu - \mathcal{B}_2\bar{\xi}_\Delta(t, \bar{\mathbf{x}}, \mathbf{u}) \quad (7.79)$$

where $\tilde{\mathbf{A}}_{11} \in \mathfrak{R}^{(n-p) \times (n-p)}$ and $\tilde{\mathbf{A}}_{21} \in \mathfrak{R}^{p \times (n-p)}$ are defined in (7.60). The submatrix $\mathcal{B}_2 \in \mathfrak{R}^{p \times p}$ results from

$$\tilde{\mathbf{B}} = \mathbf{T}_L\bar{\mathbf{B}} = \begin{bmatrix} \mathbf{0} \\ \mathbf{T}\bar{\mathbf{B}}_2 \end{bmatrix} =: \begin{bmatrix} \mathbf{0} \\ \mathcal{B}_2 \end{bmatrix} \quad (7.80)$$

Also, in the new coordinates, the matrix $\tilde{\mathbf{G}}_{NL}$ defined in (7.76) is given by

$$\tilde{\mathbf{G}}_{NL} = \mathbf{T}_L\bar{\mathbf{G}}_{NL} = \begin{bmatrix} \mathbf{0} \\ \mathbf{I}_p \end{bmatrix} \quad (7.81)$$

7.3 Stability Analysis

In the sliding mode, $\mathbf{e}_y(t) = 0$ and $\dot{\mathbf{e}}_y(t) = 0$, then

$$\dot{\tilde{\mathbf{e}}}_1(t) = \tilde{\mathbf{A}}_{11}\tilde{\mathbf{e}}_1(t) - \Delta\tilde{\mathbf{A}}_{11}(t)\tilde{\mathbf{x}}_1(t) - \Delta\tilde{\mathbf{A}}_{12}(t)\tilde{\mathbf{x}}_2(t) \quad (7.82)$$

Since $\tilde{\mathbf{A}}_{11} = \bar{\mathbf{A}}_{11} + \bar{\mathbf{L}}\bar{\mathbf{A}}_{21}$, it follows

$$\dot{\tilde{\mathbf{e}}}_1(t) = (\bar{\mathbf{A}}_{11} + \bar{\mathbf{L}}\bar{\mathbf{A}}_{21})\tilde{\mathbf{e}}_1(t) - \Delta\bar{\mathbf{A}}_{11}(t)\tilde{\mathbf{x}}_1(t) - \Delta\bar{\mathbf{A}}_{12}(t)\tilde{\mathbf{x}}_2(t) \quad (7.83)$$

but from the structure of $\bar{\mathbf{L}}$ and $\bar{\mathbf{A}}_{21}$ given in (7.54) and (7.52) yields

$$\dot{\tilde{\mathbf{e}}}_1(t) = (\bar{\mathbf{A}}_{11} + \mathbf{L}\bar{\mathbf{A}}_{21})\tilde{\mathbf{e}}_1(t) - \Delta\bar{\mathbf{A}}_{11}(t)\tilde{\mathbf{x}}_1(t) - \Delta\bar{\mathbf{A}}_{12}(t)\tilde{\mathbf{x}}_2(t) \quad (7.84)$$

Q.E.D.

In the absence of mismatched uncertainty, the error system dynamics are asymptotically stable (this is stated in Lemma 7.2). The error system is also asymptotically stable when affected by only matched uncertainties. This follows from the invariance property of sliding modes and Lemma 7.2. However, the error system dynamics given in (7.75) are clearly influenced by the effect of the mismatched uncertainty. The concept of practical stability is applied to conclude that the uncertain error system (7.75) is uniformly ultimately bounded with respect to a domain defining an ellipsoid in the state space. This domain is usually a small neighbourhood of the origin in the state space. The following lemma is related to the practical stability of the uncertain error system (7.75).

Lemma 7.3 *Let $\Omega_{\bar{\mathbf{e}}} \subset \mathbb{R}^n$ be a bounded set defined by*

$$\Omega_{\bar{\mathbf{e}}} = \left\{ \bar{\mathbf{e}}(t) \in \mathbb{R}^n : \|\bar{\mathbf{e}}(t)\| < 2\|\Delta\bar{\mathbf{A}}_u(t)\tilde{\mathbf{x}}(t)\|\gamma_\lambda^{-1} + \gamma_{\bar{\mathbf{e}}} \right\} \quad (7.85)$$

where $\gamma_\lambda \in \mathbb{R}_+$, and $\gamma_{\bar{\mathbf{e}}} \in \mathbb{R}_+$ is an arbitrary small design scalar. Assuming that $\|\Delta\bar{\mathbf{A}}_u(t)\tilde{\mathbf{x}}(t)\|$ is bounded, the estimation error $\bar{\mathbf{e}}(t)$ is ultimately bounded with respect to the set $\Omega_{\bar{\mathbf{e}}}$.

Proof Consider the *Lyapunov* function

$$\bar{V}(t) := \bar{\mathbf{e}}^T(t)\bar{\mathbf{P}}\bar{\mathbf{e}}(t) \quad (7.86)$$

where $\bar{\mathbf{P}}$ is a s.p.d matrix of the form defined in Lemma 7.2. That is,

$$\bar{\mathbf{P}} = \begin{bmatrix} \bar{\mathbf{P}}_1 & \bar{\mathbf{P}}_1\bar{\mathbf{L}} \\ \bar{\mathbf{L}}^T\bar{\mathbf{P}}_1 & \bar{\mathbf{P}}_2 + \bar{\mathbf{L}}^T\bar{\mathbf{P}}_1\bar{\mathbf{L}} \end{bmatrix} \quad (7.87)$$

with $\bar{\mathbf{P}}_1 \in \mathbb{R}^{(n-p) \times (n-p)}$ and $\bar{\mathbf{P}}_2 \in \mathbb{R}^{p \times p}$ satisfying $(\bar{\mathbf{A}} - \bar{\mathbf{G}}_L\bar{\mathbf{C}})^T\bar{\mathbf{P}} + \bar{\mathbf{P}}(\bar{\mathbf{A}} - \bar{\mathbf{G}}_L\bar{\mathbf{C}}) \prec 0$.

7.3 Stability Analysis

Differentiating (7.86) with respect to time along the error system trajectories:

$$\dot{V}(t) = \dot{\bar{\mathbf{e}}}^T(t) \bar{\mathbf{P}} \bar{\mathbf{e}}(t) + \bar{\mathbf{e}}^T(t) \dot{\bar{\mathbf{P}}} \bar{\mathbf{e}}(t) \quad (7.88)$$

$$\begin{aligned} &= \bar{\mathbf{e}}^T(t) ((\bar{\mathbf{A}} - \bar{\mathbf{G}}_L \bar{\mathbf{C}})^T \bar{\mathbf{P}} + \dot{\bar{\mathbf{P}}} (\bar{\mathbf{A}} - \bar{\mathbf{G}}_L \bar{\mathbf{C}})) \bar{\mathbf{e}}(t) - 2\bar{\mathbf{e}}^T(t) \bar{\mathbf{P}} \Delta \bar{\mathbf{A}}_u(t) \bar{\mathbf{x}}(t) \\ &\quad + 2\bar{\mathbf{e}}^T(t) \bar{\mathbf{P}} \bar{\mathbf{G}}_{NL\nu} - 2\bar{\mathbf{e}}^T(t) \bar{\mathbf{P}} \bar{\mathbf{B}} \bar{\xi}_\Delta(t, \bar{\mathbf{x}}, \mathbf{u}) \end{aligned} \quad (7.89)$$

From Lemma 7.2, it follows that

$$(\bar{\mathbf{A}} - \bar{\mathbf{G}}_L \bar{\mathbf{C}})^T \bar{\mathbf{P}} + \dot{\bar{\mathbf{P}}} (\bar{\mathbf{A}} - \bar{\mathbf{G}}_L \bar{\mathbf{C}}) = -\bar{\mathbf{Q}}_0 \prec 0 \quad (7.90)$$

where $\bar{\mathbf{Q}}_0 \in \mathfrak{R}^{n \times n}$ is a s.p.d. matrix. Therefore,

$$\begin{aligned} \dot{V}(t) &\leq -\lambda_{\min}(\bar{\mathbf{Q}}_0) \|\bar{\mathbf{e}}(t)\|^2 - 2\bar{\mathbf{e}}^T(t) \bar{\mathbf{P}} \Delta \bar{\mathbf{A}}_u(t) \bar{\mathbf{x}}(t) \\ &\quad + 2\bar{\mathbf{e}}^T(t) \bar{\mathbf{P}} \bar{\mathbf{G}}_{NL\nu} - 2\bar{\mathbf{e}}^T(t) \bar{\mathbf{P}} \bar{\mathbf{B}} \bar{\xi}_\Delta(t, \bar{\mathbf{x}}, \mathbf{u}) \end{aligned} \quad (7.91)$$

From (7.76) and (7.87),

$$\bar{\mathbf{P}} \bar{\mathbf{G}}_{NL} = \begin{bmatrix} \mathbf{0} \\ \bar{\mathbf{P}}_2 \mathbf{T}^T \end{bmatrix} \quad (7.92)$$

In addition, by using

$$\mathbf{P}_2 = \mathbf{T} \bar{\mathbf{P}}_2 \mathbf{T}^T \quad (7.93)$$

it follows

$$\bar{\mathbf{C}}^T \mathbf{P}_2 = \begin{bmatrix} \mathbf{0} \\ \mathbf{T}^T \end{bmatrix} \mathbf{T} \bar{\mathbf{P}}_2 \mathbf{T}^T = \begin{bmatrix} \mathbf{0} \\ \bar{\mathbf{P}}_2 \mathbf{T}^T \end{bmatrix} \quad (7.94)$$

Thus, the structural constraint

$$\bar{\mathbf{P}} \bar{\mathbf{G}}_{NL} = \bar{\mathbf{C}}^T \mathbf{P}_2 \quad (7.95)$$

is obtained.

In order to determine the second structural constraint, consider the input matrix given in (7.12) and the *Lyapunov* matrix defined in (7.87). The following expression is easily obtained

$$\bar{\mathbf{P}} \bar{\mathbf{B}} = \begin{bmatrix} \bar{\mathbf{P}}_1 \bar{\mathbf{L}} \bar{\mathbf{B}}_2 \\ \bar{\mathbf{P}}_2 \bar{\mathbf{B}}_2 + \bar{\mathbf{L}}^T \bar{\mathbf{P}}_1 \bar{\mathbf{L}} \bar{\mathbf{B}}_2 \end{bmatrix} \quad (7.96)$$

7.3 Stability Analysis

however from (7.15) and (7.54)

$$\bar{\mathbf{L}}\bar{\mathbf{B}}_2 = 0 \quad (7.97)$$

and therefore

$$\bar{\mathbf{P}}\bar{\mathbf{B}} = \begin{bmatrix} \mathbf{0} \\ \bar{\mathbf{P}}_2\bar{\mathbf{B}}_2 \end{bmatrix} \quad (7.98)$$

By using the output matrix given in (7.12) together with the equalities (7.93) and $\mathcal{B}_2 = \mathbf{T}\bar{\mathbf{B}}_2$ defined in (7.80),

$$\bar{\mathbf{C}}^T\mathbf{P}_2\mathcal{B}_2 = \begin{bmatrix} \mathbf{0} \\ \mathbf{T}^T \end{bmatrix} \mathbf{T}\bar{\mathbf{P}}_2\mathbf{T}^T\mathcal{B}_2 = \begin{bmatrix} \mathbf{0} \\ \bar{\mathbf{P}}_2\mathbf{T}^T\mathcal{B}_2 \end{bmatrix} = \begin{bmatrix} \mathbf{0} \\ \bar{\mathbf{P}}_2\bar{\mathbf{B}}_2 \end{bmatrix} \quad (7.99)$$

Hence, from (7.98) and (7.99) follows that

$$\bar{\mathbf{P}}\bar{\mathbf{B}} = \bar{\mathbf{C}}^T\mathbf{P}_2\mathcal{B}_2 \quad (7.100)$$

Substituting the structural constraints (7.95) and (7.100) into (7.91) produces

$$\begin{aligned} \dot{V}(t) \leq & -\lambda_{\min}(\bar{\mathbf{Q}}_0)\|\bar{\mathbf{e}}(t)\|^2 - 2\bar{\mathbf{e}}^T(t)\bar{\mathbf{P}}\Delta\bar{\mathbf{A}}_u(t)\bar{\mathbf{x}}(t) \\ & + 2\bar{\mathbf{e}}^T(t)\bar{\mathbf{C}}^T\mathbf{P}_2\nu - 2\bar{\mathbf{e}}^T(t)\bar{\mathbf{C}}^T\mathbf{P}_2\mathcal{B}_2\bar{\xi}_\Delta(t, \bar{\mathbf{x}}, \mathbf{u}) \end{aligned} \quad (7.101)$$

However, since $\mathbf{e}_y(t) = \bar{\mathbf{C}}\bar{\mathbf{e}}(t)$, it follows

$$\begin{aligned} \dot{V}(t) \leq & -\lambda_{\min}(\bar{\mathbf{Q}}_0)\|\bar{\mathbf{e}}(t)\|^2 - 2\bar{\mathbf{e}}^T(t)\bar{\mathbf{P}}\Delta\bar{\mathbf{A}}_u(t)\bar{\mathbf{x}}(t) \\ & + 2\mathbf{e}_y^T(t)\mathbf{P}_2\nu - 2\mathbf{e}_y^T(t)\mathbf{P}_2\mathcal{B}_2\bar{\xi}_\Delta(t, \bar{\mathbf{x}}, \mathbf{u}) \end{aligned} \quad (7.102)$$

Rearranging the inequality above, after substituting for ν from (7.5), results in the expression

$$\dot{V}(t) \leq -\lambda_{\min}(\bar{\mathbf{Q}}_0)\|\bar{\mathbf{e}}(t)\|^2 - 2\bar{\mathbf{e}}^T(t)\bar{\mathbf{P}}\Delta\bar{\mathbf{A}}_u(t)\bar{\mathbf{x}}(t) - 2\|\mathbf{P}_2\mathbf{e}_y(t)\|\|\mathcal{B}_2\|(\rho(\cdot) - \|\bar{\xi}_\Delta(\cdot)\|) \quad (7.103)$$

Considering the bound on the matched uncertainty given in (7.48) as well as the bound on the scalar function $\rho(t, \mathbf{y}, \mathbf{u})$, it is straightforward to verify that

$$\rho(t, \mathbf{y}, \mathbf{u}) \geq \|\bar{\xi}_\Delta(t, \bar{\mathbf{x}}, \mathbf{u})\| + \eta \quad (7.104)$$

Then,

$$\dot{V}(t) \leq -\lambda_{\min}(\bar{\mathbf{Q}}_0)\|\bar{\mathbf{e}}(t)\|^2 + 2\lambda_{\max}(\bar{\mathbf{P}})\|\bar{\mathbf{e}}(t)\|\|\Delta\bar{\mathbf{A}}_u(t)\bar{\mathbf{x}}(t)\| - 2\|\mathbf{P}_2\mathbf{e}_y(t)\|\|\mathcal{B}_2\|\eta \quad (7.105)$$

7.3 Stability Analysis

By defining

$$\gamma_\lambda = \frac{\lambda_{\min}(\bar{\mathbf{Q}}_0)}{\lambda_{\max}(\bar{\mathbf{P}})} \quad (7.106)$$

and rearranging (7.105), it is straightforward to show that

$$\dot{\bar{V}}(t) \leq \lambda_{\max}(\bar{\mathbf{P}}) \|\bar{\mathbf{e}}(t)\| (-\gamma_\lambda \|\bar{\mathbf{e}}(t)\| + 2\|\Delta\bar{\mathbf{A}}_u(t)\bar{\mathbf{x}}(t)\|) - 2\|\mathbf{P}_2\mathbf{e}_y(t)\| \|\mathbf{B}_2\| \eta \quad (7.107)$$

Inside the set $\Omega_{\bar{\mathbf{e}}}$

$$\|\bar{\mathbf{e}}(t)\| < 2\|\Delta\bar{\mathbf{A}}_u(t)\bar{\mathbf{x}}(t)\| \gamma_\lambda^{-1} + \gamma_{\bar{\mathbf{e}}} \quad (7.108)$$

and it follows that

$$\dot{\bar{V}}(t) \leq -\gamma_\lambda \gamma_{\bar{\mathbf{e}}} \lambda_{\max}(\bar{\mathbf{P}}) \|\bar{\mathbf{e}}(t)\| - 2\|\mathbf{P}_2\mathbf{e}_y(t)\| \|\mathbf{B}_2\| \eta < 0 \quad (7.109)$$

for $\bar{\mathbf{e}}(t) \notin \Omega_{\bar{\mathbf{e}}}$. Hence, the uncertain error system is ultimately bounded stable with respect to the ellipsoid $\Omega_{\bar{\mathbf{e}}}$. This means, that the estimation error $\bar{\mathbf{e}}(t)$ enters the domain $\Omega_{\bar{\mathbf{e}}}$ and remains within it thereafter.

Q.E.D.

Commensurate with the partition of the system triple $(\bar{\mathbf{A}}, \bar{\mathbf{B}}, \bar{\mathbf{C}})$ defined in (7.32) and also by using (7.53) and (7.76), the error system dynamics (7.75) can be written as follows

$$\dot{\bar{\mathbf{e}}}_1(t) = \bar{\mathbf{A}}_{11}\bar{\mathbf{e}}_1(t) + \bar{\mathbf{A}}_{12}\bar{\mathbf{e}}_2(t) - \Delta\bar{\mathbf{A}}_{11}\bar{\mathbf{x}}_1(t) - \Delta\bar{\mathbf{A}}_{12}\bar{\mathbf{x}}_2(t) - \bar{\mathbf{G}}_{L1}\mathbf{e}_y(t) + \bar{\mathbf{G}}_{NL1}\nu \quad (7.110)$$

$$\dot{\bar{\mathbf{e}}}_2(t) = \bar{\mathbf{A}}_{21}\bar{\mathbf{e}}_1(t) + \bar{\mathbf{A}}_{22}\bar{\mathbf{e}}_2(t) - \bar{\mathbf{G}}_{L2}\mathbf{e}_y(t) + \bar{\mathbf{G}}_{NL2}\nu - \bar{\mathbf{B}}_2\bar{\xi}_\Delta(t, \bar{\mathbf{x}}, \mathbf{u}) \quad (7.111)$$

Consider a similarity transformation such that $\bar{\mathbf{e}} \mapsto \mathbf{T}_L\bar{\mathbf{e}} = \tilde{\mathbf{e}}$ where the nonsingular transformation matrix $\mathbf{T}_L \in \mathfrak{R}^{n \times n}$ is given by

$$\mathbf{T}_L = \begin{bmatrix} \mathbf{I}_{(n-p)} & \bar{\mathbf{L}} \\ \mathbf{0} & \mathbf{T} \end{bmatrix} \quad (7.112)$$

From (7.110) and (7.111), in the new coordinates, the uncertain error system dynamics are governed by

$$\dot{\tilde{\mathbf{e}}}_1(t) = \tilde{\mathbf{A}}_{11}\tilde{\mathbf{e}}_1(t) - \Delta\tilde{\mathbf{A}}_{11}\bar{\mathbf{x}}_1(t) - \Delta\tilde{\mathbf{A}}_{12}\bar{\mathbf{x}}_2(t) \quad (7.113)$$

$$\dot{\tilde{\mathbf{e}}}_2(t) = \tilde{\mathbf{A}}_{21}\tilde{\mathbf{e}}_1(t) + \mathcal{A}_{22}^{stb}\mathbf{e}_y(t) + \nu - \mathcal{B}_2\bar{\xi}_\Delta(t, \bar{\mathbf{x}}, \mathbf{u}) \quad (7.114)$$

7.3 Stability Analysis

where $\tilde{\mathbf{A}}_{11} \in \mathfrak{R}^{(n-p) \times (n-p)}$ and $\tilde{\mathbf{A}}_{21} \in \mathfrak{R}^{p \times (n-p)}$ are defined in (7.60), the matrix $\mathcal{A}_{22}^{stb} \in \mathfrak{R}^{p \times p}$ is a stable matrix by design, whilst $\mathcal{B}_2 \in \mathfrak{R}^{p \times p}$ is defined in (7.80).

In the sequel, it is demonstrated that a sliding motion is induced on the sliding surface \mathcal{S}_{Obs} in finite time within a domain of attraction. This is an important result since it guarantees the existence of a sliding motion.

Lemma 7.4 *A sliding motion takes place after some finite time t_σ on the sliding surface*

$$\mathcal{S}_{Obs} = \{ \mathbf{e}(t) \in \mathfrak{R}^n : \mathbf{e}_y(t) = \mathbf{C}\mathbf{e}(t) = 0 \} \quad (7.115)$$

within the domain

$$\Omega_\sigma = \{ (\tilde{\mathbf{e}}_1(t), \mathbf{e}_y(t)) : \|\mathbf{T}\tilde{\mathbf{A}}_{21}\tilde{\mathbf{e}}_1(t)\| < \|\mathcal{B}_2\|\eta - \gamma_\sigma \} \quad (7.116)$$

where $\gamma_\sigma \in \mathfrak{R}_+$ is a small design scalar.

Proof From the definition of $\tilde{\mathbf{A}}_{21}$ given in (7.60), equation (7.114) can be written as

$$\dot{\mathbf{e}}_y(t) = \mathbf{T}\tilde{\mathbf{A}}_{21}\tilde{\mathbf{e}}_1(t) + \mathcal{A}_{22}^{stb}\mathbf{e}_y(t) + \nu - \mathcal{B}_2\bar{\xi}_\Delta(t, \bar{\mathbf{x}}, \mathbf{u}) \quad (7.117)$$

Consider the *Lyapunov* function

$$V_\sigma(t) := \mathbf{e}_y^T(t)\mathbf{P}_2\mathbf{e}_y(t) \quad (7.118)$$

where $\mathbf{P}_2 \in \mathfrak{R}^{p \times p}$ is a s.p.d matrix as defined in (7.93). Differentiating the quadratic form (7.118) with respect to time, along the error system trajectories, gives

$$\dot{V}_\sigma(t) = \dot{\mathbf{e}}_y^T(t)\mathbf{P}_2\mathbf{e}_y(t) + \mathbf{e}_y^T(t)\mathbf{P}_2\dot{\mathbf{e}}_y(t) \quad (7.119)$$

Consequently from (7.117), it follows

$$\begin{aligned} \dot{V}_\sigma(t) &= (\mathbf{T}\tilde{\mathbf{A}}_{21}\tilde{\mathbf{e}}_1(t) + \mathcal{A}_{22}^{stb}\mathbf{e}_y(t) + \nu - \mathcal{B}_2\bar{\xi}_\Delta(t, \bar{\mathbf{x}}, \mathbf{u}))^T \mathbf{P}_2\mathbf{e}_y(t) \\ &\quad + \mathbf{e}_y^T(t)\mathbf{P}_2(\mathbf{T}\tilde{\mathbf{A}}_{21}\tilde{\mathbf{e}}_1(t) + \mathcal{A}_{22}^{stb}\mathbf{e}_y(t) + \nu - \mathcal{B}_2\bar{\xi}_\Delta(t, \bar{\mathbf{x}}, \mathbf{u})) \end{aligned} \quad (7.120)$$

$$\begin{aligned} &= \mathbf{e}_y^T(t) \left((\mathcal{A}_{22}^{stb})^T \mathbf{P}_2 + \mathbf{P}_2 \mathcal{A}_{22}^{stb} \right) \mathbf{e}_y(t) + 2\mathbf{e}_y^T(t)\mathbf{P}_2\mathbf{T}\tilde{\mathbf{A}}_{21}\tilde{\mathbf{e}}_1(t) \\ &\quad + 2\mathbf{e}_y^T(t)\mathbf{P}_2\nu - 2\mathbf{e}_y^T(t)\mathbf{P}_2\mathcal{B}_2\bar{\xi}_\Delta(t, \bar{\mathbf{x}}, \mathbf{u}) \end{aligned} \quad (7.121)$$

but since

$$(\mathcal{A}_{22}^{stb})^T \mathbf{P}_2 + \mathbf{P}_2 \mathcal{A}_{22}^{stb} = -\mathbf{Q}_2 \quad (7.122)$$

7.3 Stability Analysis

where $\mathbf{Q}_2 \in \mathbb{R}^{p \times p}$ is a s.p.d. matrix defined by the designer, then

$$\begin{aligned} \dot{V}_\sigma(t) &= -\mathbf{e}_y^\top(t) \mathbf{Q}_2 \mathbf{e}_y(t) + 2\mathbf{e}_y^\top(t) \mathbf{P}_2 \mathbf{T} \bar{\mathbf{A}}_{21} \tilde{\mathbf{e}}_1(t) \\ &\quad + 2\mathbf{e}_y^\top(t) \mathbf{P}_2 \nu - 2\mathbf{e}_y^\top(t) \mathbf{P}_2 \mathcal{B}_2 \bar{\xi}_\Delta(t, \bar{\mathbf{x}}, \mathbf{u}) \end{aligned} \quad (7.123)$$

Substituting for

$$\nu = -\rho(t, \mathbf{y}, \mathbf{u}) \|\mathcal{B}_2\| \frac{\mathbf{P}_2 \mathbf{e}_y(t)}{\|\mathbf{P}_2 \mathbf{e}_y(t)\|} \quad (7.124)$$

in equation (7.123) and rearranging using the *Cauchy-Scharuz* inequality yields

$$\begin{aligned} \dot{V}_\sigma(t) &= -\mathbf{e}_y^\top(t) \mathbf{Q}_2 \mathbf{e}_y(t) + 2\mathbf{e}_y^\top(t) \mathbf{P}_2 \mathbf{T} \bar{\mathbf{A}}_{21} \tilde{\mathbf{e}}_1(t) \\ &\quad - 2\rho(t, \mathbf{y}, \mathbf{u}) \|\mathcal{B}_2\| \|\mathbf{P}_2 \mathbf{e}_y(t)\| - 2\mathbf{e}_y^\top(t) \mathbf{P}_2 \mathcal{B}_2 \bar{\xi}_\Delta(t, \bar{\mathbf{x}}, \mathbf{u}) \end{aligned} \quad (7.125)$$

$$\begin{aligned} &\leq -\mathbf{e}_y^\top(t) \mathbf{Q}_2 \mathbf{e}_y(t) + 2\mathbf{e}_y^\top(t) \mathbf{P}_2 \mathbf{T} \bar{\mathbf{A}}_{21} \tilde{\mathbf{e}}_1(t) \\ &\quad - 2\|\mathcal{B}_2\| \|\mathbf{P}_2 \mathbf{e}_y(t)\| (\rho(t, \mathbf{y}, \mathbf{u}) - \|\bar{\xi}_\Delta(t, \bar{\mathbf{x}}, \mathbf{u})\|) \end{aligned} \quad (7.126)$$

From the bound on the matched uncertainty given in (7.48) and the bound on the positive scalar $\rho(t, \mathbf{y}, \mathbf{u})$, the following relation can easily be demonstrated

$$\rho(t, \mathbf{y}, \mathbf{u}) \geq \|\bar{\xi}_\Delta(t, \bar{\mathbf{x}}, \mathbf{u})\| + \eta \quad (7.127)$$

Then,

$$\dot{V}_\sigma(t) \leq -\mathbf{e}_y^\top(t) \mathbf{Q}_2 \mathbf{e}_y(t) + 2\mathbf{e}_y^\top(t) \mathbf{P}_2 \mathbf{T} \bar{\mathbf{A}}_{21} \tilde{\mathbf{e}}_1(t) - 2\|\mathcal{B}_2\| \|\mathbf{P}_2 \mathbf{e}_y(t)\| \eta \quad (7.128)$$

$$\leq -\mathbf{e}_y^\top(t) \mathbf{Q}_2 \mathbf{e}_y(t) + 2\|\mathbf{P}_2 \mathbf{e}_y(t)\| (\|\mathbf{T} \bar{\mathbf{A}}_{21} \tilde{\mathbf{e}}_1(t)\| - \|\mathcal{B}_2\| \eta) \quad (7.129)$$

In the domain

$$\Omega_\sigma = \left\{ (\tilde{\mathbf{e}}_1(t), \mathbf{e}_y(t)) : \|\mathbf{T} \bar{\mathbf{A}}_{21} \tilde{\mathbf{e}}_1(t)\| < \|\mathcal{B}_2\| \eta - \gamma_\sigma \right\} \quad (7.130)$$

it follows

$$\dot{V}_\sigma(t) < -\mathbf{e}_y^\top(t) \mathbf{Q}_2 \mathbf{e}_y(t) - 2\|\mathbf{P}_2 \mathbf{e}_y(t)\| \gamma_\sigma < -2\|\mathbf{P}_2 \mathbf{e}_y(t)\| \gamma_\sigma \quad (7.131)$$

for all $\mathbf{e}_y(t) \neq 0$.

From the following basic algebraic manipulation

$$\|\mathbf{P}_2 \mathbf{e}_y(t)\|^2 = (\mathbf{P}_2 \mathbf{e}_y(t))^\top (\mathbf{P}_2 \mathbf{e}_y(t)) = \mathbf{e}_y^\top(t) \mathbf{P}_2 \mathbf{P}_2 \mathbf{e}_y(t) = (\mathbf{P}_2^{1/2} \mathbf{e}_y(t))^\top \mathbf{P}_2 (\mathbf{P}_2^{1/2} \mathbf{e}_y(t)) \quad (7.132)$$

the inequality

$$\|\mathbf{P}_2 \mathbf{e}_y(t)\|^2 \geq \lambda_{\min}(\mathbf{P}_2) \|\mathbf{P}_2^{1/2} \mathbf{e}_y(t)\|^2 \quad (7.133)$$

is obtained and furthermore

$$\|\mathbf{P}_2^{1/2} \mathbf{e}_y(t)\|^2 = (\mathbf{P}_2^{1/2} \mathbf{e}_y(t))^T (\mathbf{P}_2^{1/2} \mathbf{e}_y(t)) = \mathbf{e}_y^T(t) \mathbf{P}_2 \mathbf{e}_y(t) = V_\sigma(t) \quad (7.134)$$

Then, the inequality given in (7.133) can be written as

$$\|\mathbf{P}_2 \mathbf{e}_y(t)\|^2 \geq \lambda_{\min}(\mathbf{P}_2) V_\sigma(t) \quad (7.135)$$

From (7.131) and (7.135), it follows that

$$\dot{V}_\sigma(t) \leq -2\gamma_\sigma \sqrt{\lambda_{\min}(\mathbf{P}_2) V_\sigma(t)} < 0 \quad (7.136)$$

This inequality means that a sliding motion takes place on the sliding surface $\mathcal{S}_{o_{bs}}$ in finite time and remains inside the domain $\Omega_\sigma \forall t \geq t_\sigma$ thereafter.

Q.E.D.

7.4 Design Framework

The effect of the matched uncertainty $\xi_\Delta(t, \bar{\mathbf{x}}, \mathbf{u})$ is rejected by the nonlinear discontinuous vector ν , which depends upon the output estimation error injected into the observer. This is consistent with the invariance property of sliding modes with respect to the class of matched uncertainty. In this sense, sliding mode observers are more robust than the classical *Luenberger* observers. The discontinuous output error injection vector, given in (7.5), is designed in such a way that the observer trajectories are driven to the sliding surface (7.9) defined in the error space, and remain on the sliding hyperplane. Nevertheless, the invariance property is not guaranteed with respect to the mismatched uncertainty in the error system (7.51). Hence, the aim is to design a sliding mode observer so that the effect of such uncertainty is maximally attenuated. To this end, an LMI-based approach using the so-called Bounded Real Lemma (Boyd *et al.*, 1994) is proposed using a polytopic description of the mismatched uncertainty. An optimisation problem based on LMI methods is formulated in order to synthesise the matrix $\mathbf{L} \in \mathfrak{R}^{(n-p) \times (p-m)}$ which is part of the matrix

$$\bar{\mathbf{L}} = \begin{bmatrix} \mathbf{L} & \mathbf{0}_{(n-p) \times m} \end{bmatrix} \quad (7.137)$$

which defines the gain matrices \mathbf{G}_L and \mathbf{G}_{NL} .

7.4 Design Framework

Define

$$\Delta \bar{\mathbf{A}}_{u_1}(t) = \begin{bmatrix} -\Delta \bar{\mathbf{A}}_{11}(t) & -\Delta \bar{\mathbf{A}}_{12}(t) \end{bmatrix} \quad (7.138)$$

where $\Delta \bar{\mathbf{A}}_{11}(t) \in \mathfrak{R}^{(n-p) \times (n-p)}$ and $\Delta \bar{\mathbf{A}}_{12}(t) \in \mathfrak{R}^{(n-p) \times p}$ are sub-matrices of the mismatched uncertain matrix

$$\Delta \bar{\mathbf{A}}_u(t) = \begin{bmatrix} \Delta \bar{\mathbf{A}}_{11}(t) & \Delta \bar{\mathbf{A}}_{12}(t) \\ \mathbf{0} & \mathbf{0} \end{bmatrix} \quad (7.139)$$

which was established earlier in Lemma 7.1. Also, define the state vector

$$\bar{\mathbf{x}}(t) = \begin{bmatrix} \bar{\mathbf{x}}_1^T(t) & \bar{\mathbf{x}}_2^T(t) \end{bmatrix}^T \quad (7.140)$$

where $\bar{\mathbf{x}}_1 \in \mathfrak{R}^{(n-p)}$ and $\bar{\mathbf{x}}_2 \in \mathfrak{R}^p$. Then, the uncertain reduced-order uncertain error system from (7.113) can be written as

$$\dot{\tilde{\mathbf{e}}}_1(t) = (\bar{\mathbf{A}}_{11} + \mathbf{L}\bar{\mathbf{A}}_{211})\tilde{\mathbf{e}}_1(t) + \Delta \bar{\mathbf{A}}_{u_1}\bar{\mathbf{x}}(t) \quad (7.141)$$

where $\bar{\mathbf{A}}_{11} \in \mathfrak{R}^{(n-p) \times (n-p)}$ and $\bar{\mathbf{A}}_{211} \in \mathfrak{R}^{(p-m) \times (n-p)}$ are known constant matrices. The gain matrix \mathbf{L} is to be designed. The vector $\bar{\mathbf{x}} \in \mathfrak{R}^n$ is considered as an exogenous disturbance input vector. The objective is to ensure

$$\frac{\|\tilde{\mathbf{e}}_1(t)\|_2}{\|\bar{\mathbf{x}}(t)\|_2} < \gamma_{\tilde{\mathbf{e}}_1\bar{\mathbf{x}}} \quad (7.142)$$

where

$$\|\tilde{\mathbf{e}}_1(t)\|_2 = \left(\int_0^\infty \tilde{\mathbf{e}}_1^T(t)\tilde{\mathbf{e}}_1(t)dt \right)^{1/2} \quad (7.143)$$

and

$$\|\bar{\mathbf{x}}(t)\|_2 = \left(\int_0^\infty \bar{\mathbf{x}}^T(t)\bar{\mathbf{x}}(t)dt \right)^{1/2} \quad (7.144)$$

The constraint (7.142) is an \mathcal{H}_∞ performance index for all nonzero $\bar{\mathbf{x}}(t) \in \mathcal{L}_2(0, \infty)$.

Remark 7.2 The \mathcal{H}_∞ norm is the induced energy gain, and in the case presented in this section corresponds to the worst case amplification of the effect of the disturbance $\bar{\mathbf{x}}$ in the reduced-order error system.

The following is assumed throughout this section:

7.4 Design Framework

A-7.4 The matrix representing the mismatched uncertainty $\Delta\bar{\mathbf{A}}_{u1}(t)$ is affine with respect to the uncertain parameters denoted in vector form by $\boldsymbol{\theta}(t) = [\theta_1(t) \ \theta_2(t) \ \cdots \ \theta_r(t)]^T$. These uncertain parameters satisfy

$$\underline{\theta}_i \leq \theta_i \leq \bar{\theta}_i \quad \text{for } i \in I(1, r) \quad (7.145)$$

and they define a convex set in the parameter space $\Theta \subseteq \mathfrak{R}^r$.

From the assumption above, the uncertain continuous-time system (7.141) can be written in system matrix form as

$$\Sigma_{\bar{\mathbf{e}}_1\bar{\mathbf{x}}}(t) = \left[\begin{array}{c|c} (\bar{\mathbf{A}}_{11} + \mathbf{L}\bar{\mathbf{A}}_{211}) & \Delta\bar{\mathbf{A}}_{u1}(t) \\ \hline \mathbf{I}_{(n-p)} & \mathbf{0} \end{array} \right] \quad (7.146)$$

and admits a polytopic representation given by

$$\mathcal{P}_L^{Obs} = \left\{ \sum_{j=1}^N \mu_j \left[\begin{array}{c|c} (\bar{\mathbf{A}}_{11} + \mathbf{L}\bar{\mathbf{A}}_{211}) & \Delta\bar{\mathbf{A}}_{u1j} \\ \hline \mathbf{I}_{(n-p)} & \mathbf{0} \end{array} \right] : \sum_{j=1}^N \mu_j = 1, \mu_j \geq 0 \text{ for } j \in I(1, N) \right\} \quad (7.147)$$

where N is the number of vertices of \mathcal{P}_L^{Obs} .

The Bounded-Real Lemma for a polytopic description presented in (Boyd *et al.*, 1994) is adapted for the reduced-order error system (7.141) as shown in the sequel.

Let $\gamma_{\bar{\mathbf{e}}_1\bar{\mathbf{x}}}$ be a positive scalar. The continuous-time system $\Sigma_{\bar{\mathbf{e}}_1\bar{\mathbf{x}}}(t)$ defined in (7.146) is said to be stable and satisfies

$$\|\bar{\mathbf{e}}_1(t)\|_2 < \gamma_{\bar{\mathbf{e}}_1\bar{\mathbf{x}}} \|\bar{\mathbf{x}}(t)\|_2 \quad (7.148)$$

if there exists a s.p.d. matrix $\bar{\mathbf{P}}_1 \in \mathfrak{R}^{(n-p) \times (n-p)}$ such that

$$\left[\begin{array}{cc} (\bar{\mathbf{A}}_{11} + \mathbf{L}\bar{\mathbf{A}}_{211})^T \bar{\mathbf{P}}_1 + \bar{\mathbf{P}}_1 (\bar{\mathbf{A}}_{11} + \mathbf{L}\bar{\mathbf{A}}_{211}) + \mathbf{I}_{(n-p)} & \bar{\mathbf{P}}_1 \Delta\bar{\mathbf{A}}_{u1j} \\ (\bar{\mathbf{P}}_1 \Delta\bar{\mathbf{A}}_{u1j})^T & -\gamma_{\bar{\mathbf{e}}_1\bar{\mathbf{x}}}^2 \mathbf{I}_n \end{array} \right] \prec 0 \quad (7.149)$$

for $j \in I(1, N)$.

Different representations of the matrix inequality (7.149) are presented in the following lemma in which the equivalence between such formulations is stated and demonstrated.

7.4 Design Framework

Lemma 7.5 Let $\Sigma_{\bar{e}_1\bar{x}_j}$ be the j -th continuous-time system denoted by

$$\Sigma_{\bar{e}_1\bar{x}_j} = \left[\begin{array}{c|c} (\bar{\mathbf{A}}_{11} + \mathbf{L}\bar{\mathbf{A}}_{211}) & \Delta\bar{\mathbf{A}}_{u1j} \\ \hline \mathbf{I}_{(n-p)} & \mathbf{0} \end{array} \right] \quad (7.150)$$

where $\bar{\mathbf{A}}_{11}$ and $\bar{\mathbf{A}}_{211}$ are known constant matrices of appropriate dimensions, \mathbf{L} is a design matrix. Let $\bar{\mathbf{P}}_1 \in \mathfrak{R}^{(n-p) \times (n-p)}$ and $\bar{\mathbf{Q}}_1 \in \mathfrak{R}^{(n-p) \times (n-p)}$ be s.p.d. matrices, and $\gamma_{\bar{e}_1\bar{x}} \in \mathfrak{R}_+$ is a constant scalar. The following matrix inequalities are equivalent:

$$(\bar{\mathbf{A}}_{11} + \mathbf{L}\bar{\mathbf{A}}_{211})^T \bar{\mathbf{P}}_1 + \bar{\mathbf{P}}_1 (\bar{\mathbf{A}}_{11} + \mathbf{L}\bar{\mathbf{A}}_{211}) + \mathbf{I}_{(n-p)} + \gamma_{\bar{e}_1\bar{x}}^{-2} (\bar{\mathbf{P}}_1 \Delta\bar{\mathbf{A}}_{u1j}) (\bar{\mathbf{P}}_1 \Delta\bar{\mathbf{A}}_{u1j})^T \prec \mathbf{0} \quad (7.151)$$

$$\left[\begin{array}{cc} (\bar{\mathbf{A}}_{11} + \mathbf{L}\bar{\mathbf{A}}_{211})^T \bar{\mathbf{P}}_1 + \bar{\mathbf{P}}_1 (\bar{\mathbf{A}}_{11} + \mathbf{L}\bar{\mathbf{A}}_{211}) + \mathbf{I}_{(n-p)} & \bar{\mathbf{P}}_1 \Delta\bar{\mathbf{A}}_{u1j} \\ (\bar{\mathbf{P}}_1 \Delta\bar{\mathbf{A}}_{u1j})^T & -\gamma_{\bar{e}_1\bar{x}}^2 \mathbf{I}_n \end{array} \right] \prec \mathbf{0} \quad (7.152)$$

$$\left[\begin{array}{ccc} (\bar{\mathbf{A}}_{11} + \mathbf{L}\bar{\mathbf{A}}_{211})^T \bar{\mathbf{P}}_1 + \bar{\mathbf{P}}_1 (\bar{\mathbf{A}}_{11} + \mathbf{L}\bar{\mathbf{A}}_{211}) & \bar{\mathbf{P}}_1 \Delta\bar{\mathbf{A}}_{u1j} & \mathbf{I}_{(n-p)} \\ (\bar{\mathbf{P}}_1 \Delta\bar{\mathbf{A}}_{u1j})^T & -\gamma_{\bar{e}_1\bar{x}}^2 \mathbf{I}_n & \mathbf{0} \\ \mathbf{I}_{(n-p)} & \mathbf{0} & -\mathbf{I}_{(n-p)} \end{array} \right] \prec \mathbf{0} \quad (7.153)$$

$$\left[\begin{array}{ccc} (\bar{\mathbf{A}}_{11} + \mathbf{L}\bar{\mathbf{A}}_{211})^T \bar{\mathbf{Q}}_1 + \bar{\mathbf{Q}}_1 (\bar{\mathbf{A}}_{11} + \mathbf{L}\bar{\mathbf{A}}_{211}) & \bar{\mathbf{Q}}_1 \Delta\bar{\mathbf{A}}_{u1j} & \mathbf{I}_{(n-p)} \\ (\bar{\mathbf{Q}}_1 \Delta\bar{\mathbf{A}}_{u1j})^T & -\gamma_{\bar{e}_1\bar{x}} \mathbf{I}_n & \mathbf{0} \\ \mathbf{I}_{(n-p)} & \mathbf{0} & -\gamma_{\bar{e}_1\bar{x}} \mathbf{I}_{(n-p)} \end{array} \right] \prec \mathbf{0} \quad (7.154)$$

△

Proof Applying the *Schur* complement to (7.151) yields straightforwardly either (7.152) or (7.153), i.e. (7.151) \iff (7.152)-(7.153). With regard to the equivalence (7.152) \iff (7.153), this follows also by applying the *Schur* complement. Now, the equivalence between (7.151) and (7.154) is demonstrated. Multiplying both sides of the matrix inequality (7.151) by $\gamma_{\bar{e}_1\bar{x}}^{-1}$ and substituting for $\bar{\mathbf{Q}}_1 = \gamma_{\bar{e}_1\bar{x}}^{-1} \bar{\mathbf{P}}_1$ yields

$$\begin{aligned} & (\bar{\mathbf{A}}_{11} + \mathbf{L}\bar{\mathbf{A}}_{211})^T \bar{\mathbf{Q}}_1 + \bar{\mathbf{Q}}_1 (\bar{\mathbf{A}}_{11} + \mathbf{L}\bar{\mathbf{A}}_{211}) \\ & + \gamma_{\bar{e}_1\bar{x}}^{-1} \mathbf{I}_{(n-p)} + \gamma_{\bar{e}_1\bar{x}}^{-1} (\bar{\mathbf{Q}}_1 \Delta\bar{\mathbf{A}}_{u1j}) (\bar{\mathbf{Q}}_1 \Delta\bar{\mathbf{A}}_{u1j})^T \prec \mathbf{0} \end{aligned} \quad (7.155)$$

Then, applying the *Schur* complement to the *Riccati* inequality (7.155) produces the matrix inequality (7.154). Since (7.151) \iff (7.152)-(7.153) and (7.151) \iff (7.154), the equivalence (7.152)-(7.153) \iff (7.154) follows immediately.

Q.E.D.

7.4 Design Framework

The main result of this section proposes a synthesis method for designing a gain matrix \mathbf{L} through an optimisation problem involving LMIs. The following proposition allows a gain matrix \mathbf{L} to be designed for the polytopic representation of system (7.141). This result consists of a convex optimisation problem formulated using LMIs methods.

Proposition 7.1 *Consider a continuous-time reduced-order error system given in matrix form by*

$$\Sigma_{\bar{\mathbf{e}}_1\bar{\mathbf{x}}}(t) = \left[\begin{array}{c|c} (\bar{\mathbf{A}}_{11} + \mathbf{L}\bar{\mathbf{A}}_{211}) & \Delta\bar{\mathbf{A}}_{u1}(t) \\ \hline \mathbf{I}_{(n-p)} & \mathbf{0} \end{array} \right] \quad (7.156)$$

where $\bar{\mathbf{A}}_{11}$ and $\bar{\mathbf{A}}_{211}$ are known constant matrices of appropriate dimensions such that the pair $(\bar{\mathbf{A}}_{11}, \bar{\mathbf{A}}_{211})$ is detectable. The solution of the convex optimisation problem

$$\min_{\gamma_{\bar{\mathbf{e}}_1\bar{\mathbf{x}}}>0, \bar{\mathbf{Q}}_1, \mathbf{F}_L} \gamma_{\bar{\mathbf{e}}_1\bar{\mathbf{x}}}$$

s.t.

$$\left[\begin{array}{ccc|c} \bar{\mathbf{A}}_{11}^T \bar{\mathbf{Q}}_1 + \bar{\mathbf{Q}}_1 \bar{\mathbf{A}}_{11} + \bar{\mathbf{A}}_{211}^T \mathbf{F}_L^T + \mathbf{F}_L \bar{\mathbf{A}}_{211} & \bar{\mathbf{Q}}_1 \Delta\bar{\mathbf{A}}_{u1j} & \mathbf{I}_{(n-p)} & \\ & (\bar{\mathbf{Q}}_1 \Delta\bar{\mathbf{A}}_{u1j})^T & -\gamma_{\bar{\mathbf{e}}_1\bar{\mathbf{x}}} \mathbf{I}_n & \mathbf{0} \\ & \mathbf{I}_{(n-p)} & \mathbf{0} & -\gamma_{\bar{\mathbf{e}}_1\bar{\mathbf{x}}} \mathbf{I}_{(n-p)} \end{array} \right] \prec 0 \quad (7.157)$$

$$\bar{\mathbf{Q}}_1 \succ 0 \quad (7.158)$$

guarantees

$$\|\bar{\mathbf{e}}_1(t)\|_2 < \gamma_{\bar{\mathbf{e}}_1\bar{\mathbf{x}}}^* \|\bar{\mathbf{x}}(t)\|_2 \quad (7.159)$$

where $\gamma_{\bar{\mathbf{e}}_1\bar{\mathbf{x}}}^* = \inf(\gamma_{\bar{\mathbf{e}}_1\bar{\mathbf{x}}})$, and the gain matrix \mathbf{L} can be straightforwardly computed as

$$\mathbf{L} = \bar{\mathbf{Q}}_1^{-1} \mathbf{F}_L \quad (7.160)$$

△

Proof Suppose there exists a $\bar{\mathbf{Q}}_1 \succ 0$ such that

$$\left[\begin{array}{ccc|c} \bar{\mathbf{A}}_{11}^T \bar{\mathbf{Q}}_1 + \bar{\mathbf{Q}}_1 \bar{\mathbf{A}}_{11} + \bar{\mathbf{A}}_{211}^T \bar{\mathbf{F}}_L^T + \bar{\mathbf{F}}_L \bar{\mathbf{A}}_{211} & \bar{\mathbf{Q}}_1 \Delta\bar{\mathbf{A}}_{u1j} & \mathbf{I}_{(n-p)} & \\ & (\bar{\mathbf{Q}}_1 \Delta\bar{\mathbf{A}}_{u1j})^T & -\gamma_{\bar{\mathbf{e}}_1\bar{\mathbf{x}}} \mathbf{I}_n & \mathbf{0} \\ & \mathbf{I}_{(n-p)} & \mathbf{0} & -\gamma_{\bar{\mathbf{e}}_1\bar{\mathbf{x}}} \mathbf{I}_{(n-p)} \end{array} \right] \prec 0 \quad (7.161)$$

for $j \in I(1, N)$ for some $\mathbf{F}_L \in \mathfrak{R}^{(n-p) \times (p-m)}$ and $\gamma_{\bar{\mathbf{e}}_1\bar{\mathbf{x}}} \in \mathfrak{R}_+$.

Defining and replacing $\mathbf{F}_L = \bar{\mathbf{Q}}_1 \mathbf{L}$ in (7.161) yields

$$\left[\begin{array}{ccc|c} (\bar{\mathbf{A}}_{11} + \mathbf{L}\bar{\mathbf{A}}_{211})^T \bar{\mathbf{Q}}_1 + \bar{\mathbf{Q}}_1 (\bar{\mathbf{A}}_{11} + \mathbf{L}\bar{\mathbf{A}}_{211}) & \bar{\mathbf{Q}}_1 \Delta\bar{\mathbf{A}}_{u1j} & \mathbf{I}_{(n-p)} & \\ & (\bar{\mathbf{Q}}_1 \Delta\bar{\mathbf{A}}_{u1j})^T & -\gamma_{\bar{\mathbf{e}}_1\bar{\mathbf{x}}} \mathbf{I}_n & \mathbf{0} \\ & \mathbf{I}_{(n-p)} & \mathbf{0} & -\gamma_{\bar{\mathbf{e}}_1\bar{\mathbf{x}}} \mathbf{I}_{(n-p)} \end{array} \right] \prec 0 \quad (7.162)$$

for $j \in I(1, N)$.

From Lemma 7.5, the matrix inequality above is equivalent to the quadratic expression

$$\begin{bmatrix} \tilde{\mathbf{e}}_1(t) \\ \tilde{\mathbf{x}}(t) \end{bmatrix}^T \begin{bmatrix} (\bar{\mathbf{A}}_{11} + \mathbf{L}\bar{\mathbf{A}}_{211})^T \bar{\mathbf{P}}_1 + \bar{\mathbf{P}}_1(\bar{\mathbf{A}}_{11} + \mathbf{L}\bar{\mathbf{A}}_{211}) + \mathbf{I}_{(n-p)} & \bar{\mathbf{P}}_1 \Delta \bar{\mathbf{A}}_{u_{1j}} \\ (\bar{\mathbf{P}}_1 \Delta \bar{\mathbf{A}}_{u_{1j}})^T & -\gamma_{\tilde{\mathbf{e}}_1 \tilde{\mathbf{x}}}^2 \mathbf{I}_n \end{bmatrix} \begin{bmatrix} \tilde{\mathbf{e}}_1(t) \\ \tilde{\mathbf{x}}(t) \end{bmatrix} < 0 \quad (7.163)$$

for $j \in I(1, N)$. It follows

$$\begin{aligned} \sum_{j=1}^N \mu_j \left(\tilde{\mathbf{e}}_1^T(t) \left((\bar{\mathbf{A}}_{11} + \mathbf{L}\bar{\mathbf{A}}_{211})^T \bar{\mathbf{P}}_1 + \bar{\mathbf{P}}_1(\bar{\mathbf{A}}_{11} + \mathbf{L}\bar{\mathbf{A}}_{211}) \right) \tilde{\mathbf{e}}_1(t) \right. \\ \left. + 2\tilde{\mathbf{e}}_1^T(t) \bar{\mathbf{P}}_1 \Delta \bar{\mathbf{A}}_{u_{1j}} \tilde{\mathbf{x}}(t) \right) + \tilde{\mathbf{e}}_1^T(t) \tilde{\mathbf{e}}_1(t) - \gamma_{\tilde{\mathbf{e}}_1 \tilde{\mathbf{x}}}^2 \tilde{\mathbf{x}}^T(t) \tilde{\mathbf{x}}(t) < 0 \end{aligned} \quad (7.164)$$

since $\mu_j \geq 0$ and $\sum_{j=1}^N \mu_j = 1$ for all $j \in I(1, N)$.

Consider the *Lyapunov* function

$$V(\tilde{\mathbf{e}}_1) := \tilde{\mathbf{e}}_1^T \bar{\mathbf{P}}_1 \tilde{\mathbf{e}}_1 > 0 \quad (7.165)$$

Then (7.164) is equivalent to

$$\dot{V}(\tilde{\mathbf{e}}_1(t)) + \tilde{\mathbf{e}}_1^T(t) \tilde{\mathbf{e}}_1(t) - \gamma_{\tilde{\mathbf{e}}_1 \tilde{\mathbf{x}}}^2 \tilde{\mathbf{x}}^T(t) \tilde{\mathbf{x}}(t) < 0 \quad (7.166)$$

where

$$\dot{\tilde{\mathbf{e}}}_1(t) = \sum_{j=1}^N \mu_j \left((\bar{\mathbf{A}}_{11} + \mathbf{L}\bar{\mathbf{A}}_{211}) \tilde{\mathbf{e}}_1(t) + \Delta \bar{\mathbf{A}}_{u_{1j}} \tilde{\mathbf{x}}(t) \right) \quad (7.167)$$

which corresponds to the polytopic description of the uncertain reduced-order system (7.141) with $\mu_j \geq 0$ and $\sum_{j=1}^N \mu_j = 1$ for $j \in I(1, N)$.

By integrating (7.166) with respect to time along the time interval $t \in [0, T]$ and assuming the initial condition $\tilde{\mathbf{e}}_1(0) = 0$, yields

$$V(\tilde{\mathbf{e}}_1(T)) + \int_0^T \left(\tilde{\mathbf{e}}_1^T(t) \tilde{\mathbf{e}}_1(t) - \gamma_{\tilde{\mathbf{e}}_1 \tilde{\mathbf{x}}}^2 \tilde{\mathbf{x}}^T(t) \tilde{\mathbf{x}}(t) \right) dt < 0 \quad (7.168)$$

Since $V(\tilde{\mathbf{e}}_1(T)) > 0$, the inequality (7.168) implies that

$$\|\tilde{\mathbf{e}}_1(t)\|_2 < \gamma_{\tilde{\mathbf{e}}_1 \tilde{\mathbf{x}}} \|\tilde{\mathbf{x}}(t)\|_2 \quad (7.169)$$

A convex optimisation problem is required in order to find the greatest lower bound of $\gamma_{\tilde{\mathbf{e}}_1 \tilde{\mathbf{x}}} \in \mathfrak{R}_+$, i.e. $\gamma_{\tilde{\mathbf{e}}_1 \tilde{\mathbf{x}}}^* \in \mathfrak{R}_+$, and the matrix variables $\bar{\mathbf{Q}}_1$ and \mathbf{F}_L . To this end, the

7.5 Design and Simulation Example

following optimisation problem is formulated

$$\min_{\gamma_{\bar{\epsilon}_1}, \bar{\mathbf{Q}}_1, \mathbf{F}_L} \gamma_{\bar{\epsilon}_1}$$

s.t.

$$\begin{bmatrix} \bar{\mathbf{A}}_{11}^T \bar{\mathbf{Q}}_1 + \bar{\mathbf{Q}}_1 \bar{\mathbf{A}}_{11} + \bar{\mathbf{A}}_{21}^T \mathbf{F}_L^T + \mathbf{F}_L \bar{\mathbf{A}}_{21} & \bar{\mathbf{Q}}_1 \Delta \bar{\mathbf{A}}_{u1j} & \mathbf{I}_{(n-p)} \\ (\bar{\mathbf{Q}}_1 \Delta \bar{\mathbf{A}}_{u1j})^T & -\gamma_{\bar{\epsilon}_1} \mathbf{I}_n & \mathbf{0} \\ \mathbf{I}_{(n-p)} & \mathbf{0} & -\gamma_{\bar{\epsilon}_1} \mathbf{I}_{(n-p)} \end{bmatrix} \prec 0 \quad (7.170)$$

$$\bar{\mathbf{Q}}_1 \succ 0 \quad (7.171)$$

for $j \in I(1, N)$.

Q.E.D.

Once the matrix $\mathbf{L} \in \mathfrak{R}^{(n-p) \times (p-m)}$ is designed then the observer gain matrices $\bar{\mathbf{G}}_L \in \mathfrak{R}^{n \times p}$ and $\bar{\mathbf{G}}_{NL} \in \mathfrak{R}^{n \times p}$, in the original coordinates, can be computed as follows

$$\mathbf{G}_L = \mathbf{T}_o^{-1} \bar{\mathbf{G}}_L \quad (7.172)$$

$$\mathbf{G}_{NL} = \mathbf{T}_o^{-1} \bar{\mathbf{G}}_{NL} \quad (7.173)$$

where

$$\mathbf{T}_o = \mathbf{T}_C \mathbf{T}_B \mathbf{T}_A \quad (7.174)$$

with \mathbf{T}_C , \mathbf{T}_B and \mathbf{T}_A defined in (7.20), (7.26) and (7.31) respectively.

7.5 Design and Simulation Example

Here the design methodology presented in the last section is illustrated through a numerical example involving a 4th order uncertain linear system.

Example 7.1 Consider an uncertain linear dynamical system described in state space form by

$$\dot{\mathbf{x}}(t) = \begin{bmatrix} -6 & 1 + \theta_1(t) & 0 & 2 + \theta_2(t) \\ 0 & -2 & -1 + \theta_3(t) & 1 \\ 0 & 3 & 0 & 0 \\ 2 & 1 & -2 & -1 \end{bmatrix} \mathbf{x}(t) + \begin{bmatrix} 0 \\ 0 \\ 0 \\ 1 \end{bmatrix} (u(t) + \xi(\cdot)) \quad (7.175)$$

$$\mathbf{y}(t) = \begin{bmatrix} 0 & 0 & 1 & 0 \\ 0 & 0 & 0 & 1 \end{bmatrix} \mathbf{x}(t) \quad (7.176)$$

7.5 Design and Simulation Example

where

$$\theta_1(t) = 0.5 \sin(2t) \quad \theta_2(t) = \sin(4t) \quad \theta_3(t) = 0.5 \sin(6t) \quad \xi(\cdot) = 0.5 \sin(10\pi t) \quad (7.177)$$

The system is already in the canonical form defined in Lemma 7.1 then $\mathbf{T}_o = \mathbf{I}_4$. Another feature of the system represented in (7.175)-(7.176) is that the open loop nominal system ($\theta_1(t) = \theta_2(t) = \theta_3(t) = 0$) is unstable. This is easy to see by inspection of the nominal system's open loop eigenvalues

$$\{-6.6799, -2.3793, 0.0296 \pm j1.6254\} \quad (7.178)$$

The uncertain parameters define a hyper-rectangle in the parameter space $\Theta \in \mathfrak{R}^3$ when considering

$$|\theta_1(t)| \leq 0.5 \quad |\theta_2(t)| \leq 1 \quad |\theta_3(t)| \leq 0.5 \quad (7.179)$$

In addition, the state matrix is affine in $\boldsymbol{\theta}(t) = [\theta_1(t) \ \theta_2(t) \ \theta_3(t)]^T$. Thus, a polytope \mathcal{P}_L^{obs} composed of 8 vertices can be constructed using

$$\bar{\mathbf{A}}_{11} = \begin{bmatrix} -6 & 1 \\ 0 & -2 \end{bmatrix} \quad (7.180)$$

$$\Delta \bar{\mathbf{A}}_{w_{1j}} = \begin{bmatrix} 0 & \theta_{1j} & 0 & \theta_{2j} \\ 0 & 0 & \theta_{3j} & 0 \end{bmatrix} \quad \text{for } j \in I(1, 8) \quad (7.181)$$

$$\bar{\mathbf{A}}_{211} = [\ 0 \ 3 \] \quad (7.182)$$

The pair $(\bar{\mathbf{A}}_{11}, \bar{\mathbf{A}}_{211})$ is not completely observable but is detectable. Hence, only one pole may be placed arbitrarily.

The convex optimisation problem formulated in Proposition 7.1 can be implemented in MATLAB and has a solution giving $\gamma_{\hat{e}_{1\bar{x}}}^* = 0.1863$ as the worst amplification of the disturbance effect and the gain matrix

$$\mathbf{L} = \begin{bmatrix} -0.3333 \\ -1.8087 \end{bmatrix} \quad (7.183)$$

for which

$$\lambda(\bar{\mathbf{A}}_{11} + \mathbf{L}\bar{\mathbf{A}}_{211}) = \{-6, -7.4260\} \quad (7.184)$$

7.5 Design and Simulation Example

Furthermore,

$$\bar{\mathbf{L}} = \begin{bmatrix} -0.3333 & 0 \\ -1.8087 & 0 \end{bmatrix} \quad (7.185)$$

Defining

$$\mathcal{A}_{22}^{stb} = \begin{bmatrix} -13 & 0 \\ 0 & -13 \end{bmatrix} \quad (7.186)$$

and $\mathbf{Q}_2 = \mathbf{I}_2$, the following *Lyapunov* matrix is obtained

$$\mathbf{P}_2 = \begin{bmatrix} 0.0385 & 0 \\ 0 & 0.0385 \end{bmatrix} \quad (7.187)$$

From (7.185) and $\mathbf{T}_o = \mathbf{I}_2$, the gain matrices $\bar{\mathbf{G}}_L$ and $\bar{\mathbf{G}}_{NL}$ are computed using equations (7.53) and (7.76). Moreover, since the system is in the canonical form, the observer gain matrices $\mathbf{G}_L = \bar{\mathbf{G}}_L$ and $\mathbf{G}_{NL} = \bar{\mathbf{G}}_{NL}$ are given by

$$\mathbf{G}_L = \begin{bmatrix} 4.1420 & 2 \\ 18.8952 & 1 \\ 18.4260 & 0 \\ 0.4753 & 12 \end{bmatrix} \quad (7.188)$$

$$\mathbf{G}_{NL} = \begin{bmatrix} 0.3333 & 0 \\ 1.8087 & 0 \\ 1 & 0 \\ 0 & 1 \end{bmatrix} \quad (7.189)$$

The gain matrix (7.188) yields the following eigenvalues of the nominal error system, *i.e.* when $\theta_1(t) = \theta_2(t) = \theta_3(t) = 0$,

$$\lambda(\mathbf{A}_0 - \mathbf{G}_L \mathbf{C}) = \{-13, -6, -13, -7.4260\} \quad (7.190)$$

where $\mathbf{A}_0 \in \mathbb{R}^{4 \times 4}$ is the nominal state matrix in (7.175).

For simulation purposes a state feedback control law of the form $u(t) = -\mathcal{K}_{SF}\mathbf{x}(t)$ has been designed using the polytopic representation of the uncertain system (7.175)-(7.176) and the LMI region shown in Figure 7.1.

The controller gain is given by

$$\mathcal{K}_{SF} = [3.2181 \quad 4.8737 \quad -3.3614 \quad 3.9105] \quad (7.191)$$

In order to demonstrate the ability of the proposed sliding mode observer to track the state behaviour of the uncertain system (7.175)-(7.176), the following control signal is used for the computer simulations

$$u(t) = -\mathcal{K}_{SF}\mathbf{x}(t) + 20 \sin(5\pi t) \quad (7.192)$$

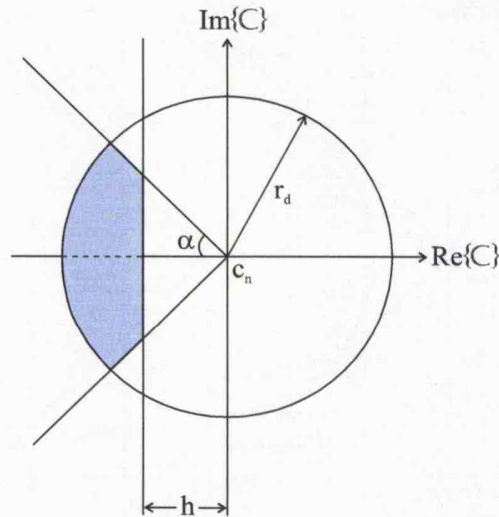


Figure 7.1: Convex Region $\mathcal{D}(h, c_n, r_d, \alpha) = \mathcal{D}(0.1, 0, 6, \pi/4)$ for robust pole placement of a full state feedback controller

Computer simulation results are presented in the sequel using the initial conditions $\mathbf{x}_0 = [1 \ -1 \ 0 \ 1]^T$ and $\hat{\mathbf{x}}_0 = [0 \ 0 \ 0 \ 0]^T$ for the plant and observer respectively. The time evolution of the uncertain parameters is depicted in Figure 7.2.

The true and estimated states are plotted in Figures 7.3–7.6 for comparison. It can be seen that after approximately 0.5 sec the estimated states $x_3(t)$ and $x_4(t)$ track the true states perfectly. With regard to state variable $x_2(t)$ perfect tracking of the estimated state is achieved after 2 sec. A perceptible estimation error occurs in terms of the true and estimated state variable $x_1(t)$. However, $|e_1(t)| = |\hat{x}_1(t) - x_1(t)| < 0.08$ after 2.5 sec. This can be seen in Figure 7.7.

Estimation errors are depicted in Figures 7.7–7.10. These plots demonstrate the effectiveness of the sliding mode observer design methodology for plants with mismatched uncertainties. The acceptable margin for the magnitude of the estimation error is application-related and is part of the performance specifications. The time evolution of the switching functions is shown in Figure 7.11. This plot shows that the sliding motion is induced on the sliding hyperplane \mathcal{S}_{Obs} .

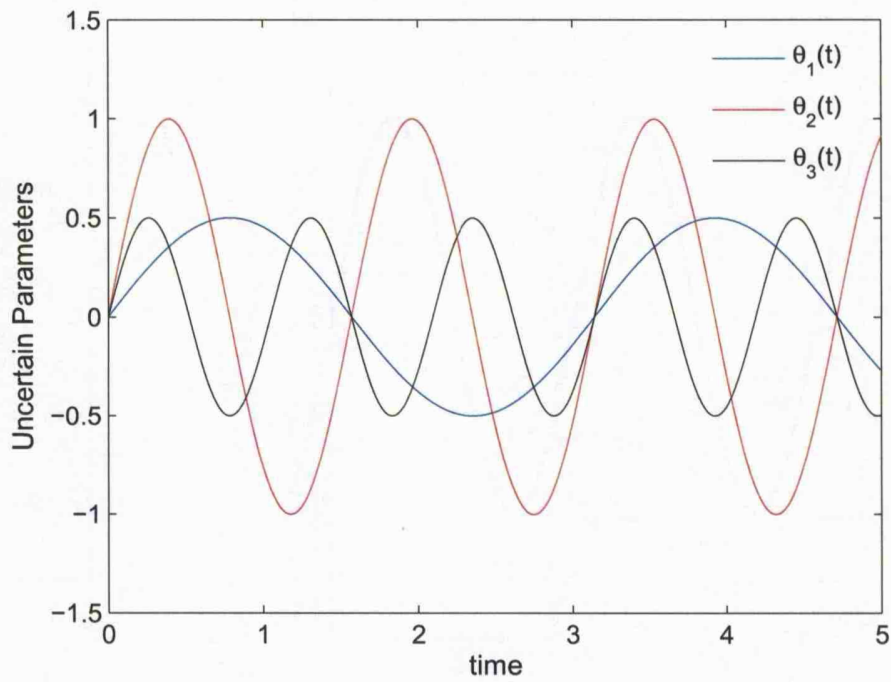


Figure 7.2: Time evolution of the uncertain parameters $\theta_1(t)$, $\theta_2(t)$ and $\theta_3(t)$

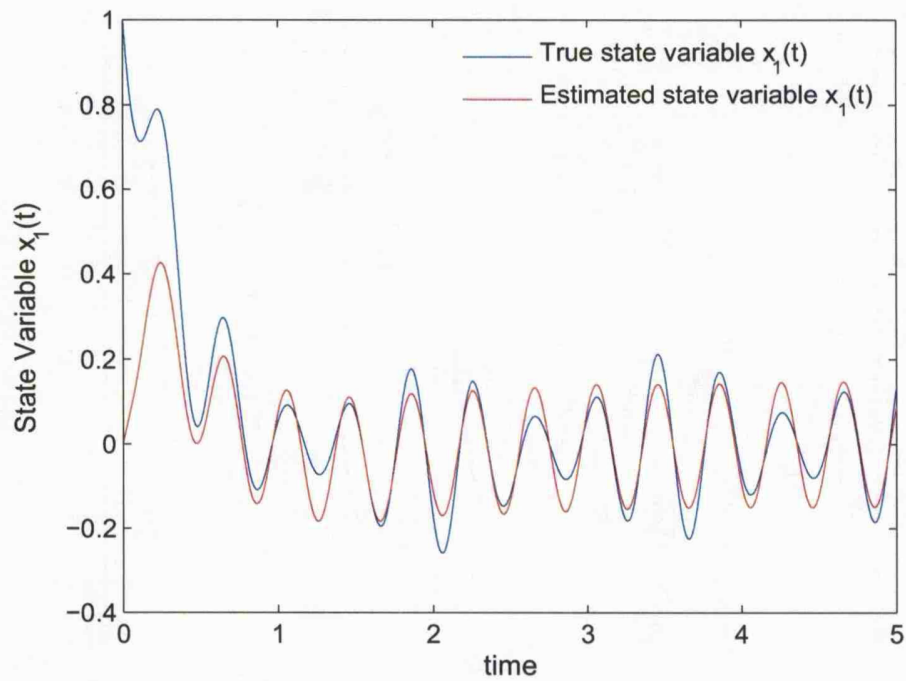
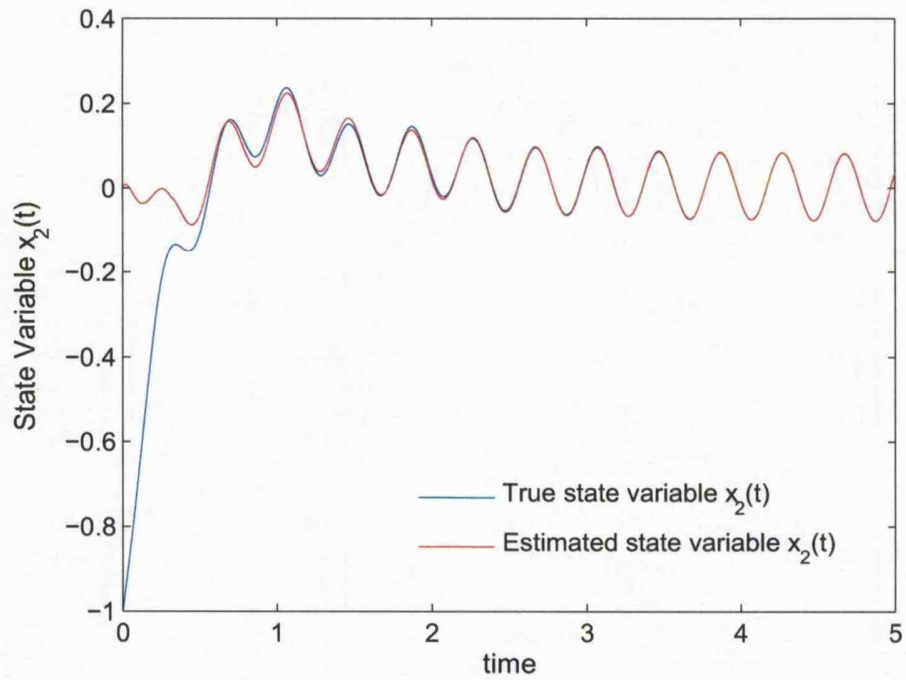
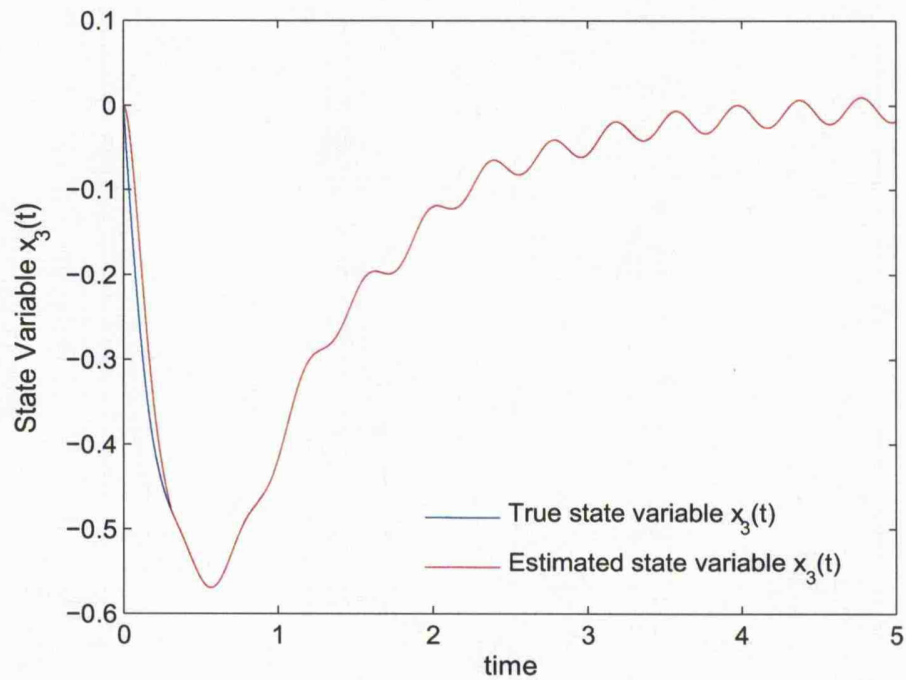
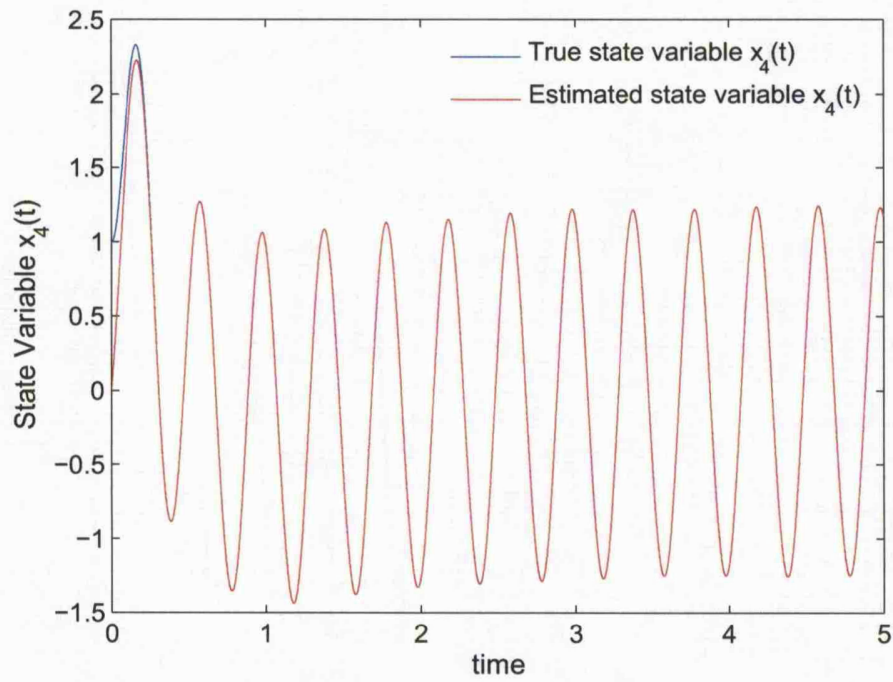
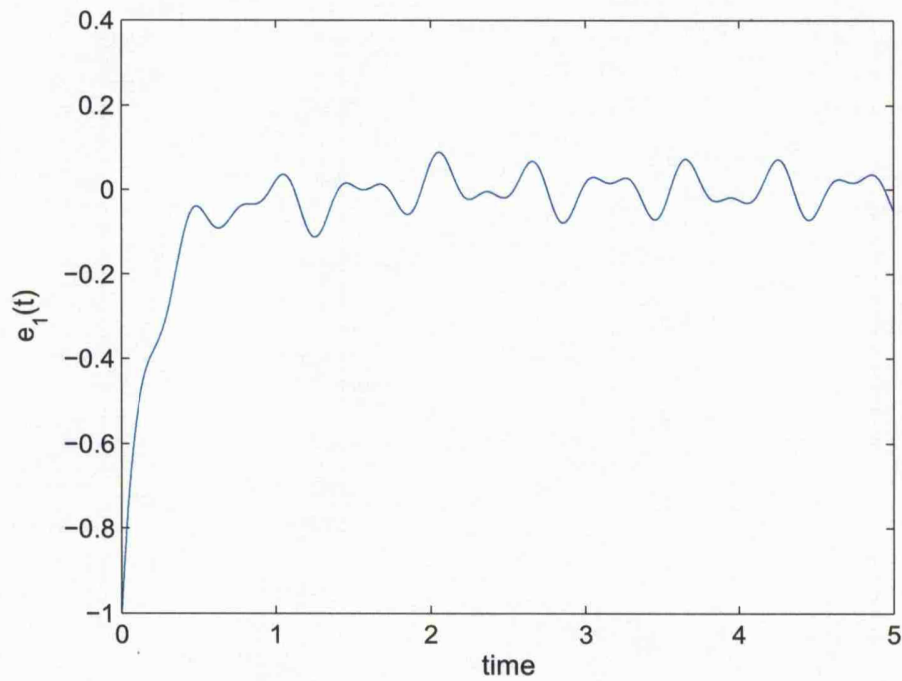
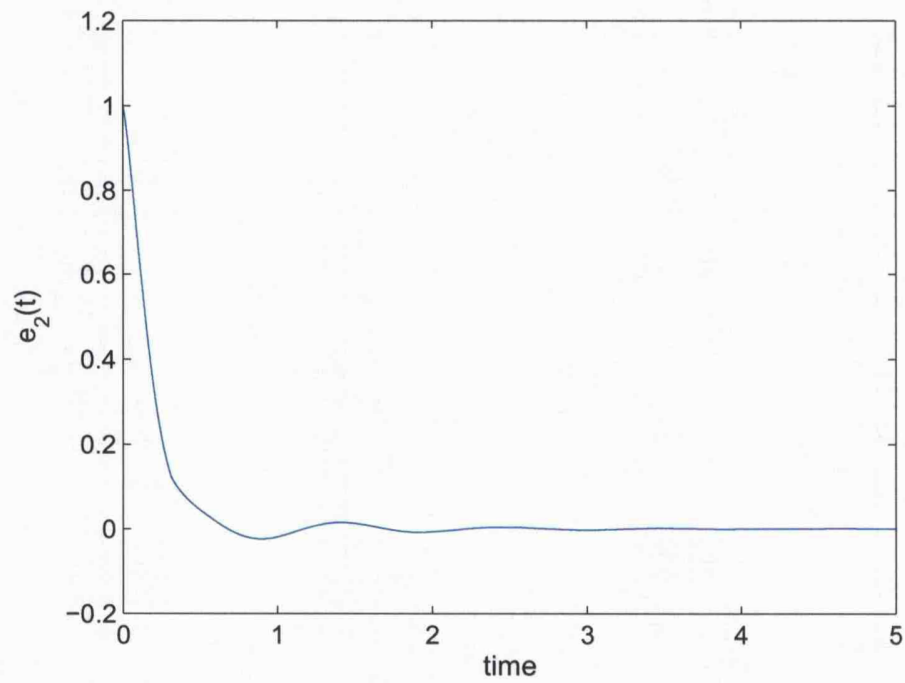
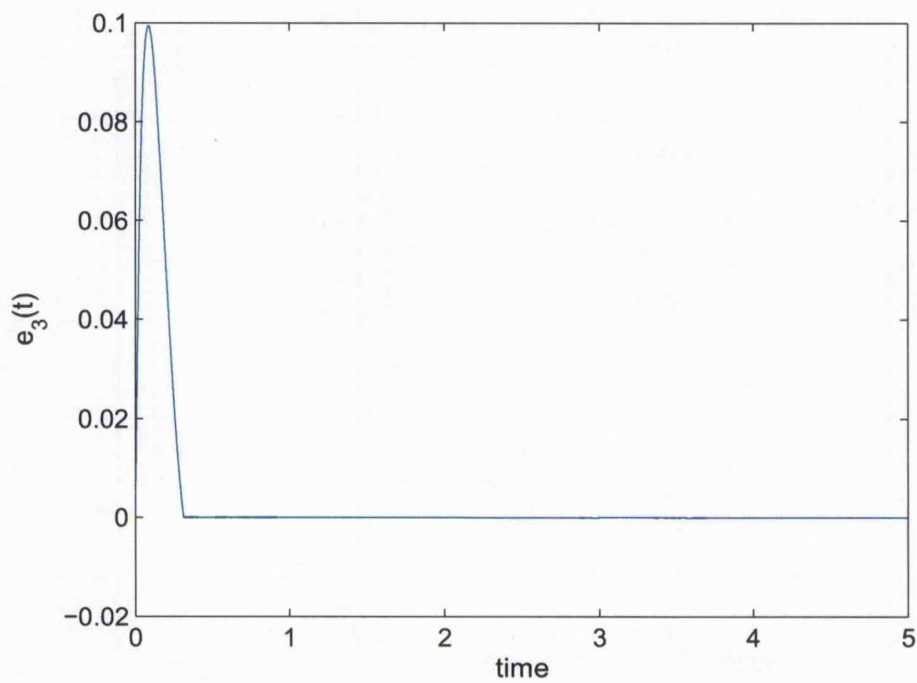


Figure 7.3: Time evolution of the true and estimated state $x_1(t)$

Figure 7.4: Time evolution of the true and estimated state $x_2(t)$ Figure 7.5: Time evolution of the true and estimated state $x_3(t)$

Figure 7.6: Time evolution of the true and estimated state $x_4(t)$ Figure 7.7: Estimation error $e_1(t) = \hat{x}_1(t) - x_1(t)$

Figure 7.8: Estimation error $e_2(t) = \hat{x}_2(t) - x_2(t)$ Figure 7.9: Estimation error $e_3(t) = \hat{x}_3(t) - x_3(t)$

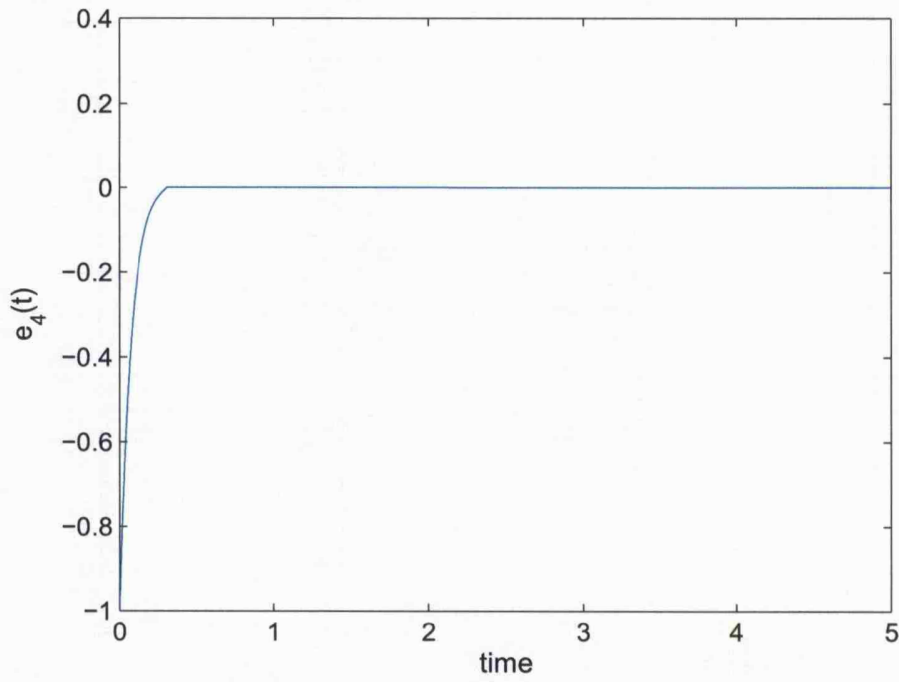


Figure 7.10: Estimation error $e_4(t) = \hat{x}_4(t) - x_4(t)$

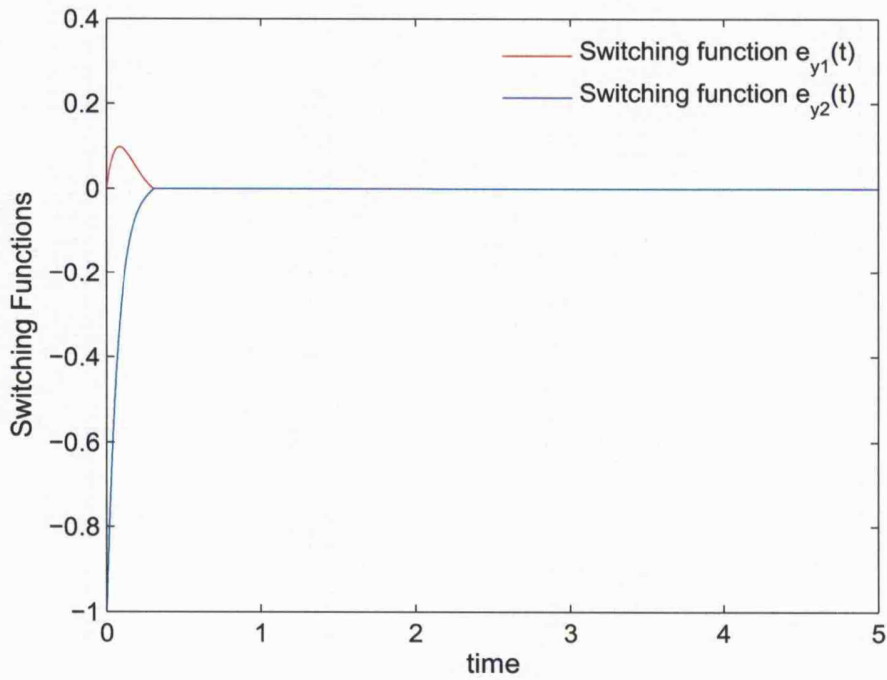


Figure 7.11: Time evolution of switching functions $\mathbf{e}_y(t) \in \mathbb{R}^2$

7.6 Summary

An LMI-based synthesis framework requiring only input and output signals from the plant has been described for designing the gain matrices of a sliding mode observer. The effect of the mismatched uncertain component is considered as a disturbance whose effect on the output estimation error has to be minimised. The observer gain matrices are parameterised in terms of only one design matrix. This matrix is obtained by solving a convex optimisation problem involving LMIs with a polytopic description of the reduced-order error system in terms of \mathcal{H}_∞ performance. A detailed stability analysis has been carried out for the sliding mode observer and the class of uncertain systems considered. A numerical example has illustrated the proposed approach and demonstrated its efficacy through computer simulations.

"If a man will begin with certainties, he shall end in doubts; but if he will be content to begin with doubts, he shall end in certainties."

Francis Bacon (1561 - 1626)
The Advancement of Learning (1605)

8

Conclusions

8.1 Concluding Remarks

The problem of designing variable structure systems with sliding modes for uncertain continuous time plants involving mismatched parametric uncertainties and matched uncertainties, nonlinearities and/or disturbances has been addressed in this thesis. Full and partial state information cases were considered. The proposed synthesis approaches are based on LMI methods and involve polytopic models for describing the mismatched parametric uncertainty which usually affects real world systems. The form of the sliding mode control law considered throughout consists of linear and nonlinear (discontinuous) components.

In the full state information case, a design framework for state feedback sliding mode controllers has been proposed. Robust pole clustering in LMI regions, considering a polytopic description of the reduced-order system governing the sliding dynamics, has been employed for synthesising a parameterised switching gain matrix which defines a sliding surface. The control law uses the state vector in its entirety. A feasibility LMI problem has been formulated, involving a polytopic model of the plant, for designing the gain matrix in the linear component of the control law. In turn, the switched part of the control law takes into account the matched term associated with uncertainties, nonlinearities and/or exogenous perturbations. The design of the nonlinear component is dependent on the solution of the feasibility problem when synthesising the gain matrix of the linear state feedback component. Angular position control of an uncertain DC motor has demonstrated the applicability of the proposed state feedback sliding mode control approach. In addition, computer simulations have demonstrated the effectiveness of this control scheme.

New sliding mode control approaches using only measurable state variables have been proposed in this thesis. Thus, only output signals are required for the class of sliding surfaces and control laws considered. This is useful in many engineering

8.1 Concluding Remarks

applications since the state vector in its entirety might not be measurable because some internal states are not available, lack physical meaning and/or software and hardware overhead costs may be high. Two approaches have been proposed: sliding mode static output feedback and sliding mode dynamic output feedback. Conclusions on these two approaches are drawn in the sequel.

Firstly, an output feedback sliding mode controller which is static in nature and uses polytopic models has been developed. The existence problem has been formulated as a static output feedback problem in terms of a polytopic model of the reduced-order sliding mode dynamics. Without loss of generality, an LMI-based algorithm was adapted and can be applied to design the sliding surface. In addition, the control law requires only output signals. The linear component is designed through an optimisation LMI problem involving LMI regions and a polytopic model of the plant considering the mismatched uncertainty, whilst the discontinuous term is designed in such a way that the invariance with respect to matched uncertainties is achieved. As in the state feedback approach, the design of the nonlinear part depends on one of the matrix variables obtained if the optimisation problem formulated for the design of the linear output feedback gain matrix has a solution. The control law does not incur high control effort and does not induce chattering since the unit vector has been smoothed using the differentiable approximation introduced in Section 2.5.4. Two design studies have been carried out. The former corresponds to a numerical example borrowed from a paper studying the problem of designing a sliding mode static output feedback controller for systems of the class considered in this thesis. The latter is concerned with the lateral control of an aircraft in which some parameters have been assumed uncertain. Computer simulations were carried out in order to assess the proposed sliding mode static output feedback control (SMSOFC) approach. The results obtained were satisfactory and reflected the applicability of this new approach to solve control problems when only output information is available.

Secondly, although the SMSOFC strategy proposed in this dissertation, and indeed static output feedback in general, is the simplest approach when only a sub-set of the state variables are available for measurement, it may not be applied in some particular cases when a system is not static output feedback stabilisable or if the closed loop performance requires improvement. In this thesis, a sliding mode dynamic output feedback control approach has been proposed to deal with such situations. The reduced-order system representing the sliding mode dynamics is augmented and described using a polytopic model. Then, the sliding surface synthesis problem can be posed as a static output feedback problem. The algorithm employed in the sliding mode static output feedback control approach has been adapted and employed to design a compensator-based sliding surface. The mismatched parametric uncertainty is considered in the formulation of the problem using a polytopic description and LMI methods. With regard to the control law design, an LMI optimisation problem using an augmented

8.1 Concluding Remarks

representation of the plant has been formulated in order to synthesise the linear output feedback gain matrix. The switched component of the control law tackles the mismatched uncertainties, nonlinearities and/or external disturbances. This part of the control law, as in the previous described control schemes, is dependent on the design of the linear component. An augmented output vector is used in both components of the control law. A numerical example considering an uncertain plant, whose reduced-order system is not static output feedback stabilisable, has been used to illustrate the proposed control scheme. Simulation results have provided evidence of the applicability of the sliding mode dynamic output feedback controller developed in this dissertation using polytopic models and based on LMIs.

Another problem considered in this thesis was the synthesis of a single sliding mode output feedback controller, if such a controller exists, for the simultaneous stabilisation of a finite collection of plant models. One approach to the simultaneous stabilisation problem is to split the operating space into a finite number of operating conditions. This has practical relevance since it facilitates several applications, *e.g.* stabilisation of uncertain plants; fault tolerant control where the operating conditions are regarded as the fault-free and various fault affected plant models; stabilisation of plants investigating different operation conditions. The plant model belongs to the class of continuous-time systems described in state-space form by a finite set of different state matrices, but common input and output matrices. Furthermore a term associated with mismatched uncertainties, nonlinearities and/or exogenous perturbations is also included. The problem of simultaneous stabilisation has been addressed from the multi-model paradigm rather than using polytopic models in order to encompass a wider number of systems and control engineering problems. Moreover, it facilitates exploration of the use of a finite set of *Lyapunov* matrices instead of a single *Lyapunov* matrix as in the strategies currently proposed in this thesis using polytopic models¹. Synthesis frameworks for static and dynamic output feedback variable structure controllers with sliding modes have been proposed. These sliding mode output feedback control strategies can be applied to a set of uncertain linear systems whose matched and mismatched uncertainties can be dealt with. An interpretation of the different state matrices is that they constitute mismatched uncertainty. This is a noteworthy feature since most of the existing sliding mode output feedback control approaches only tackle matched uncertainties and a ‘one plant’ model. Some conclusions about the deployed sliding mode output feedback approaches are given below.

A sliding mode static output feedback controller design based on LMIs has been proposed for the problem of simultaneous stabilisation of a finite collection of uncertain system. The sliding mode existence problem has been formulated as a static output feedback problem considering a family of uncertain LTI models. The LMIs involved

¹The use of parameter-dependent *Lyapunov* matrices will be briefly discussed here in Section 8.2.

8.1 Concluding Remarks

in the solution of the existence problem have as many *Lyapunov* matrices as models considered. An iterative algorithm involving LMIs was adapted to solve numerically the sliding mode existence problem. An LMI optimisation problem has been formulated in order to synthesise the linear output feedback gain matrix of the control law. The nonlinear component is designed in such a way that the system response is not sensitive with respect to the matched uncertainty. Moreover, as in the previous approaches proposed in this thesis, the design of the nonlinear component is dependent on one of the matrix variables resulting from the solution, if such a solution exists, of the LMI optimisation problem for the linear component. The proposed sliding mode static output feedback controller has demonstrated, through computer simulations, its efficacy in simultaneously stabilising a lateral motion autopilot for a remotely piloted vehicle when different flight conditions were considered.

A design framework for a compensator-based sliding mode controller using only output information, which simultaneously stabilises a finite set of models, has been proposed. This synthesis methodology can be applied when the collection of sliding mode reduced-order systems is not static output feedback stabilisable. As in Chapter 5, the reduced-order system, which describes the sliding mode dynamics, is augmented by adding a compensator, consequently introducing further dynamics to the sliding motion. A static output feedback problem has been formulated and the iterative algorithm used for designing the sliding mode static output feedback controller has been re-cast to design the compensator-based sliding surface. An LMI optimisation problem has been posed for designing the linear part of the control law considering an augmented representation of the plant due to the inclusion of a compensator. An augmented output vector is available to the control law. The nonlinear part of the control law depends on the solution of an LMI optimisation problem for the linear component. Two design examples have been considered. Firstly, a set of plant models which are not static output feedback stabilisable have been stabilised by means of the proposed sliding mode dynamic output feedback (SMDOF) controller. This makes the proposed approach appealing. Secondly, a sixth-order gas absorber operating under different conditions has been considered as a collection of models and a single SMDOF controller stabilises the plant in all the operating conditions considered. These two examples have demonstrated the efficacy of the approach through computer simulations.

An LMI-based design framework requiring only input and output signal from the plant has been described for synthesising the gain matrices of a sliding mode observer. The observer gain matrices were parameterised in terms of only one design matrix. All other components of the gain matrices are part of the system sub-matrices written in a canonical form. The class of systems to which the design approach can be applied consists of uncertain plants with both matched and mismatched uncertainties. The effect of the mismatched uncertain component is considered as a disturbance whose effect on the output estimation error has to be minimised. For this purpose, a convex

8.2 Brief Suggestion for Future Research

optimisation problem is formulated using a polytopic description of the reduced-order error system in terms of \mathcal{H}_∞ performance. This reflects the maximal amplification of the disturbance which can be interpreted as the worst case gain of the reduced-order error system with respect to the disturbance. The optimisation problem involves LMIs and can be solved numerically using any available LMI software. An exhaustive stability analysis has been carried out for the sliding mode observer and the class of uncertain systems considered. The concept of practical stability, formally called uniformly ultimate bounded stability, has been applied. The proposed methodology has been illustrated through a detailed design involving a numerical example. The results obtained from computer simulations demonstrate the applicability and effectiveness of the approach.

8.2 Brief Suggestion for Future Research

The concept of quadratic stability, considered within the design frameworks in Chapters 4 and 5, imposes the condition that a single *Lyapunov* matrix must exist over the entire polytopic domain. This is an inherent source of conservatism that can be reduced by considering parameter dependent *Lyapunov* matrices. Hence, a natural extension of the work presented in the aforementioned chapters is: the formulation of the sliding mode existence and reachability problems in terms of parameter-dependent *Lyapunov* matrices, the study of LMI-based algorithms for state feedback and static output feedback problems employing such classes of *Lyapunov* matrices, and the adaptation of the most suitable algorithms to the sliding mode context considering polytopic models. Note that new nonlinear components for the control laws have to be developed since such components, in the current approaches proposed in this thesis, depend on a single *Lyapunov* matrix (\mathbf{P}_2 in the state and static output feedback cases, and \mathbf{P}_{a2} in the dynamic output feedback approach).

Another area for future research lies in the investigation of the discrete-time counterparts of the problems addressed in this dissertation. This could be pursued by initially considering a single *Lyapunov* matrix and then parameter-dependent *Lyapunov* matrices.

The application of the design frameworks proposed in this thesis to real world plants would be appealing as further research in the future. Technical issues associated with the implementation of these variable structure controllers with a sliding mode and involving sliding mode observers could be challenging though.

Another possible extension of the synthesis methodologies developed in this dissertation lies in considering more general mathematical models of the plant. For example,

8.2 Brief Suggestion for Future Research

$$\dot{\mathbf{x}}(t) = (\mathbf{A} + \Delta\mathbf{A}(t))\mathbf{x}(t) + \mathbf{B}(\mathbf{u}(t) + \xi(t, \mathbf{x}, \mathbf{u})) + \mathbf{D}_m \mathbf{f}_m(t, \mathbf{x}) + \mathbf{D}_f \mathbf{f}_f(t) \quad (8.1)$$

$$\mathbf{y}(t) = (\mathbf{C} + \Delta\mathbf{C}(t))\mathbf{x}(t) \quad (8.2)$$

and

$$\dot{\mathbf{x}}(t) = \mathbf{A}_i \mathbf{x}(t) + \mathbf{B}(\mathbf{u}(t) + \xi_i(t, \mathbf{x}, \mathbf{u})) \quad (8.3)$$

$$\mathbf{y}(t) = \mathbf{C}_i \mathbf{x}(t) \quad (8.4)$$

for $i \in I(1, N)$. These models are quite attractive from a passive fault tolerant control viewpoint, since faults in sensors could be dealt with. Recall that faults affecting the state and input matrix can be handled using the class of systems already considered in this thesis. Nevertheless, the models presented in (8.1)-(8.2) and (8.3)-(8.4) allow a wider class of systems to be considered. Note that, $\mathbf{D}_m \mathbf{f}_m$ represents mismatched uncertainties, nonlinearities and/or external disturbances which are not associated with the state matrix, whilst $\mathbf{D}_f \mathbf{f}_f(\cdot)$ may be used for modelling faults.

Fault estimation using a sliding mode observer for plants with matched and mismatched parametric uncertainties described by polytopic models represents an important area for future investigation. Its practical significance resides in the fact that real physical plants are uncertain and their operation is subject to faults in any of their components. Any fault has to be detected in order to avoid performance degradation or even the complete breakdown of the system.

"The purpose of computation is insight, not numbers."

Richard W. Hamming (1915 - 1998)



High-level Implementation of LMIs

The main attraction for posing problems as LMIs, is that LMI problems can be tackled using efficient numerical tools and solved in polynomial time (Boyd *et al.*, 1994). Solving an LMI problem involves (1) determining whether the problem is feasible, and, if the problem is indeed feasible, (2) finding a solution. In this thesis, the LMI toolbox of Matlab (Gahinet *et al.*, 1995) and the toolbox SeDuMi (Sturm, 1999) have been used. Both of these toolboxes use interior point methods¹. With these toolboxes, LMI problems can be formulated, in the Matlab environment, in a high-level symbolic form which is relatively transparent to the user. The toolboxes then translate these high-level symbolic forms into numerical optimisation problems and then solve the LMI problems as described above.

In order to illustrate the implementation of LMI problems using the LMI control toolbox of MATLAB and SeDuMi, partial pieces of code are presented in the sequel. It is important to highlight that the code shown in this appendix represents only a small fraction of all MATLAB scripts developed during this research project.

The following code, using commands of the LMI control toolbox, corresponds to the switching gain matrix synthesis considered in the design example presented in Section 4.3.3.

¹Details on the interior-point methods can be found in (Bland *et al.*, 1981), (Boyd *et al.*, 1994) and (Scherer & Weiland, 1999).

```

% Definition of LMIs
setlmis([]);

% Definition of Decision Variables
Q_1 = lmivar(1, [(n - m) 1]);
L_1 = lmivar(2, [m (n - m)]);

% Definition of the LMI Region as LMI constraints
% Strip constraint
for i = 1 : N
    lmiterm([i 1 1 Q_1], 1, (A_11{i})', 's');
    lmiterm([i 1 1 - L_1], -1, (A_12{i})', 's');
    lmiterm([i 1 1 Q_1], (2 * h), 1);
end

% Circle Constraint
for i = 1 : N
    lmiterm([(2 + i) 1 1 Q_1], -rd, 1);
    lmiterm([(2 + i) 1 2 Q_1], A_11{i}, 1);
    lmiterm([(2 + i) 1 2 L_1], A_12{i}, -1);
    lmiterm([(2 + i) 1 2 Q_1], cn, 1);
    lmiterm([(2 + i) 2 2 Q_1], -rd, 1);
end

% Conic Constraint
for i = 1 : N
    lmiterm([(4 + i) 1 1 Q_1], sin(alpha), (A_11{i})', 's');
    lmiterm([(4 + i) 1 1 L_1], -sin(alpha) * A_12{i}, 1, 's');
    lmiterm([(4 + i) 1 2 Q_1], cos(alpha) * A_11{i}, 1);
    lmiterm([(4 + i) 1 2 Q_1], -cos(alpha), (A_11{i})');
    lmiterm([(4 + i) 1 2 L_1], -cos(alpha) * A_12{i}, 1);
    lmiterm([(4 + i) 1 2 - L_1], cos(alpha), (A_12{i})');
    lmiterm([(4 + i) 2 2 Q_1], sin(alpha), (A_11{i})', 's');
    lmiterm([(4 + i) 2 2 L_1], -sin(alpha) * A_12{i}, 1, 's');
end

lmiterm([-7 1 1 Q_1], 1, 1);

LMI_Sys = getlmis;

% Feasibility Problem
[tmin_LMIP, x_feas_LMIP] = feasp(LMI_Sys);

% Results
Q1 = dec2mat(LMI_Sys, x_feas_LMIP, Q_1);

```

```

L1 = dec2mat(LMI_Sys, x_feas.LMIP, L_1);
K = L1 * inv(Q1);
Gamma = [K eye(m)];

```

In what follows, the optimisation problem in Proposition 7.1 is presented using SeDuMi commands.

```

cvx_precision high
cvx_begin sdp
variable Q1((n-p),(n-p)) symmetric
variable FL((n-p),(p-m))
variable gamma
minimize (gamma)
Q1 > 0
for i = 1 : N
    [ A_bar_11' * Q1 + Q1 * A_bar_11 + A_bar_211' * FL' + FL * A_bar_211
      Q1 * DeltaA_bar_u_1{i} eye(n - p);
      DeltaA_bar_u_1{i}' * Q1 - gamma * eye(n) zeros(n, (n - p));
      eye(n - p) zeros((n - p), n) - gamma * eye(n - p)] < 0
end
cvx_end
L = inv(Q1) * FL

```

"The farther backward you can look,
the farther forward you are likely to see."

Sir Winston Leonard Spencer Churchill (1874 - 1965)

References

- ALWI, H., EDWARDS, C., STROOSMA, O. & MULDER, J.A. (2008). Fault tolerant sliding mode control design with piloted simulator evaluation. *AIAA Journal of Guidance, Control, and Dynamics*, **31**, 1186–1201. 4
- ANDERSON, B.D.O. & MOORE, J.B. (2007). *Optimal Control - Linear Quadratic Methods*. Dover Books in Engineering, N.Y. - U.S.A. 101
- ANDRADE-DA SILVA, J.M. & EDWARDS, C. (2009a). Compensator-based sliding mode output feedback simultaneous stabilisation controller design via LMIs for uncertain systems. In *48th IEEE Conference on Decision and Control*, 7735–7740, IEEE, Shanghai, P.R. China. 12
- ANDRADE-DA SILVA, J.M. & EDWARDS, C. (2009b). An LMI approach for sliding mode static output feedback simultaneous stabilisation. In *7th IEEE International Conference on Control and Automation*, 903–908, IEEE, Christchurch, New Zealand. 12
- ANDRADE-DA SILVA, J.M. & EDWARDS, C. (2010a). Sliding mode controller design for systems with mismatched uncertainties described using polytopic models. Accepted for the 2010 IEEE Multi-conference on Systems and Control to be held in Yokohama, Tokyo on September 8-10. 11
- ANDRADE-DA SILVA, J.M. & EDWARDS, C. (2010b). Sliding mode observer for systems with mismatched parametric uncertainties. In *11th International Workshop on Variable Structure Systems*, IEEE, Mexico City - Mexico. 12
- ANDRADE-DA SILVA, J.M., SPURGEON, S.K. & EDWARDS, C. (2008a). Sliding mode output feedback controller design using linear matrix inequalities with application to aircraft systems. In *10th International Workshop on Variable Structure Systems*, 227–232. 11
- ANDRADE-DA SILVA, J.M., SPURGEON, S.K. & EDWARDS, C. (2008b). Sliding mode static output feedback control for uncertain systems: A polytopic approach. In *17th IFAC World Congress*, 8630–8635, The International Federation of Automatic Control, Seoul, Korea. 11

REFERENCES

- ANDRADE-DA SILVA, J.M., EDWARDS, C. & SPURGEON, S.K. (2009a). Linear matrix inequality based dynamic output feedback sliding mode control for uncertain plants. In *American Control Conference*, 763–768, IEEE - AACC, Hyatt Regency Riverfront, St. Louis, MO, U.S.A. 11
- ANDRADE-DA SILVA, J.M., EDWARDS, C. & SPURGEON, S.K. (2009b). Sliding-mode output-feedback control based on LMIs for plants with mismatched uncertainties. *IEEE Transactions on Industrial Electronics*, **56**, 3675–3683. 11
- ARZELIER, D., ANGULO, M.I. & BERNUSSOU, J. (1997). Sliding surface design by quadratic stabilization and pole placement. In *Proceedings of the European Control Conference*. 5, 11
- BARBASHIN, E.A. (1967). *Introduction to Stability Theory (in Russian)*. Nauka, Moscow. 2
- BARTOLINI, G., PISANO, A., PUNTA, E. & USAI, E. (2004). Motion control of underwater objects by using second order sliding mode techniques. In *Variable Structure Systems: From Principles to Implementation*, IEE Control Engineering Series 66, chap. 16, 353–375, IEE, London, U.K. 4
- BASHEIN, G. (1971). A simplex algorithm for on-line computation of time optimal controls. *IEEE Transactions on Automatic Control*, **16**, 479–482. 141
- BEJARANO, F.J., FRIDMAN, L. & POZNYAK, A. (2007). Exact state estimation for linear systems with unknown inputs based on hierarchical super-twisting algorithm. *International Journal of Robust and Nonlinear Control*, **17**, 1734–1753. 9
- BENTON, R.E. & SMITH, D. (1999). A non-iterative LMI-based algorithm for robust static-output-feedback stabilization. *International Journal of Control*, **72**, 1322–1330. 11, 89, 90, 106, 114
- BERNSTEIN, D.S. (2005). *Matrix mathematics: theory, facts, and formulas with application to linear systems theory*. Princeton University Press., U.S.A. 27
- BIEL-SOLE, D. & FOSSAS-COLET, E. (2004). SMC applications in power electronics. In *Variable Structure Systems: From Principles to Implementation*, IEE Control Engineering Series 66, chap. 12, 265–293, IEE, London, U.K. 3
- BIRDWELL, J., CASTANON, D. & ATHANS, M. (1979). On reliable control system designs with and without feedback reconfigurations. *Proceedings of the IEEE Conference on Decision and Control*, 419–426. 7
- BLAND, R.G., GOLDFARB, D. & TODD, M.J. (1981). The ellipsoid method: A survey. *Operations Research*, **29**, 1039–1091. 49, 188

REFERENCES

- BONDAREV, A.G., BONDAREV, S.A., KOSTYLEVA, N.E. & UTKIN, V.I. (1985). Sliding modes in systems with asymptotic state observers. *Automation and Remote Control*, **46**, 49–64. 2, 35
- BOYD, S. & VANDENBERGHE, L. (2008). *Convex Optimization*. Cambridge University Press. 41, 42, 44, 46, 49
- BOYD, S., EL GHAOUI, L., FERON, E. & BALAKRISHNAN, V. (1994). *Linear Matrix Inequalities in System and Control Theory*, vol. 15 of *SIAM Studies in Applied Mathematics*. Philadelphia - U.S.A. 4, 10, 12, 41, 47, 49, 50, 52, 166, 168, 188
- BURTON, J.A. & ZINOBER, A.S.I. (1986). Continuous approximation of variable structure control. *International Journal of Systems Science*, **17**, 876–885. 35
- CAO, Y.Y. & SUN, Y.X. (1998). Static output feedback simultaneous stabilization: An ILMI approach. *International Journal of Control*, **70**, 803–814. 7, 12, 119, 120, 131, 132
- CHANG, Y. & CHENG, C.C. (2007). Design of adaptive sliding surfaces for systems with mismatched perturbations to achieve asymptotical stability. *IEE Proceedings on Control Theory*, **1**, 417–421. 5
- CHAPMAN, S.J. (2005). *Electric Machinery Fundamentals*. McGraw-Hill Higher Education, 4th edn. 76
- CHEN, W. & SAIF, M. (2006). Novel sliding mode observers for a class of uncertain systems. In *Proceedings of the American Control Conference*, 2622–2627, IEEE, Minneapolis, Minnesota, U.S.A. 8
- CHEN, W. & SAIF, M. (2008). Output feedback controller design for a class of MIMO nonlinear systems using high-order sliding-mode differentiators with application to a laboratory 3-D crane. *IEEE Transactions on Industrial Electronics*, **55**, 3985–3997. 6, 9
- CHEN, Y.P. & CHANG, J.L. (2000). A new method for constructing sliding surfaces of linear time-invariant systems. *International Journal of Systems Science*, **31**, 417–420. 5
- CHILALI, M. & GAHINET, P. (1996). H_∞ design with pole placement constraints: An LMI approach. *IEEE Transactions on Automatic Control*, 358–367. 52, 53
- CHILALI, M., GAHINET, P. & APKARIAN, P. (1999). Robust pole placement in LMI regions. *IEEE Transactions on Automatic Control*, **44**, 2257–2270. 52, 53, 68, 97
- CHOI, H. (1997). A new method for variable structure control system design: A linear matrix inequality approach. *Automatica*, **33**, 2089–2092. 4

REFERENCES

- CHOI, H. (2002). Variable structure output feedback control design for a class of uncertain dynamic systems. *Automatica*, **38**, 335–341. 6
- CHOI, H. (2003). An LMI-based switching surface design method for a class of mismatched uncertain systems. *IEEE Transactions on Automatic Control*, **48**, 1634–1638. 5
- CHOI, H.H. (2008a). Output feedback variable structure control design with an \mathcal{H}_2 performance bound constraint. *Automatica*, **44**, 2403–2408. 6
- CHOI, H.H. (2008b). Sliding-mode output feedback control design. *IEEE Transactions on Industrial Electronics*, **55**, 4047–4054. 6
- CHOI, H.H. (2009). Output feedback stabilization of uncertain fuzzy systems using variable structure system approach. *Fuzzy Sets and Systems*, **160**, 2812–2823. 6
- CHOI, H.H. & RO, K.S. (2005). LMI-based sliding-mode observer design method. *IEE Proceedings on Control Theory Applications*, **152**, 113–115. 8, 38
- CULLEN, C.G. (1990). *Matrices and Nonlinear Transformations*. Dover Publications, Inc., New York, U.S.A., 2nd edn., an unabridged, slightly corrected republication of the second edition (1972) of the work originally published in 1966 by Addison-Wesley Publishing Company, Reading, Massachusetts, U.S.A. 26
- DATTORRO, J. (2005). *Convex Optimization and Euclidean Distance Geometry*. Meboo, v2009.12.02 edn. 43
- DAVISON, E. (1970). On pole assignment in linear systems with incomplete state feedback. *IEEE Transactions on Automatic Control*, 348–351. 7
- DECARLO, R.A., ŽAK, S.H. & MATTHEWS, G.P. (1988). Variable structure control of nonlinear multivariable systems: tutorial. *Proceedings of the IEE*, **76**, 212–232. 3, 16, 35
- DORLING, C.M. & ZINOBER, A.S.I. (1986). Two approaches to hyperplane design in multivariable variable structure control systems. *International Journal of Control*, **44**, 65–82. 4, 20
- DOYE, Y. & HOFT, R.G. (1980). Microprocessor based sliding mode controller for a DC motor drive. *Presented at the Ind. Applicat. Soc. Annu. Meeting*. 3
- DRAKUNOV, S. & UTKIN, V.I. (1995). Sliding mode observers - tutorial. *Proceedings of the 34th CDC*, 3376–3378. 8
- DRAKUNOV, S.V., IZOSIMOV, D.B., LUKYANOV, A.G., UTKIN, V.A. & UTKIN, V.I. (1990a). Block principle i. *Automation and Remote Control*, **51**, 601–609. 3, 35

REFERENCES

- DRAKUNOV, S.V., IZOSIMOV, D.B., LUKYANOV, A.G., UTKIN, V.A. & UTKIN, V.I. (1990b). Block principle ii. *Automation and Remote Control*, **52**, 737–746. 3, 35
- DRAŽENOVIĆ, B. (1969). The invariance conditions in variable structure systems. *Automatica*, **5**, 287–295. 2, 29, 63
- EDWARDS, C. (2004). A practical method for the design of sliding mode controllers using linear matrix inequalities. *Automatica*, **40**, 1761–1769. 4
- EDWARDS, C. & SPURGEON, S.K. (1994). On the development of discontinuous observers. *International Journal of Control*, **59**, 1211–1229. 8, 36, 37, 38, 147, 148
- EDWARDS, C. & SPURGEON, S.K. (1995). Sliding mode stabilization of uncertain systems using only output information. *International Journal of Control*, **62**, 1129–1144. 6, 12, 21, 24, 25, 26, 85, 117, 151, 152
- EDWARDS, C. & SPURGEON, S.K. (1998a). Compensator based output feedback sliding mode controller design. *International Journal of Control*, **71**, 601–614. x, 7, 33, 147, 152
- EDWARDS, C. & SPURGEON, S.K. (1998b). *Sliding Mode Control—Theory and Applications*, vol. 7 of *Systems and Control Series*. Taylor & Francis. x, 2, 3, 5, 8, 16, 17, 22, 23, 27, 30, 32, 34, 36, 38, 65, 79, 148
- EDWARDS, C. & SPURGEON, S.K. (2000). On the limitations of some variable structure output feedback controller designs. *Automatica*, **36**, 743–748. 6
- EDWARDS, C. & SPURGEON, S.K. (2003). Linear matrix inequality methods for designing sliding mode output feedback controllers. *IEEE Proceedings on Control Theory Applications*, **150**, 539–545. 11, 87, 104
- EDWARDS, C., AKOACHERE, A. & SPURGEON, S.K. (2001). Sliding-mode output feedback controller desing using linear matrix inequalities. *IEEE Transactions on Automatic Control*, **46**, 115–119. 6, 12
- EL-GHEZAWI, O.M.E., ZINOBER, A.S.I. & BILLINGS, S. (1983). Analysis and design of variable structure systems using a geometric approach. *International Journal of Control*, **38**, 657–671. 4, 20, 26, 27, 29
- EL-KHAZALI, R. & DECARLO, R. (1995). Output feedback variable structure control design. *Automatica*, **31**, 805–816. 6
- EMEL'YANOV, S.Y. (1957). A method of producing complex control laws using only the error signal or controlled coordinate plus their first derivatives. *Automation and Remote Control*, **18**, 921–931. 2

REFERENCES

- EMEL'YANOV, S.Y. (1959a). Control of a first order delayed system by means of an astatic regulator and nonlinear correction. *Automation and Remote Control*, **20**, 983–991. 2
- EMEL'YANOV, S.Y. (1959b). The use of nonlinear correcting devices of the "key" type for improving the quality of second-order automatic control systems. *Automation and Remote Control*, **20**, 844–859. 2
- EMEL'YANOV, S.Y. (1967). *Variable Structure Control Systems (in Russian)*. Nauka, Moscow. 2, 31, 32
- EMEL'YANOV, S.Y. & KOROVIN, S.K. (2000). *Control of Complex and Uncertain Systems - New Types of Feedback*. Communications and Control Engineering, Springer-Verlag, London, Great Britain. 3
- FILIPPOV, A.F. (1964). Differential equations with discontinuous right-hand sides. *American Mathematical Society Translations*, **42**, 199–231. 19
- FINSLER, P. (1937). Über das vorkommen definiter un semi-definiter formen in scharen quadratischer formen. *Comentarii Mathematici Helvetici*, **9**, 192–199. 52
- FLOQUET, T. & BARDOT, J.P. (2007). Super twisting algorithm-based step-by-step sliding mode observers for nonlinear systems with unknown inputs. *International Journal of Systems Science*, **38**, 803–815. 9
- FOSSAS, E., ROS, R.M. & FABREGAT, J. (2001). Sliding mode control in a bioreactor model. *Journal of Mathematical Chemistry*, **30**, 203–218. 3
- FRANKLIN, G.F., POWELL, J.D. & EMAMI-NAEINI, A. (2002). *Feedback Control of Dynamic Systems*. Prentice-Hall–Pearson Education International, 4th edn. x, 76, 77
- FRIDMAN, L., LEVANT, A. & DAVILA, J. (2006). High-order sliding-mode observer for linear systems with unknown inputs. In *Proceedings of the International Workshop on Variable Structure Systems*, 202–207, Alghero, Italy. 9
- FRIDMAN, L., DAVILA, J. & LEVANT, A. (2008). High-order sliding-mode observation of linear systems with unknown inputs. In *Proceedings of the 17th International Federation of Automatic Control World Congress*, 4779–4790, IFAC, Seoul, Korea. 9
- FULLER, A.T. (1974). Simplification of some time-optimal control switching functions. *IEEE Transactions on Automatic Control*, **19**, 65–68. 2
- GAHINET, P. & APKARIAN, P. (1994). A linear matrix inequality approach to \mathcal{H}_∞ control. *International Journal of Robust and Nonlinear Control*, **4**, 421–448. 52

REFERENCES

- GAHINET, P., NEMIROVSKI, A., LAUB, A.J. & CHILALI, M. (1995). *LMI Control Toolbox for use with Matlab*. The MathWorks, Natick, Massachusetts. 10, 12, 41, 46, 49, 58, 188
- GAUTHIER, J.P., HAMMOURI, H. & OTHMAN, S. (1992). A simple observer for non-linear systems—application to bioreactors. *IEEE Transactions on Automatic Control*, **37**, 875880. 8
- GOH, K.B., SPURGEON, S.K. & JONES, N.B. (2004). The application of sliding mode control algorithms to a diesel generator set. In *Variable Structure Systems: From Principles to Implementation*, IEE Control Engineering Series 66, chap. 15, 333–351, IEE, London, U.K. 4
- HADDAD, W.M. & CHELLABOINA, V. (2008). *Nonlinear Dynamical Systems and Control - A Lyapunov-Based Approach*. Princeton University Press, New Jersey, U.S.A. 9
- HASHIMOTO, H., MARUYAMA, K. & HARASHIMA, F. (1987). A microprocessor based robot manipulator control with sliding mode. *IEEE Transactions on Industrial Electronics*, **IE-34**, 11–18. 3
- HECK, B.S., YALLAPRAGADA, S.V. & FAN, M.K.H. (1995). Numerical methods to design the reaching phase of output feedback variable structure control. *Automatica*, **31**, 275–279. 12
- HERRMANN, G., EDWARDS, C., HREDZAK, B., VENKATARAMANAN, V. & SPURGEON, S.K. (2008). A novel discrete sliding mode technique and its application to a HDD dual-stage track-seek and track-following servo system. *International Journal of Adaptive Control and Signal Processing*, **22**, 344–358. 4
- HOWITT, G.D. & LUUS, R. (1991). Simultaneous stabilization of linear single-input systems by linear state feedback. *International Journal of Control*, **54**, 1015–1030. 12
- HOWITT, G.D. & LUUS, R. (1993). Control of a collection of linear systems by linear state feedback control. *International Journal of Control*, **58**, 79–96. 141, 142, 143
- HUNG, J.Y., GAO, W. & HUNG, J.C. (1993). Variable structure control: A survey. *IEEE Transactions on Industrial Electronics*, **40**, 2–22. 3, 16, 18, 31, 32, 34
- ISERMANN, R. (2006). *Fault-Diagnosis Systems*. Springer-Verlag, Berlin-Germany. 8
- ITKIS, U. (1976). *Control Systems of Variable Structure*. New York. 2, 31, 32
- KALMAN, R.E. (1960). A new approach to linear filtering and prediction problems. *Transactions on the ASME Journal of Basic Engineering*, **82**, 35–45. 8

REFERENCES

- KIM, K.S., PARK, Y. & OH, S.H. (2000). Designing robust sliding hyperplanes for parametric uncertain systems: A riccati approach. *Automatica*, **36**, 1041–1048. 5
- KIMURA, H. (1975). Pole assignment by gain output feedback. *IEEE Transactions on Automatic Control*, **AC-20**, 509–516. 7
- KIMURA, H. (1977). A further result on the problem of pole assignment by output feedback. *IEEE Transactions on Automatic Control*, 458–463. 7
- KOSHKOUEI, A.J. & ZINOBER, A.S.I. (2004). Sliding mode state observation for nonlinear systems. *International Journal of Control*, **77**, 118–127. 8
- KULEBAKIN, V. (1932). On the theory of vibration controller for electric machines (in russian). *Theoretical and Experimental Electronics*, **4**. 1
- KWAN, C. (2001). Further results on variable output feedback controllers. *IEEE Transactions on Automatic Control*, **46**, 1505–1508. 6
- LAVAEI, J. & AGHDAM, A. (2007). Simultaneous LQ control of a set of lti systems using constrained generalized sampled-data hold functions. *Automatica*, **43**, 274–280. 7
- LEE, P.H. & SOH, Y.C. (2004). Simultaneous H_∞ stabilization. *International Journal of Control*, **77**, 111–117. 7
- LEVANT, A. (1998). Robust exact differentiation via sliding mode technique. *Automatica*, **34**, 379–384. 8
- LUENBERGER, D.G. (1964). Observing the state of a linear system. *IEEE Transactions on Military Electronics*, **MIL-8**, 74–80. 7, 8
- LUUS, R. (2000). *Iterative Dynamic Programming*. Chapman & Hall/CRC Monographs and Surveys in Pure and Applied Mathematics 110, U.S.A. xi, 140, 141, 142
- MARINO, R. & TOMEI, P. (1995). Adaptive observer with arbitrary exponential rate of convergence for nonlinear systems. *IEEE Transactions on Automatic Control*, **40**, 1300–1304. 8
- MARSDEN, J.E. (1974). *Elementary Classical Analysis*. W. H. Freeman and Company, U.S.A. 18
- MICHEL, A.N. & HERGET, C.J. (1981a). *Applied Algebra and Functional Analysis*. Dover Publications, Inc., New York, U.S.A. 26

REFERENCES

- MICHEL, A.N. & HERGET, C.J. (1981b). *Mathematical Foundations in Engineering and Science - Algebra and Analysis*. Prentice-Hall, Inc., Englewood Cliffs, New Jersey, U.S.A. 18, 20
- MSIRDI, N. & NADJAR-GAUTHIER, N. (2002). Application of sliding mode control to robotic systems. In N. Munro, ed., *Sliding Mode Control in Engineering*, Control Engineering Series, chap. 13, 351–390, Marcel Dekker, Inc., U.S.A. 3
- NIKOLSKI, G. (1934). On automatic stability of a ship on a given course (in russian). *Proceedings of the Central Communication Laboratory*, **1**, 34–75. 2
- OGATA, K. (2002). *Modern Control Engineering*. Prentice Hall, 4th edn. 77
- PAN, Y., OZGÜNER, D. & DAĞCI, O.H. (2008). Variable-structure control of electronic throttle valve. *IEEE Transactions on Industrial Electronics*, **55**, 3899–3907. 4, 6
- PARK, P., CHOI, D.J. & KONG, S.G. (2007). Output feedback variable structure control for linear systems with uncertainties and disturbances. *Automatica*, **43**, 72–79. 7
- RYAN, E.P. & CORLESS, M. (1984). Ultimate boundedness and asymptotic stability of a class of uncertain dynamical systems via continuous and discontinuous feedback control. *IMA Journal of Mathematical Control & Information*, **1**, 223–242. 5, 147
- SABANOVIC, A. & JEZERNIK, K. (2004). Sliding modes in motion control systems. In *Variable Structure Systems: From Principles to Implementation*, IEE Control Engineering Series 66, chap. 13, 295–318, IEE, London, U.K. 3
- SAEKS, R. & MURRAY, J. (1982). Fractional representations, algebraic geometry and the simultaneous stabilization problem. *IEEE Transactions on Automatic Control*, **AC-27**, 895–903. 7
- SCHERER, C. & WEILAND, S. (1999). *Lecture notes on Linear Matrix Inequalities in Control*. University of Technology - The Netherlands. 41, 44, 49, 50, 51, 188
- SELLAMI, A., ARZELIER, D., M'HIRI, R. & ZRIDA, J. (2007). A sliding mode control approach for systems subjected to a norm-bounded uncertainty. *International Journal of Robust and Nonlinear Control*, **17**, 327–346. 5
- SIRA-RAMIREZ, H. & SPURGEON, S.K. (1994). On the robust design of sliding mode observers for linear systems. *Systems and Control Letters*, **23**, 9–14. 8
- SLOTINE, J.J. (1984). Sliding controller design for nonlinear systems. *International Journal of Control*, **40**, 421–434. 2, 35

REFERENCES

- SLOTINE, J.J. & SASTRY, S.S. (1983). Tracking control of nonlinear systems using sliding surfaces with application to robot manipulators. *International Journal of Control*, **38**, 465–492. 2, 35
- SLOTINE, J.J.E. & LI, W. (1991). *Applied Nonlinear Control*. Prentice-Hall International, U.S.A. 3, 31, 32
- SLOTINE, J.J.E., HEDRICK, J.K. & MISAWA, E.A. (1986). On sliding observers for nonlinear systems. *Proceedings of the American Control Conference*, 1794–1800. 8
- SPURGEON, S.K. & DAVIES, R. (1993). A nonlinear control strategy for robust sliding-mode performance in the presence on unmatched uncertainty. *International Journal of Control*, **57**, 1107–1123. 5, 35
- STURM, J.F. (1999). Using SeDuMi 1.02, a matlab toolbox for optimization over symmetric cones. *Optimization methods and software*, **11**, 625–653. 49, 61, 188
- SYRMOS, V.L., ABDALLAH, C.T., DORATO, P. & GRIGORIADIS, K. (1997). Static output feedback - a survey. *Automatica*, **33**, 125–137. 6
- TAKAHASHI, R.H.C. & PERES, P.L.D. (1999). \mathcal{H}_2 guaranteed cost-switching surface design for sliding modes with nonmatching disturbances. *IEEE Transactions on Automatic Control*, **44**, 2214–2218. 5
- TAN, C.P. & EDWARDS, C. (2001). An LMI approach for designing sliding mode observers. *International Journal of Control*, **74**, 1559–1568. 8, 38, 156, 159
- TAN, C.P. & EDWARDS, C. (2008). A robust sensor fault tolerant control scheme implemented on a crane. *Asian Journal of Control*, **9**, 340–344. 4
- TAN, S.C., LAI, Y. & TSE, C. (2008). General design issues of sliding-mode controllers in DC-DC converters. *IEEE Transactions on Industrial Electronics*, **55**, 1160–1174. 4, 6
- TEIXEIRA, M.C.M., COVACIC, M.R. & ASSUNÇÃO, E. (2006). Design of SPR systems with dynamic compensators and output variable structure control. *Proceedings of the 9th International Workshop on Variable Structure Systems (VSS'06)*, 328–333. 6
- UTKIN, V. (1974). *Sliding modes and their application in variable structure systems*. Nauka, Moscow, in Russian. 2
- UTKIN, V., GULDNER, J. & SHI, J. (1999). *Sliding Mode Control in Electromechanical Systems*. CRC Press Systems and Control, CRC Press - Biddles/IBT Global, London, U.K. 1, 2, 3, 35

REFERENCES

- UTKIN, V.I. (1971). Equations of sliding mode in discontinuous systems I. *Automation and Remote Control*, **12**, 1897–1907, moscow. Translated from *Avtomatika i Telemekhanika*, No. 12, pp. 42-54, December, 1971. 2
- UTKIN, V.I. (1972). Equations of sliding mode in discontinuous systems II. *Automation and Remote Control*, **2**, 211–219, moscow. Translated from *Avtomatika i Telemekhanika*, No. 2, pp. 51-61, February, 1972. 2
- UTKIN, V.I. (1977). Variable struture systems with sliding modes. *IEEE Transactions on Automatic Control*, **AC-22**, 212–222. 2, 3, 18, 19, 20, 21, 22, 31, 32
- UTKIN, V.I. (1978). *Sliding Modes and Their Application in Variable Structure Systems*. MIR Publishers Moscow, english translation edn., revised from the 1974 Russian Edition. 34
- UTKIN, V.I. (1981). Principles of identification using sliding regimes. *Soviet Physics: Doklady*, **26**, 271–272. 8, 36
- UTKIN, V.I. (1992). *Sliding Modes in Control Optimization*. Springer-Verlag, Berlin. 1, 2, 3, 8, 18, 33, 34, 36, 65
- UTKIN, V.I. (1993). Sliding mode control design principles and applications to electric drives. *IEEE Transactions on Industrial Electronics*, **40**, 23–36. 3, 6, 35
- UTKIN, V.I. (2002). First stage of VSS: People and Events. In X. Yu & J.X. Xu, eds., *Variable Structure Systems: Towards the 21st Century*, vol. 274 of *Lecture Notes in Control and Information Sciences*, 1–32, Springer-Verlag, Berling Heidelberg. 2
- UTKIN, V.I. & CHANG, H.C. (2004). Sliding mode control for automobile applications. In *Variable Structure Systems: From Principles to Implementation*, IEE Control Engineering Series 66, chap. 14, 319–332, IEE, London, U.K. 4
- UTKIN, V.I. & SHI, J. (1996). Integral sliding mode in systems operating under uncertainty conditions. In *IEEE Conference on Decision and Control*, 4591–4596, IEEE, Kobe, Japan. 3, 35
- UTKIN, V.I. & YANG, K.D. (1986). Methods for constructing discontinuity planes in multidimensional variable structure systems. *Automation and Remote Control*, **9**, 1466–1470. 31
- UTKIN, V.I. & YOUNG, K.K.D. (1978). Methods for constructing discontinuity planes in multidimensional variable structure systems. *Automation and Remote Control*, **39**, 1466–1470. 4
- VANDENBERGHE, L. & BOYD, S. (1996). Semidetinite programming. *Society for Industrial and Applied Mathematics (SIAM) Review*, **38**, 49–95. 49

REFERENCES

- VIDYASAGAR, M. & VISWANADHAM, N. (1982). Algebraic design techniques for reliable stabilization. *IEEE Transactions on Automatic Control*, **AC-25**, 1085–1095. 7
- WALCOTT, B.L. & ŽAK, S.H. (1987). State observation of nonlinear uncertain dynamical systems. *IEEE Transactions on Automatic Control*, **32**, 166–170. 8, 36
- WHITE, B.A. (1990). *Applications of Output Feedback in Variable Structure Control*, chap. 8, 144–169. Peter Peregrinus, U.K. 127
- WILLEMS, J.C. (1971). Least squares stationary optimal control and the algebraic ricatti equation. *IEEE Transactions on Automatic Control*, **AC-16**, 621–634. 46
- WU, J.L. & LEE, T.T. (2005). Optimal static output feedback simultaneous regional pole placement. *IEEE Transactions on Systems, Man, and Cybernetics - Part B: Cybernetics*, **35**, 881–893. 7
- XIANG, J., WEI, W. & SU, H. (2006). An ILMI approach to robust static output feedback sliding mode control. *International Journal of Control*, **79**, 959–967. 6, 98, 99
- XIE, W.F. (2007). Sliding-mode-observer-based adaptive control for servo actuator with friction. *IEEE Transactions on Industrial Electronics*, **54**, 1517–1527. 6
- YOUNG, K.K. (1993). *Variable Structure Control for Robotics and Aerospace Systems*. Elsevier, Amsterdam, The Netherlands. 3
- ŽAK, S.H. & HUI, S. (1993). On variable structure output feedback controllers for uncertain dynamics systems. *IEEE Transactions on Automatic Control*, **38**, 1509–1512. 6, 12
- ZINOBER, A.S.I. (1994). *An Introduction to Sliding Mode Variable Structure Control, Variable Structure and Lyapunov Control*. Lecture Notes in Control and Information, Springer-Verlag, Berlin - Germany. 3